
Citation:

Hemingray, CS (2015) Colour prediction for sustainable fibre blending. Doctoral thesis, University of Leeds.

Link to Leeds Beckett Repository record:

<https://eprints.leedsbeckett.ac.uk/id/eprint/2921/>

Document Version:

Thesis (Published Version)

Creative Commons: Attribution-Noncommercial-Share Alike 3.0

The aim of the Leeds Beckett Repository is to provide open access to our research, as required by funder policies and permitted by publishers and copyright law.

The Leeds Beckett repository holds a wide range of publications, each of which has been checked for copyright and the relevant embargo period has been applied by the Research Services team.

We operate on a standard take-down policy. If you are the author or publisher of an output and you would like it removed from the repository, please [contact us](#) and we will investigate on a case-by-case basis.

Each thesis in the repository has been cleared where necessary by the author for third party copyright. If you would like a thesis to be removed from the repository or believe there is an issue with copyright, please contact us on openaccess@leedsbeckett.ac.uk and we will investigate on a case-by-case basis.

Colour prediction for sustainable fibre blending

Caroline Suzanne Hemingray

Submitted in accordance with the requirements for the degree of Doctor of Philosophy

The University of Leeds

School of Design

September 2014

The candidate confirms that the work submitted is her own and that appropriate credit has been given where reference has been made to the work of others.

This copy has been supplied on the understanding that it is copyright material and that no quotation from the thesis may be published without proper acknowledgement.

© 2014 The University of Leeds and Caroline Suzanne Hemingray

The right of Caroline Suzanne Hemingray to be identified as Author of this work has been asserted by her in accordance with the Copyright, Designs and Patents Act 1988.

Acknowledgements

I would like to thank my supervisor Professor Stephen Westland for all of his encouragement, support and guidance throughout my PhD. Steve you have been a true mentor to me. You have been a constant source of inspiration and knowledge and have given me the confidence to challenge myself both academically and personally. I would also like to thank my second supervisor Dr. Richard Blackburn for all his knowledge and help in the areas of fibres and dyeing.

I feel very fortunate and grateful to have been sponsored by both the Clothworkers' Foundation and Lenzing AG, both of whom have given me not only financial support to do my PhD but also rich experiences and unique opportunities. In particular I would like to thank Andrew Blessley of The Clothworkers' Company and Jim Taylor and Marina Crnoja from Lenzing AG. Thank you also to Lenzing AG for the supplies of fibre that have been made available to me for my experimental work. I would also like to thank NIRI for the use of the carding machine and Richard Noyes and Progressive Threads for their dyeing expertise.

I am privileged to have studied and worked within the School of Design. Thank you to all the members of staff who have helped and supported me since I first came to Leeds to study BA Textile Design. In particular I would like to thank Chris Harris, Jean Mitchell and Azim Abadi.

My deepest thanks go to my parents and to my siblings who have supported and encouraged me throughout my personal and academic life. Without your love and support I would not be where I am today, thank you. I would also like to thank my god-parents and all my wonderful friends who have also encouraged me along my way and who I am truly blessed to have in my life. Finally, I would like to thank my two PhD 'partners in crime', Sophie and Nick; you two have made me laugh, smile and believe in myself when I have needed it the most, thank you.

Abstract

The blending of coloured fibre is explored as a sustainable method of colouration when coupled with sustainable fibre and dyeing choices such as spun-dyed Lenzing Viscose Austria. It was found that a selection of spun-dyed colours (primaries) can be used to create homogenous 4-colour blends when mixed in specific groups. The use of 4-colour blends ensures that the optimal amount of colours within a gamut are produced with the lowest possible number of primaries depending on the acceptable mean colour difference of the 4-colour blends. The acceptable mean colour difference of a blend (measured by averaging each pair of colour differences between the primaries in a blend) can be derived using example 4-colour blends and participant observations at a set viewing distance.

Using MATLAB, a method of estimating the number of primaries required to fill a given gamut in CIELAB colour space was developed. Primaries can be distributed across CIELAB colour space and grouped into tetrahedral groups of four for blending. The mean colour difference of the tetrahedral 4-colour blends can be increased or decreased by varying the number of primaries within a gamut. It was also found that the maximum mean colour difference of blends in order for them to appear solid (when viewed at a specific viewing distance) was transferable to blends in knit form.

Comparisons of existing blend prediction models with the prediction possibilities of a standard neural network and novel neural network were undertaken using data gathered from 333 blended samples. The results showed that neural networks outperformed the existing prediction models and can be successfully used to predict the colour of blends to an industry standard.

The investigations of this thesis have shown that a sustainable colouration system using spun-dyed viscose blends is possible and that accurate colour predictions of these blends can be made.

Table of contents

Acknowledgements.....	ii
Abstract.....	iii
Table of contents	iv
Table of figures.....	viii
List of tables	xii
Abbreviations and symbols	xv
Chapter 1 Introduction and literature review	1
1.1 Introduction.....	1
1.1.1 Aims and objectives	2
1.2 Textiles for fashion: the demand	3
1.2.1 Textile fibres.....	5
1.2.2 Natural and synthetic fibres.....	8
1.3 Colouration of fibres for fashion and textiles	18
1.3.1 Environmental impact of dyeing textiles	19
1.3.2 Spun-dyed fibres	20
1.3.3 Blending coloured fibre to produce colours	22
1.4 Colour: what is it?.....	23
1.4.1 Colour vision.....	24
1.4.2 Light sources	26
1.4.3 Light and objects	28
1.4.4 Organising colour	32
1.5 Models for predicting the colour of blended fibre	39
1.5.1 Kubelka-Munk equation.....	40
1.5.2 Stearns-Noechel equation	41

1.5.3	Friele equation	43
1.6	Artificial neural networks	46
1.6.1	What are neural networks?	46
1.6.2	Neural networks and colour prediction	49
1.6.3	Standard neural network for predicting fibre blends	51
1.6.4	Novel neural network for predicting fibre blends	52
1.7	Primaries within blended samples	52
Chapter 2	Materials and methods	56
2.1	Materials.....	56
2.1.1	Lenzing viscose	56
2.1.2	Lenzing spun-dyed viscose	56
2.1.3	Lenzing viscose pack dyed.....	56
2.2	Fibre blending.....	57
2.2.1	Preparation of samples	57
2.2.2	Carding machine	58
2.3	Colour measurement.....	59
2.3.1	Spectrophotometer.....	60
2.3.2	Reflectance data in MATLAB.....	61
2.4	Preparing knitted samples.....	62
2.5	Visual assessment of carded samples	62
2.5.1	Participant selection	63
2.5.2	Experiment environment	64
2.5.3	Experiment procedure	64
Chapter 3	Colour difference and sample appearance.....	67
3.1	Introduction.....	67

3.2	Experiment 1: Creating fibre blends with mean colour differences of between 11 and 119 CIELAB ΔE	68
3.2.1	The primaries	69
3.2.2	Preparing the blended samples	71
3.2.3	Visual assessment of blended samples.....	74
3.2.4	Conclusions	84
3.3	Experiment 2: Creating fibre blends with mean colour differences of between 15 and 25 CIELAB ΔE	85
3.3.1	The primaries	86
3.3.2	Preparing the blended samples	92
3.3.3	Visual assessment of blended samples.....	95
3.3.4	Discussion of results.....	98
3.3.5	Conclusions	99
3.4	Summary.....	100
Chapter 4	Developing a relevant colouration system for industry	102
4.1	Introduction.....	102
4.2	Colour space and the distribution of primaries within a large gamut	103
4.2.1	Producing a large gamut	106
4.2.2	Filling the large gamut with primaries	108
4.2.3	Creating 4-primary tetrahedra using maxminc and Delaunay triangulation	110
4.2.4	Results	114
4.3	Colour space and the distribution of primaries within a small gamut.....	116
4.3.1	Producing a small gamut.....	117
4.3.2	Results	118
4.4	Applying fibre blending in a fashion context.....	121

4.4.1	The primaries	122
4.4.2	Preparing blended samples.....	123
4.4.3	Producing knitted samples.....	125
4.4.4	Conclusions	127
Chapter 5	Colour prediction of fibre blends	129
5.1	Standard prediction models	129
5.1.1	Stearns-Noechel equation	130
5.1.2	Friele's equation.....	131
5.2	Standard neural network model	132
5.2.1	Standard network results.....	135
5.3	Novel neural network model.....	144
5.3.1	Novel network results	146
5.4	Comparison and conclusions of all models using the test set	155
Chapter 6	Conclusions and future work	159
6.1	Conclusions.....	159
6.2	Further work.....	164
	References.....	166
	Appendices.....	183

Table of figures

Figure 1.1 Examples of natural and man-made textile fibres.....	9
Figure 1.2 Process of photosynthesis	13
Figure 1.3 Structure of cellobiose	14
Figure 1.4 Cross-section diagram of the structure of the eye	26
Figure 1.5 Illustration of transmission, reflection, scattering and absorption characteristics of light with materials.....	29
Figure 1.6 Diagram of the Spectraflash® 600 spectrophotometer.....	31
Figure 1.7 Example of a single-layer perceptron neural network	47
Figure 1.8 Example of a fully connected multi-layer perceptron network (MLP)	48
Figure 1.9 Two primaries produce blending along a line within CIELAB colour space (one-dimension).....	53
Figure 1.10 Three primaries create a plane within CIELAB colour space (two- dimensional).....	53
Figure 1.11 Four primaries create a three-dimensional tetrahedron within CIELAB colour space (three-dimensional blending)	54
Figure 2.1 Layout of small sample Tathams carding machine.....	58
Figure 2.2 Blended sample number 2.23 with a mean colour difference of 15 CIELAB ΔE (1:1 scale)	59
Figure 2.3 Datacolor 600™ Spectrophotometer	60
Figure 2.4 Knitted sample number 2.23 with a mean colour difference of 15 CIELAB ΔE (1:1 scale)	62
Figure 2.5 Pie chart showing the proportion of female to male participants in the visual assessments	63
Figure 2.6 Pie chart showing the country of origin of the participants used in the visual assessments	64

Figure 2.7 Participant viewing carded sample	65
Figure 3.1 Position of primaries in CIELAB colour space.....	69
Figure 3.2 CIELAB colour space with the positions of the 325 blends and 8 primaries .	73
Figure 3.3 Position of the blended samples in CIELAB colour space from directly above the L* axis, looking down on to the a* and b* axes	74
Figure 3.4 Comparison of the mean, max and median values of the colour differences within 2-colour blends, both with (left-hand graphs) and without (right-hand graphs) the white and black primaries included.....	76
Figure 3.5 Comparison of the mean, max and median values of the colour differences for 3-colour blends, both with (left-hand graphs) and without (right-hand graphs) the white and black primaries included	77
Figure 3.6 Comparison of the mean, max and median values of the colour differences for 4-colour blends, both with (left-hand graphs) and without (right-hand graphs) the white and black primaries included	78
Figure 3.7 Experiment 2 primaries in CIELAB colour space	86
Figure 3.8 Group 1: blended samples in CIELAB colour space.....	93
Figure 3.9 Group 2: blended samples in CIELAB colour space.....	93
Figure 3.10 Group 3: blended samples in CIELAB colour space.....	94
Figure 3.11 Group 4: blended samples in CIELAB colour space.....	94
Figure 3.12 Group 5: blended samples in CIELAB colour space.....	95
Figure 3.13 Mean colour difference (CIELAB ΔE) of blends and % of participants who perceived the blends as a solid colour	99
Figure 4.1 Flow chart showing the process of defining n number of primaries within a gamut	105
Figure 4.2 The 12 CIELAB colours to define the size of experimental gamut	107
Figure 4.3 The CIELAB colours seen from directly above the L* axis	107
Figure 4.4 The 10,012 colours plotted in CIELAB colour space.....	109

Figure 4.5 The 10,012 colours in CIELAB colour space, looking directly down the L^* axis onto the a^* and b^* axes.....	109
Figure 4.6 Example of a two-dimensional Delaunay triangle	110
Figure 4.7 Example of a two-dimensional Delaunay triangle	111
Figure 4.8 Example of an incorrect Delaunay triangle	111
Figure 4.9 Three-dimensional Delaunay tetrahedron	112
Figure 4.10 Example of 50 primaries connected using Delaunay triangulation in CIELAB colour space	113
Figure 4.11 Number of primaries versus mean colour difference of blends.....	115
Figure 4.12 Small gamut of dark colours plotted within CIELAB colour space	117
Figure 4.13 Number of primaries versus mean colour difference (CIELAB ΔE) of blends	119
Figure 4.14 The 15 primaries used to produce 22 blended samples, plotted in CIELAB colour space	124
Figure 4.15 Position of the blends in CIELAB colour space	125
Figure 5.1 Variation of mean CIELAB ΔE (for the training data) with b varied for the Stearns-Noechel model.....	131
Figure 5.2 Variation of average colour difference (training data) with s for the Friele model	132
Figure 5.3 Illustration of the standard neural network using 8 input vectors, 35 output vectors and two hidden units (note that each hidden and output unit also receives weighted input from a bias unit, but this is not illustrated)	133
Figure 5.4 The mean training and test errors of Standard Network 1 using CIELAB ΔE (varying the number of hidden units from 1 to 60)	137
Figure 5.5 Mean training errors of Standard Network 1 using CIELAB ΔE with the standard errors shown.....	139

Figure 5.6 Mean testing errors of Standard Network 1 using CIELAB ΔE with the standard errors shown	139
Figure 5.7 The mean training and testing errors of Standard Network 2 using CIELAB ΔE (varying the number of hidden units from 1 to 40)	141
Figure 5.8 Mean training errors of Standard Network 2 using CIELAB ΔE with the standard errors shown	143
Figure 5.9 Mean testing errors of Standard Network 2 using CIELAB ΔE with the standard errors shown	143
Figure 5.10 Diagram showing a small neural network used to predict the reflectance of a sample at 360 nm	145
Figure 5.11 The mean training and test errors of Novel Network 1 using CIELAB ΔE (varying the number of hidden units from 1 to 20)	147
Figure 5.12 Mean training errors of Novel Network 1 using CIELAB ΔE with the standard errors shown	149
Figure 5.13 Mean testing errors of Novel Network 1 using CIELAB ΔE with the standard errors shown	149
Figure 5.14 The mean training and testing errors of Novel Network 2 using CIELAB ΔE (varying the number of hidden units from 1 to 20)	152
Figure 5.15 Mean training errors of Novel Network 2 using CIELAB ΔE with the standard errors shown	154
Figure 5.16 Mean testing errors of Novel Network 2 using CIELAB ΔE with the standard errors shown	154

List of tables

Table 1.1 Variations of b for different fibre types as derived by different studies within literature	42
Table 1.2 Variations of s for different fibre types as derived by different studies within literature	44
Table 3.1 $L^*a^*b^*$ and sRGB values and appearance of first experiment primaries	70
Table 3.2 The Euclidean CIELAB colour difference (ΔE) between each pair of primaries	71
Table 3.3 Generic blend recipes	71
Table 3.4 Comparison of mean, max and median values for the blended samples	79
Table 3.5 Blends that were judged as a solid colour by 100 % of observers	80
Table 3.6 Comparison of blends scored as a solid colour by 100 % of participants	81
Table 3.7 Blends that were evaluated as not a solid colour by all observers	83
Table 3.8 $L^*a^*b^*$ and sRGB values and appearance of second experiment primaries ..	87
Table 3.9 Primaries within group 1 with a mean colour difference of 25 CIELAB ΔE	88
Table 3.10 Primaries within group 2 with a mean colour difference of 22 CIELAB ΔE ...	88
Table 3.11 Primaries within group 3 with a mean colour difference of 19 CIELAB ΔE ...	88
Table 3.12 Primaries within group 4 with a mean colour difference of 18 CIELAB ΔE ...	89
Table 3.13 Primaries within group 5 with a mean colour difference of 15 CIELAB ΔE ...	89
Table 3.14 Group 1 colour differences (CIELAB ΔE)	89
Table 3.15 Group 2 colour differences (CIELAB ΔE)	90
Table 3.16 Group 3 colour differences (CIELAB ΔE)	90
Table 3.17 Group 4 colour differences (CIELAB ΔE)	91
Table 3.18 Group 5 colour differences (CIELAB ΔE)	91
Table 3.19 Generic blend recipes for groups 1 to 5	92

Table 3.20 Group 1 visual assessment results showing the percentage of participants who believed that a sample speared as a solid colour	96
Table 3.21 Group 2 visual assessment results showing the percentage of participants who believed that a sample speared as a solid colour	96
Table 3.22 Group 3 visual assessment results showing the percentage of participants who believed that a sample speared as a solid colour	96
Table 3.23 Group 4 visual assessment results showing the percentage of participants who believed that a sample speared as a solid colour	97
Table 3.24 Group 5 visual assessment results showing the percentage of participants who believed that a sample speared as a solid colour	97
Table 3.25 Visual assessment results of the primaries showing the percentage of participants who believed that a sample speared as a solid colour	98
Table 4.1 MATLAB results showing the number of primaries within the gamut versus the number and mean colour difference of tetrahedral blends	114
Table 4.2 MATLAB results showing the number of primaries within the gamut against the mean colour difference of the tetrahedral blends	118
Table 4.3 $L^*a^*b^*$ and sRGB values for the primaries used in experiment 3	123
Table 4.4 Experiment 3 generic blend recipes	124
Table 4.5 Visual assessment results of knitted fabrics composed of one or more primaries	126
Table 5.1 The progress parameters for the standard neural network using the built- in MATLAB toolbox settings	134
Table 5.2 Number of hidden units versus mean training and testing errors for Standard Network 1 using CIELAB ΔE	136
Table 5.3 The standard error of the mean training and testing errors of Standard Network 1 using CIELAB ΔE (varying the number of hidden units from 1 to 60)	138
Table 5.4 Number of hidden units versus mean training and testing errors for Standard Network 2 using CIELAB ΔE	140

Table 5.5 The standard error of the mean training and testing errors of Standard Network 2 using CIELAB ΔE (varying the number of hidden units from 1 to 40)	142
Table 5.6 Number of hidden units versus mean training and testing errors for Novel Network 1 using CIELAB ΔE	146
Table 5.7 The standard errors of the mean training and testing errors for Novel Network 1 using CIELAB ΔE (varying the number of hidden units from 1 to 20)	148
Table 5.8 Number of hidden units versus mean training and testing errors for Novel Network 2 using CIELAB ΔE	151
Table 5.9 The standard errors of the mean training and testing errors for Novel Network 2 using CIELAB ΔE (varying the number of hidden units from 1 to 12)	153
Table 5.10 Comparison of results of blend prediction methods using CIELAB ΔE	156
Table 5.11 Comparison of results of blend prediction methods using CIEDE2000	156

Abbreviations and symbols

ANN	artificial neural network
b	empirically derived constant for Stearns-Noechel formula
cd/m^2	candela per square meter
CIELAB colour space	CIE 1976 $L^*a^*b^*$ colour space
CIELAB ΔE	CIE 1976 colour difference formula ΔE_{ab}^*
CIEDE2000	CIE 2000 colour difference formula ΔE_{00}^*
EPI	ends per inch
f_{SN}	Stearns-Noechel function
f_F	Friele function
g	gram
K	Kelvin
kg	kilogram
$L^*a^*b^*$ values	CIE 1976 $L^*a^*b^*$ values
m	metre
MJ	megajoules
MLP	multi-layer perceptron neural network
n	number of primaries
nm	nanometre
PPI	picks per inch
R	reflectance
r	number of primaries in a recipe
R^2	coefficient of determination
R_∞	reflectance of an infinitely thick sample
R_M	reflectance of a blend
s	scattering coefficient for Friele's formula
%	percent

Chapter 1 Introduction and literature review

1.1 Introduction

Fibre blending is the method of blending a limited number of pre-dyed coloured fibres together, in specific proportions, to create new colours. Coloured fibre blending has been suggested as an alternative, more environmentally sustainable, method of textile colouration (Philips-Invernizzi *et al.*, 2000).

Fibre blending is thought of as a sustainable method of colouring textiles as it limits the amount of secondary dyeing processes that are normally involved in textile colouration; instead of altering a dye recipe, the recipe of the blended fibres is altered. To truly promote the use of fibre blending as a means of sustainable colouration for textiles and fashion, spun-dyed viscose fibres (from Lenzing Austria) are used in the experimental work within this thesis due to their environmental merit. Benefits of blending spun-dyed fibre include limiting the amount of fibre wasted as a result of unmatched colouration and limiting the amount of dye, water and chemicals used to colour textile fibres due to the spun-dyeing process. The blending of coloured fibre could be extended to recycled fibre. Fibre blending of coloured fibres from recycled materials already exists as a method of re-engineering second-hand textiles. Textiles are deconstructed through cutting, shredding and carding to produce fibres for blending, spinning and knitting, giving the textile fibre new value (Hawley, 2006).

For coloured fibre blending to become a viable competitor to conventional dyeing practices, a method of accurately predicting the colour of blends from a set of coloured fibres (or primaries) must be established. A primary can be defined as a colour from which all other colours can be created by combining the primary colours in different proportions (OED, 2014). In fibre blending, primaries are coloured fibre which are blended together to create multiple new colours. Whilst there are some existing methods of coloured blend prediction, their success has been limited due to the complex relationship between incident light and the surface characteristics of fibre blends (Burlone, 1983).

1.1.1 Aims and objectives

The aim of this research was to investigate a sustainable method of colouring textiles for fashion and textiles which is flexible, accurate and environmentally sustainable. The application of this research within the fashion industry was of particular interest due to the speed at which fashion trends and seasons are changing. It was anticipated that a system of colouration can be developed which allows small amounts of coloured textiles to be produced with accuracy. To do this, it is proposed that instead of dyeing fibre, yarns and fabrics to a specific colour for a particular design, that coloured fibre is instead blended together in various proportions to achieve homogenous, solid appearing colours. By doing this, only a selected number of dyed colours (primaries) would be required.

In order for coloured fibre blending to become a commercially viable form of textile colouration, investigations were made into the processes involved. This broadly included three areas; firstly, the process of choosing which fibres to blend together so that solid colour effects are produced, secondly, the estimated number of primaries a colouration system would need, and finally, the development of an accurate system for the colour prediction of the fibre blends.

The research objectives to achieve this model were therefore:

1. To identify the maximum colour-difference tolerance between a pair or group of primaries so that once blended they produce solid colour effects;
2. To define the number of primaries that a fibre blending colouration system requires so that almost any colour could be produced as a blend from a set of primaries;
3. To test existing methods of blend prediction and compare these to prediction models using neural networks.

This thesis approaches these different objectives over the course of five chapters. This first chapter includes the literature review which outlines the current fibre, fashion and textiles industry. In particular, the environmental impact of different fibre types,

and the way in which they are consumed within the fast-fashion and textiles industry, is considered. The benefits of spun-dyeing, rather than conventional dyeing, is discussed as well as the benefits of blending spun-dyed fibre to produce new colours. Existing blend prediction models are identified before the possibility of using neural networks is proposed. Chapter 2 outlines the materials and methods used within this thesis. This includes the materials and methods used to produce blended samples, colour measurement and the methods used to assess blended samples using observers. Chapter 3 is composed of two experiments in which blended samples were prepared using a variety of primaries. The blended samples were assessed by observers with normal colour vision in order to understand when different primaries appear as one colour when blended. This allowed calculations to be made as to the threshold of colour difference (in CIELAB ΔE) between individual primaries within a blend so that once blended they appear as a solid colour. Chapter 4 builds upon the work in chapter 3, investigating the number of primaries a fibre blending colouration system may require to create a large (or specific) range of solid fibre blends. Finally, chapter 5 tests existing and novel blend prediction models for the application of accurate fibre blending within industry.

1.2 Textiles for fashion: the demand

Each year the global population continues to increase. The current estimate for global population is over 7 billion people and this is projected to rise to over 8 billion people by 2025 (United Nations, 2013). With this continued rise in population comes an unavoidable increase in global demand for the world's limited resources, textiles being one of them. In 2012, over 85.9 million tonnes of fibre was produced globally; of this, 68 % (58.6 million tonnes) of the production was composed of man-made fibres. Within Europe, 4.6 million tonnes of man-made fibre was manufactured, including over 1 million tonnes of polyester and 562,000 tonnes of cellulosic fibres (CIRFS, 2014). The environmental and social impact and sustainability of producing these vast amounts of different fibres (and consequently fashion and textiles) is wide ranging and diverse as different fibres require different inputs and processing techniques. Within textiles for fashion, both natural and man-made fibres are used to sustain global clothing demand, an area which has seen rapid changes in recent years.

The fashion industry has traditionally promoted new trends for consumers across the course of two main fashion seasons; spring/summer and autumn/winter. Fashion trends and garment collections are often predicted and planned months or years in advance. More recently, however, there has been a shift by retailers to move towards a fast-fashion formula. Anson (2010) identifies that some markets are producing fashion garments in cycles of up to 12 seasons per year. Fast-fashion is profit-led with short lead times and a high turnover of garments. These garments are often of poor quality, as there is an increasing presumption that they may only be worn a few times before being discarded, garment price therefore being of upmost importance (Tham, 2013). The economic push to produce cheap and readily available garments has compromised the quality and durability of the garments being produced (Fletcher, 2015). Fast-fashion is popular for retailers as it allows them to give multiple short seasons of trends which react directly to consumer demand. Zara is an example of a retailer that has implemented this method of supply and demand very successfully, producing huge ranges of garments compared to their competition (The Economist, 2005). A whole collection of garments, from design concept to completed manufacture, can be ready for sale in Zara stores within three to four weeks (Chu, 2014). With over 450 million garments distributed in over 1,700 stores across the globe, Zara only decides up to 50 % of its collections before the start of a season, the rest is introduced depending on sales figures and changing trends (Berfield & Baigorri, 2013; Ferdows *et al.*, 2005). One benefit of producing clothes in this fast and tightly controlled supply and demand method, is that Zara only produce more of the garments which are selling well, limiting their end of season surplus and therefore waste. Zara's high turnover, fast-fashion formula is a particularly extreme example of fast-fashion; however it highlights the changing shape of the fashion industry where the successful sale and demand of small runs of clothing leads to a quick turnover of successful products and trends. Consumers want more clothes and more variety and the industry is responding quickly.

The fashion retail industry is big business within the UK with £38.4 billion spent on clothing in 2005. The average amount spent in the UK on clothes per person was estimated to be £625 in 2004 (Allwood *et al.*, 2006). Fletcher (2008) describes the

consumer's desire for new clothes as a means of re-formulating ones identity in response to changing fashion trends. Campbell (2006) views the consumption of goods as a means of satisfying the consumer's desire for new and novel pleasurable experiences. Michael Flanagan, chief executive of Clothescource, highlights that the majority (86 %) of the world's spending on fashion originates from only 15 % of the planet's population. Flanagan argues that the consumption of fashion garments is not solely motivated by a need to follow fashion trends but a desire by the wealthy for real or perceived comfort or performance benefits (Flanagan, 2013). Fashion consumption in the UK has shown significant growth in recent years, with the amount of clothes purchased per capita increasing rapidly. For example, between 2001 and 2005 the UK saw a 37 % increase in the amount of clothes purchased per capita. Concurrently, almost 40 kg of clothing and textile waste per person was disposed of within each of those years (Allwood *et al.*, 2006). Currently, Europeans consume 90 m² of clothing per year; this is in stark contrast to an average Bangladeshi who consumes less than 1 m² per year (Flanagan, 2013). Flanagan (2013) calculates that when the world's twenty poorest and most populous countries consume as many clothes as are consumed in Europe and America, then the world will need to produce three times more fabric and energy than it is currently producing. Whilst the motivations behind the consumption of fashion textiles are complex, the reality of the industry is clear; that the global demand and consumption of textiles is increasing alongside a growing global population. Sustainable methods of textile manufacture and colouration must therefore be considered if the rate of textile consumption is to be fulfilled responsibly.

1.2.1 Textile fibres

A variety of fibres, both natural and man-made, are being used within fashion and textiles. The selection of fibre type, method of manufacture and method of colouration of textiles for fashion all depend on a variety of design decisions including the garment end use, the season in which the garment is to be sold, the cost of manufacture, the market level at which the garments will be sold and availability of the fibres or textiles. Ultimately, however, the choice of fibre is often based on the cost and speed of production, rather than the environmental impact of the fibre (Sherburne, 2009).

Fletcher and Grose (2012) highlight various important impacts that the creation of a garment has on ecological and social systems. These include the inputs of producing a fibre or garment (how much water, energy and/or chemicals have been used); the waste outputs produced in the manufacturing process (waste water, chemicals, airborne emissions); the use stage (how is the garment washed); the end-of-life disposal (is the fibre or garment biodegradable or is it destined for landfill?); the social impact of workers producing the fibres (working conditions and pay); and finally the impact of fibre production on local communities (including health and natural resources) (Fletcher & Grose, 2012). These complex issues all have a role in the environmental, social and economic sustainability of fashion. One way of quantifying the sustainability of a product is through life cycle assessments.

Life cycle assessments (LCAs) of products, such as fashion garments, have become a commonly used and trusted method of assessing the environmental, social and economic impact that the life of a product has, from raw material (cradle), to end of life disposal (grave) (Lee, 2013a). The International Organisation for Standardisation (ISO) has produced two ISO standards; ISO 14040 (2006a) and ISO 14044 (2006b) which provide guidelines for companies and organisations to produce reliable LCAs of products and services. LCAs can highlight particular negative processes or materials within the life cycle of a product. Companies and organisations can use this information to change or improve a product's environmental performance (Lewis & Gertsakis, 2001).

Lee (2013b) identifies five life cycle stages to consider when looking at the impact of a product from cradle to grave:

- 1) Raw materials stage: the natural resources and processes used to produce the raw materials;
- 2) Manufacturing stage: the processes and activities used to produce a product from manufacturing entrance to exit gate;
- 3) Distribution stage: the processes or activities involved between manufacturer's exit gate and sale of product;
- 4) Use stage: how long a product will last and how much use and energy will be consumed within the product's lifetime;
- 5) End of life stage: the recycling, reuse and disposal (including incineration or landfill) of a product.

From an environmental point of view, Lewis *et al.* (2001) identify the design stage of a product, specifically where the materials for a product are selected, as being the key point at which the life cycle impact of a product is decided. If a product is designed with consideration as to the amount of waste, raw materials, energy and water consumption that will be used, then those properties are known and can be altered to influence (and potentially improve) the life cycle of a product (Lewis *et al.*, 2001). Sherburne (2009) argues that for textiles, the highest impacts on the LCA of textile fibres (excluding the social impacts) include the over use of water in production processes (which can have associated effects such as de-oxygenation and salinisation of water supplies), the over use of chemicals including pesticides and chemicals used in production, exploitation of non-renewable materials and energy sources, waste and transportation. Other environmental impacts specific to textiles include de-oxygenation of water supplies, loss of biodiversity and loss of soil fertility (Sherburne, 2009).

The dyeing stage of textiles is also an area of high environmental impact, with large amounts of additional water and chemicals used. It is estimated that 378 billion litres of water a year are used by the textile industry (Clay, 2004). The use stage of garment

has also been shown to have a deceptively large impact on the LCA of a fibre. In 1993, Franklin Associates produced a report on the LCA of a polyester blouse. The report illustrated that the majority of energy use (82 %), majority of carbon dioxide emission (83 %) and large percentage of solid waste (66 %) of the LCA of the blouse occurred through washing and drying (Franklin Associates, 1993). Whilst this study is now perhaps relatively outdated as consumer purchasing and use of fashion garments has evolved (for example, washing machines have become more energy efficient and the frequency at which we wear garments (particularly trend fashion pieces) is reducing) the study does highlight the complexity of LCA of fashion garments (ENDS Report, 2007; Fletcher & Tham, 2004; Gibson, 2013).

1.2.2 Natural and synthetic fibres

Depending on the fibre type, the LCA of a textile garment can vary. Textile fibres can be broadly divided into natural and man-made fibres. Natural fibres are those made from vegetable fibres such as cotton, animal protein fibres such as wool and mineral fibres such as asbestos.

Figure 1.1 shows some commonly used natural and man-made fibres within fashion and textiles industry.

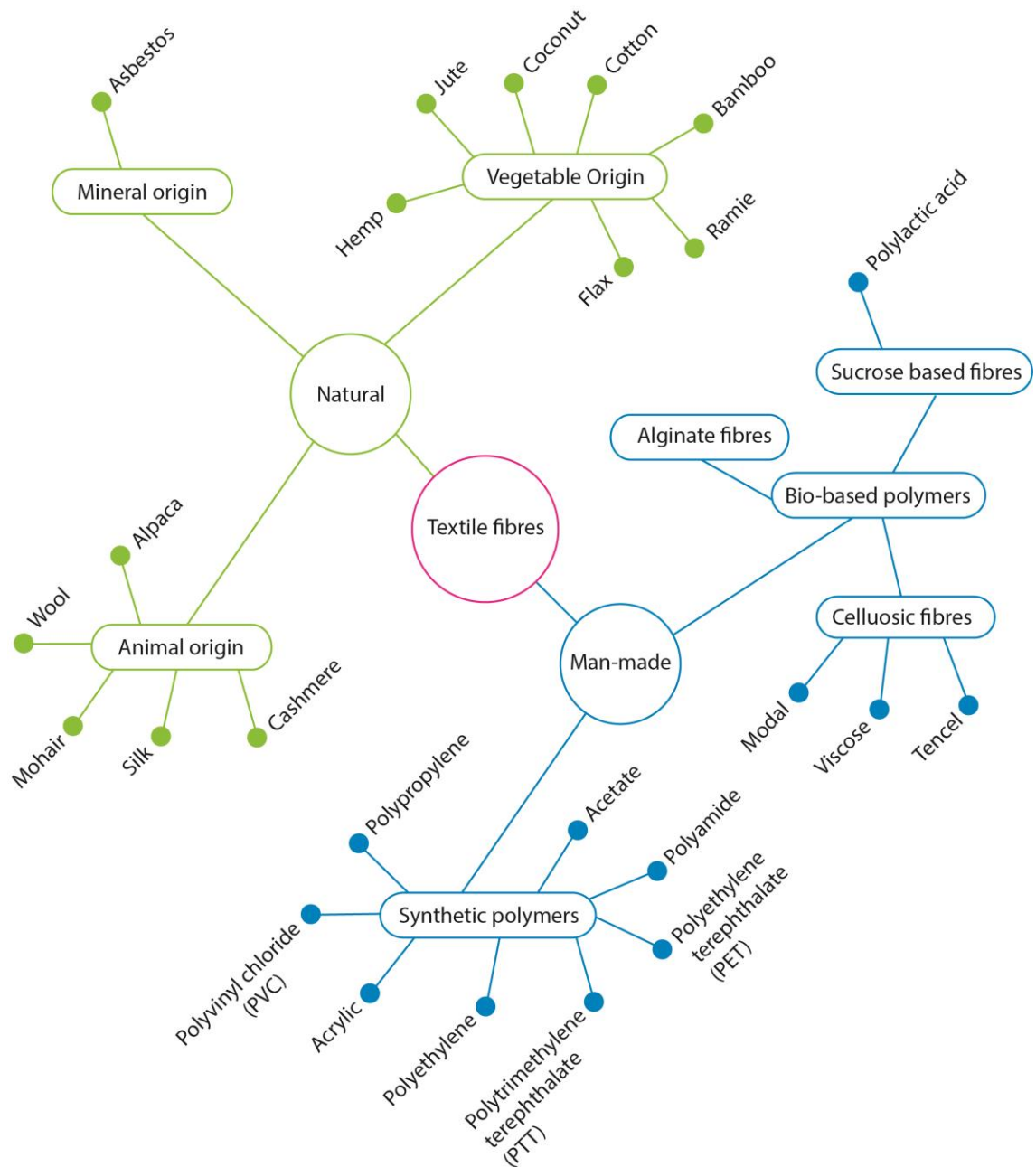


Figure 1.1 Examples of natural and man-made textile fibres

The separation within man-made fibres of those fibres made from synthetic polymers and those fibres made using natural (or bio-based) polymers can also be seen in Figure 1.1. Synthetic polymer-based fibres are those manufactured from polymers which have been synthesised from chemical elements or compounds, whereas natural-based polymer fibres (often called regenerated fibres) are made from naturally occurring fibre-forming polymers (Denton & Daniels, 2002; McIntyre, 2005). Synthetic polymers are manufactured using petrochemicals and minerals and these create fibres including polyurethane and polyester (Fletcher & Grose, 2012). One group of synthetic bio-based fibres are produced using regenerated cellulose polymers (extracted from natural fibres such as beech wood and bamboo) to create fibres including viscose and lyocell.

Natural fibres, and synthetic fibres which have been produced from bio-polymers, are fundamentally biodegradable. In contrast, synthetic polymer-based fibres can take hundreds of years to decompose in landfill (Black, 2011). Biodegradability is an important consideration when assessing the LCA of fibres and textiles (Ciechanska & Nousiainen, 2005). The renewability of natural and synthetic fibres is also different. Fibres are said to be renewable if they can be cultivated over months or years and, crucially, be replenished without detriment to the rate of their harvest (Fletcher & Grose, 2012). Examples of renewable fibres include natural fibres such as cotton and bamboo, and regenerated cellulose fibres such as viscose and lyocell. Non-renewable fibres are manufactured using materials (such as oil or minerals) which take hundreds of thousands or even millions of years to replenish. Non-renewable fibres include polyester and nylon (Fletcher & Grose, 2012). With limited access and supplies of non-renewable source materials such as crude oil, renewable fibres are a much more reliable and sustainable source for long term textile production.

The renewability and biodegradability of natural fibres contributes to the common perception that natural fibres must always be more environmentally friendly compared to man-made fibres. However, the whole life cycle of a fibre from raw material to eventual disposal must be considered. Whilst natural fibres are sustainable in the fact that they are renewable, the farming and processing of natural fibres such

as cotton and wool are often highly intensive with un-sustainable environmental consequences (Lewis *et al.*, 2001). The following sub-sections discuss some of the global environmental and social impacts that the production of popular fibres, including cotton, wool, polyester and viscose, have within the fashion and textile industry.

1.2.2.1 Cotton

Cotton is the most highly produced natural fibre within the textile industry. In 2012, 24.68 million tonnes of raw cotton fibre was consumed globally (Fibre Organon, 2013). Approximately three quarters of the global supply of cotton is produced in the developing world and 45 % of this cotton is consumed in Europe and America (Black, 2011). Cotton uses high levels of water in both the irrigation and processing stages. Over 50 % of the world's cotton is irrigated in dry countries such as Egypt and Uzbekistan where water is scarce (Soth, 1999). Depending on the environment in which it is grown, it is estimated that it can take between 7,000 and 29,000 litres of water to grow 1 kg of cotton (WWF, 2003). One study estimated that it can take over 2,700 litres of water to produce one cotton t-shirt (EJF, 2014). In a 2006 study into the life cycle of a plain, dyed cotton t-shirt, it was estimated that a total of 109 megajoules (MJ) of energy was consumed across the product's life span; 24 MJ was consumed in the production of the t-shirt and 65 MJ consumed in the use stage, showing that washing, drying and ironing can also have a significant impact of the LCA of a garment (Allwood *et al.*, 2006).

Added to the water and energy demands of both the production and use stages of cotton garments, there is also the chemical use in the growing of cotton crops. Many cotton crops are treated with fertilisers, pesticides and herbicides which can leech into the surrounding water and soil (Wakelyn & Chaudhry, 2007). The high demand for water and use of harmful chemicals to support cotton growth can have hugely detrimental effects on regions and countries. In Uzbekistan, poor irrigation practices and water contamination have resulted in the Aral Sea basin being dramatically reduced to 10 % of its original size (Hecht, 2014). The dry desert basin has left the local

population exposed to agricultural chemicals and contaminated drinking water (Grose, 2009; EJF & Pesticide Action Network UK, 2007).

1.2.2.2 Wool

Wool is the fibrous protein hairs from the fleece of sheep. The term wool is also often used to include other sources of animal hair such as cashmere or alpaca within the textile industry (Black, 2011). The global demand for wool is much smaller than cotton, with only 1.08 million tonnes, as opposed to 23.46 million tonnes of cotton, consumed globally in 2012 (Fiber Economics Bureau, 2013). However the amount of wool consumed in Western Europe in 2012 (352.7 million lb) was not far from the amount of cotton that was also consumed (396.8 million lb) (Fiber Economics Bureau, 2013). The cleaning of wool in order for it to be suitable for fashion and textiles is fairly intensive. The fleece of a sheep is sheared off in one piece at which point it can weigh approximately 3.6 kg, this raw weight is reduced however after cleaning and scouring (Black, 2011). Approximately two thirds of the weight of raw wool is dirt, grease, dried sweat and skin flakes (Lewis *et al.*, 2001). To clean the wool of these impurities, large amounts of water, detergent, chemicals and scouring are required. This in turn produces large amounts of harmful effluent (Lewis *et al.*, 2001; Russell, 2009). Conversely, some of the natural grease in wool is a useful by-product of the cleaning process and is made into lanolin for use in soap and cosmetics (Black, 2011).

1.2.2.3 Polyester

Synthetic man-made fibres made from petrochemicals have dominated the textile industry in recent years. In 2012, polyester fibres, most commonly in the form of poly(ethylene terephthalate) (PET) fibres, contributed to 88 % (43.3 million tonnes) of the total synthetic polymer fibres produced globally (Fiber Economics Bureau, 2013). Polyester fibres are appealing within the fashion and textile industry as they are durable, lightweight, easy to dye and inexpensive to produce (East, 2005).

The main chemicals used in the manufacture of PET are terephthalic acid (TA) and ethylene glycol (EG) (East, 2005). After polymerisation, the liquid polymer is extruded into strands of fibre where it is solidified and either cut to a required length or made

into a continuous filament yarn (East, 2005). It is argued that the highest impact stage in the life cycle of polyester for fashion and textiles is the environmental and social cost of oil exploration and oil extraction (Fletcher, 2008). The production of polyester uses much less water than cotton; however, the energy consumed during polyester production is fairly high, at 109 megajoules (MJ) per kilogram of polyester. Of this, 46 MJ is consumed at the raw material stage and 63 MJ consumed in the processing of the raw material into fibre (Fletcher, 2008; Laursen & Hansen, 1997).

1.2.2.4 Viscose

Whilst regenerated cellulosic man-made fibres such as viscose are yet to compete with the vast amounts of polyester produced globally and within Europe, cellulosic fibres have established themselves as an appealing alternative to other man-made fibres (Textiles Intelligence, 2013). Reasons for this include their biodegradability, renewability, and comfort properties.

Viscose is most commonly made from wood, of which approximately 40-50 % is composed of cellulose (Lenzing, 2012). Cellulose can also be extracted from plants and some bacterium; any living organism which uses photosynthesis (Figure 1.2).

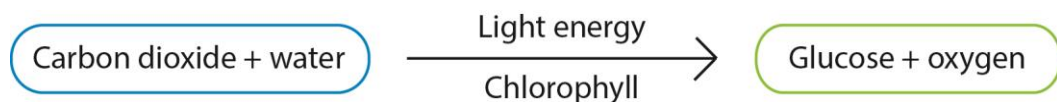


Figure 1.2 Process of photosynthesis

First recognised by French chemist Anselme Payen in 1838, cellulose ($C_6H_{10}O_5$)_n is an organic polysaccharide (repeating glucose structure) with diverse and far reaching applications. Cellulose is a linear-chain polymer, comprising of repeating β -D-glucopyranose molecules, with a C4-OH group at one end and a C1-OH group at the other end (see Figure 1.3). The large number of hydroxyl groups present in cellulose allow for high rates of changeability and hydrogen bonding (Klemm *et al.*, 2005).

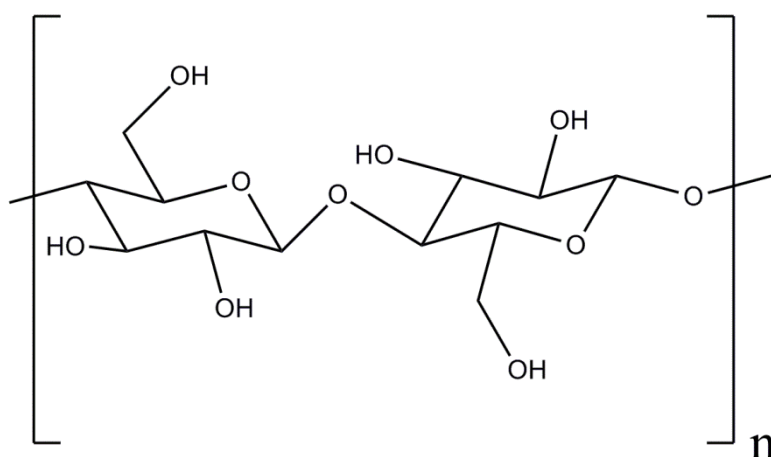


Figure 1.3 Structure of cellobiose

Viscose, a type of regenerated cellulose, dates back to the late 19th century. In 1891, British chemists Charles Cross, Edward Bevan and Clayton Beadle first discovered that cotton and wood cellulose could be treated with an alkali and carbon disulphide to produce cellulose xanthate. This was then coagulated in aqueous ammonium sulphate before being returned to pure cellulose through treatment with dilute sulphuric acid. Cross and Bevan successfully patented this process in 1893 (Woodings, 2000). Meanwhile, Charles Henry Stearn and Charles Fred Topham were working on a method of spinning filaments; Stearn patenting a successful procedure in 1898 (Stearn, 1898; Woodings, 2000). In May 1898, Cross and Stearn combined their expertise in cellulose dissolution and spinning technology, and launched the Viscose Spinning Syndicate Ltd. The company sold its viscose process rights and patents to Samuel Courtauld & Co Ltd in July 1904. Courtaulds grew from strength to strength, and by 1909 the company was producing good quality viscose in both the UK and America. Production of viscose increased worldwide following the expiration of the viscose patents and production increased from 14,000 tonnes to 225,000 tonnes per year from 1920 to 1931. The production of viscose continued to increase and by 1973, annual production had increase to 3,856,000 tonnes (Woodings, 2000). In 2012, 4.07 million tonnes of man-made cellulosic fibres were produced globally, indicating the growth that regenerated cellulose fibres have seen (Fiber Economics Bureau, 2013).

Since Cross and Bevan's patent in 1893, the production of viscose has developed to become a more efficient process. The modern viscose process most commonly involves the following process. Wood is chipped, pulped and soaked in sodium hydroxide (NaOH) (commonly known as caustic soda) to break the internal hydrogen bonds, in turn swelling the fibres. This slurring process changes the cellulose into sodium cellulosate, or alkali cellulose to use its common name. This is then pressed and the remaining caustic soda is recycled back into the process. The alkali cellulose is then oxidised and mixed with carbon disulphide (CS₂) to produce sodium cellulose xanthate. This is then dissolved in more caustic soda to finally produce viscose. The viscose is held in a vacuum to ripen and remove any trapped air, after which it is passed through a filter to ensure its purity. Finally the viscose is passed through a spinneret, coagulating and neutralising as it enters a bath of sulphuric acid, sodium sulphate, zinc sulphate and water. The resulting filaments are either collected in bales of short staple fibre or in continuous yarns (Wilkes, 2000). The rate of coagulation and stretching, as well as the concentration of the viscose solution, all contribute to the particular characteristics of the viscose end product (Nevell, 1995).

Depending on the exact method of production, the LCA of viscose production can vary. In the same 2006 study into the LCA of a cotton t-shirt as discussed in section 1.2.2.1, the LCA of a viscose blouse was also considered (Allwood *et al.*, 2006). In this case, the energy consumed in the manufacture of the viscose blouse (11 MJ) was much less than the energy consumed in the manufacture of the cotton t-shirt (24 MJ). The use phase of the viscose blouse also consumed considerably less energy (7 MJ) compared to the cotton t-shirt (65 MJ) (Allwood *et al.*, 2006). Perhaps the greatest impact on the LCA of viscose for fashion and textiles is the chemical emissions and waste water effluent. These important areas have been highlighted within the textile industry and companies are beginning to change their manufacturing processes so that chemicals are recycled and reused (Lewis *et al.*, 2001).

European market leaders of cellulosic fibres, such as Lenzing AG, have enthusiastically promoted cellulosic fibres such as Lenzing Viscose Austria and Tencel® (a form of lyocell) as more sustainable fibre choices for fashion and textile products. Their focus

on environmental sustainability, in particular with regard to materials and production have given Lenzing industrial recognition with awards such as the European Commission's Ecolabel (Lenzing 2014a). The label, awarded to Lenzing in 2002 recognises products and services which have less impact on the environment and health throughout their life cycle compared to comparative goods and services (Lenzing 2014a).

Lenzing Viscose Austria is produced using wood sourced from beech and eucalyptus trees which have been grown in compliance with the sustainable forestry legislation. Neither beech nor eucalyptus trees require artificial irrigation so the water consumption to grow them is minimised (Lenzing, 2008). Lenzing Viscose Austria is produced in a similar way to the common viscose process described above. Pulp from an integrated plant is alkalisied in caustic soda, depolymerised and mixed with carbon disulphide (CS_2) to produce cellulose xanthate. The cellulose xanthate is then dissolved in caustic soda before being filtrated, degassed and aged. The viscose solution is put into a spin-bath containing sulphuric acid, sodium sulphate and zinc sulphate. It is then spun in an acid salt bath to create the viscose filaments. Finally, the fibres are bleached, finished and dried. Importantly, up to 70 % of the CS_2 used to produce the viscose is recycled back into the production process, reducing the LCA of the fibre production stage (Shen *et al.*, 2010).

The integrated plant allows the whole production process of Lenzing Viscose Austria, from wood to fibre, to be done on one site, reducing the amount of fossil fuel consumed in the production of the fibre. Bark waste and waste from the pulp production process contributes to the fuelling of the pulp and fibre production processes with the remaining energy for production (40 %) sourced using externally purchased bark and municipal solid waste from an incineration plant next to the factory (Shen & Patel, 2008).

1.2.2.5 Tencel®

Lenzing Tencel® (a form of lyocell) is produced in a similar way to viscose; however, the production process has been altered so that less chemicals are used and the

production of the fibre is done in a closed-loop process, that is, almost 100 % of the solvents used in the manufacture of Tencel® fibres is recovered and the remaining emissions are treated in biological water treatment plants (Lenzing, 2014d).

Unlike the viscose production process, Tencel uses NMMO (N-methylmorpholine-N-oxide) to dissolve the wood pulp to regenerate cellulose. The use of the highly toxic chemical carbon disulphide (CS_2) is completely eliminated and the production process steps are reduced (Shen & Patel, 2008). This method of production reduces the amount of water consumed; with Tencel® using 10-20 times less water compared to the equivalent amount of cotton (Shen & Patel, 2008). The yield of Tencel® per m^2 of soil is also much higher than cotton. For every 6 m^2 of soil, 1 cotton t-shirt is produced as opposed to ten Tencel® t-shirts (Lenzing, 2014d).

As the global demand for textiles continues to increase, viable and sustainable methods of producing fibres for fashion and textiles must be considered. Whilst natural fibres such as cotton are perceived to be the ultimate fibre choice for sustainability, as they are completely natural, this is not necessarily the case when the whole life cycle of a fibre (including the environmental, social and economic impacts) of a fibre is considered. Regenerated cellulose fibres such as Lenzing Viscose Austria and Tencel® are an exciting option for the future of textiles for fashion. The main benefits of using these fibres include; reduced water consumption in both raw material production and fibre processing; reduced pesticide use; high yield; biodegradability; and renewability of raw materials.

It is therefore proposed that this research may be used to develop a colour blend prediction model for regenerated cellulose fibres such as Lenzing Viscose Austria and Tencel®. The resulting model would promote the use of environmentally responsible fibre choices in combination with commercially viable colouration techniques.

1.3 Colouration of fibres for fashion and textiles

Textile colouration is of great importance, adding value and aesthetic quality to all types of textile products; from fashion to transport furnishings. Fletcher and Grose (2012) describe textile colouration as one of the most important elements in the commercial appeal of fashion products. Colour can rapidly change the appearance of a garment and even prompt additional purchases (Fletcher & Grose, 2012).

The colouration of textiles has been popular for thousands of years. Textile colouration using natural materials is thought to date back to before 2500 BC. Plants, insects and shells were popular resources for colouring materials right up to the late nineteenth century. The range and intensities of colours were however limited and dyed materials often had a low resistance to fading from daylight. The discovery of synthetic dyes in 1856 revolutionised the dyeing industry, with synthetic dyes completely replacing the use of natural dyes within commercial industries by the 1940s (Ingamells, 1993).

W.H. Perkin discovered the first synthetic dye, Mauveine, in 1856. Since then, a plethora of synthetic dyes have been produced, dramatically increasing the amount of colours available and allowing the colouration of both natural and synthetic fibres. The basic principles of dyeing textiles include diffusion of soluble dye particles within a dye-bath, adsorption of the dye by the material, diffusion of the dye from the surface of the fibre to its interior, and the fixation of a dye to the fibre through physical bonds (Cegarra *et al.*, 1992). This form of dyeing can be described as wet-processing. Depending on the fibre type, different dyes are used. Whilst natural fibres such as cotton have good permeability, synthetic fibres such as polyesters have a higher crystallinity, and are therefore much harder to penetrate (Cegarra *et al.*, 1992). Consequently, different classes of dyes have been developed with specific molecular structures which enable the colouration of specific fibre types. The degree to which a dye transfers from a dye bath to fibre is called exhaustion. To aid exhaustion of dye to fibre, chemical auxiliaries are often used (Perkins, 1996). The rate of fixation varies between fibre and dye types and any dye which is not fixated to a fibre during exhaustion remains within the effluent (Fletcher & Grose, 2012).

1.3.1 Environmental impact of dyeing textiles

Regardless of the type of dye or fibre, the colouration of textiles has, like the production of textiles, its own range of environmental impacts. As already identified in section 1.3, the dyes manufactured in today's commercial environment are synthetic. Unfortunately, the use of synthetic dyes in both the dyeing and finishing processes of textiles can consume large amount of chemicals, water and energy and produce harmful waterborne and airborne pollutants (Cattoor, 2007; Lewis *et al.*, 2001). Globally, over half of the production of colorants (estimated to be over 1 million tonnes per year) is used for dyeing textiles (Nousiainen, 1997). Cattoor (2007) identifies discharge water as a particular environmental impact from dyeing and finishing due to the high chemical load that the waste water contains.

Whilst the earliest form of dyeing using natural dyes used small quantities of dye (which was applied to fibres without the need for additional chemical processes), the discovery of synthetic dyes changed the scale and process of dyeing on a vast scale (Gregory, 2007). A large number of the earliest workers involved in the production of synthetic dyes such as fuchsine and auramine (between 1930 and 1960), suffered from bladder cancer due to the carcinogenic nature of the dye ingredients (Hunger, 2003). Since the discovery that some dye ingredients could be harmful, assessment of the toxicology and ecotoxicology of dyes and pigments has become conventional practice with tight safety regulations implemented in most industrial countries (Gregory, 2007). However, the presence of any dye or chemical within waste water can be harmful and consequently waste water must be treated accordingly. Whilst there are environmental regulations in place, such as the European Union environmental legislation or the United States Environmental Protection Agency, regulations are not consistent across the globe (Christie, 2007). It ultimately remains the responsibility of the dye-house to minimise its environmental impact beyond the given regulations. Minimisation of the use of harmful chemical auxiliaries, re-use of dye-baths and reduction of water consumption are among the possible options for reducing the negative impact of textile dyeing, but this is often unfortunately subjective to commercial and monetary considerations (Bide, 2007).

1.3.2 Spun-dyed fibres

Spun-dyed fibres can provide an environmentally positive alternative to conventional dyeing techniques. As outlined in section 1.3, one of the main areas of environmental concern related to textile dyeing is related to the use of water, but with spun-dyeing, water consumption associated with conventional dyeing techniques is removed. Up to 30 litres of water per meter of viscose fabric can be saved through spun-dyeing compared to conventional dyeing (Birla Cellulose, 2012a). Spun-dyeing is a method of dyeing man-made fibres during their production. When manufacturing regenerated or synthetic man-made fibres such as viscose or polyester, a colorant can be added to the spin-bath. The spinning dope is then extruded through a spinneret with the colour inherent to the resulting fibre (AATCC, 2000; Manian *et al.*, 2007). Other benefits of spun-dyed fibres include; good light-fastness, uniformity of colouration, exact reproducibility of colour and ability to dye fibres which are normally more difficult to dye, such as polypropylene, due to their high crystalline structure (Filature Miroglio, 2009; Manian, *et al.*, 2007).

The environmental benefits of spun-dyeing are even more substantial when using fibres which have been manufactured in a particularly environmentally way. As identified, Lenzing Viscose Austria and Tencel® are examples of this; integrating pulping and fibre manufacturing, recycling and reusing harmful solvents and gases, and extracting useable by-products. The amount of water and energy saved through spun-dyed is also considerable. It is estimated that just over 50 litres of water is saved when spun-dyeing black Lenzing Viscose Austria, with a reduction in processing energy of up to 80 % when compared to conventional dyed viscose (Taylor, 2012).

Due to the environmental and social impact of conventional wet-process dyeing, the colouration of textiles can have a large impact on the LCA of fashion and textiles. A recent study by Terinte *et al.* (2014) compared the cradle-to-gate LCA of conventionally dyed knitted modal (jet dyed) with spun-dyed modal fibre. The results showed that across all LCA categories, including categories such as acidification, eutrophication and ozone layer depletion, the spun-dyed fibres caused less environmental impact (often less than half the environmental impact) compared to the

conventionally dyed fabric (Terinte *et al.*, 2014). With regards to water consumption, it was found that the spun-dyed fibre used only 86 litres of water per kg of fibre which was almost half the amount used in the jet-dyeing of the modal fabric which consumed 162 litres per kg of fibre. The benefit of spun-dyeing is even greater when compared to conventionally dyed cotton which was found to use 25 times more water than the spun-dyed modal (Terinte *et al.*, 2014).

Whilst the environmental benefits of spun-dyeing are clear, spun-dyeing is not without its limitations. The main limitation to spun-dyeing, and therefore its current limited application within the textiles for fashion industry, is that large quantities of each spun-dyed colour must be produced at a time in order for the process to be economically worthwhile. The machines for example must be cleaned between the manufacture of different spun-dyed colours. This process takes time away from production and so manufacture of individual spun-dyed colours must be of a quantity substantial enough to be worthwhile. Companies such as Lenzing and Birla Cellulose produce minimum runs of between 5 and 10 tonnes of individual spun-dyed colours (Birla Cellulose, 2012b; Taylor, 2012). This limits both the range of spun-dyed colours companies can offer and also the markets to which they sell to. As identified, the fast-fashion formula employed by many fashion companies requires smaller volumes of textiles to be produced at one time, (as they increasingly respond to consumer demand). Companies such as these many not therefore use spun-dyed fibre (despite their environmental appeal) as the volume of production is too high for their needs. This is where the benefits of blending coloured fibre are advantageous. Instead of producing unique spun-dyed colours, unique colours in smaller quantities can be produced by blending a selection of primary spun-dyed colours. Companies need only stock a set number of spun-dyed primaries with which to blend, reducing the amount of surplus dyed fibre. It is also thought that spun-dyeing can be used to improve brand reputation due to the large environmental savings (Terinte *et al.*, 2014). Economical savings can also be made with the use of spun-dyeing. Spun-dyeing not only uses less water as already identified, but also uses less colorant (with 80 % less pigment used in the spin bath compared to conventional dyeing), and also less energy (consuming 50 % less non-renewable energy compared to conventional dyeing) (Terinte *et al.*, 2014).

Spun-dyeing is therefore an appealing alternative to conventional dyeing and coupled with fibre blending its application within textiles for fashion could become a much more sustainable and appealing method of textile colouration.

1.3.3 Blending coloured fibre to produce colours

The blending of coloured fibres to produce new colours has been well documented in the literature (Burlone, 1983; Burlone, 1990; Miller *et al.*, 1963; Guthrie *et al.*, 1962). In 1957, Guthrie and Oliver discussed the possibilities of using a catalogue of 3-colour blends, their X, Y, Z values calculated and listed in a catalogue (Guthrie & Oliver, 1957). Guthrie and Oliver included discussion on the means with which coloured fibres should be blended, encouraging the blending of colours using a carding machine to produce homogenous blends akin to subtractive mixing (Guthrie & Oliver, 1957). Burlone identified that careful sample preparation and measurement is also essential for colour matching accuracy (Burlone, 1983).

Blending coloured fibre has also attracted increased interest from a recycling point of view. Waste textile materials can be mechanically reduced to fibres before being carded and spun into yarn for knitting or weaving (Black, 2011). From an industrial point of view, the option of having a set number of primary colours from which to produce a wealth of additional colours could be appealing if the blending is accurate and predictable. Having a set of primaries would limit the amount of dyeing required. Once the core primaries are dyed, these can be blended to produce a wealth of new colours. The combination of coloured fibre blending with spun-dyeing in particular would prove beneficial from both an environmental and industry stand point. As identified, the production of spun-dyed fibres is usually done in high volumes (often over 5 tonnes) so that the process is financially viable (Birla Cellulose, 2012; Taylor, 2012). This limits the application of spun-dyed fibre within the fashion industry in particular, as companies often require relatively small amounts of coloured fibre or textiles due to the fast-fashion turnover of trends and garments. If spun-dyeing were to be used in the form of a palette of primaries from which thousands of colours could be blended then it would be possible to supply smaller amounts of coloured fibre to industry. Rather than producing specific coloured fibres for a company, colour would

be matched using a blend of specific primaries. The number of primaries that would be required to match a large range of colours is of particular interest; if too many primaries are required such that it is not feasible to store them then coloured fibre blending would not be a viable option for colouring textiles. Companies such as Birla Cellulose, who specialise in cellulosic fibres, already stock large numbers of spun-dyed fibres (up to 69 readily available colours) (Birla Cellulose, 2012b). If these 69 colours were carefully selected primaries then it would be possible to create thousands of new colours, which are all discernible from one another, through fibre blending.

1.4 Colour: what is it?

Whilst the perceived meaning and symbolism associated with colour can vary from culture to culture, it is thought that the fundamental physiology of the human eye, which allows us to see colour, gives all humans approximately the same visual experience of colour (though of course this is only true for people without colour deficiencies).

Colour is greatly important in enriching our environment. A natural phenomenon, colour can help us to distinguish our surroundings and differentiate between similar objects within it. Differentiating objects not only by their shape, size and texture, but also by their colour has a great evolutionary advantage. For example, two berries which may appear the same in shape and size may be more or less edible, even poisonous, but if we can distinguish them by their different colours, we can choose to eat the one we know to be safe and discard the other.

Colours can be symbolic, their meaning varying greatly between cultures. For example, white is a colour traditionally worn by Western brides on their wedding day. The colour is associated with purity and the beginning of a new life as a married woman; however, in China, the colour white has very different associations, being linked to death and mourning. So whilst it is thought that we all physically see colour in the same way the meaning of colour may change culturally. Within textiles and fashion, colour is a key design tool. Colour greatly influences the feel of a garment and inspires colour palettes for trends and fashion seasons (Fletcher & Grose, 2012).

There are three important contributors to the way we see colour. Firstly there is the human visual system itself, the source of light and finally the material with which the light interacts.

1.4.1 Colour vision

The human experience of colour is possible due to the visual system's ability to detect a small section of the electromagnetic spectrum, ranging between 360 and 780 nm (Berns, 2000). This section is called the visible spectrum and is commonly referred to as light. Light entering the eye is absorbed by light-sensitive photoreceptors called rods and cones. The information received by the photoreceptors is interpreted by the brain as colour. Whilst light itself is not coloured, the varying wavelengths of light that enter our eyes are perceived as different colours by the brain.

Rods and cones are the light-sensitive photoreceptors found in the retinas of our eyes. There is only one type of rod and three types of cones. Rods have a peak sensitivity of around 500 nm and are only activated in low levels of light (Tilley, 2011). When the light source is 0.003 candela per square meter (cd/m^2) or lower, the rods are activated, giving us monochromatic or scotopic vision (Ohta *et al.*, 2005). The three varieties of cones (referred to as L, M and S cones) have different peak sensitivities in the long-, medium- and short-wavelength regions of the visible spectrum (Hunt, 1998). L cones are most sensitive to the green-yellow region (560 nm), M cones most sensitive to the green region (530 nm) and S cones most sensitive to the blue region (420 nm) (Tilley, 2011). The overlapping of the spectral sensitivities of the cones contributes to better colour discrimination (Hunt, 1998). At high light levels, greater than 3 cd/m^2 , the cones activate and we have colour or photopic vision. When the light source is of intensity somewhere in the middle, or suddenly changes from dark to light, then the rods and cones can both be active at the same time and this is called mesopic vision (Ohta & Robertson, 2005). When light enters the eye the photoreceptors are excited and relay electrical pulses to the brain via the optic nerve. The brain in turn perceives the particular ratio of cone responses at any specific location as colour (Hunt, 1998).

The approximately spherical structure of the eye is integral in allowing the optimum amount of light to enter the eye and focus upon the light sensitive cells contained within the retina at the back of the eye. Light enters the eye through a transparent area of tissue called the cornea. The cornea is part of the tough, white outer layer of the eye, called the sclera. Light then passes through the anterior chamber, the lens and through the vitreous humor; a solution that fills the inner chamber of the eye. Light finally reaches the rods and cones within the retina, the innermost lining of the eye. The information received is relayed to the brain via the optic nerve and interpreted by the brain as colour. In order to optimise the amount of light entering the eye, the iris, contained within the choroid layer which is located between the sclera and the retina, can expand and contract to adjust the amount of light entering the eye through the pupil (Viqueira Pérez *et al.*, 2010).

A simple illustration of the structure of the eye can be seen in Figure 1.4.

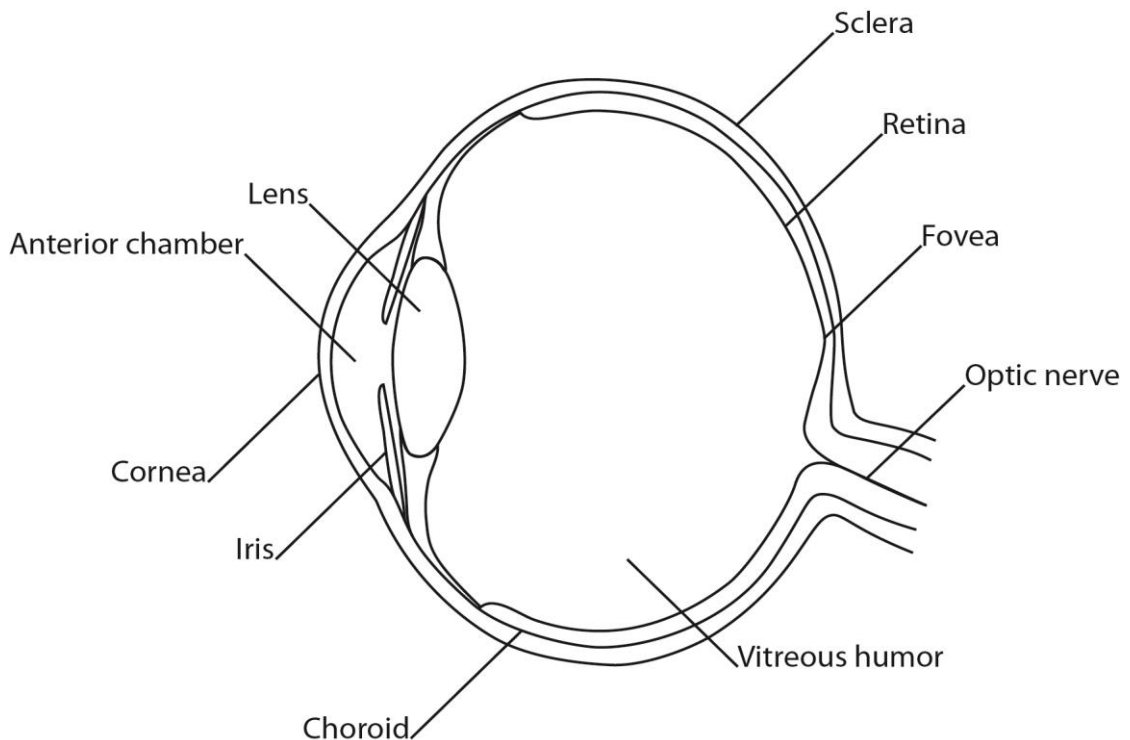


Figure 1.4 Cross-section diagram of the structure of the eye

As already stated, the rods and cones can be found within the retinal layer of the eye. They do not cover the whole of the retina however and are located centrally at the back of the eye around a small area, around 1.5 mm in diameter, called the fovea centralis. This area has the highest concentration of cones and does not usually include any rods. Rods are distributed around the wider surrounding area (Ohta & Robertson, 2005). It should be noted that there are more L and M cones than S cones and that the specific number of cones can vary from person to person (Berns, 2000). Another area located in the back of the eye is the optic disc, where ganglion cells carrying information to the brain via the optic nerve are situated. There are no photoreceptors here which results in a blind spot (Viqueira Pérez *et al.*, 2010).

1.4.2 Light sources

As identified, our visual system is activated by light. Sources of light can vary from the natural, such as the sun, to man-made sources such as filament light bulbs. The source

of light greatly influences the amount of electromagnetic energy, namely relative power, which is emitted at each wavelength of the visible spectrum. For example, daylight emits high amounts of all wavelengths across the visible spectrum, giving it a high relative power (Berns, 2000). Light sources such as the sun, candles and burning coal are described as incandescent. This means that their light, and resulting colour, are a result of a material being heated up enough to emit increased amounts of radiation in the form of light (Berns, 2000). As the temperature of a material increases, so does the amount of light being emitted. Black body radiators, or Planckian radiators, rely solely on their temperature and are objects or materials which absorb and emit all wavelengths (Hunt, 1998). Perfect black bodies do not actually exist in nature, but the characteristics of natural light sources such as the sun are very close. The temperature of a perfect black body, in kelvins (K), can be compared with and used to describe a non-black body object by comparing their colour, and therefore their correlated colour temperature (Kuehni, 2005). Unlike perfect black body radiators, artificial light sources such as mercury and fluorescent lamps do not emit all wavelengths. Depending on the particular light source, a light source may have different spectral peaks within the visible spectrum. This can result in the colour of an object being distorted under different lighting conditions (Berns, 2000).

In order to accommodate for this potential change in colour within commercial fields such as textile colouration, illuminating conditions are specified using CIE standard illuminants. The most popular CIE standard illuminants are D65 (for average daylight) and standard Illuminant A (for incandescent light). These standards are a representation of the two most common forms of light interacted with on a daily basis. D65 has a correlated colour temperature of approximately 6500 K and Illuminant A has a correlated colour temperature of approximately 2856 K (CIE & IEC, 1987; ISO, 2011b; Ohta & Robertson, 2005). Objects viewed under different illuminants can appear differently. If two objects appear to match under one illuminant and not another, the objects are described as exhibiting illuminant metamerism (Berns, 2000). One way to assess the visual appearance of a light source is by measuring its radiance. Radiance is the amount of light from the visible spectrum that is emitted from a light source. This information is often plotted on a normalised relative spectral power distribution curve,

and this allows the appearance of different light sources to be compared (Fairchild, 2005).

1.4.3 Light and objects

Colour perception also depends greatly upon the physical composition of a material that light comes into contact with. When light penetrates the surface of an object, photons of light interact with the molecular structure of the material. This interaction of light and material give the surface appearance of a material including colour. Depending on the interaction of light and material, either all or part of the radiation is refracted, reflected, scattered or absorbed.

Refraction occurs when light travelling through a medium of one refractive index (for example air) reaches a medium of a different refractive index (such as paint) and this interaction changes the direction in which the light was travelling (Sinclair, 1997). This phenomenon can be seen when light passing through the air meets a transparent object at an angle such as light entering a glass prism. In this instance the light passes through the glass prism and is separated as it leaves due to the different refractive indices of the various wavelengths; producing a rainbow effect (Kuehni, 2005). The refractive index describes the amount to which light is slowed down as it passes through a material, in comparison to its speed in air. The refractive index can vary from one material to another, and when light passes through two adjoining materials with different refractive indices, some of the light is reflected (Berns, 2000).

Reflection is when light comes into contact with a smooth surface and changes direction on impact. The angle at which the incident light makes contact with a material is the same angle at which the light is reflected, making the prediction of reflectance easily calculable (Kuehni, 2005). This type of reflection is specifically called specular reflection and causes objects to appear glossy (Berns, 2000). The prediction of the scattering of light is however much more difficult. Scattering is an irregular form of reflection where incident light comes into contact with a rough surface and is scattered in many directions (Kuehni, 2005). When light is scattered by a rough surface, specular reflection is reduced and light is diffusely reflected (Berns, 2000). The

extent of scattering will depend on the material that the light comes into contact with. For textile fibres and fabrics, scattering is often very high and irregular due to the complex structures of the fibres and fabrics (Sinclair, 1997). Scattering is affected by the particle size that wavelengths come into contact with. Whilst small particles scatter small amounts of light, larger particles scatter increasingly more light. When the particles are larger than the wavelengths interacted with, the amount of scattered light begins to decrease. Transmission can also occur, where light passes directly through a material. Transmission is usually observed with transparent objects or materials (Berns, 2000; Kuehni, 2005).

Absorption is when photons of light respond to the energy levels of a material, so much so that the light loses its energy and is no longer visible to the human eye; it has been absorbed by the material. When this happens, some of the energy absorbed is re-emitted as heat (Kuehni, 2005). Black bodies are an excellent example of this. If an object absorbs all visible wavelengths then it appears black, as all the energy that we could interpret as colour, is removed. No real objects absorb all the light energy falling on to them and in most cases, an object or material will selectively absorb some of the light and reflect or scatter the remainder (Kuehni, 2005).

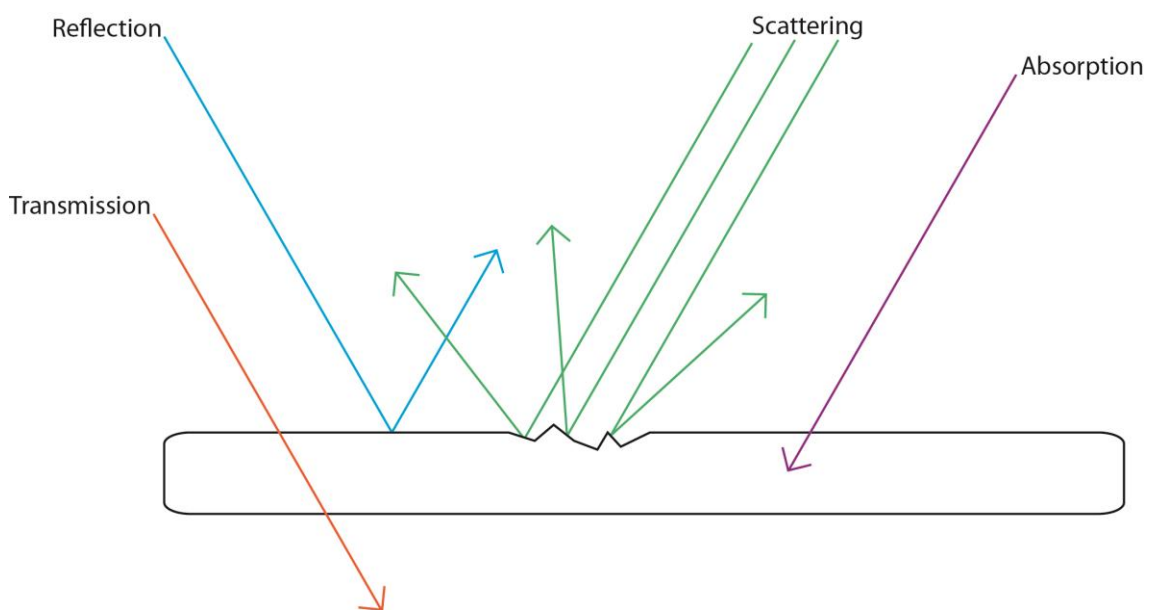


Figure 1.5 Illustration of transmission, reflection, scattering and absorption characteristics of light with materials

This combination of absorption, scattering and reflectance results in the appearance of coloured materials such as textile fabrics; the colour we see being mediated by the eye's response to those wavelengths which are scattered and reflected.

The spectral reflectance of an object can be measured using a spectrophotometer. Most devices measure spectral reflectance data at 10 nm intervals; however, this is dependent on the device used. A spectrophotometer is comprised of a light source, CIE standardised illuminating and viewing geometry, monochromator and detector. The illuminating and viewing geometries define the illuminating angle and viewing angle, for example, 45°/0°. The monochromator disperses the reflected light so that it passes to the detector (Gupte, 2010). For non-self-luminous coloured samples such as textile fibres, a light source that emits light across the spectrum is required. Spectrophotometers measure the reflectance of a given sample across a defined range of wavelengths, taking measurements at specified intervals. The Spectraflash® 600 PLUS spectrophotometer, which is used in this study, records at wavelengths at 10 nm intervals between 360 nm and 700 nm. The instrument uses a barium-coated integrated (or Ulbricht) sphere with an 8° angle of collection (d/8°) (Datacolor, 2007). Samples placed in the viewing port are illuminated (usually using D65 lighting) and light reflected from the sample at the 8° angle is collected. A second reference beam consisting of the light reflected from the inner sphere surface can also be collected if the option for specular reflection is included (Battle, 1997; Datacolor, 2007).

An illustration of the Spectraflash® 600 PLUS spectrophotometer used in this study can be seen in Figure 1.6.

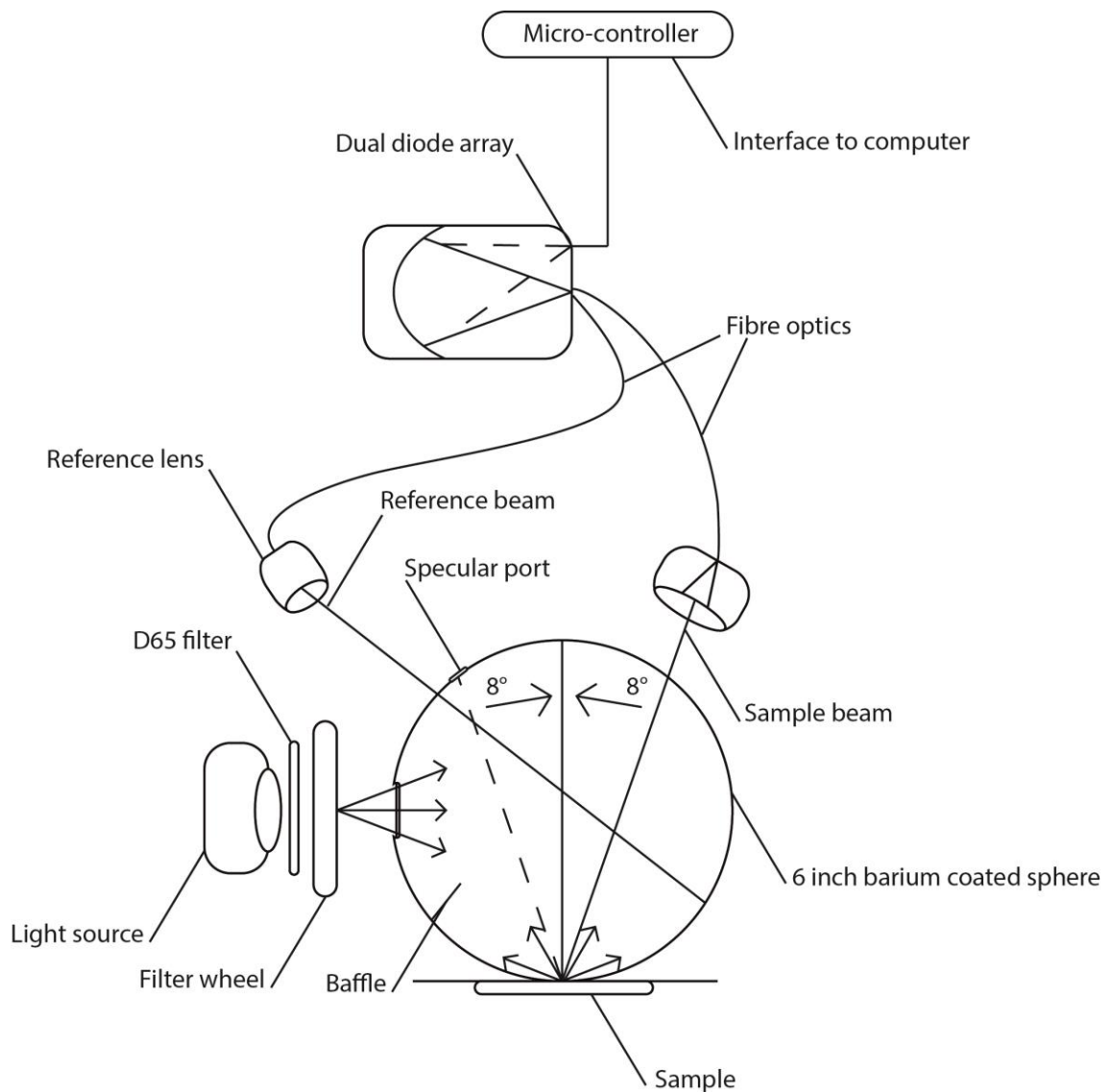


Figure 1.6 Diagram of the Spectraflash® 600 spectrophotometer

Spectrophotometers can be used to accurately measure the reflectance factors of textile samples. When measuring loose fibre, particular care must be taken to ensure that the specimen is uniform. It is also recommended that several measurements are taken in order to obtain an average measurement (Gangakhedkar, 2010; Hunter Associates Laboratory, Inc., 2008). Spectrophotometers are also integral pieces of equipment for the accurate calculation of colour differences and colour matching. Spectral reflectance data can be converted into tristimulus values (such as CIE XYZ) so

that comparisons of colour can be made (Hunt, 1998). This will be discussed further in the following section 1.4.4.

1.4.4 Organising colour

When discussing colour, we commonly use names such as red, yellow, orange etc., to describe the colours we see. We also often use adjectives with these colours to further indicate their appearance, such as vivid red or mustard yellow. However, due to the vast variations of colours we are able to perceive (MacAdam, 1947), it would perhaps be impossible to allocate descriptive names to them all. There is then the problem of whether a descriptive name of a colour effectively conveys its appearance to another person. It must also be considered that each person may perceive the same colour slightly differently due to our unique visual systems. Whilst the communication of a colour is not usually a problem when talking about colour in general, for example when describing the colour of an everyday object in conversation, it can be a problem within the fashion and textile industry. For example, a designer within the UK may design a dress with a specific colour in mind; in order for the dyehouse in China to match that specific colour quickly and efficiently there must be a reliable way of communicating it.

The communication, description and organisation of colour is not a new concept and many artists, designers and scientists past and present have strived to create effective colour systems. There are two main types of colour specification systems. The first is based on the orderly arrangement of colours based on their appearance and includes systems such as the Munsell system and the Swedish Natural Colour system (NCS). The second specification system is based on additive colour mixing and this includes the Commission Internationale de l'Eclairage (CIE) system. There are also colour naming systems, such as the Pantone System, which is predominantly used to communicate colour between designers and manufacturers. Originally a system developed for graphic designers, the Pantone system has expanded and now provides references for a wide variety of industries including fashion and architecture. The Pantone System consists of reference books containing individually named coloured swatches, or stock. Pantone references are widely used by fashion and textile designers as a creative tool

for assembling seasonal colour palettes and communicating them to manufacturers (Pantone, 2014). Naming systems such as the Pantone System provide a good basis for communicating the general appearance of a colour; however, the colours are not exhaustive are often ordered in an aesthetic rather than perceptually ordered system.

1.4.4.1 Colour appearance systems

The Munsell system is perhaps the most well-known colour appearance system and dates back to 1905. American artist Albert Munsell used painted colour chips to arrange colours by their hue, value (lightness) and chroma (chromatic intensity). The structure of Munsell's system is cylindrical with five main hues (red, yellow, green, blue and purple) and five intermediate hues (yellow-red, green-yellow, blue-green, purple-blue and red-purple) radiating from a central axis. The value (or lightness) is the height of the cylinder with white at the top and black at the bottom. The chroma is represented by concentric circles around the axis. Whilst Munsell originally wanted a uniform sphere shape to his system, he soon realised that the maximum chroma of the different hues varied and consequently produced an irregular spherical shape called the Munsell tree (Kuehni, 2005; Munsell, 1905). In 1907 Munsell published his first 'Atlas of the Munsell Color System' which was revised and extended in 1915 (Munsell, 1907; Munsell, 1915). In 1929 the Munsell Color Company produced another revised version of Munsell's Atlas and called it the Munsell Book of Color (Munsell Color Company, 1929). The visual scales of this book were subsequently revised by the Colorimetry Committee of the Optical Society of America (OSA), to produce the 1943 Munsell Renotations which are still in use today (Newhall *et al.*, 1943). The revisions included revising aim colours of the Munsell system using the CIE system of colorimetry (Kuehni, 2005). A total of 2746 chromatic and 9 achromatic colours have been defined, of which 65 % have been produced as colour chips for reference (Kuehni, 2003).

1.4.4.2 Colour mixing systems

Colour mixing systems, such as the CIE system, are based on the additive mixing of three coloured primary lights in order to match a specific colour (Ohta & Robertson, 2005). The amounts of each coloured light, or primary, required to match a given

colour can then be quantified numerically (rather than being described using a name or coordinate from a system such as Munsell's) (Rigg, 1997). Additive mixing itself is the mixing of two or more coloured lights which we then perceive as one colour. This is different to subtractive colour mixing which is most commonly seen in the mixing of physical materials such as paint, ink or dyes. Whilst the mixture of the three primaries used in ink jet printing (cyan, magenta and yellow) will produce an almost black colour, the mixing of the additive primaries (usually red, green and blue) will produce white light. The additive primaries produced in one lab can be accurately produced in another (Rigg, 1997). This is unlike the subtractive mixing of paints and dyes which is subject to a person's unique visual systems and human error.

In 1931 the Commission Internationale de l'Eclairage (CIE) standardised the colour matching functions (red, green and blue primaries) so that additive colour systems would use consistent stimuli, where $[R] = 700.00 \text{ nm}$, $[G] = 546.1 \text{ nm}$ and $[B] = 435.8 \text{ nm}$ (ISO, 2011a). These functions were determined in two separate studies using observers with normal colour vision. The first in 1929 by Wright (Wright, 1929) used 10 observers, and the second in 1931 by Guild (Guild, 1931) used 7 observers. In the experiments, observers were asked to match a target colour (generated using an incandescent lamp) using light from the red, green and blue primaries using a small 2° field of view. The results of each experiment were averaged and slightly adjusted so that proportions of $[R]$, $[G]$ and $[B]$, as colour matching functions $\bar{r}(\lambda)$, $\bar{g}(\lambda)$ and $\bar{b}(\lambda)$, could be used to create a function identical to the CIE luminous efficiency $V(\lambda)$ (ISO, 2011a).

In reality, the use of $\bar{r}(\lambda)$, $\bar{g}(\lambda)$ and $\bar{b}(\lambda)$ posed difficulties as it is not possible to match all possible colours using combinations of the three $[R]$, $[G]$, $[B]$ primaries as some colours are too pure (Rigg, 1997).

In order to match a very pure colour, for example colour [C], it is sometimes necessary to first add one primary, for example [R], to [C], so that primaries [G] and [B] can match [C] as in Equation 1.

$$C[C] + R[R] \equiv G[G] + B[B]$$

Equation 1

Equation 1 can be arranged as Equation 2 which shows that the recipe for [C] is now $-R$, G and B .

$$C[C] \equiv -R[R] + G[G] + B[B]$$

Equation 2

Having a negative value (in this case $-R$) posed difficulties in early colour matching practices when calculations of tristimulus values were done manually (Ohta & Robertson, 2005). In order to solve this problem, the CIE introduced new primaries [X], [Y] and [Z] using the following Equation 3, Equation 4 and Equation 5 (ISO, 2011a);

$$\bar{x}(\lambda) = [0,46\bar{r}(\lambda) + 0,31\bar{g}(\lambda) + 0,20\bar{b}(\lambda)]n$$

Equation 3

$$\bar{y}(\lambda) = [0,17697\bar{r}(\lambda) + 0,81240\bar{g}(\lambda) + 0,01063\bar{b}(\lambda)]n$$

Equation 4

$$\bar{z}(\lambda) = [0,00\bar{r}(\lambda) + 0,01\bar{g}(\lambda) + 0,99\bar{b}(\lambda)]n$$

Equation 5

where n is a normalising constant, found using Equation 6 (ISO, 2011a);

$$n = \frac{V(\lambda)}{0,17697\bar{r}(\lambda) + 0,81240\bar{g}(\lambda) + 0,01063\bar{b}(\lambda)}$$

Equation 6

This created the CIE 1931 Standard Colorimetric System (CIE & EIC, 1987; CIE, 2004; ISO, 2011a) with reference colour stimuli [X], [Y] and [Z]. The amount of [X], [Y] and [Z] required to match any given colour can be given using the tristimulus values X, Y and Z. Sometimes it is useful to calculate the tristimulus values as proportional amounts, and then they are known as chromaticity coordinates (see Equation 7, Equation 8 and Equation 9).

$$x = \frac{X}{X + Y + Z}$$

Equation 7

$$y = \frac{Y}{X + Y + Z}$$

Equation 8

$$z = \frac{Z}{X + Y + Z}$$

Equation 9

The new colour matching functions ensured that the tristimulus values to match a colour would always be positive numbers (unlike for the $\bar{r}(\lambda)$, $\bar{g}(\lambda)$ and $\bar{b}(\lambda)$, colour matching functions). It is important to note that the CIE 1931 Standard Colorimetric System was based on the 1931 RGB system and therefore 1931 RGB standard 2° observers. The RGB standard 2° observers were therefore adopted as virtual observers for the CIE 1931 system and called the CIE Standard Colorimetric Observer (CIE, 2004; ISO, 2011a; Ohta & Robertson, 2005).

In 1964 two new standard observer experiments were carried out by Stiles and Burch (1959) and Speranskaya (1959). Like the work of Wright (1929) and Guild (1931), the experiments used observers to additively match a target wavelength colour using three lights sources. However in Stiles and Burch and Speranskaya's work, the field of view was increased from 2° to 10° (Stiles & Burch, 1959; Speranskaya, 1959). The

results of the two studies were averaged to produce the 10° CIE Supplementary Standard Observer (Rigg, 1997). Increasing the viewing field was important as whilst samples viewed at 2° may be perceived to be a good match in colour matching, the same samples may appear differently at 10° due to the fact that the photoreceptors are not uniformly distributed in the retina of the eye. This is closely linked to metamerism where two samples may appear the same under one set of viewing conditions (for example D65 lighting at a 2° field of view) however when seen under a different set of conditions the samples appear different. The two samples are said to be a metameric pair; they are spectrally different but appear the same under certain conditions or by a certain observer. Using a field of view of 10° (as in the CIE 1964 Supplementary Colorimetric Observer) will usually highlight the occurrence of metamerism (Hunt, 1998; ISO, 2011a).

A chromaticity diagram is a two-dimensional, horseshoe-shaped plane produced when two of the chromaticity coordinates (by tradition this is usually x and y) are plotted against each other. The two ends of the horse shoe shape (the spectrum locus) are joined together using a straight line. This line shows the additive mixtures of the two colour-matching functions. All possible additive mixtures of the functions fall within or along the outline of horseshoe shape (Kuehni, 2005; Ohta & Robertson, 2005). If the third colour matching function is included then a triangle is formed with the gamut of all possible colours using the three colour-matching functions inside (Westland *et al.*, 2012).

There are thought to be two main restrictions of the CIE colorimetry system using $[X]$, $[Y]$ and $[Z]$ (Westland *et al.*, 2012). The first restriction is that the system was based on colour specification, rather than colour appearance. The second restriction is the non-uniformity of the system, making it difficult to define that magnitude of perceptual difference between two points with different tristimulus values. To combat this problem a new three-dimensional colour space was proposed by the CIE in 1976 called the CIE (1976) $L^*a^*b^*$ colour space (also known as CIELAB) (ISO, 2011c).

In CIELAB, the tristimulus values of a measured object or material (given in X , Y and Z) and the tristimulus values of a perfect reflecting diffuser under the same illumination (given in X_n , Y_n and Z_n) are normalised so that $Y_n = 100$. This is done using the following Equation 10, Equation 11 and Equation 12 (CIE, 2004);

$$L^* = 116 \left(\frac{Y}{Y_n} \right)^{\frac{1}{3}} - 16$$

Equation 10

$$a^* = 500 \left[\left(\frac{X}{X_n} \right)^{\frac{1}{3}} - \left(\frac{Y}{Y_n} \right)^{\frac{1}{3}} \right]$$

Equation 11

$$b^* = 200 \left[\left(\frac{Y}{Y_n} \right)^{\frac{1}{3}} - \left(\frac{Z}{Z_n} \right)^{\frac{1}{3}} \right]$$

Equation 12

This gives L^* , a^* and b^* coordinates where L^* is the variation in lightness on a scale of 0 to 100 where 0 = black and 100 = white; a^* is the variation of red to green; and b^* is the variation from yellow to blue. The a^* and b^* axes form one plane with the L^* axis intersecting the plane at right angles. The CIELAB system is used to assess the colour appearance of materials and objects and provide more accurate colour difference measurements between two sets of stimuli. Euclidean colour difference is calculated using the following Equation 13;

$$\Delta E_{ab}^* = [(\Delta L^*)^2 + (\Delta a^*)^2 + (\Delta b^*)^2]^{\frac{1}{2}}$$

Equation 13

where ΔE is proportional to the colour difference perceived between two stimuli. For an indication as to the scale of CIELAB ΔE colour differences, Rigg (1997) compares the colour difference between black and white (100 CIELAB ΔE) with acceptable

commercial colour differences in colour matching (between 1 and 2 CIELAB ΔE). It is thought that a colour difference of 0.5 is the approximate threshold of perceptibility for a person with normal colour vision (Westland & Ripamonti, 2004).

Most recently, the CIE recommended the CIEDE2000 colour difference formula as seen in Equation 14 (Luo *et al.*, 2000). Whilst the CIEDE2000 colour difference formula is based on the CIELAB colour difference formula, it does not simply measure the Euclidean distance between two stimuli. Instead, the CIEDE2000 formula measures difference in lightness, chroma and hue and weights them depending upon where in colour space the stimuli are, as well as improving the performance of blue colours and grey colours (Luo *et al.*, 2000). The CIEDE2000 colour difference formula has been shown to produce the most reliable colour difference data when compared to other formula such as CIELAB colour difference (Luo, 2002). However, it has been suggested that the formula is most accurate when the colour difference between two stimuli is less than 5 units, and that above this, CIEDE2000 performs less accurately than CIELAB ΔE (Kuehni, 2005).

$$\Delta E_{00} = \left[(\Delta L' / (k_L S_L))^2 + (\Delta C' / (k_C S_C))^2 + (\Delta H' / (k_H S_H))^2 + R_T (\Delta C' / (k_C S_C)) (\Delta H' / (k_H S_H)) \right]^{\frac{1}{2}}$$

Equation 14

1.5 Models for predicting the colour of blended fibre

In order to predict the colour of a blend of fibres composed of more than one coloured fibre (or primary), different prediction models have been explored. The most rudimental method of prediction is using the average reflectance of a set of primaries, weighted by their proportion within a blend. For example, see Equation 15;

$$R_M(\lambda) = c_1 R_1(\lambda) + c_2 R_2(\lambda)$$

Equation 15

where the reflectance of the mixture $R_M(\lambda)$ at wavelength λ is the weighted reflectance of component $R_1(\lambda)$ and $R_2(\lambda)$ and c_1 and c_2 are the fractional quantities of the two primaries ($c_1 + c_2 = 1$).

However, many studies have shown that Equation 15 is a poor method of blend prediction as reflectance is not linearly related to the proportion of each primary within a blend (Burlone, 1984; Park & Stearns, 1944). Instead, most popular methods use functions which transform reflectance with the aim of developing an additive model.

1.5.1 Kubelka-Munk equation

For predicting the reflectance of dyed substrates, the most widely used formula is Kubelka-Munk (Kubelka & Munk, 1931). The Kubelka-Munk equation has been used within the textile and paint industry to predict dye and pigment recipes by calculating a linear relationship between reflectance and colorant concentration of a substrate. Equation 16 shows the Kubelka-Munk equation where K is the absorption coefficient, S is the scattering coefficient and R_∞ is the reflectance of an infinitely thick sample.

$$\frac{K}{S} = \frac{(1 - R_\infty)^2}{2R_\infty}$$

Equation 16

Measures of the reflectance of an infinitely thick textile fabric sample can be obtained, for example, by folding the fabric sufficiently so that it is opaque.

The K/S of both the individual dyes and the substrate and the K/S of the whole mixture can be defined (Ingamells, 1993). One limitation with the Kubelka-Munk model is that it presumes that the incident light is either directly absorbed or upwardly reflected by a substrate and that the substrate is homogenous. Scattering where light is lost through the edges of a substrate is not accounted for (Nobbs, 1985; Sinclair, 1997). This therefore limits the application of the Kubelka-Munk model within textiles as the absorption and scattering of textile fibres is much more complex.

Whilst the single constant Kubelka-Munk model is less effective when used to predict the colour of textiles compared to its use in colorant prediction, as discussed by Burlone (1983), the two-constant Kubelka-Munk model is seen to perform much better (Burlone, 1984). In two-constant Kubelka-Munk theory, each primary has two constants; a pseudoabsorption constant K and a pseudoscattering constant S which take into account the physical form of a sample of blended fibres. Using the two-constant Kubelka-Munk model, Burlone achieved a 1.6 CIELAB colour difference between prepared blends and blend predictions (Burlone, 1984). However, it is thought that this method is not completely reliable however as it is (similarly to single-constant Kubelka-Munk) based on subtractive mixing. In reality, blended fibres have both subtractive and additive properties (Philips-Invernizzi *et al.*, 2002a; Burlone, 1990).

1.5.2 Stearns-Noechel equation

In 1944, Stearns and Noechel published a new model for predicting the colour of wool blends (Stearns & Noechel, 1944), see Equation 17;

$$f_{SN}(R_M(\lambda)) = c_1 F(R_1(\lambda)) + c_2 F(R_2(\lambda))$$

Equation 17

where $R_M(\lambda)$ is the blend reflectance. The formula (function f_{SN}) that transforms the reflectance factors is shown in Equation 18;

$$[f_{SN}(\lambda)] = \frac{1 - R(\lambda)}{[b(R(\lambda) - 0.01) + 0.01]}$$

Equation 18

where b is a dimensionless constant. Stearns and Noechel (1944) empirically derived b as 0.15 for wool blends.

As b is empirically derived, it is expected to vary depending on fibre type. This has been shown in the work of subsequent authors who have optimised b to be between 0.09 for viscose (Rong & Feng, 2005) and 0.25 for acrylic (Davidson & Taylor, 1965). Table 1.1 summarises some of the various b values derived for different fibres within the literature.

Table 1.1 Variations of b for different fibre types as derived by different studies within literature

Reference	b value	Fibre type	No. colours in blend
Stearns and Noechel, 1944	0.15	Wool	2
Davidson and Taylor, 1965	0.25	Acrylic	2, 3 and 4
Burlone, 1984	0.11	Nylon	4
Aspland and Zhou, 2000	0.189	Polyester	2
Philips-Invernizzi <i>et al.</i> , 2002	0.109	Cotton	2
Rong and Feng, 2005	0.09	Viscose	2, 3 & 4

Davidson and Taylor (1965) produced ten blended samples with ten corresponding blend predictions. The mean colour difference between the actual measured blended samples and the predicted colour of the blends was 5.8 MacAdam units (Davidson & Taylor, 1965). Burlone used 42 blended samples to test Stearns-Noechel's model, the result of which produced a minimum mean colour difference of 2.4 CIELAB ΔE (where b was varied between 0.07 and 0.11) between blend samples and blend predictions (Burlone, 1983; Burlone, 1984). Whilst Stearns-Noechel's model has had limited success in its original form as a method of predicting blend colours, variations of the equation have proved encouraging.

Philips-Invernizzi *et al.* (2002a) used Stearns-Noechel's model to predict the colour of 234 cotton blends in both the classic form and in modified forms. They found b to be 0.109 for the classical use of the Stearns-Noechel's equation, which gave a mean colour difference between measured colour of blend and predicted colour of blend as 1.85 CIELAB ΔE .

The most practical and successful form of the Stearns-Noechel equation that they investigated required optimising b for each wavelength (see Equation 19). This produced improved results with a mean CIELAB ΔE of 1.66 (Philips-Invernizzi *et al.*, 2002a).

$$b = \frac{(0.12\lambda + 42.75)}{1000}$$

Equation 19

Li *et al.* (2009) more recently produced a spectrophotometric algorithm based on Stearns-Noechel's model to optimally derive b . Using 36 three-component blends and 12 four-component blends, b was derived as 0.09. The three- and four-colour blends produced an overall mean of 0.89 CIELAB ΔE .

1.5.3 Friele equation

In 1952, Friele produced a less empirical model than Stearns-Noechel's equation which built upon the principals of Kubelka-Munk theory. Friele related K/S to the function $f_F(R(\lambda))$ to produce his own equation as seen in Equation 20 (Friele, 1952);

$$f_F(R(\lambda)) = \frac{-s(1 - R(\lambda))^2}{2R(\lambda)}$$

Equation 20

where s is the Friele parameter, or scattering coefficient. In Friele's original work on wool blends the scattering coefficient was theoretically derived as $s = 0.30$ (Friele, 1952).

Successive authors within the literature have altered the s coefficient depending on the fibre type, as seen in Table 1.2.

Table 1.2 Variations of s for different fibre types as derived by different studies within literature

Reference	s value	Fibre type	No. colours in blend
Friele, 1952	0.30	Wool	2
Miller <i>et al.</i> , 1963	0.28	Viscose rayon	3
Davidson & Taylor, 1965	0.11	Acrylic	2,3 & 4
Burlone, 1984	0.25	Nylon	4

In the same paper in which Burlone tested Stearns-Noechel's equation with 42 blended sampled, Burlone also tested Friele's equation. In this case a minimum mean colour difference of 2.7 CIELAB $\Delta E \pm 1$ unit was recorded when s was varied from 0.19 to 0.27, showing larger colour differences between measured colour of a blend and predicted colour of a blend compared to the results found using Stearns-Noechel's model (Burlone 1983; Burlone 1984).

Philips-Invernizzi *et al.* (2002b) more recently tested Friele's equation using 17 coloured cotton primaries to create 28 blends (each composed of three colours). The mean colour difference between prepared blends and blend predictions was 5.77 CIELAB ΔE . It is possible that lower colour differences may have been achieved if a larger number of primaries were used to make four-, rather than three-colour blends (Philips-Invernizzi, 2002b).

Miller *et al.* employed Friele's equation for coloured viscose rayon blends where s was found to be 0.28 (Miller *et al.*, 1963). To empirically derive this value, the reflectance values of a large amount of fibre blends were measured and compared to the predicted values given by Friele's equation, the s factor was then adjusted so that the best agreement between the two sets of data was achieved. A total of 22 coloured fibres were used in the experiment. The reflectance of each colour was measured and

a National Elliot 405 computer made blend predictions for two- and three-colour blend combinations at 10 % increments. The result was a catalogue of approximately 57,000 predicted colour blends in the form of X, Y and Z tristimulus values and blend recipes. The difference in colour, ΔE , between actual blended samples and colour predictions averaged 4.1 units of the National Bureau of Standards (NBS, now the National Institute of Standards and Technology), on a scale of 1-9 units (Miller *et al.*, 1963). For a colour difference to be commercially insignificant to an observer, the NBS unit should be less than one (Hunter, 1942). Whilst Friele's model was not particularly successful within the work of Miller *et al.* (1963), the work did highlight that to achieve solid colour effects more than three colours should be blended together.

The question of how many primaries would be required to produce a large variety of blends is important if colour blending is to be a viable option for textile industries. It has been estimated by a number of authors that at least 50 primaries should be used if a large range of solid blends are to be produced (Guthrie *et al.*, 1962; Miller *et al.*, 1963; Philips-Invernizzi *et al.*, 2002a). Philips-Invernizzi *et al.* also suggested that the more colours within a blend, the more accurate a match will be (Philips-Invernizzi *et al.*, 2002a).

In other research, Guthrie and Oliver (1957) proposed that the colour of the primaries selected should be as far apart in the colour spectrum, and as colourful and as saturated as possible to achieve the greatest gamut of blended colours. This would also take into account the possible dulling of colours once blended (Guthrie & Oliver, 1957). Further to these recommendations, it has been recommended that to create homogenous blends that are appropriate for accurate colour measurement, consideration must be made as to the amount of times the primaries within a blend are carded. The length and fineness of the fibres may also affect the blend appearance (Philips-Invernizzi *et al.*, 2002a; Philips-Invernizzi *et al.*, 2002b; Warburton & Lund, 1956).

It is clear that there are two important elements to creating a viable solution to textile colouration by the blending of coloured fibre. Firstly, an accurate method of blend

prediction that takes into account the complicated absorption and reflectance of textile material is essential. Secondly, the selection of the primaries, including the number of them and their position in colour space, is vital and must be well considered so that a large number of blends with a solid colour appearance can be produced.

1.6 Artificial neural networks

The following sub-sections look at the application of neural networks as a method of predicting colour. The first part looks at what neural networks are and explains the basic principles of multi-layer perceptron networks. The second part of this section looks into the practical and theoretical applications of neural networks in predicting colour from existing sources. The third section outlines a typical neural network structure for blend prediction. Finally, the fourth section proposes a novel application of neural networks for predicting the colour of fibre blends which has not yet been tested within the literature.

1.6.1 What are neural networks?

Artificial neural networks (ANNs) are computing systems based on the biology of the brain. Within the brain, interconnected neurons process vast amounts of information to perform complex computations (Haykin, 1999; Mehrotra *et al.*, 1997). For example, light entering the eye is processed by photoreceptors which transmit electrical signals through the optic nerve to be interpreted by the neurons within the brain as colour (Tilley, 2011). Complex processes such as this are done quickly by the brain neurons; with tasks such as perceptual recognition taking 100-200 milliseconds for the brain to compute (Haykin, 1999). Like the neurons within the brain, artificial neural networks, or neural networks, are able to process complex relationships between a set of inputs and outputs. Neural networks can be trained with example data using a learning algorithm so that they can compute complex, non-linear tasks. Learning algorithms allow neural networks to vary different parameters, or weights, so that the correct relationship between the input vector and the output vector is achieved (Haykin, 1999).

Neural networks can be structured in many ways. There are three main units which are included in feed-forward networks; input units, output units and hidden units. Input units are weighted by the input vector, for the prediction of fibre blends this could be a number of primaries. The output units are weighted by the output vector, again for the prediction of colours blends this could be reflectance at 35 different wavelengths (from 360 nm to 700 nm in 10 nm increments). Finally, the hidden units are free parameters which are weighted by the complexity of the internal relationship between inputs and outputs (Rumelhart & McClelland, 1987; Westland, 1998). The optimum number of hidden units must be derived empirically by running the neural network and varying the number of hidden units used.

One of the simplest structures of neural networks is the single-layer feed-forward network (or single-layer perceptron network) where only input and output units exist. A single input layer will compute directly to an output layer (see Figure 1.7) and this type of network is therefore used in simple, linear problem solving. This type of network would not be appropriate for predicting the colour of blended fibre as that is considered a non-linear relationship due to the complex nature of the blends with regard to additive and subtractive colour mixing (Burlone, 1990; Warburton & Lund, 1956; Warburton & Oliver, 1956;).

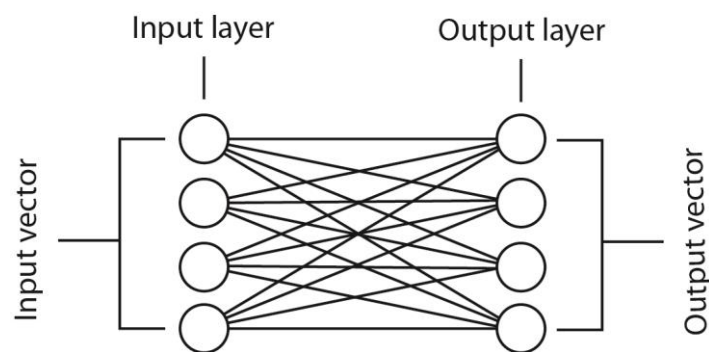


Figure 1.7 Example of a single-layer perceptron neural network

One of the most widely used neural network structures, that does include the input, output and hidden units, is the multi-layer feed-forward network, otherwise known as a multi-layer perceptron network (MLP). In MLPs the input vector informs the number

of input units which interact with the hidden units, within one or more hidden layers, before continuing to the output layer (the size of which is informed by the output vector). Each unit within the hidden layers and output layer also receives a weighted input from a bias unit which is fixed as unity (Westland, 2012). The bias unit is not shown in the example of an MLP in Figure 1.8 for simplicity.

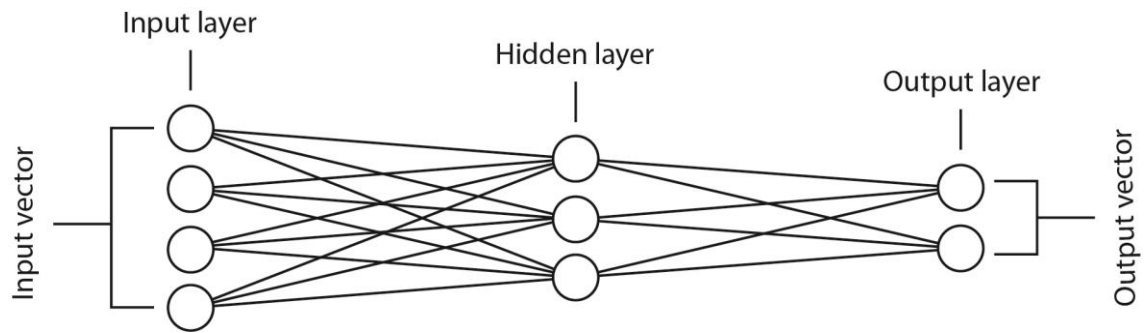


Figure 1.8 Example of a fully connected multi-layer perceptron network (MLP)

The function between any input and output unit is described as the activation function (or transfer function). In MLPs the transfer function is usually non-linear (Westland *et al.*, 2012). The number of hidden layers within a MLP network can vary depending on the complexity of the problem being solved. With increased hidden layers the network will produce statistical results of a higher-order which, it is suggested, is more relevant when there are a very large number of inputs within the input vector (Haykin, 1999). It has been shown that for a large number of computations one hidden layer can sufficiently produce accurate transformations between input and output data (Funahashi, 1989).

1.6.1.1 Multi-layer perceptron networks and supervised learning

An advantage of using MLP networks is that they use supervised learning. Supervised learning is when a neural network is given example input to output pairs of data in the form of training sets. After training, the neural network is tested for its ability to generalise and predict using unseen test sets (Schalkoff, 1997). During the training stage, the network adjusts the weights (hidden units) within the hidden layers of the network to learn the relationship between the two. As the network trains it calculates the error (generalised delta rule) between input and output pairs. The training cycle

(or training epoch) for all input-output pairs is repeated until the mean error between the input and output pairs is sufficiently low (Haykin, 1999; Schalkoff, 1997; Westland, 2012). The training of the network can also be stopped by other stopping criteria such as time elapsed or the number of epochs the data has used (this is dependent on the design of the network). Once the network is trained the weights are fixed and the testing set (which should comprise of data that the network has not seen before but which is comprised of the same set of inputs), can be used to test the network. The performance of the network can be measured using the results of the test data. A good performance is quantified by small differences between the test data and corresponding predictions.

It can be seen that the training of an MLP network is an important tool in allowing the neural network to build knowledge, generalise and consequently make predictions of data that it has not seen before (Shamey & Hussain, 2003; Westland *et al.*, 1991). The number of training samples required to train a network is important and depends on the size of the network. As indicated, the size of the network is dependent on the input and output as well as the number of hidden units (or weights) within the hidden layer(s). Most importantly, when training a neural network, the number of weights must be proportional to the number of training samples, as this affects the network's ability to generalise. If there are a large number of weights but only a small number of training samples then the network will most likely over train, this will consequently have a negative effect on any predictions (Westland, 1998). Whilst the training data is likely to improve with an increased number of hidden units, this can cause over training and subsequently affect the network's ability to predict unseen data (Westland, 2012).

1.6.2 Neural networks and colour prediction

The idea of using neural networks as a colour prediction tool is seen within the literature from the early nineties (Bishop *et al.*, 1991; Westland *et al.*, 1991). Most of this early colour prediction work and literature concerned the use of neural networks as a method of colour prediction for dyes or printing inks rather than fibres (Bishop *et al.*, 1991; Westland, 1994; Westland, 1998; Westland *et al.*, 1991;). Bishop *et al.* (1991)

for example used a neural network to predict three dye concentrations (outputs) from three CIELAB coordinates (inputs). The network was quite large with two hidden layers composing of 8 and 16 units. The results showed a mean error of 1.46 CIELAB ΔE for two-colorant mixtures, with 78.8 % of the predictions producing a CIELAB ΔE of less than 0.8 (Bishop *et al.*, 1991). It was subsequently recommended that for most applications, colour prediction from recipe to reflectance is more advantageous than colorant recipe prediction from reflectance as seen in the work of Bishop, *et al.* (Westland, 2001).

To illustrate the use of MLP networks for colour prediction, Westland (2001) used 6 printing inks to produce 163 blends of printed colours. The network was trained using 123 samples and tested using 40 unseen samples. The network predicted the colour appearance of the 40 blends with a mean colour difference between the actual printed blend reflectance and predicted blend reflectance of approximately 1 CMC colour difference unit (Westland, 2001).

One problem encountered with much of the early work using neural networks for colour and colorant prediction was the ratio of training samples to weights within the network. Often the number of training samples was very similar to the number of weights. For example, Bezerra and Hawkyard's work into the prediction of dye recipes used 391 weights and 283 training samples and the results concluded that the neural network was unsuccessful (Bezerra & Hawkyard, 2000). Cheung *et al.* used 129 weights and 166 training samples for their investigation into the characterisation of colour cameras, producing a median error of 2.89 CIELAB ΔE between target characterisation colour and predicted colour (Cheung *et al.*, 2004).

In order to produce reliable data predictions and avoid over-training, Sarle (2002) recommends that the number of training samples should be at least 30 times the number of weights. Sarle also estimates that a network with 20 hidden units may require between 150 to 2500 training data (Sarle, 2002). One limitation in predicting the colour of blends at 35 output units is that the network is immediately of a substantial size. In order to successfully train a MLP network with a good testing error,

a substantial training set must be used. The training and testing data can be used to determine the optimum number of weights for the network by varying the number of hidden units. An optimum number of weights will be found when both the training error and testing error are low. It is likely that the training error will continue to improve as the number of hidden units increases. The training error will improve fairly evenly to a point, after which the errors will increase again or become irregular which is a sign that the network has become over-trained.

1.6.3 Standard neural network for predicting fibre blends

In section 1.6.1 the suitability of using MLPs for solving complex problems, such as predicting the colour of blended fibre, was identified. The prediction of reflectance of fibre blends is complex due to the mixed absorption and scattering properties of blended fibre. In this thesis, a MLP neural network is used to predict the colour of the blended samples prepared in chapter three.

The number of inputs will be determined by the number of primaries within the output vector, which is the number of primaries used to create the set of blended samples in chapter three (8). The number of outputs will be determined by the spectral reflectance factors of blends in 10 nm intervals, from 360 nm to 700 nm (35). The network will be trained using 273 training samples and tested using 60 unseen testing samples. The network will use one hidden layer and the number of hidden units will be optimally derived by varying the number of hidden units until the smallest mean colour difference (CIELAB ΔE) between the measured reflectance of a blend and predicted reflectance of a blend is found.

Depending on the optimum number of hidden units, the 273 training set may or may not be sufficiently large. For example, the network will use 8 inputs and 35 outputs, if there are 3 hidden units then the number of weights will be $9 \times 3 + 4 \times 35 = 167$. Whether the number of training samples is enough will be determined through training and testing.

1.6.4 Novel neural network for predicting fibre blends

As well as a standard feed-forward MLP network, this thesis will also test a novel application of ANN technology (in this thesis this will be referred to as a novel neural network). The novel neural network uses a number of small networks which all have the same inputs. Each small network is weighted and produces its own output. This type of network could be compared to a modular-structured neural network to an extent as both modular networks and this proposed novel network are comprised of small networks which compute independently of one another. However, the individual neural networks within a modular neural network are each informed by different input vectors (Osherson *et al.*, 1990). This is not the case with the novel network as each of the individual networks is informed by the same inputs within the input vector.

The structure of the novel network will be such that instead of using eight input vectors (8 primaries) to predict 35 output vectors (35 reflectance factors between 360 nm and 700 nm) as in the standard network, the novel network will use 35 small networks, each one with the same eight input vectors (8 primaries) but each one predicting its own spectral reflectance factor. The 35 small networks will predict the spectral reflectance of 35 individual wavelengths from 360 nm to 700 nm in 10 nm intervals. These 35 individual networks will culminate in the final output vector where the whole reflectance of a blend is consequently known.

Using this novel structure has a substantial impact on the ratio of training samples to weights as each individual network is now much smaller. Each of the 35 networks will compute 8 inputs to 1 output. Again, if three hidden units within this network are used as an example, then the number of weights for each individual network will be $9 \times 3 + 4 \times 1 = 31$. This gives a much greater proportion between number of training samples (273) and number of weights (31).

1.7 Primaries within blended samples

An important consideration that has been touched upon by some authors testing existing blend prediction models is the number of colours to mix within a blend. When we consider that colour space is three-dimensional, it lends itself to the idea that

colour blending of fibres should also be three-dimensional. If there are two primaries in colour space then we create a line between two points on which we can make any mixture of the two, for example see Figure 1.9 (one-dimensional blending).



Figure 1.9 Two primaries produce blending along a line within CIELAB colour space (one-dimension)

When there are three primaries a plane is created (see Figure 1.10). By mixing these three colours, any colour along or within the boundary of the plane can be produced (two-dimensional blending).

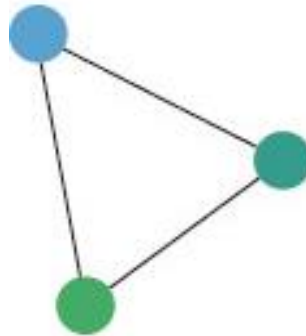


Figure 1.10 Three primaries create a plane within CIELAB colour space (two-dimensional)

When a fourth primary is used a three-dimensional tetrahedron is produced, where any colour along the boundaries or within the space of the four colours can be made, thus giving three-dimensional blending (see Figure 1.11). The hue, chroma and value (lightness) can all be varied depending on the point within the three-dimensional space.

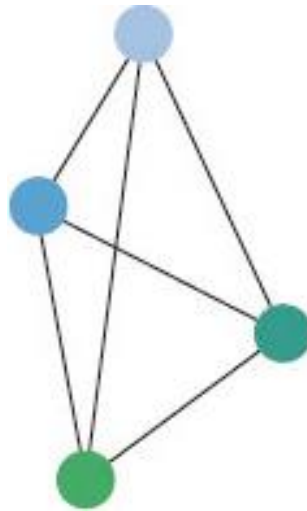


Figure 1.11 Four primaries create a three-dimensional tetrahedron within CIELAB colour space (three-dimensional blending)

It is clear that using four primaries within a blend produces a much larger gamut of blended colours than only blending two or three colours. When translating this concept into a model for predicting the colour of blend recipes so that the blends appear solid in colour, it is possible that a three-dimensional colour palette of primaries could be produced. Primaries could be grouped into tetrahedral groups of four. Depending on the target colour, a different tetrahedron of primaries may be used so that the four primaries enclose the target colour. The next important consideration to this is the spacing of the four primaries within each tetrahedron. The distance between each pair of primaries within a tetrahedron can be measured using CIELAB ΔE . With four primaries there would be six pairs of colour differences. The mean of these six colour differences could be used to determine the number and spacing of primaries (organised as a number of tetrahedron throughout colour space). Depending on the mean colour difference of the tetrahedra and the size of the desired gamut, the number of primaries to cover an area of colour space will vary. If a very large gamut of

colours is desired then there will be more tetrahedra and therefore more primaries. If only a very small gamut is required then the number of tetrahedra and therefore primaries will be reduced. This is very much dependent on the even distribution of the tetrahedra and the colour difference between each primary within each tetrahedron. The mean colour difference required so that a four-colour blend will appear as a solid colour must be determined. Once this is known it would be possible to produce a palette of colours which are evenly divided into tetrahedra with specific mean colour differences so that when blended they produce solid colour effects. Equally it would be possible to deliberately increase the colour difference between the four primaries within each tetrahedral group so that melange blends could be produced.

In order to achieve this, the point at which four colours appear as one, and not a melange, must be defined. This is in itself an important question and one which is dependent on a range of variables including; the distance at which a blend is seen; the shadowing produced from the layering of carded fibre; and the eyesight of the observer. It should also be noted that the appearance of a blend as a solid colour in blended fibre form, may differ once in a knitted or woven form.

All these important considerations as to the primaries which are blended together must be weighted with a method of blend prediction which is both reliable and easy to use if fibre blending is to be used successfully within industry. Whilst the existing blend prediction models have produced encouraging results, in particular the Stearns-Noechell model, improved methods of prediction will be explored through the use of artificial neural networks (ANNs).

Chapter 2 Materials and methods

In this chapter the materials and methods used within the experimental work of this thesis are outlined. Section 2.1 details the type of fibre used and the way in which the fibres were coloured. Section 2.2 details the way in which the coloured fibres were prepared and carded to create blended samples. Section 2.3 describes the methods used for measuring the spectral reflectance of the blended samples using a spectrophotometer, and the calculation of CIE (1976) $L^*a^*b^*$ values using MATLAB. CIELAB ΔE colour differences between the primaries within a blended sample could also then be calculated using MATLAB. Some of the blended samples were spun and knitted and the method and specification of the knitted samples can be found in section 2.4. Finally, both the blended samples and the knitted samples were observed by a group of participants. The method of selecting the participants, the demographic of the participants and the method of running the participant observations are detailed in section 2.5.

2.1 Materials

The specification of the fibres used in this study and the methods in which they were dyed are detailed in the following sub-sections.

2.1.1 Lenzing viscose

Virgin viscose staple fibre was provided by Lenzing AG. The denier of the fibre was 1.7 dtex and fibre length was 50 mm (Lenzing 2014c).

2.1.2 Lenzing spun-dyed viscose

Virgin spun-dyed viscose staple fibre was also provided by Lenzing AG. The denier of the fibre was 1.7 dtex and the fibre length was 50 mm (Lenzing 2014c).

2.1.3 Lenzing viscose pack dyed

In some instances it was required that the same fibre that is described in section 2.1.1 was pack dyed to specific colour requirements. To do this, primary colours were first selected in $L^*a^*b^*$ colour space. The $L^*a^*b^*$ values were converted to sRGB values and matched as closely as possible to the sRGB values of Pantone colour references in

Adobe Illustrator. Once the colours were closely matched, Pantone's online colour finder allowed the digital colour to be converted to the equivalent dyed cotton reference in the Pantone Cotton Planner (Pantone, 2011). Using the Pantone Cotton Planner, independent dyer Richard Noyes formulated the dye recipes to match the Pantone colours as closely as possible. After each adjustment of the dye recipe, a sample of the fibres was carded and measured using the spectrophotometer to ensure that the colour differences were approximately the same as originally desired. Once the dye recipes were agreed upon, ecru Lenzing viscose fibre was pack dyed by outsourced company Progressive Threads. Pack dyeing allowed the fibres to be dyed as evenly as possible and with minimal tangling of the individual fibres. This was important as any knotting of the fibres may have affected the even carding of the primaries.

After dyeing, each primary was again carded and measured so that accurate CIELAB tristimulus values were known. Precise colour differences between each primary could then be calculated (as despite appearing similar to the Pantone references by eye, the spectral data would most likely be different to the original references due to metamerism factors).

2.2 Fibre blending

In order to create uniform webs of fibre composed of one or more primaries, it was necessary to open and inter-mix the fibres through machine carding. The preparation and carding of the samples is described in the following sub-sections.

2.2.1 Preparation of samples

The fibre used in this experiment was conditioned in a controlled environment for 48 hours prior to weighing for sample preparation. The fibre for each sample was weighed to 2 decimal places. The room temperature was 20°C and the relative humidity was 65 ± 5 %.

After the fibre was weighed it was opened by hand in ambient conditions. The fibre was arranged evenly in a sample area size of 210 mm x 148 mm. When two or more

primaries were used, care was taken to distribute the different colours as evenly as possible across the sample area. An example of the fibre

2.2.2 Carding machine

In order to blend the fibre into a non-woven web, a small sample Tathams carding machine was used. The machine comprised of an automatic feed belt, interconnecting feed rollers, lick-in, a single main cylinder with three pairs of workers and strippers, a single doffer and a fly comb. A second conveyor belt at the end of the fly comb transported the web to a lapper which laid the web in a parallel batt formation. The dimensions of the machine and direction of rollers can be seen in Figure 2.1.

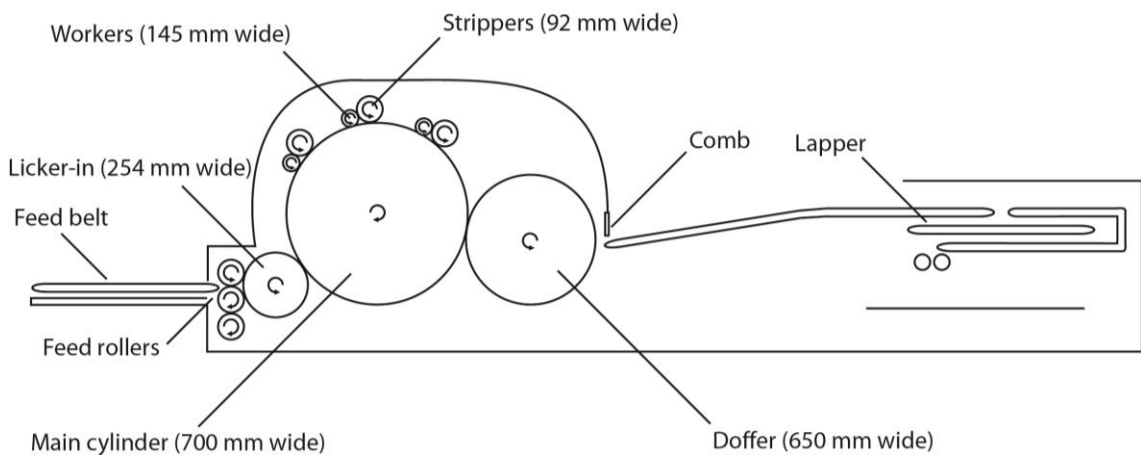


Figure 2.1 Layout of small sample Tathams carding machine

Each fibre sample was placed onto the feed belt and processed through the carding machine. After the first pass, the parallel batt was rotated 90° and passed through the machine a second time. This action was repeated a third time to ensure homogenous blending. To determine the optimum number of times to pass the batt through the carding machine, the carded webs were measured using the spectrophotometer after each pass through the carding machine. It was found that there was no significant advantage to passing the samples through the carding machine a fourth time as the resulting spectral reflectance measurements were consistent with the measurements taken at three passes.

As identified in the literature, careful preparation and handling of the carded blends was essential for accurate colour measurement (Burlone, 1983; Guthrie & Oliver, 1957). The carding machine was cleaned of loose fibre between every sample in order to minimise fibre cross-contamination between samples. The samples were carded in ambient conditions. An example of blended sample 2.23 can be seen in Figure 2.2. The sample was a 4-colour blend with a mean colour difference of 15 CIELAB ΔE .



Figure 2.2 Blended sample number 2.23 with a mean colour difference of 15 CIELAB ΔE (1:1 scale)

2.3 Colour measurement

After carding, the spectral reflectance of each blended sample was measured using a spectrophotometer. The reflectance was then exported into MATLAB for data analysis, comparison and conversion to L*a*b* coordinates.

2.3.1 Spectrophotometer

A Spectraflash® 600 PLUS spectrophotometer (see Figure 2.3) and ColorTools software was used to measure the spectral reflectance of each carded sample (Datacolor, 2007).



Figure 2.3 Datacolor 600™ Spectrophotometer

The measurement device had an optical geometry of $d/8^\circ$ and D65 lighting. A 30 mm (illuminated) Large Aperture View (LAV) plate was used to give a large sample area for measurement, as recommended by the Datacolor 600™ User's Guide for measuring samples with an irregular or textured sample surface (Datacolor 2007). The measurements were taken using 100 % UV, no UV filter with the specular component excluded (SCE).

Before measuring the samples, the machine was calibrated and a standard was measured. Samples were carefully folded until opaque before measuring. For each sample 10 reflectance measurements were taken and the average reflectance was calculated. The reflectance data of each primary was recorded at 10 nm intervals between 360 nm and 700 nm.

2.3.2 Reflectance data in MATLAB

Using MATLAB, the reflectance data for each primary and blended sample was converted to tristimulus values (X , Y and Z) using the MATLAB function 'r2xyz' (Westland *et al.*, 2012). These tristimulus values were then converted to CIE (1976) $L^*a^*b^*$ values using the MATLAB function 'xyz2lab' (Westland *et al.*, 2012). The CIE (1976) $L^*a^*b^*$ values (referred to in this thesis as CIELAB or $L^*a^*b^*$ values) were used to plot the position of each sample in CIELAB colour space. In order to illustrate the approximate visual appearance of each sample, sRGB values for each sample were calculated in MATLAB using the function 'xyz2srgb' and plotted in CIELAB using the corresponding sRGB colour (Westland *et al.*, 2012). Example code can be seen in Appendix I.

2.3.2.1 Calculating colour differences

The colour difference between two samples in CIELAB colour space can be calculated by measuring the Euclidean distance between two pairs of $L^*a^*b^*$ points. This is done using the CIELAB colour difference equation outlined in section 1.4.4.2. In this thesis, MATLAB was used to calculate the colour differences (CIELAB ΔE) using the function 'cielabde' (Westland *et al.*, 2012). Example code for calculating the colour difference between two samples can be seen in Appendix II.

The calculation of colour differences (CIELAB ΔE) between two samples was particularly important when looking at the primaries within a blend of two or more colours. By calculating the colour difference between pairs of primaries, the average colour difference of a group of primaries could be calculated. For example, a blended sample made from the primaries p_1 , p_2 and p_3 would have three possible pairs of colour differences; p_1 and p_2 , p_1 and p_3 , and p_2 and p_3 . By averaging these three

numbers, the average colour difference for the blend could be calculated. Example code can be seen in Appendix III.

2.4 Preparing knitted samples

Once the fibres were blended using the method described in section 2.2, some blended samples were made into knitted samples. Webs of blended fibre were spun and knitted by Lenzing AG, Austria. The plain knit samples were produced on a circular knit machine. The knitted samples had a thread count of 68, 24 ends per inch (EPI) and 44 picks per inch (PPI). An example of knitted sample 2.23, which is shown in web form in section 2.2.2, can be seen in Figure 2.4. The sample was a 4-colour blend with a mean colour difference of 15 CIELAB ΔE .



Figure 2.4 Knitted sample number 2.23 with a mean colour difference of 15 CIELAB ΔE (1:1 scale)

2.5 Visual assessment of carded samples

In order to understand the relationship between the average colour difference (CIELAB ΔE) of a blended sample and the sample's appearance (as a solid colour or not), participants were selected and asked to observe carded samples and rate them. A total of 16 participants were recruited. Only observers with normal colour vision partook in the visual assessments and this was determined using the methods described in section 2.5.1. The results of the participant observations were used to determine the optimum range of average colour differences (CIELAB ΔE) of a blend of primaries in order for the blend to appear as a solid colour.

2.5.1 Participant selection

In order to gather results representative of 98 % of the population, participants were required to have normal colour vision (Hall, 1997). Under controlled viewing conditions, using D65 lighting, the 16 participants were firstly tested for normal colour vision using the Ishihara tests (Ishihara, 1972). Participants were also asked to complete the Farnsworth-Munsell 100-hue test under the same controlled viewing conditions in order to ensure that they were able to detect small differences in sample hue and therefore be able to discriminate accurately between the many blended samples (Hill, 1997; X-rite, 2007). All 16 participants passed the Farnsworth-Munsell 100-hue test and groups of ten participants were used in each visual assessment experiment. An indication as to the variety of participants within the visual assessments can be seen in Figure 2.5 and Figure 2.6

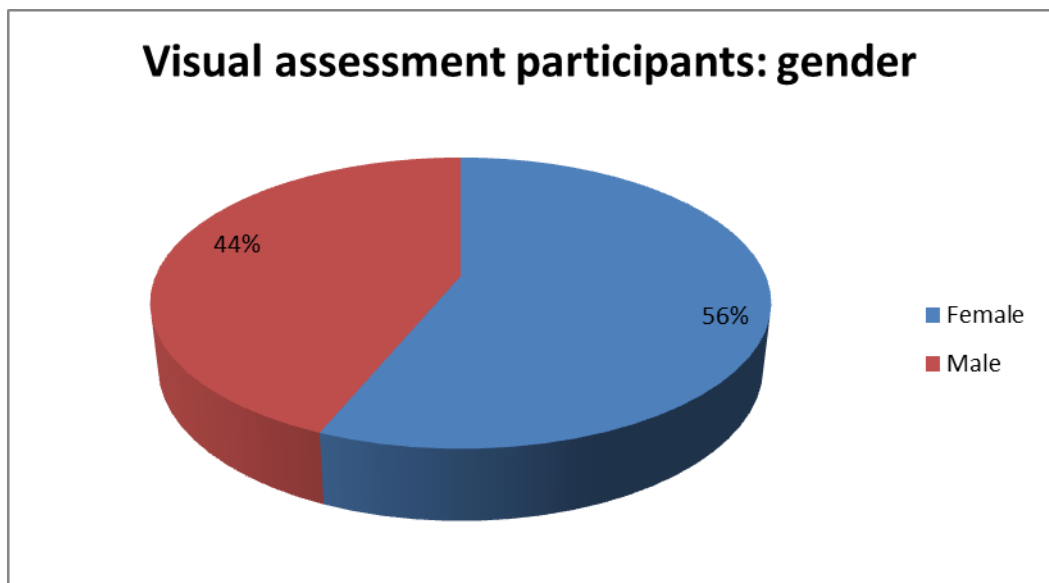


Figure 2.5 Pie chart showing the proportion of female to male participants in the visual assessments

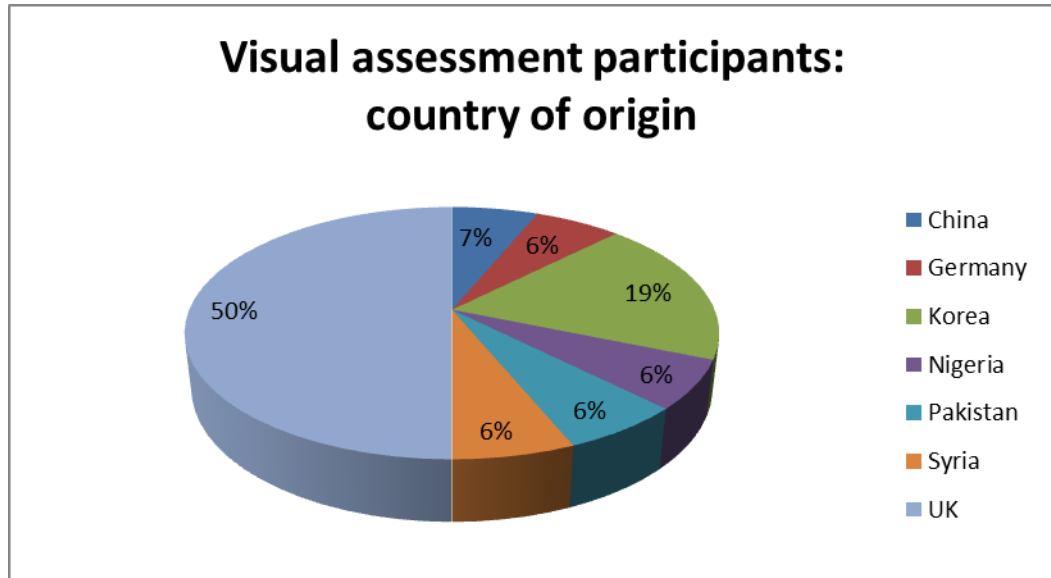


Figure 2.6 Pie chart showing the country of origin of the participants used in the visual assessments

2.5.2 Experiment environment

All visual assessment experiments were done under controlled viewing conditions. Using a Verivide viewing cabinet, D65 lighting was used to illuminate the fibre samples.

2.5.3 Experiment procedure

Participants were shown one sample at a time. The samples were presented in an 8 x 8 cm viewing frame that was coloured grey to match the viewing cabinet. The frame was placed on an inclined, grey presentation board at a 45° angle. The lighting box and samples were a distance of 45 cm in front of the participant. The 45 cm viewing distance and 45° viewing angle was chosen so that samples would be observed by participants in consistent conditions. The distance of 45 cm represented a comfortable viewing distance that a garment may be observed in a retail environment.

Figure 2.7 shows an example of a participant in the laboratory viewing conditions.



Figure 2.7 Participant viewing carded sample

Due to the length of the experiment, participants were able to take regular breaks to rest their eyes. Participants were asked not to lean forward or touch the samples. Before the start of each experiment, participants were given written instructions, an example of which can be seen in Appendix IV.

Participants were asked to assess the carded samples and respond using the following options depending on their observation;

a) A solid colour

(the sample appears like one colour)

b) Almost a solid colour

(the sample is very close to appearing like it is one colour, but you can see that there may be another colour present)

c) Not a solid colour

(the sample definitely appears to be made up from more than one colour)

For each response above the corresponding number of points was given as show below;

a) 1 point

a) 0.5 points

b) 0 points

The results were recorded using a data capture form, an example of which can be seen in Appendix V. On average, participants completed observations of six samples per minute. The total participant score was calculated by adding up the responses for each sample from each participant. For example, if 10 participants all perceived sample 1 as 'a) A solid colour' then the total participant score for this sample would be 10 (100 % success). Conversely, a sample that was perceived as 'c) Not a solid colour' by all ten participants would score a total participant score of 0 (0 % success). The participant score could consequently be compared to the average colour difference (CIELAB ΔE) of a blend.

Chapter 3 Colour difference and sample appearance

3.1 Introduction

In this chapter the relationship between a selection of primaries in a blend and the resulting visual appearance of the blend as either a mélange or solid colour was explored. A mélange can be defined as a blend appearing to have clear heterogeneous primary elements (OED, 2013). Conversely, a blend with a solid colour appearance would appear homogeneous, despite being composed of more than one primary. The aim was to determine a method for predicting in advance whether a particular blend (with known primaries and amounts) would be likely to be judged as being visually solid. If such a prediction is possible then it could, for example, be used to estimate how many primaries a colouration system would need in order that most or all of mixed primary blends would be solid. It is expected that as the number of primaries in a colouration system increases, so does the likelihood that the primaries within a blend (if chosen correctly) will appear solid; however, as the number of primaries increases so does the cost of producing or storing those primaries. Therefore understanding the expected appearance of a blend based on its composition is integral to a successful colouration system. It is important to ensure that blends appear solid whilst at the same time optimising the number of primaries in the system so that it is commercially viable.

In this chapter, two experiments were conducted, during which a large number of blended samples were prepared. With each experiment certain variables were altered including:

- The number of primaries used in each experiment;
- The colour of the primaries used;
- The blend recipes;
- The colour difference between each pair of primaries within a blend;
- The overall average colour difference of a selection of primaries within a blend;
- The number of samples made.

The first experiment was a preliminary experiment whereby eight primaries were used to create 325 2-, 3- and 4-colour blends. The blends were evaluated visually and it was shown that there was a relationship between how similar the primaries used to create the blend were and the likelihood that the blend would be perceived as solid. However, all of the 4-colour blends had very high intra-blend colour differences (and hence most did not appear solid at all). As suggested in the literature review, it is likely that blends composed of four primaries may be advantageous as they produce three-dimensional tetrahedral gamuts in colour space. Further analysis of 4-colour blends was therefore important for this project. Consequently a second experiment was conducted whereby only 4-colour blends were considered and the primaries were selected to be much closer than in the first experiment. The colours of the primaries used were subject to some commercial constraints as they were selected from fibres made available in small quantities by Lenzing AG.

3.2 Experiment 1: Creating fibre blends with mean colour differences of between 11 and 119 CIELAB ΔE

In experiment one, one undyed viscose primary and seven spun-dyed viscose primaries (that is, a white and seven colours) were used to create a range of blended samples. A total of 325 blended samples were made from these primaries with varying colour differences between the primaries within each blend. A group of 10 participants with normal colour vision took part in the visual assessment of the blended samples. The assessments were used to understand which blended samples appeared solid in colour and to evaluate methods for predicting whether a set of primary colours will create solid blends. Three candidate methods were tested to try to predict the results of the visual assessments; these were the *mean colour difference*, the *maximum colour difference* and the *median colour difference* between the primaries of each blend. The coefficient of determination (R^2) was calculated for each of the methods in relation to the participants' results. This was used as a measure of the ability of the mean, maximum or median as methods for predicting which colours would successfully blend together.

3.2.1 The primaries

The first primary in this experiment was undyed viscose (white), the specifications of which are described in section 2.1.1. The other primaries were spun-dyed viscose of different colours. Their appearance could generally be described as being black, pink, orange, yellow 1, yellow 2, blue and purple. The specifications of the fibres are described in section 2.1.2. The fibres were provided by Lenzing AG and the primaries selected were those that were available in small quantities.

Each primary was carded using the method described in section 2.2. The resulting webs were uniformly blended so that the fibres were aligned and the primaries evenly distributed throughout the batt of fibre. The webs were then folded until opaque and measured using a spectrophotometer, as described in section 2.3, to record the spectral reflectance factors of each primary. The spectral reflectance factors of the samples were then converted to $L^*a^*b^*$ and sRGB values using the methods described in section 2.3.2. The position of the primaries in CIELAB colour space, coloured using their sRGB values for visualisation, can be seen in Figure 3.1.

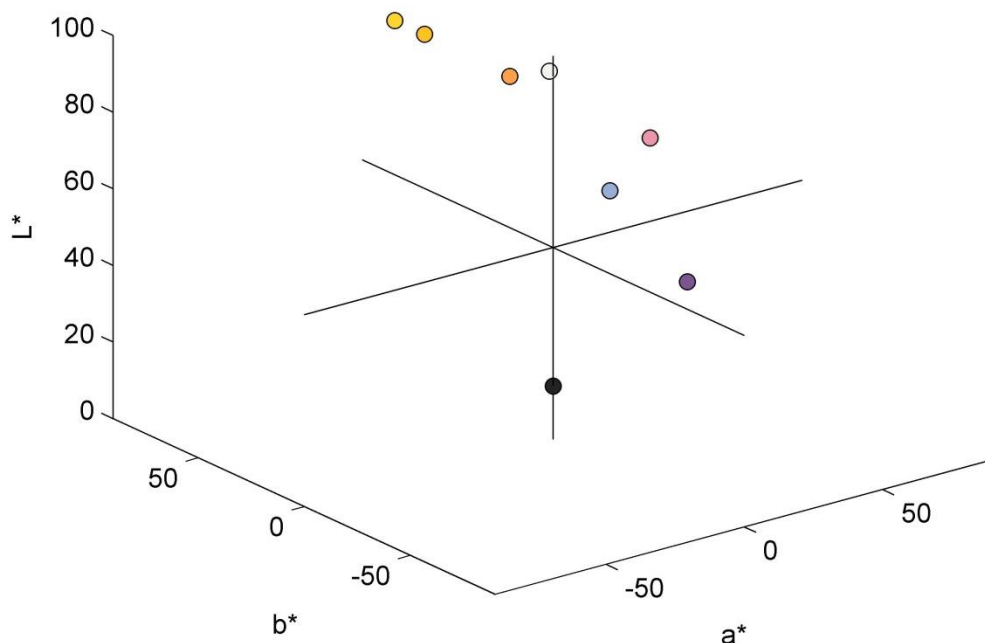


Figure 3.1 Position of primaries in CIELAB colour space

Table 3.1 shows the $L^*a^*b^*$ and sRGB values for each primary. A coloured key is also included which shows the general appearance of the primaries, using the sRGB values, to give a representation of their colour appearance.

















Table 3.1 $L^*a^*b^*$ and sRGB values and appearance of first experiment primaries

Primary number	L^*	a^*	b^*	R	G	B	General appearance (sRGB)
1.1	95.72	-0.21	1.56	244	243	238	
1.2	13.87	-0.03	-0.05	36	36	36	
1.3	71.36	35.82	1.06	237	150	173	
1.4	74.34	28.66	57.84	255	161	74	
1.5	82.67	14.42	79.38	255	194	35	
1.6	87.84	4.50	80.48	255	214	48	
1.7	70.52	2.13	-23.88	152	174	214	
1.8	42.48	27.89	-26.90	125	85	144	

Using the $L^*a^*b^*$ values of the primaries the Euclidean CIELAB colour difference (ΔE) between each pair of primaries was calculated in MATLAB using the method described in section 2.3.2.1. The largest colour difference between a pair of primaries was 119 CIELAB ΔE and the lowest colour difference was 11 CIELAB ΔE .

The colour difference (in CIELAB ΔE) between each pair of primaries is shown in Table 3.2.

Table 3.2 The Euclidean CIELAB colour difference (ΔE) between each pair of primaries

Primary	No.	1.1	1.2	1.3	1.4	1.5	1.6	1.7	1.8
No.									
1.1		0	82	43	67	80	79	36	67
1.2		82	0	68	88	106	109	61	48
1.3		43	68	0	57	82	87	42	41
1.4		67	88	57	0	27	36	86	91
1.5		80	106	82	27	0	11	105	114
1.6		79	109	87	36	11	0	106	119
1.7		36	61	42	86	105	106	0	38
1.8		67	48	41	91	114	119	38	0

3.2.2 Preparing the blended samples

To produce blended samples from the eight primary colours, a selection of blend recipes was required. A total of six generic recipes were used; two containing 2 colours, two containing 3 colours, and two containing 4 colours. These recipes can be seen in Table 3.3.

Table 3.3 Generic blend recipes

	Primary a (%)	Primary b (%)	Primary c (%)	Primary d (%)
Recipe 1	50	50	-	-
Recipe 2	25	75	-	-
Recipe 3	25	25	50	-
Recipe 4	33	33	33	-
Recipe 5	25	25	25	25
Recipe 6	16.66	16.66	16.66	50

With six recipes and eight primaries, the total number N of blends that could be produced if every combination of primary was used for each generic recipe was calculated to be 658 using Equation 21,

$$N = \frac{n!}{r!(n-r)!}$$

Equation 21

where n is the total number of primaries that is being selected from and r is the number of primaries in a recipe. For example, if we consider Recipe 5 (in Table 3.3) there are 70 different combinations of 4 primaries from 8 ($n = 8$; $r = 4$). However, for Recipe 6, although there are 70 different combinations of 4 primaries from 8, there are 4 unique permutations for each one giving rise to 280 different recipes.

To provide a substantial data set for the participant visual experiments, 325 recipes were randomly selected from the possible 658 recipes (generating the full 658 recipes would have been impractical). This large sample set would also be sufficient to test and train neural networks as part of further subsequent experimental work as discussed in chapter 5.

The total sample weight for each of the 325 blends was 6 g and the samples were prepared and carded in the same way as described in section 2.2. The spectral reflectance factors of the blends were measured and converted into $L^*a^*b^*$ values as described in section 2.3.

The position of all 325 blends and the eight primaries can be seen in Figure 3.2. The plots of the blends have been coloured using the corresponding sRGB values.

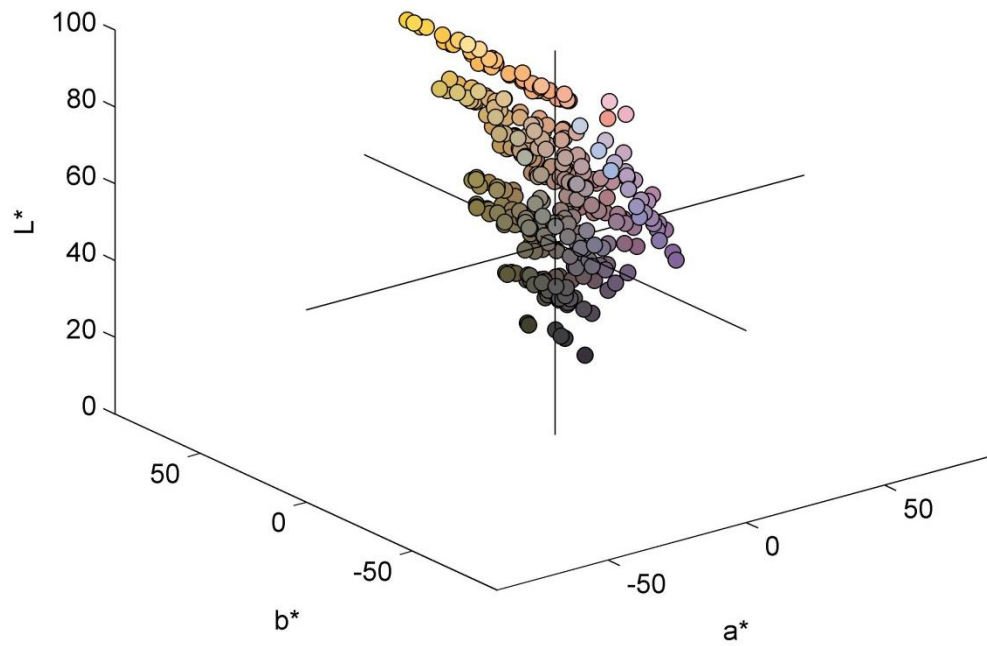


Figure 3.2 CIELAB colour space with the positions of the 325 blends and 8 primaries

Figure 3.3 also shows these blends in CIELAB colour space, this time from an angle directly looking down the L^* axis to see the a^* and b^* plane. This figure gives an indication as to the gamut of the primaries and consequent blends.

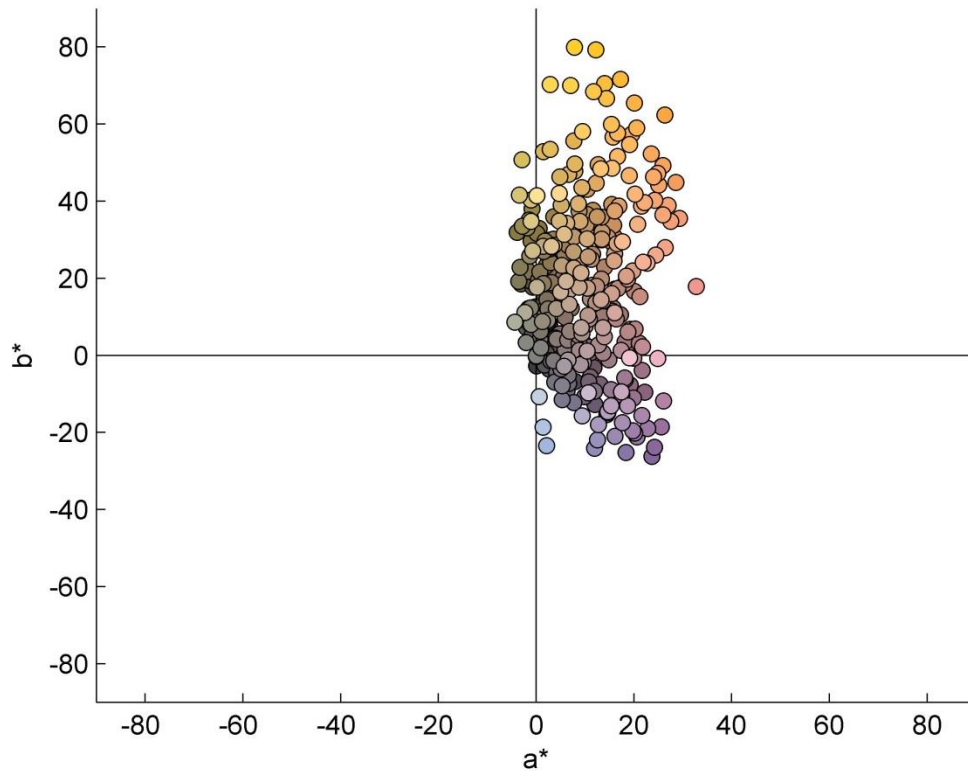


Figure 3.3 Position of the blended samples in CIELAB colour space from directly above the L^* axis, looking down on to the a^* and b^* axes

Using the $L^*a^*b^*$ values of the primaries, a mean colour difference for each blend was calculated by taking an average of the colour differences between each pair of primaries within a blend (so, for example, for a four-component blend there would be 6 colour differences to average); the MATLAB code to do this is described in section 2.3.2.1. The maximum colour difference within a blend and the median colour difference were also calculated.

3.2.3 Visual assessment of blended samples

All 325 blended samples and the 8 primary samples were visually assessed by ten participants using the procedure described in section 2.5. The samples were randomised before being presented to the participants and the participants were not

told how many colours were present within each sample. The results of the participant observations were collated and scored as outlined in section 2.5.

3.2.3.1 Calculating the mean, max and median values of a blend sample

There are a variety of ways with which to relate the results of the participant observations with the composition of a blend. Methods include calculating the mean (or average) of the colour differences of each pair of primaries within a blend, the maximum (max) colour difference of a pair of primaries within a blend and finally the median (middle value) of the colour differences of each pair of primaries within a blend. These three possible methods are explored in this experiment to assess which of the methods provides the best correlation between blend composition and sample appearance. The best correlation is determined by plotting, for each sample, the calculated value (either mean, max or median) against the participant scores in a scatter graph, applying a linear trend line and calculating the corresponding coefficient of determination (R^2).

When comparing the mean, max and median values for each blend with the total participant scores, the visual assessment results were analysed separately for 2-, 3- and 4-colour blends.

The following figures show the results for each group of blends. The first columns show the results including all eight colours; the second column shows the results without white or black. For the 2-colour blends, when recipes that contained white and black were removed (the right-hand column figures), the correlations between the different values and participant scores were better. This trend was not as consistent when looking at 3- and 4-colour blends, however this is most likely due to the increased colour differences between the primaries within the blends.

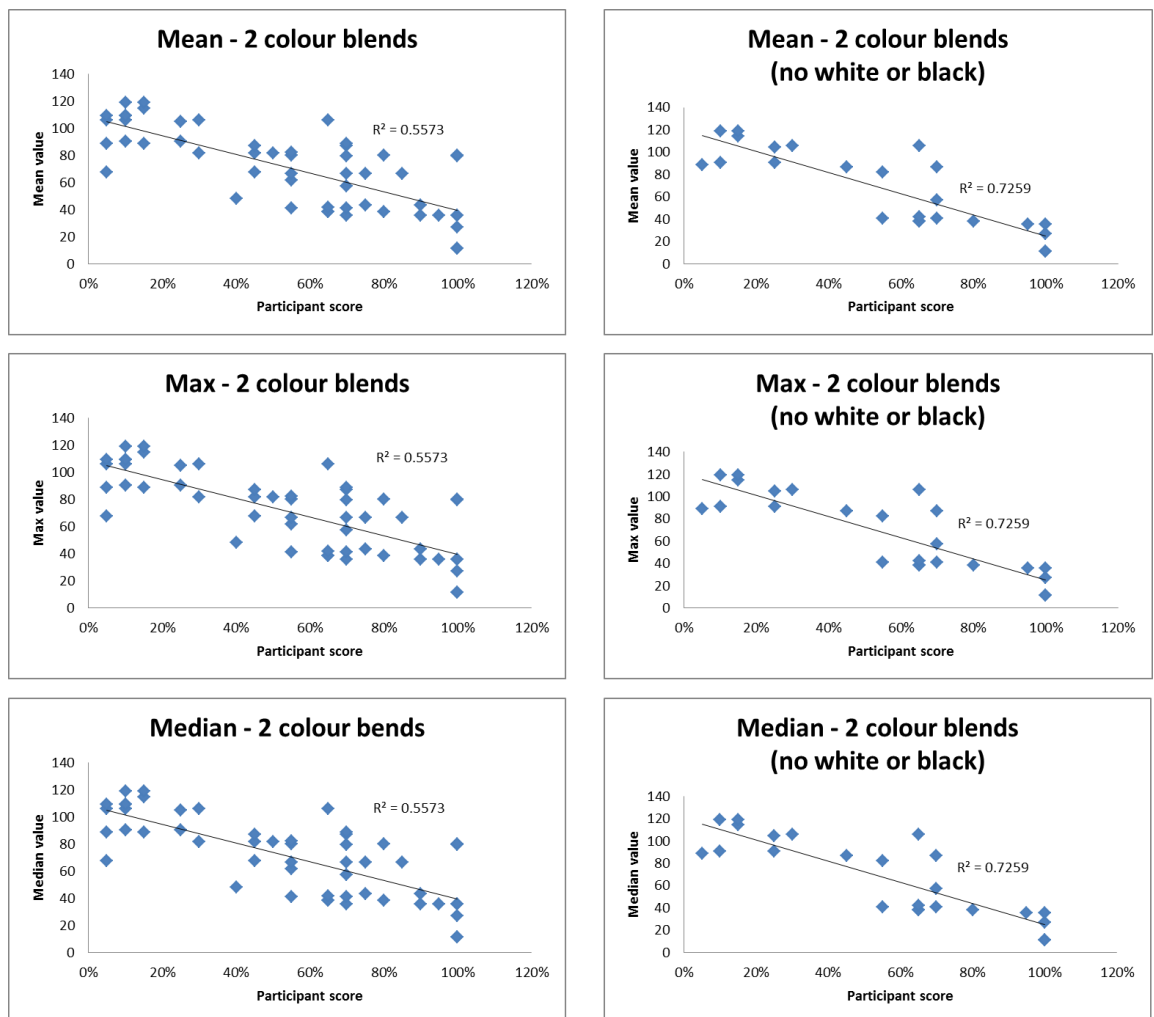


Figure 3.4 Comparison of the mean, max and median values of the colour differences within 2-colour blends, both with (left-hand graphs) and without (right-hand graphs) the white and black primaries included

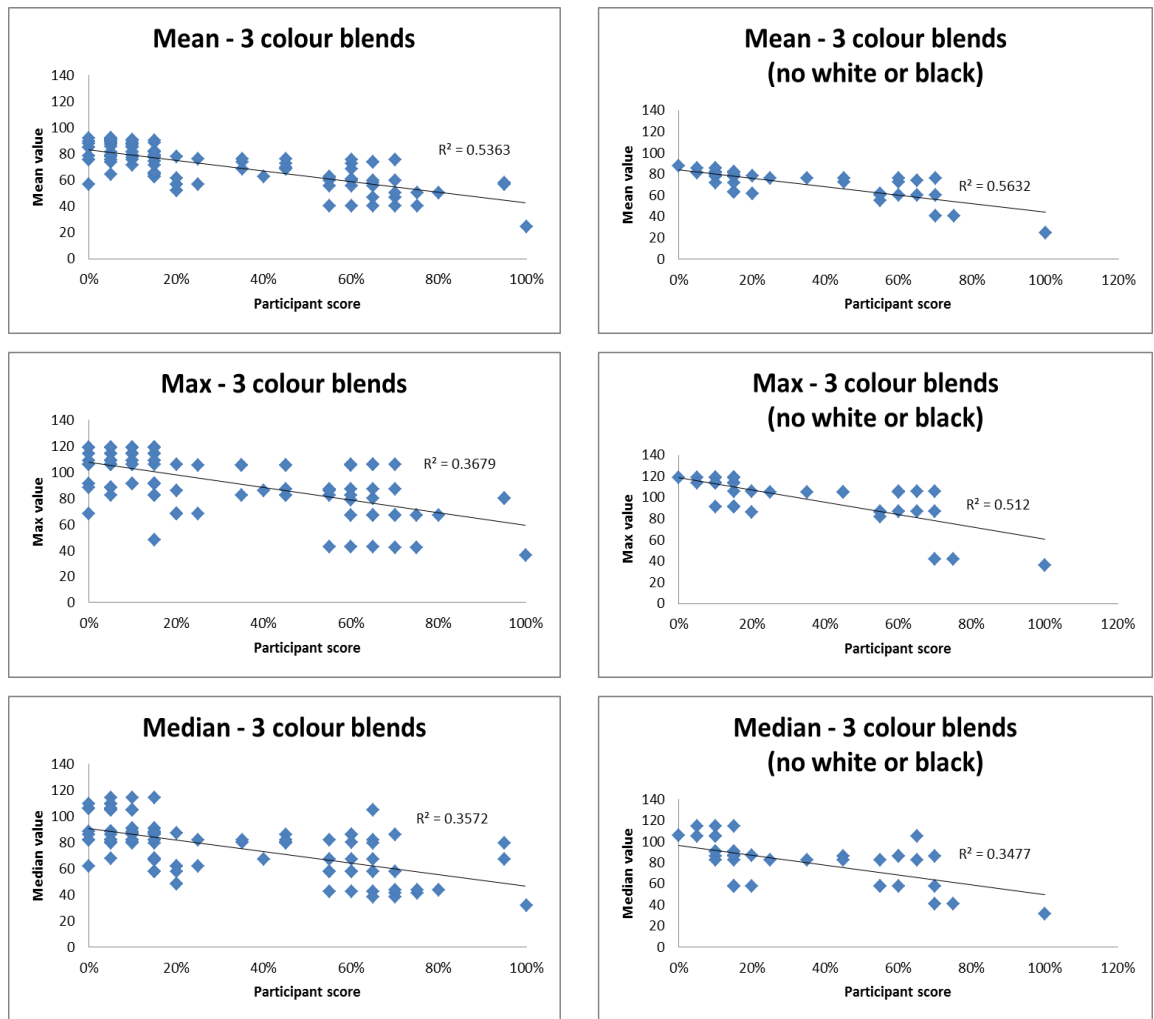


Figure 3.5 Comparison of the mean, max and median values of the colour differences for 3-colour blends, both with (left-hand graphs) and without (right-hand graphs) the white and black primaries included

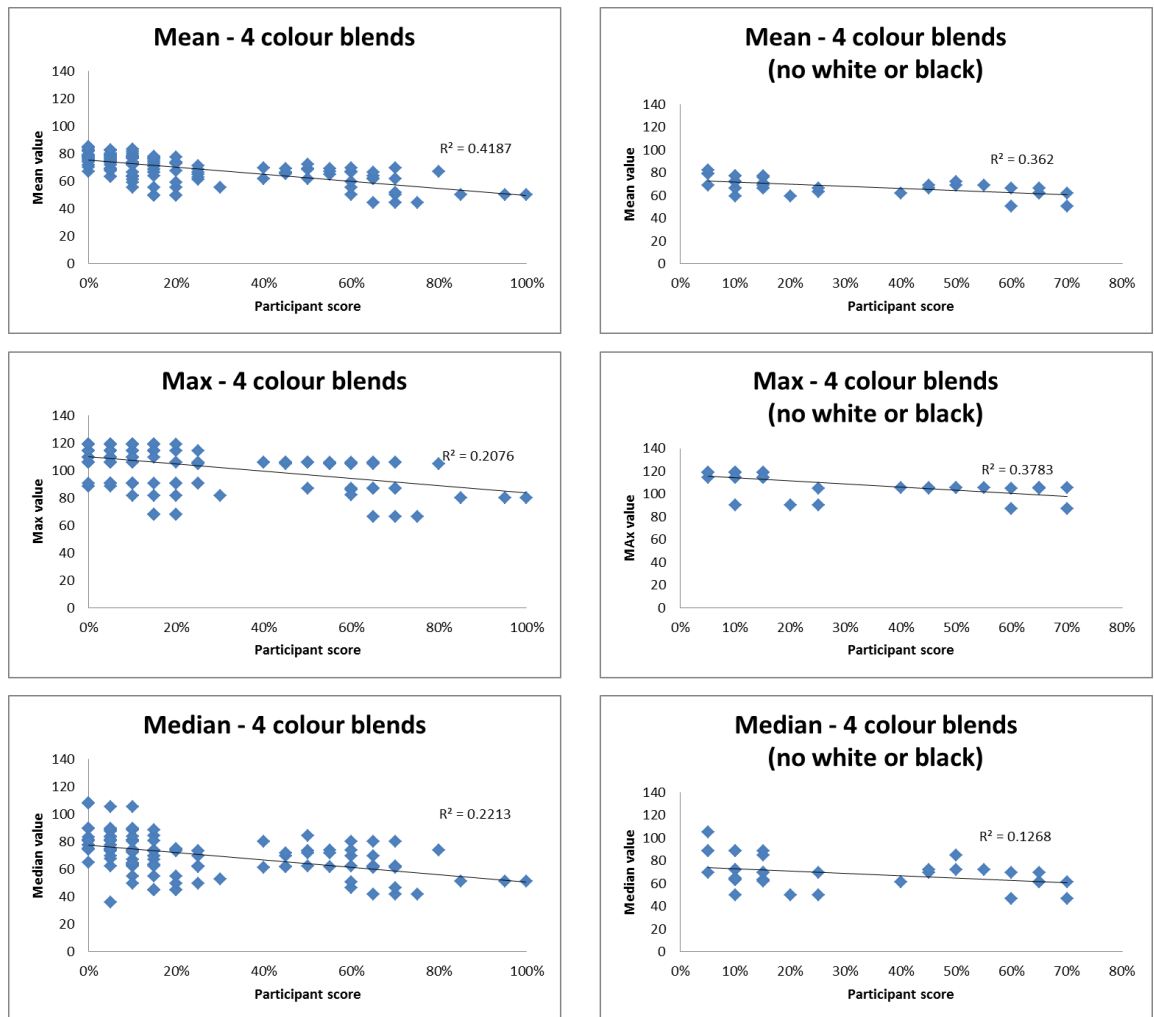


Figure 3.6 Comparison of the mean, max and median values of the colour differences for 4-colour blends, both with (left-hand graphs) and without (right-hand graphs) the white and black primaries included

Table 3.4 summarises the results (in terms of R^2) of the comparison of mean, max and median methods using 2-, 3- and 4-colour blends, both with and without including the white and black primaries. The highest R^2 value was seen for 2-colour blends which excluded the white and black primaries. In this instance, the R^2 value for the mean, max and median values were all 0.7148 (this is because when there are only two primaries there is only one colour difference and therefore the mean, max and median are all the same). The mean of the colour differences between primaries within a blend also performed well for the 3- and 4-colour blends, indicating that this gave the best correlation between blends and participant observations. The mean performed best for 3- and 4-colour blends using all primaries and also for 3-colour blends excluding the white and black primaries. The mean colour difference of a blend was therefore considered to be the best of the three methods and was used subsequently and compared to the participants' visual assessments.

Table 3.4 Comparison of mean, max and median values for the blended samples

All primaries	Mean (R^2)	Max	Median
2 colour blends	0.5573	0.5573	0.5573
3 colour blends	0.5363	0.3679	0.3572
4 colour blends	0.4187	0.2076	0.2236
Blends with no white or black	Mean (R^2)	Max	Median
2 colour blends	0.7148	0.7148	0.7148
3 colour blends	0.5632	0.512	0.3477
4 colour blends	0.362	0.3783	0.1268










3.2.3.2 Mean colour difference and visual assessment results

The results of the visual assessment were ordered from the highest scoring blends (total score of 10 and therefore solid in appearance to 100 % of observers) to the lowest scoring blends (total score of 0 and therefore seen as a solid colour by 0 % of participants). All 8 primaries were observed to be a solid colour by all participants. The full list of results can be seen in Appendix VII.

3.2.3.3 Blends which appeared solid to 100 % of participants

There were 9 blended samples which were scored as a solid colour by 100 % of participants. Table 3.5 shows the results for these blends including the blend names, mean colour differences (CIELAB ΔE) and a representation of the primaries within each blend using the corresponding sRGB values. The full list of blend names and recipes can be found in Appendix VI.

Table 3.5 Blends that were judged as a solid colour by 100 % of observers

Sample name	Mean CIELAB ΔE	Total score	sRGB colours
Blend 1.48	27	100 %	
Blend 1.65	80	100 %	
Blend 1.76	11	100 %	
Blend 1.87	25	100 %	
Blend 1.96	11	100 %	
Blend 1.121	79	100 %	
Blend 1.128	36	100 %	
Blend 1.210	50	100 %	
Blend 1.240	36	100 %	

As Table 3.5 shows, the mean colour difference of the most successful blended samples ranged from 11 CIELAB ΔE to 80 CIELAB ΔE and utilised only five of the eight primaries. Interestingly, the blends which included the white primary generally had higher colour differences (36 CIELAB ΔE to 80 CIELAB ΔE) than those without the white (11 CIELAB ΔE to 36 CIELAB ΔE).

This is examined more closely in Table 3.6 where the blends including or excluding the white primary are separated. The first section of the table looks at the results of the successful blends which were made using a white primary and the second half of the table looks at the successful blends made without a white primary. Each section is also separated into 2-, 3- and 4-colour blends.

Table 3.6 Comparison of blends scored as a solid colour by 100 % of participants

Blend including white	Lowest mean CIELAB ΔE	Highest mean CIELAB ΔE	Participant score	No. of blends
2-colour blends	36	80	100 %	3
3-colour blends	n/a	n/a	n/a	0
4-colour blends	50	50	100 %	1
Blends without white	Lowest mean CIELAB ΔE	Highest mean CIELAB ΔE	Participant score	No. of blends
2-colour blends	11	36	100 %	4
3-colour blends	25	25	100 %	1
4-colour blends	n/a	n/a	n/a	0

The results show that for blends which include the white primary, the mean colour difference of the primaries within a blend can be much higher (between 36 CIELAB ΔE and 80 CIELAB ΔE) than the blends which are made from primaries excluding white. For blends without the white primary, the mean colour difference is much lower (between 11 CIELAB ΔE and 36 CIELAB ΔE). It may be that having a white, or undyed, primary within a blend could have a transparent effect, increasing the mean colour difference for a blend without compromising its appearance as a solid colour. For 2-colour blends which are made from a white and one other colour, the colour difference between the two primaries can be as high as 80 CIELAB ΔE . However, this is reduced, in this case to 50 CIELAB ΔE , when the blend is composed of four colours. There were no 3-colour blends that included white that were perceived as a solid colour by all participants. However there were two 3-colour blends (Blend 1.38 and Blend 1.108) which contained the white primary and were perceived as a solid colour by 9 out of 10

participants. Blend 1.38 had a mean colour difference of 58 CIELAB ΔE and Blend 1.108 had a mean colour difference of 57 CIELAB ΔE .

For blends excluding the white primary, the highest mean colour difference for 2- and 3-colour blends that still allowed them to appear as a solid colour to 100 % of participants was 36 CIELAB ΔE . There were no 4-colour blends (which excluded the white primary) that appeared as a solid colour to 100 % of observers. Only one 4-colour blend, as shown in Table 3.6, was perceived as a solid colour by 100 % of observers and this blend had a mean colour difference of 50 CIELAB ΔE . When looking closely at the results, all 4-colour blends prepared had mean colour difference of between 45 CIELAB ΔE and 85 CIELAB ΔE . In other words, the reason that the 4-colour blends did not appear solid was because they had large mean colour differences (and this is a consequence of the limited and arbitrary set of eight primaries that were used in the study).


























The results of this analysis highlight that the mean colour difference of the 4-colour blended samples produced in this first experiment were not sufficiently wide ranging. The results suggest that much lower colour differences for 4-colour blends need to be studied in order to fully understand the relationship between a 4-colour blend and its appearance as a solid colour (or not).














3.2.3.4 Samples which appeared not solid to 100 % of participants

Table 3.7 shows the 38 blended samples which were all perceived as not a solid colour by 100 % of participants. Out of these 38 blends, all apart from one blended sample contained the black primary. The samples were all 3- or 4-colour blends; there were no 2-colour blends. The mean colour difference of the primaries within each blend ranged from 57 CIELAB ΔE to 92 CIELAB ΔE .

When looking at the general appearance of the primaries within each blend (see Table 3.7), it is perhaps intuitive that the primaries would not blend successfully enough to appear as one colour as the colours within each blend are very chromatically different.

Table 3.7 Blends that were evaluated as not a solid colour by all observers

Sample name	Mean CIELAB ΔE	Total score	sRGB colour
Blend 1.3	74	0 %	
Blend 1.7	78	0 %	
Blend 1.8	76	0 %	
Blend 1.10	71	0 %	
Blend 1.12	79	0 %	
Blend 1.25	71	0 %	
Blend 1.42	77	0 %	
Blend 1.50	78	0 %	
Blend 1.53	85	0 %	
Blend 1.80	90	0 %	
Blend 1.82	85	0 %	
Blend 1.85	85	0 %	
Blend 1.93	76	0 %	
Blend 1.104	90	0 %	
Blend 1.105	79	0 %	
Blend 1.124	79	0 %	
Blend 1.134	88	0 %	
Blend 1.149	70	0 %	
Blend 1.151	79	0 %	
Blend 1.155	84	0 %	
Blend 1.157	82	0 %	
Blend 1.160	79	0 %	
Blend 1.174	85	0 %	
Blend 1.191	83	0 %	
Blend 1.213	67	0 %	

Blend 1.214	92	0 %	
Blend 1.222	74	0 %	
Blend 1.235	77	0 %	
Blend 1.237	75	0 %	
Blend 1.238	79	0 %	
Blend 1.254	77	0 %	
Blend 1.270	57	0 %	
Blend 1.271	85	0 %	
Blend 1.276	78	0 %	
Blend 1.284	84	0 %	
Blend 1.293	82	0 %	
Blend 1.296	77	0 %	
Blend 1.301	85	0 %	

As shown previously in Table 3.2 the colour differences between the black primary and 7 other primaries was high, ranging from 48 CIELAB ΔE to 109 CIELAB ΔE . This will have had a significant impact on the mean colour differences of these blends. The 2-colour blended samples which contained the black primary and one other primary had mean colour differences ranging from 11 CIELAB ΔE to 119 CIELAB ΔE . Whilst none of these blends were scored being a solid colour to 0 % of participants, four 2-colour blends were scored as 5 % and these blended samples had mean colour differences ranging between 68 CIELAB ΔE and 109 CIELAB ΔE .

3.2.4 Conclusions

The results of this first experiment strongly indicate that there is a relationship between the mean of the colour differences between a given number of primaries within a blend and whether that blend appears to be solid or not. However, the large colour differences that were between each of the primaries in this experiment did not allow a thorough-enough exploration of the threshold mean colour difference of a 4-colour blend in order for it to appear as a solid colour. Despite this, the experiment did

give some indications as to the colour difference required and these are discussed below.

For 2-colour blends containing white, even when the mean colour difference between the two colours was as high as 80 CIELAB ΔE the blend appeared as a solid colour to all participants. For 2-colour blends composed of two dyed primaries, the colour difference between two primaries needed to be much lower (36 CIELAB ΔE or lower) in order for the some of the blends to appear solid to 100 % of observers.

For 3-colour blends which contained the white primary, blends appeared as a solid colour to 90 % of participants even when the mean colour difference of the primaries was 58 CIELAB ΔE . For 3-colour blends made from 3 dyed primaries (excluding white) the mean colour difference of the primaries within a blend needed to be as low as 25 CIELAB ΔE .

For 4-colour blends containing the white primary, the mean colour difference of the primaries for a solid blend could be up to 50 CIELAB ΔE . It is not clear what the mean colour difference of a 4-colour blend, composed of four dyed primaries, should be from these results if the blend is to successfully appear as a solid colour to 100 % of participants. This is because that particular result did not occur in this experiment. This is most likely due to the absence of any 4-colour blends made from four dyed primaries with a mean colour difference of less than 50 CIELAB ΔE .

In order to progress this research further, a more concentrated range of primaries, with a smaller range of colour differences between them, was required. Experiment 2 used a new set of dyed primaries with the mean colour differences of each blend equal to 25 CIELAB ΔE or less.

3.3 Experiment 2: Creating fibre blends with mean colour differences of between 15 and 25 CIELAB ΔE

Following the results of the first experiment it became clear that new primaries (with smaller colour differences between them) were required. In addition, only 4-colour

blends were considered because in most practical applications of this work the recipes are likely to contain four primaries. For this experiment, 25 blends were prepared using five groups of four primaries. As already identified, blends prepared using four primaries will have a total of six colour differences within the blend. The average of these colour differences gives the mean colour difference of the blend. The primaries for the blends were selected so that the mean colour difference of the blends would be 25 CIELAB ΔE or less.

3.3.1 The primaries

Sixteen new spun-dyed viscose colours were made available by Lenzing AG. The specification of the fibre is described in section 2.1.2. Each primary (30 g) was carded using the method described in section 2.2. This created uniform webs of fibre where the fibres were aligned in one direction. The primary webs were then folded until opaque and measured using a spectrophotometer, as described in section 2.3, to record the spectral reflectance factors of each primary. The spectral reflectance factors of the primaries were converted to $L^*a^*b^*$ and sRGB values using the methods described in section 2.3.2. The position of the primaries in CIELAB colour space, coloured using their corresponding sRGB values, can be seen in Figure 3.7.

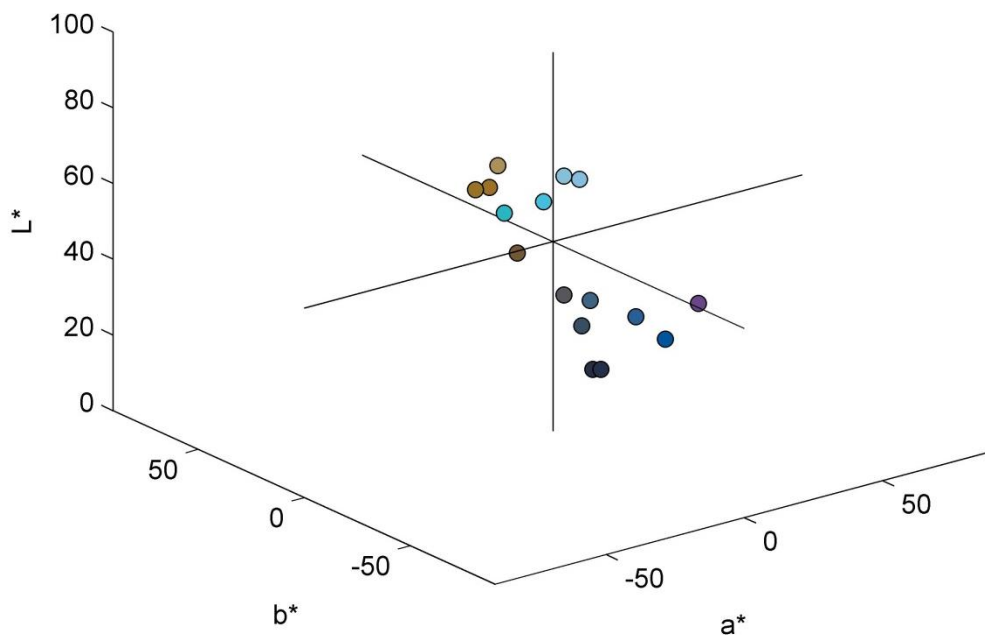


















Figure 3.7 Experiment 2 primaries in CIELAB colour space

Table 3.8 details the $L^*a^*b^*$ and sRGB values for each primary. A coloured key is also included to show the general appearance of the primaries using the sRGB values.

Table 3.8 $L^*a^*b^*$ and sRGB values and appearance of second experiment primaries

Primary number	L^*	a^*	b^*	R	G	B	General appearance (sRGB)
2.1	36.91	0.57	-4.31	85	87	93	
2.2	39.22	6.59	25.61	115	88	51	
2.3	61.31	3.98	31.38	173	145	92	
2.4	68.13	-31.15	-17.54	41	183	196	
2.5	74.36	-9.05	-24.13	134	190	225	
2.6	20.23	3.28	-18.18	37	49	75	
2.7	71.76	-23.54	-26.05	69	191	221	
2.8	74.52	-11.25	-19.71	136	192	218	
2.9	39.07	1.91	-36.39	40	95	151	
2.10	40.86	-3.73	-22.30	62	100	132	
2.11	32.00	-1.00	-15.00	58	78	99	
2.12	36.21	28.28	-31.63	105	71	136	
2.13	19.42	3.06	-14.58	39	47	68	
2.14	50.63	7.11	45.89	152	115	38	
2.15	35.37	4.40	-47.05	0	86	158	
2.16	50.82	11.15	44.65	158	113	41	

Using the $L^*a^*b^*$ values of each primary the colour difference between each pair of primaries was calculated using the method described in section 2.3.2.1. The sixteen primaries were divided into five groups of four primaries (some of the primaries were used more than once). The primaries within each group were selected so that the mean colour difference of each group (calculated by averaging each possible pair of colour differences between the four given primaries), varied from a maximum of 25 CIELAB ΔE for group 1 to a minimum of 15 CIELAB ΔE for group 5. The five groups of

primaries were used to create new blended samples. These samples would be used to further investigate the relationship between the mean colour difference of a group of four primaries and the resulting appearance of blends produced from these primaries as a solid colour or not. The hypothesis was that blends from group 5 should appear more solid than blends from group 1, for example, because the mean colour difference is lower. Table 3.9 to Table 3.13 show the five groups of primaries and their mean colour differences. The sRGB values of the primaries have been used to illustrate the appearance of the primaries within each blend.

Table 3.9 Primaries within group 1 with a mean colour difference of 25 CIELAB ΔE

Group 1: Mean CIELAB ΔE = 25	General appearance (sRGB)
Primary 2.1	
Primary 2.10	
Primary 2.11	
Primary 2.12	

Table 3.10 Primaries within group 2 with a mean colour difference of 22 CIELAB ΔE

Group 2: Mean CIELAB ΔE = 22	General appearance (sRGB)
Primary 2.6	
Primary 2.9	
Primary 2.10	
Primary 2.15	

Table 3.11 Primaries within group 3 with a mean colour difference of 19 CIELAB ΔE

Group 3: Mean CIELAB ΔE = 19	General appearance (sRGB)
Primary 2.9	
Primary 2.10	
Primary 2.11	
Primary 2.13	

Table 3.12 Primaries within group 4 with a mean colour difference of 18 CIELAB ΔE





Group 4: Mean CIELAB ΔE = 18	General appearance (sRGB)
Primary 2.2	
Primary 2.3	
Primary 2.14	
Primary 2.16	

Table 3.13 Primaries within group 5 with a mean colour difference of 15 CIELAB ΔE




Group 5: Mean CIELAB ΔE = 15	General appearance (sRGB)
Primary 2.4	
Primary 2.5	
Primary 2.7	
Primary 2.8	

Table 3.14 to Table 3.18 show the individual colour differences between each pair of primaries within each group. The mean colour difference and maximum colour difference for each group of primaries is also shown. As the mean colour difference of the groups reduces, so does the maximum colour difference.

Table 3.14 Group 1 colour differences (CIELAB ΔE)













Primary no.	sRGB	Primary no.	sRGB	Colour difference (CIELAB ΔE)
Primary 2.1		Primary 2.10		19
Primary 2.1		Primary 2.11		12
Primary 2.1		Primary 2.12		39
Primary 2.10		Primary 2.11		12
Primary 2.10		Primary 2.12		34
Primary 2.11		Primary 2.12		34
Mean colour difference				25
Maximum colour difference				39

Table 3.15 Group 2 colour differences (CIELAB ΔE)













Primary no.	sRGB	Primary no.	sRGB	Colour difference (CIELAB ΔE)
Primary 2.6		Primary 2.9		26
Primary 2.6		Primary 2.10		22
Primary 2.6		Primary 2.15		33
Primary 2.9		Primary 2.10		15
Primary 2.9		Primary 2.15		12
Primary 2.10		Primary 2.15		27
Mean colour difference				22
Maximum colour difference				33

Table 3.16 Group 3 colour differences (CIELAB ΔE)













Primary no.	sRGB	Primary no.	sRGB	Colour difference (CIELAB ΔE)
Primary 2.9		Primary 2.10		15
Primary 2.9		Primary 2.11		22
Primary 2.9		Primary 2.13		29
Primary 2.10		Primary 2.11		12
Primary 2.10		Primary 2.13		24
Primary 2.11		Primary 2.13		13
Mean colour difference				19
Maximum colour difference				29

Table 3.17 Group 4 colour differences (CIELAB ΔE)

























Primary no.	sRGB	Primary no.	sRGB	Colour difference (CIELAB ΔE)
Primary 2.2		Primary 2.3		23
Primary 2.2		Primary 2.14		23
Primary 2.2		Primary 2.16		23
Primary 2.3		Primary 2.14		18
Primary 2.3		Primary 2.16		18
Primary 2.14		Primary 2.16		4
Mean colour difference				18
Maximum colour difference				23

Table 3.18 Group 5 colour differences (CIELAB ΔE)

Primary no.	sRGB	Primary no.	sRGB	Colour difference (CIELAB ΔE)
Primary 2.4		Primary 2.5		24
Primary 2.4		Primary 2.7		12
Primary 2.4		Primary 2.8		24
Primary 2.5		Primary 2.7		15
Primary 2.5		Primary 2.8		5
Primary 2.7		Primary 2.8		14
Mean colour difference				15
Maximum colour difference				24

3.3.2 Preparing the blended samples

Five generic recipes were chosen to produce blended samples from each group of primaries. For each group, one sample was made per recipe. This gave a total of 25 blends to prepare. Table 3.19 shows the generic recipes of the blends. The sample size for each blend was 30 g and the blends were prepared using the same method as described in section 2.2.

Table 3.19 Generic blend recipes for groups 1 to 5

	Primary a (%)	Primary b (%)	Primary c (%)	Primary d (%)
Recipe 1	25	25	25	25
Recipe 2	20	30	20	30
Recipe 3	50	25	15	10
Recipe 4	15	15	15	55
Recipe 5	30	20	30	20

Once the samples were prepared, the spectral reflectance factors for each blend were recorded using the spectrophotometer and the data was converted to $L^*a^*b^*$ and sRGB values in MATLAB using the method described in section 2.3.

The following graphs show the position of the carded blends, for each group of primaries, in CIELAB colour space.

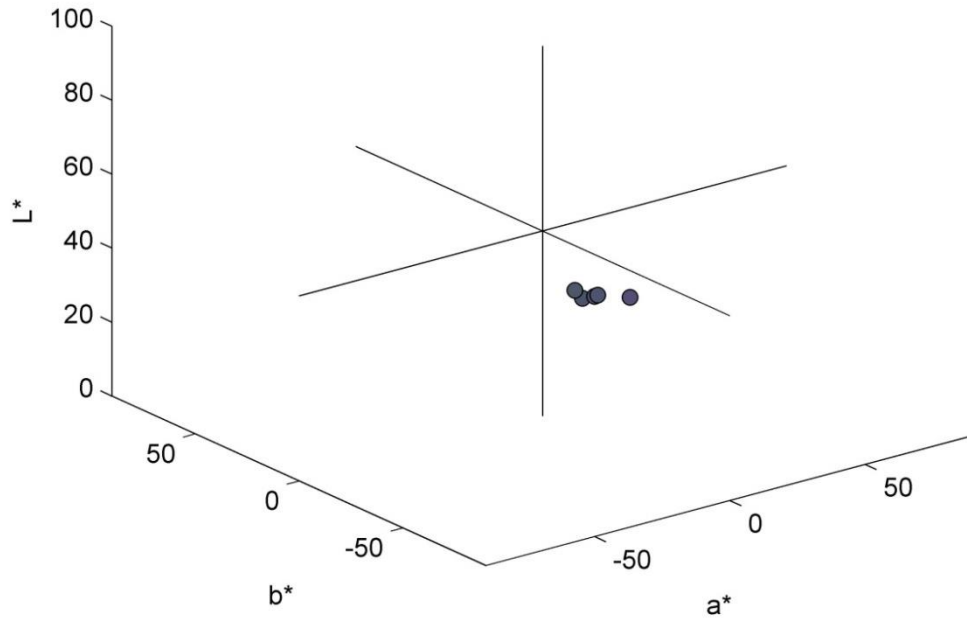


Figure 3.8 Group 1: blended samples in CIELAB colour space

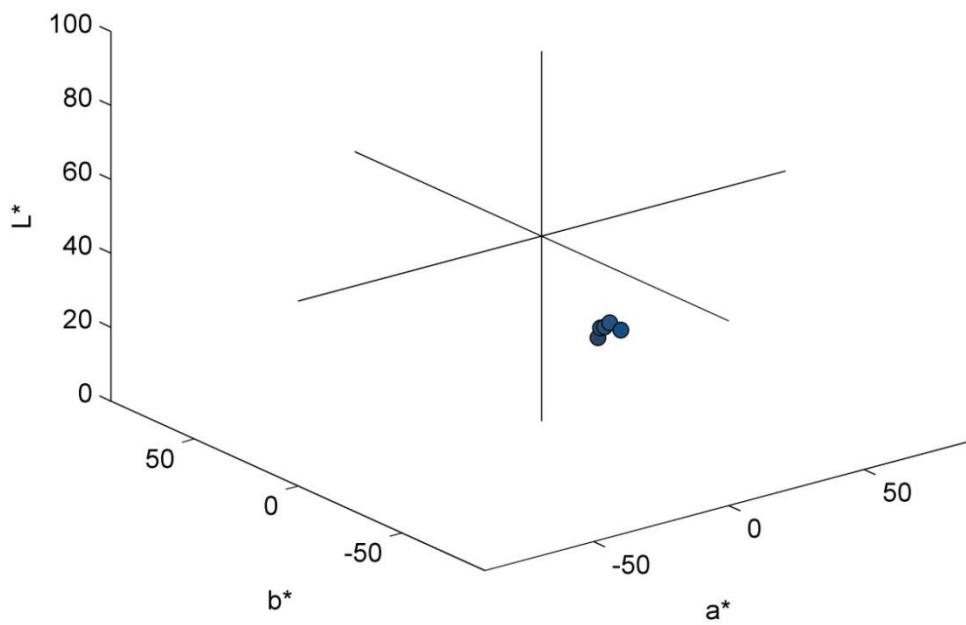


Figure 3.9 Group 2: blended samples in CIELAB colour space

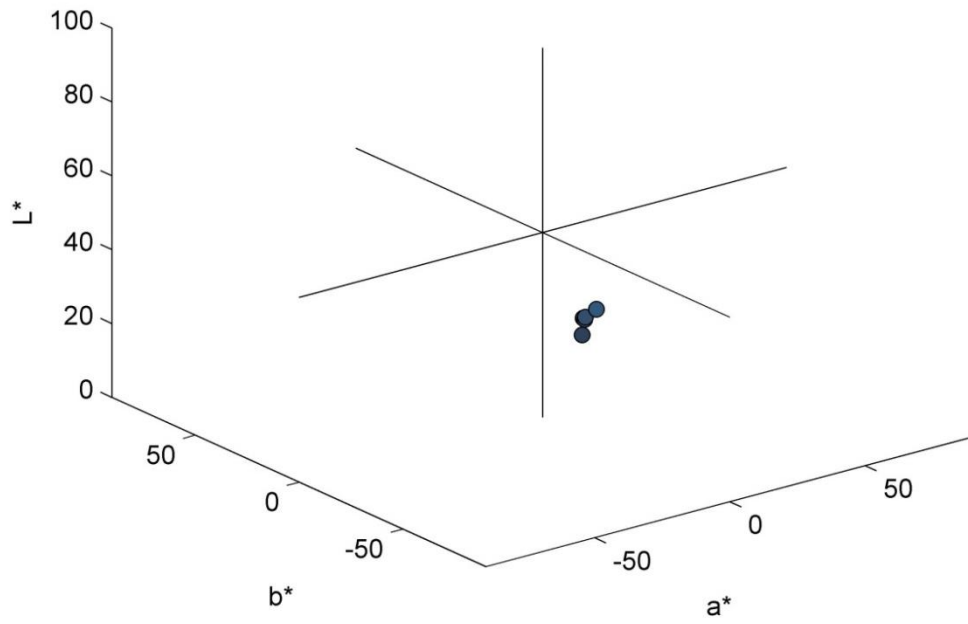


Figure 3.10 Group 3: blended samples in CIELAB colour space

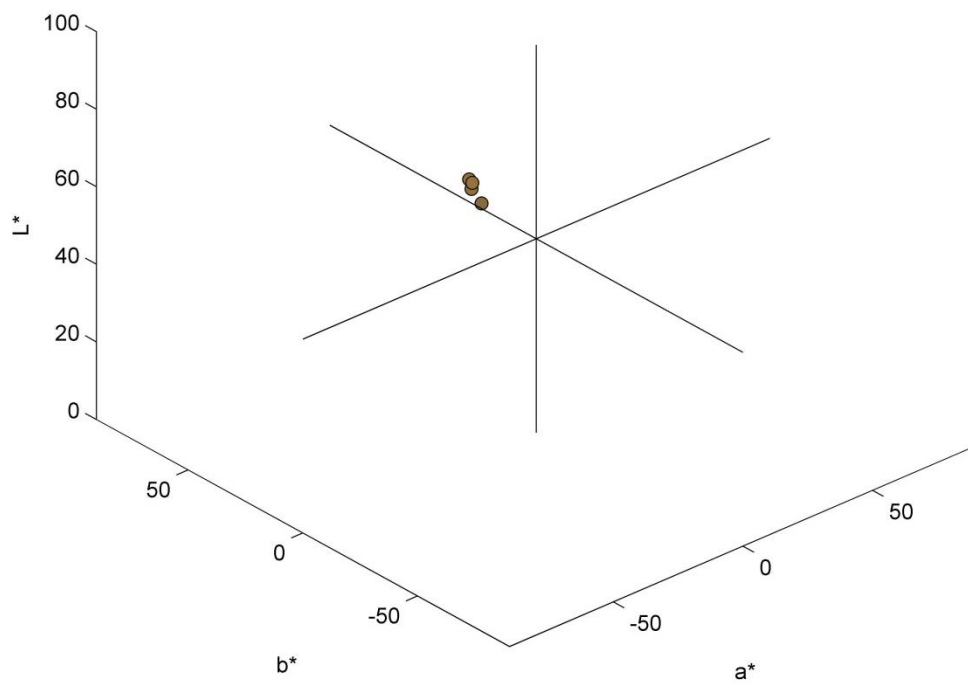


Figure 3.11 Group 4: blended samples in CIELAB colour space

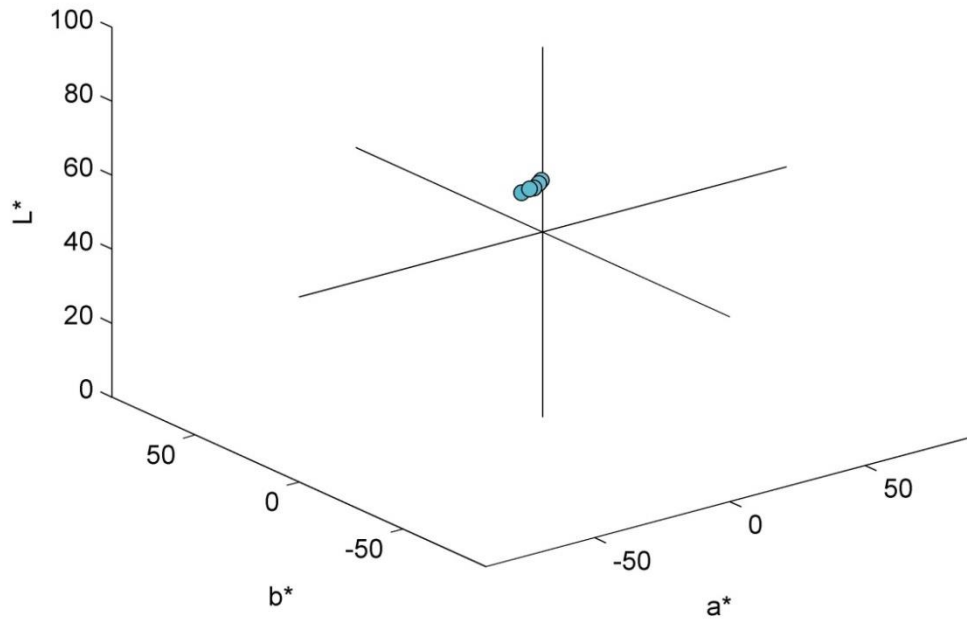


Figure 3.12 Group 5: blended samples in CIELAB colour space

3.3.3 Visual assessment of blended samples

The 25 blended samples and 8 primary samples were visually assessed by ten participants (some, but not all, of the participants took part in Experiment 1) using the procedure described in section 2.5. The samples were randomised before being presented to the participants and the participants were not told how many primaries were within each sample. The participants were again asked to assess the visual appearance of the samples in terms of solidity of colour.

3.3.3.1 Visual assessment results

The results of the participant observations were collated and scored as outlined in section 2.5. The results for each group can be seen in Table 3.20 to

Table 3.24.

Table 3.20 Group 1 visual assessment results showing the percentage of participants who believed that a sample speared as a solid colour






Group 1	Mean CIELAB ΔE	Participant score	sRGB colour
Blend 2.1	25	5 %	
Blend 2.2	25	5 %	
Blend 2.3	25	5 %	
Blend 2.4	25	10 %	
Blend 2.5	25	15 %	

Table 3.21 Group 2 visual assessment results showing the percentage of participants who believed that a sample speared as a solid colour






Group 2	Mean CIELAB ΔE	Participant score	sRGB colour
Blend 2.6	22	35 %	
Blend 2.7	22	55 %	
Blend 2.8	22	60 %	
Blend 2.9	22	40 %	
Blend 2.10	22	45 %	

Table 3.22 Group 3 visual assessment results showing the percentage of participants who believed that a sample speared as a solid colour






Group 3	Mean CIELAB ΔE	Participant score	sRGB colour
Blend 2.11	19	50 %	
Blend 2.12	19	45 %	
Blend 2.13	19	75 %	
Blend 2.14	19	50 %	
Blend 2.15	19	55 %	

Table 3.23 Group 4 visual assessment results showing the percentage of participants who believed that a sample speared as a solid colour











Group 4	Mean CIELAB ΔE	Participant score	sRGB colour
Blend 2.16	18	80 %	
Blend 2.17	18	85 %	
Blend 2.18	18	85 %	
Blend 2.19	18	95 %	
Blend 2.20	18	80 %	









Table 3.24 Group 5 visual assessment results showing the percentage of participants who believed that a sample speared as a solid colour

Group 5	Mean CIELAB ΔE	Participant score	sRGB colour
Blend 2.21	15	100 %	
Blend 2.22	15	90 %	
Blend 2.23	15	100 %	
Blend 2.24	15	95 %	
Blend 2.25	15	100 %	

Unlike experiment 1, in this experiment not all of the primary blends were scored as a solid colour by 100 % of participants. It is likely that this is an effect of the reduced colour differences between the primaries within the blended samples. The primaries within the blended samples have blended more successfully, producing blended webs which appear more homogenous in colour compared to those in experiment 1, and are therefore more difficult to distinguish as being composed of one colour or more.

The results of the visual assessments for the primary blends are included in Table 3.25.

Table 3.25 Visual assessment results of the primaries showing the percentage of participants who believed that a sample speared as a solid colour

Primaries	Mean ΔE	Participant score	sRGB colour
Primary 2.3	n/a	95 %	
Primary 2.5	n/a	95 %	
Primary 2.6	n/a	95 %	
Primary 2.7	n/a	100 %	
Primary 2.9	n/a	80 %	
Primary 2.10	n/a	85 %	
Primary 2.14	n/a	100 %	
Primary 2.16	n/a	100 %	

3.3.4 Discussion of results

The results of this experiment showed a clear trend between the mean colour difference of a group of four primaries and the appearance of these blends as a solid colour or not. This is illustrated in Figure 3.13 which shows the mean colour difference of the blends plotted against the percentage (%) of participants who assessed the blends to be a solid colour. As the mean colour difference of the blends reduces, the percentage of participants who observe the blends as solid colours increases, from 5 % to 100 %. The high R^2 (coefficient of determination) value, 0.8869, indicates a high relationship between the mean CIELAB ΔE and the appearance of a blend as a solid colour.

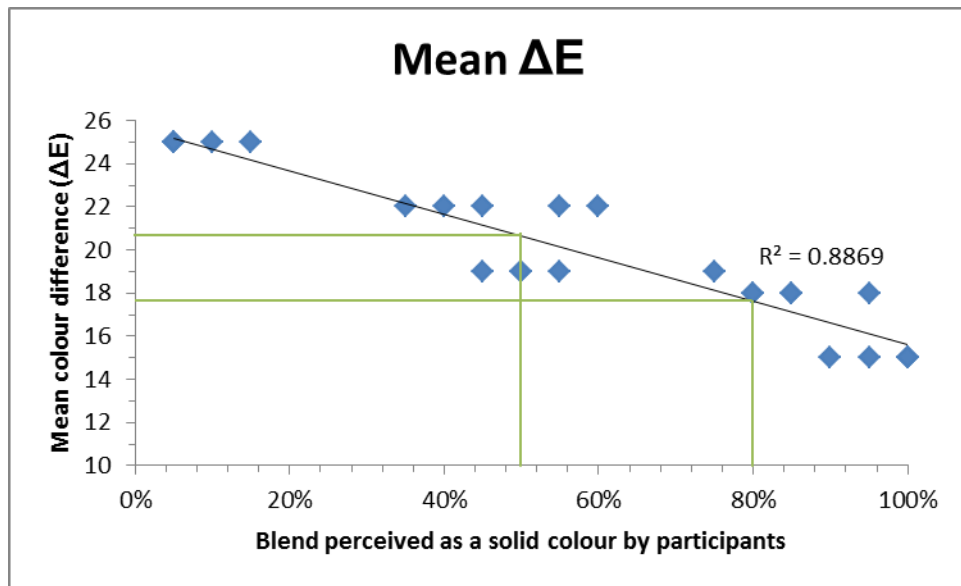


Figure 3.13 Mean colour difference (CIELAB ΔE) of blends and % of participants who perceived the blends as a solid colour

As identified, the primaries that were individually blended and observed alongside the mixed-blends did not score as a solid colour to 100 % of participants every time. In this experiment the primaries scored as being seen as a solid colour by between 80-100 % of participants. This indicates that being able to determine whether a web of coloured fibre is composed of one colour (or more than one colour), when the average colour difference of the primaries within a blend is low, is difficult even at close proximity. Using Figure 3.13, an estimate can be taken as to what the mean colour difference of a group of primaries should be in order for a blend to appear as a solid colour to a selected percentage of participants. If a reading is taken from the figure at 80 %, the lowest percentage that a primary scored, then the mean colour difference for blends to appear as a solid colour is less than 18 CIELAB ΔE . However, this threshold is probably too severe. If we take a lower threshold of 50 % of people viewing the sample as solid (or people viewing it as solid 50 % of the time) then the threshold for the mean colour difference of four primaries in a blend is approximately 21 CIELAB ΔE .

3.3.5 Conclusions

Experiment 2 used a new range of spun-dyed fibre to create 4-colour blended samples with a mean colour difference of between 15 CIELAB ΔE and 25 CIELAB ΔE , much lower

than in experiment 1. The mean colour difference was calculated by averaging the colour differences of the six possible colour differences between the four primaries within a blend. It was observed that similarly to experiment 1, as the mean colour difference of a blended sample reduced, the more likely the sample was to appear as a solid colour to participants.

The participants who took part in the visual assessment of the blends saw both the 25 blended samples and 8 primary samples. It was noted that the participants did not always identify primary blends as appearing as a solid colour, with some primary blends appearing as a solid colour to 80 % of participants (rather than 100 % of participants as seen in experiment 1). The increased difficulty in discriminating between samples composed of one primary and samples composed of multiple primaries can be attributed to the lower colour differences between the primaries within the blends. The threshold for determining the mean colour difference required for a blend to appear as a solid colour was reduced to 50 % to reflect the participant's responses. In addition, the threshold of 50 % reflects the standard threshold for colour difference detection in colour psychophysics.

The results showed good correlation between the mean colour difference of a blend and its appearance as a solid colour. The coefficient of determination (R^2) was used to quantify this relationship and the high R^2 value (0.8869) indicated that there was a good relationship between the two sets of data. Using Figure 3.13, a reading was taken at 50 % of participants viewing a sample as a solid colour which gave a recommended mean colour difference of less than 21 CIELAB ΔE for a 4-colour blend to appear as a solid colour. The samples in this experiment were viewed at quite a close distance of 45 cm. If this distance were to increase then we would expect to see a rise in the acceptance of blends which had a higher mean colour difference as a solid colour.

3.4 Summary

If the mean CIELAB colour difference (ΔE) required for a 4-colour blend to appear as a solid colour is known, then it is possible to define the number of primaries required to cover a specific volume of colour space so that the primaries are appropriately spaced.

The volume of colour space could be a large area which covers the majority of colour space, or it could be a smaller volume focusing on one hue, for example blues. Primaries could be spaced using the optimum mean CIELAB ΔE colour difference, in this case to be less than 21 CIELAB ΔE , to fill the required volume of colour space. As the volume of colour space increases, so would the number of primaries required to cover the given area.

This novel approach to producing coloured webs, which could then be spun into yarn and knitted or woven, could provide a credible way for textile companies to utilise spun-dyed fibres with environmental and economic benefits. Depending on the range of colours required, calculations could be made as to how many primaries would be needed in order to produce those colours through blending four colours. By increasing the colour difference between primaries it would also be possible to produce blends with the intention of create melanges.

In order to calculate how many primaries may be required to cover a certain volume of colour space, further work was required. The next chapter explores this idea with consideration as to its application within the textile industry. This will include an investigation into the number of primaries to cover both a large volume of CIELAB colour space and a smaller volume of CIELAB colour space. Knitted samples will also be made from these blends in order to assess whether the perception of the 4-colour blends as a solid colour is affected in any way by the change from webbed fibre to knitted fabric.

Chapter 4 Developing a relevant colouration system for industry

4.1 Introduction

In chapter 3 the concept that four different coloured primaries could be blended together to create a solid web was explored. The results showed a strong relationship between the mean colour difference of a 4-colour blended sample and its appearance as a solid colour. In both experiment 1 and experiment 2 of chapter 3 it was observed that as the mean colour difference (calculated by averaging the colour differences between each pair of primaries within a blend) of a blend reduced, the likelihood of a blend appearing as a solid colour increased. In experiment 2 of chapter 3 the mean colour difference of a 4-colour blend, in order for it to appear as a solid colour, was less than 21 CIELAB ΔE . If the method of blending four solid colours to produce multiple new solid colours is to be acceptable as a competitive method of colouring textiles in industry, then further work is required to understand the scale or number of primaries required to cover either a large proportion, or selected area of colour space.

Important research questions for this chapter therefore included:

1. Identifying the number of primaries required to cover a given volume of gamut within colour space so that all 4-colour groups are blended to appear as solid colours;
2. Identifying how the mean colour difference of 4-colour blends is affected as the number of primaries is varied;
3. Identifying whether the number of primaries required to cover a specific area of colour space is feasible for industry or not.

To answer these important questions, investigative work was undertaken using both MATLAB and practical experiments using dyed fibre. MATLAB was used to simulate the distribution and number of primaries within a given gamut and fibre blending was used to check that the application of the theory into practice within the fashion industry could be successful.

4.2 Colour space and the distribution of primaries within a large gamut

Firstly, the size of a given gamut and the consequent distribution of primaries within that gamut, depending on the distance between each primary, were explored. To do this, two different sized gamuts within CIELAB colour space (one large and one small) were created.

Three important MATLAB functions are used in this chapter and these are described in the following:

inhull.m – The inhull function is a MATLAB command that simply calculates whether a point is within the convex hull; the three-dimensional space within a specified gamut outlined by a set of points. The convex hull is the. The inhull.m file is available for download from MATLAB Central (D'Errico, 2012). The point of this function is that if a gamut is defined by a set of points in 3-dimensional colour space, then it is possible to randomly select other points in the colour space and use the inhull function to deduce whether they are inside the gamut of the original set of points or not. If they are within the gamut then they can be added and in this way the gamut can be populated.

maxminc.m – This function was written by Cheung and Westland (2006) and selects a set of n points from N points (where $N > n$). The n points are selected from CIELAB colour space so that they are optimally dissimilar. This method has been adopted as a way to select n primaries from a larger set of N points.

delaunay.m – Delaunay triangulation is a method of covering a 2-dimensional space by points so that every part of the space falls into a triangle whose vertices are formed by three of the points. The delaunay.m file is part of MATLAB and the input to the function is a set of points in the 2-dimensional space; the function groups the points into triangles so that every possible point in the space falls into one, and only one, of the triangles (MathWorks. 2014a). The function also works in 3-dimensional space and is used in this way in this thesis. In the 3-dimensional case the delaunay.m function takes a set of points (colour primaries) as input and generates tetrahedra from these points so that every part of the colour space covered by the primaries falls into one of

the tetrahedra; the vertices of each tetrahedron being formed by four of the colour primaries.

Using the functions `inhull`, `maxminc` and `delaunay` it was possible to distribute a specified number of primaries within each gamut and group these primaries into 4-colour groups or tetrahedra. The `inhull` function was used to densely populate a 3-dimensional colour gamut in CIELAB space defined by a small set of samples on the periphery. The `maxminc` function was then used to select n primaries from the gamut. The `delaunay` function was then used to group the primaries so that they formed tetrahedra. The mean colour difference for the primaries for each tetrahedron was then calculated in the same way as previously calculated in chapter 3; by calculating the colour difference between each pair of primaries within the group of four primaries and averaging the colour differences to produce the mean.

Figure 4.1 further illustrates this process.

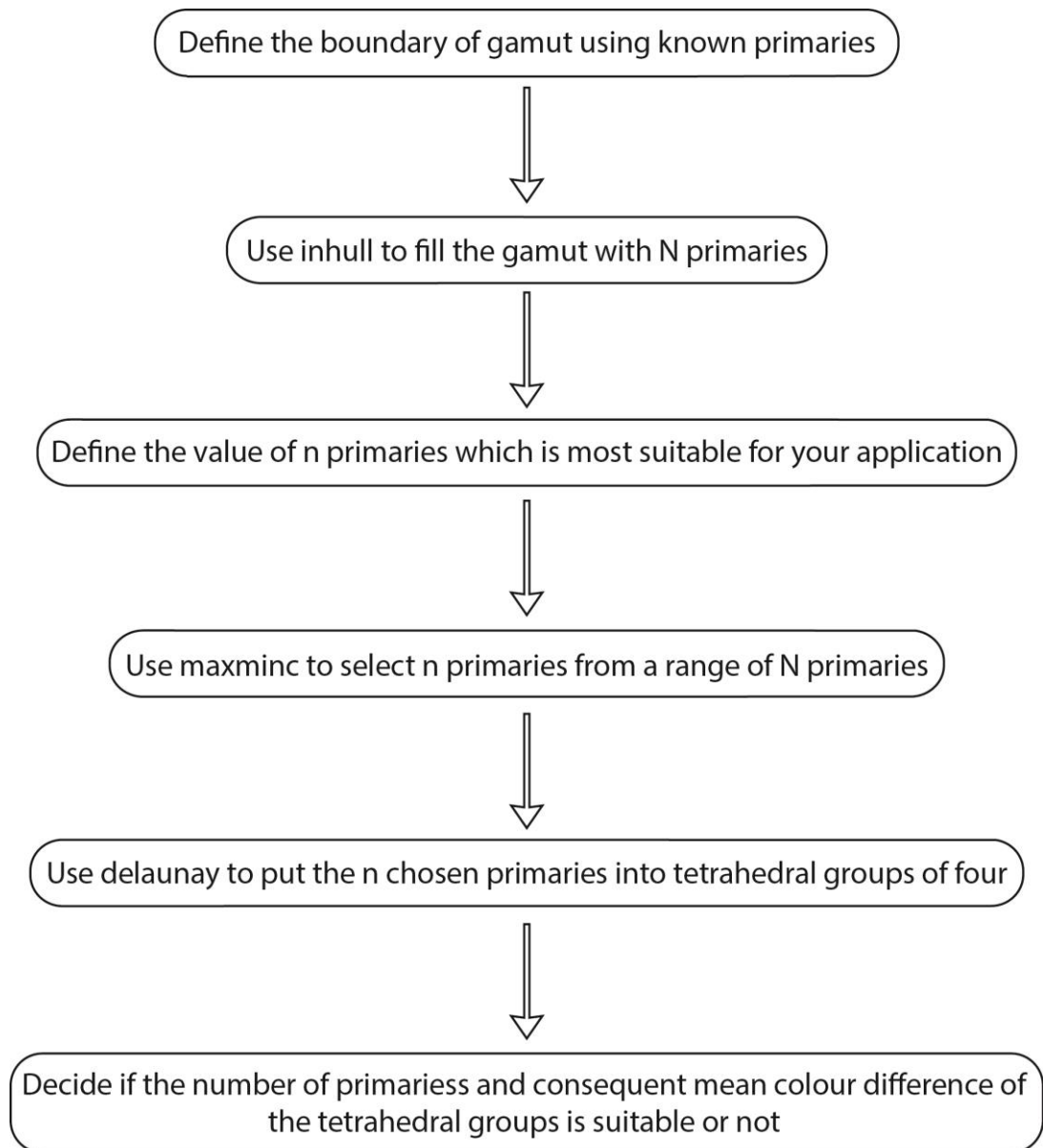


Figure 4.1 Flow chart showing the process of defining n number of primaries within a gamut

It was possible to vary the number of primaries (n), and therefore the number and spacing of the tetrahedra, within the gamuts. When the number of primaries was increased, the mean colour difference of the tetrahedra decreased. It was also possible to predict how many primaries would be required to fill a specific sized gamut depending on the required mean colour difference of the tetrahedral blends. The following sub-sections outline the investigative method used in MATLAB.

4.2.1 Producing a large gamut

A large gamut within CIELAB colour space was defined by firstly selecting a number of primaries to form the outer perimeter of the desired gamut. Munsell's understanding of the non-uniformity of colour space gave an appropriate starting place to define the primaries. Using a virtual Munsell colour atlas (VCS, 2013) one hue from each of the 5 main Munsell hues (red, yellow, green, blue and purple) and 5 intermediate hues (yellow-red, green-yellow, blue-green, blue-purple and red-purple) were selected. Samples of each hue were selected so that they had the highest possible chroma (note that this varies depending upon the hue; the Munsell value at maximum chroma also varies depending upon the hue). If a hue had more than one sample with the same maximum chroma then the sample with a Munsell value closest to 5 was chosen. The hues were referenced on the virtual atlas using CIE XYZ coordinates. These coordinates were converted to $L^*a^*b^*$ values using MATLAB to give 10 highly chromatic samples. The $L^*a^*b^*$ values of the white and black primaries used in experiment 1 of chapter 2 were also added to the 10 Munsell colours to give a total of 12 points in CIELAB colour space. The $L^*a^*b^*$ values of the white and black primaries from experiment 1 were used – rather than using, say $L^* = 100$, $a^* = 0$, $b^* = 0$ for the white - because they represented realistic colours in a textile system. It would be unrealistic to expect to create a white fibre with maximum lightness ($L^* = 100$) or a black fibre with zero lightness. Example code for producing the 12 outer points of the colour gamut can be seen in Appendix VIII.

These 12 points formed the boundary of the gamut as illustrated in Figure 4.2. Figure 4.3 shows the primaries on the a^* and b^* axes, as seen from directly above the L^* axis, giving an illustration as to the shape of the gamut. Note that the lightness at which the maximum chroma occurs is different for each hue which is a reflection of Munsell's irregular colour space.

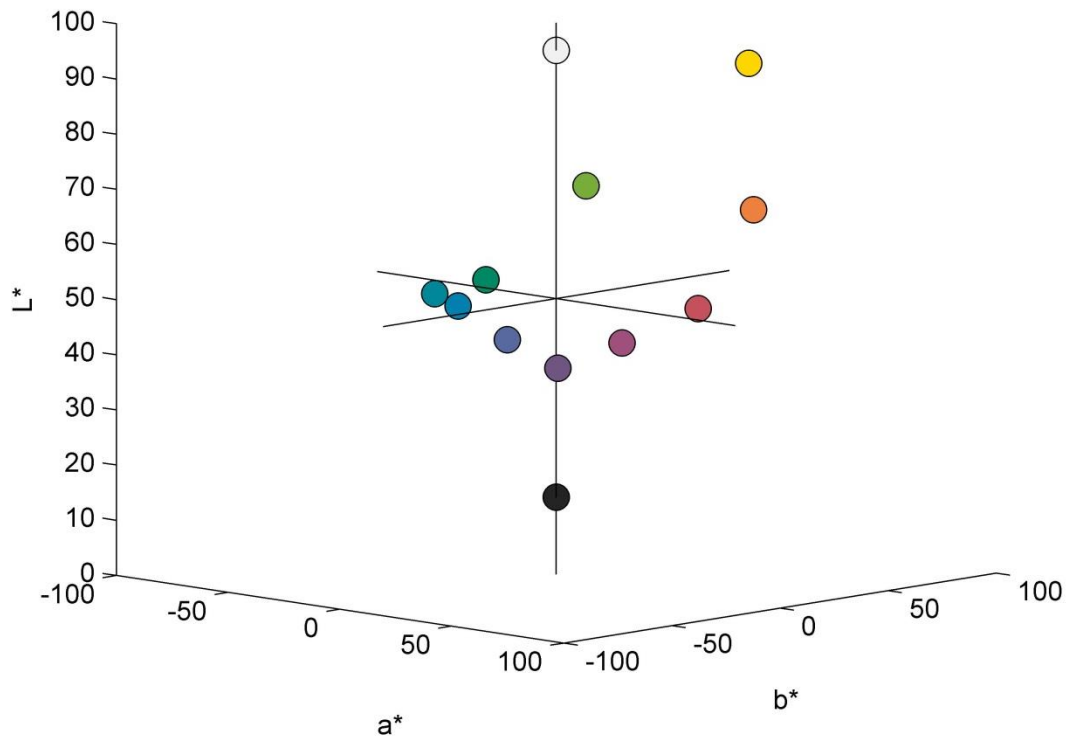


Figure 4.2 The 12 CIELAB colours to define the size of experimental gamut

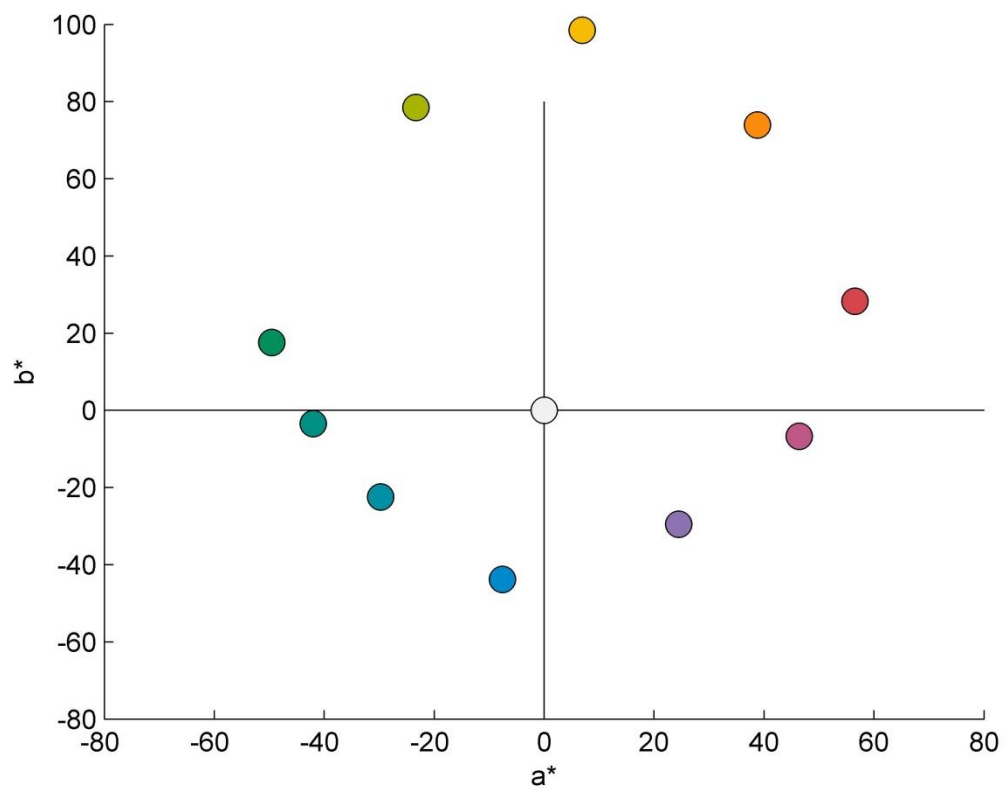


Figure 4.3 The CIELAB colours seen from directly above the L^* axis

4.2.2 Filling the large gamut with primaries

The 12 colours define the gamut that will be explored. The space within the boundaries of the 12 colours can be referred to as the gamut or the hull. The next step was to fill the hull with a dense number of potential primaries using the function `inhull` (D'Errico, 2012). It may have been possible to express the gamut mathematically; however, in this work, a more pragmatic approach was adopted whereby the gamut was populated by points to form a set of points that were all within the gamut. One reason why this approach was taken was because the unit required for the `maxminc` function (see section 4.2.3) is a set of points rather than a mathematical description of a gamut.

The gamut was densely populated by creating a loop of MATLAB code whereby a random colour was generated. If the random colour was within the hull then the random colour was accepted and the $L^*a^*b^*$ coordinates saved. If the random colour was outside of the hull then a new random colour was generated until the next colour did fit inside the hull. This loop was continued until 10,000 colours were distributed within the hull of the 12 boundary colours. The use of 10,000 primaries was an arbitrary number which sufficiently filled the hull defined by the 12 outer colours. Example code can be seen in Appendix IX.

The dense distribution of the 10,012 colours (the 12 original colours and the 10,000 that were added) can be seen in Figure 4.4 and Figure 4.5. Figure 4.4 in particular shows the non-uniform shape of the gamut within CIELAB colour space.

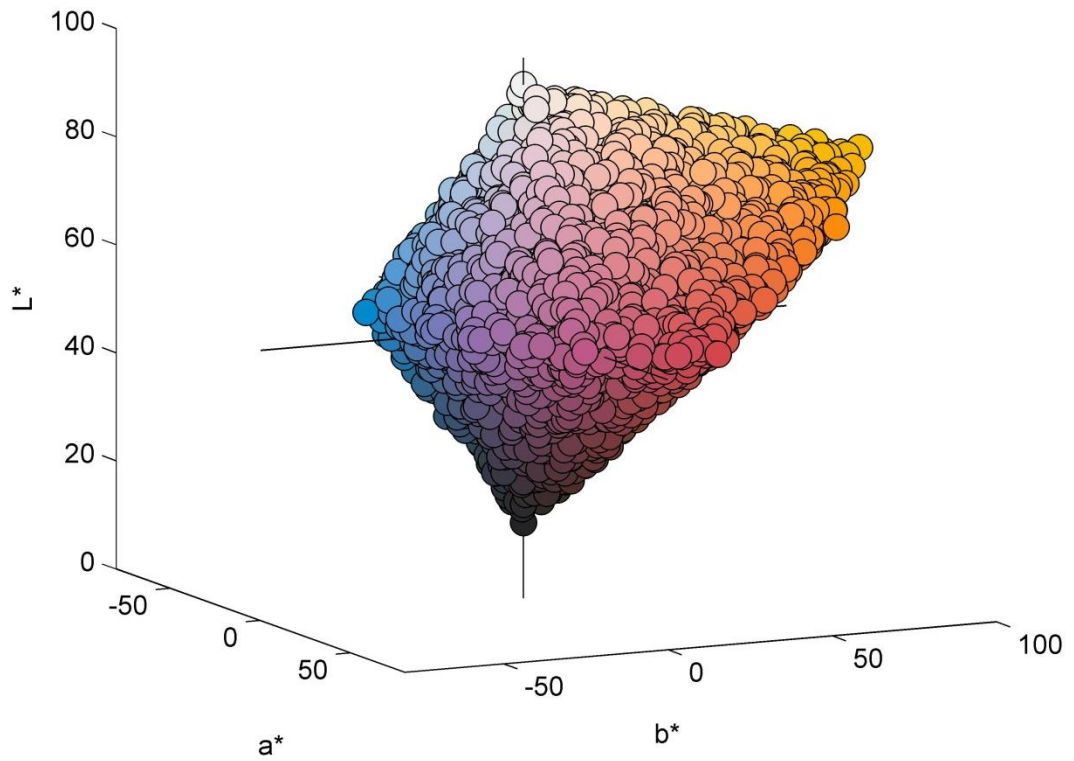


Figure 4.4 The 10,012 colours plotted in CIELAB colour space

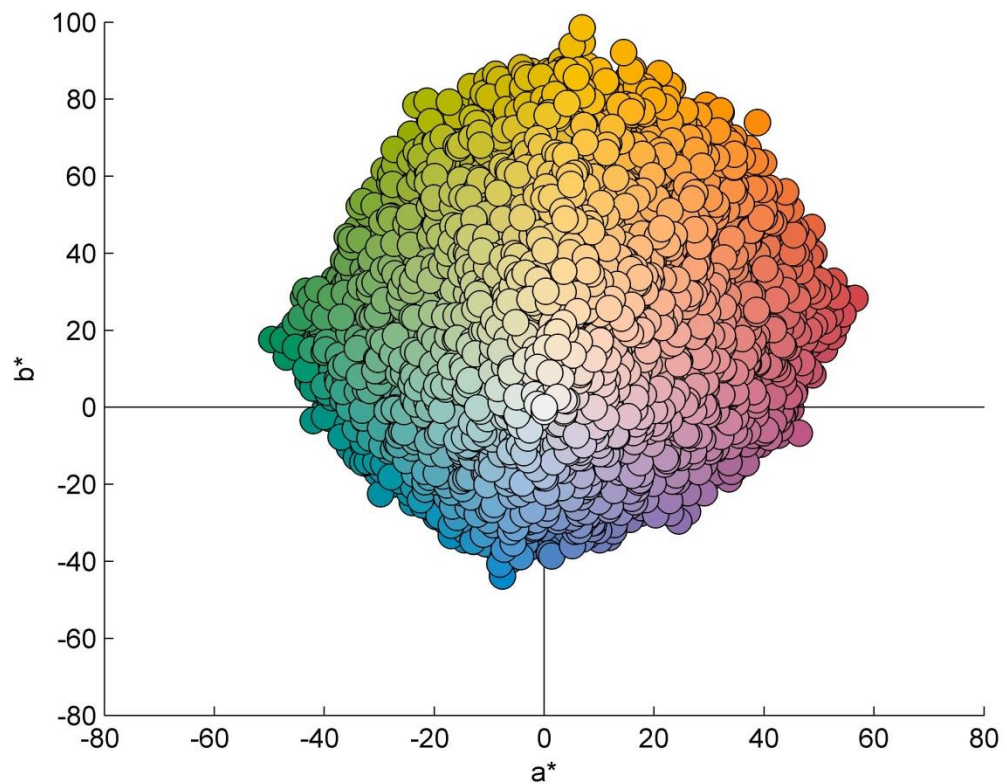


Figure 4.5 The 10,012 colours in CIELAB colour space, looking directly down the L^* axis onto the a^* and b^* axes

4.2.3 Creating 4-primary tetrahedra using maxminc and Delaunay triangulation

The next step used maxminc (Cheung & Westland, 2006) to select a subset of the 10,012 colours so that the points in the subset were as far apart as they can be from one another. The maxminc code can be used to create a subset of 1 to 10,012 samples. This was done to produce 12 alternative primary systems with 10, 20, 30, 40, 50, 60, 65, 70, 80, 90, 100 and 150 primaries. As is expected, as the number of primaries is increased the primaries become less spaced out.

For each of the primary systems Delaunay triangulation was used to define the four primaries of each 4-colour group or tetrahedron. In two-dimensional space, Delaunay triangles are three points connected to make a triangle whose three vertices are intersected by a circle which includes no other points, for example see Figure 4.6. Points A, B and C make a green triangle and there are no other points within the circumcircle (MathWorks, 2014a; Weisstein, 2014).

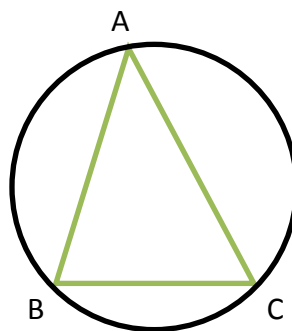


Figure 4.6 Example of a two-dimensional Delaunay triangle

Figure 4.7 shows another example of a Delaunay triangle. Despite there being another triangle (the red triangle) present, the third vertex (D) of the red triangle is outside of the circumcircle containing the green triangle.

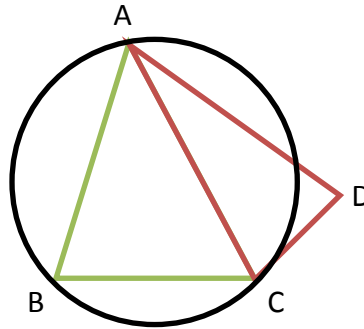


Figure 4.7 Example of a two-dimensional Delaunay triangle

Figure 4.8 is not a Delaunay triangle as there are more than 3 points within the circumcircle making two triangles.

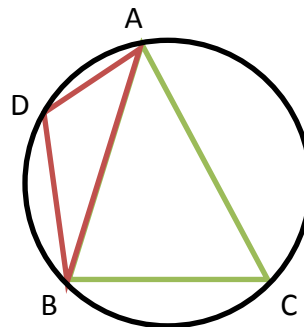


Figure 4.8 Example of an incorrect Delaunay triangle

The fundamentals of Delaunay triangulation can be applied to three-dimensional spaces. The principal is the same; however, because the points are in three dimensions, the points are connected to produce a tetrahedron within a sphere, for an example see Figure 4.9.

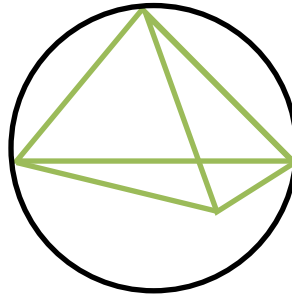


Figure 4.9 Three-dimensional Delaunay tetrahedron

With an increase in points, there is an increase in the number of tetrahedra that can be defined. Delaunay triangles can be produced in MATLAB using the standard function `Delaunay` (MathWorks, 2014a). Appendix X gives example code for applying the Delaunay triangulation function in 3-dimensional space.

Figure 4.10 shows the outcome of the Delaunay triangulation for the example data set in Appendix X.

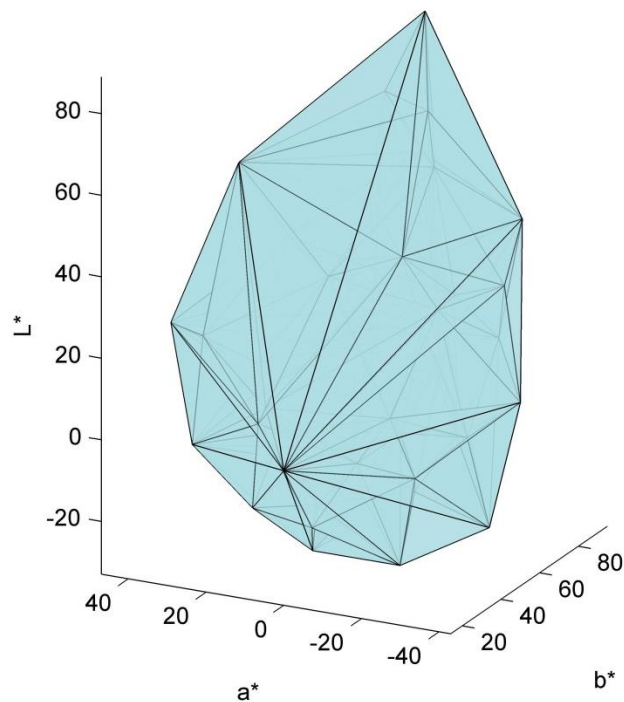


Figure 4.10 Example of 50 primaries connected using Delaunay triangulation in CIELAB colour space

MATLAB script was written to combine the delaunay and maxminc functions, using a loop to vary the number of primaries within the hull. The number of primaries was varied from 10 to 200. The first primary selected was always the white primary (this is a property of the maxminc function). The following primaries were selected according to the delaunay and maxminc functions. Appendix XI shows example code for creating a loop for selecting the tetrahedra using points within the gamut. For each loop of the script (10 primaries, 20 primaries etc.), the number of tetrahedra required to fill the hull and the average mean colour difference of the tetrahedra for each condition was recorded. The whole script was run ten times so that average calculations could be made as to the number of primaries, tetrahedra and mean colour difference of the tetrahedra. The standard deviation of the results was recorded to identify whether the results were consistent with each new generation of 10,000 primaries.

4.2.4 Results

The results showed that as the number of primaries selected within the hull increased, so did the number of tetrahedra. This was an expected result as with each increase in the number of primaries, the three-dimensional space was divided more finely. With an increase in tetrahedra, it was also expected that the mean colour difference of the tetrahedral primaries would decrease. It was not however known to what extent the mean colour difference of the tetrahedra would decrease as the number of primaries increased. Table 4.1 shows the average results (using 10 runs of the script) for the number of tetrahedra and the mean colour difference of the tetrahedra within the gamut depending on how many primaries were used.

Table 4.1 MATLAB results showing the number of primaries within the gamut versus the number and mean colour difference of tetrahedral blends

Number of primaries	Average no. of tetrahedra	Standard deviation of no. of tetrahedra	Average mean CIELAB ΔE of tetrahedra	Standard deviation of mean CIELAB ΔE of tetrahedra
10	16	0.82	60	0.62
20	61	1.84	44	0.38
30	112	2.57	38	0.54
40	165	3.92	33	0.45
50	220	4.54	31	0.41
60	275	6.92	28	0.33
70	333	7.62	27	0.42
80	394	8.03	25	0.34
90	452	4.43	24	0.22
100	517	7.76	23	0.20
150	817	9.60	20	0.26
200	1131	11.21	18	0.23

It can be seen that as the number of primaries increases, so does the number of tetrahedra used to fill the gamut. It is also noted that with the increase in the number of tetrahedra, the mean colour difference of the tetrahedra decreases. Whilst the standard deviation of the results of the average number of tetrahedra within the gamut increases with the increase in the number of primaries (from 0.82 to 11.21), the standard deviation of the mean colour difference of the tetrahedra generally decreases with the more primaries that are used. The standard deviation of the mean colour difference of the tetrahedra is also much lower (between 0.20 and 0.62) than the average results for the number of tetrahedra (between 0.82 and 11.21).

Figure 4.11 shows the results of the number of primaries plotted against the mean colour difference of the tetrahedral blends. Using the graph, a reading can be taken depending on the acceptable mean colour difference of the blends. For example, if a mean colour difference of 20 CIELAB ΔE is acceptable for producing solid blends then 125 primaries would be needed to cover this particular gamut. However, if a higher mean colour difference of 23 CIELAB ΔE was acceptable then the number of primaries needed would reduce to approximately 85 primaries.

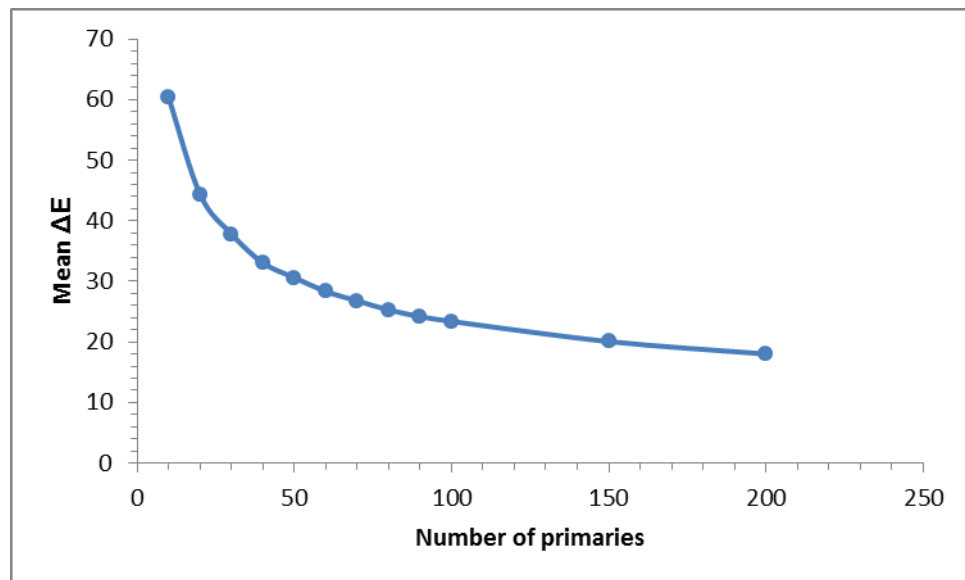


Figure 4.11 Number of primaries versus mean colour difference of blends

The results of the participant observations in chapter 3 suggest that a mean colour difference of a group of 4 primaries should be less than 21 CIELAB ΔE in order for the blend to appear as a solid colour to 50% or more of observers. From these results, it would require approximately 125 primaries to fulfil this criterion. In the literature review it was noted that Birla Cellulose (2012b) readily stock 69 spun-dyed colours. Whilst 125 primaries is quite an increase on this number, it is not unrealistic, especially when the potential number of new colours that could be created as blends from the 125 primaries is considered. Using Table 4.1 as a reference, if 100 primaries are used in a colouration system, then there are approximately 517 tetrahedral blends of four-primaries. If ten colours are made from each of these tetrahedral groups then there are already 5,170 solid blends that can be produced (517×10). This is a huge increase in the number of spun-dyed colours a company could offer and allows unique colours to be produced in varying quantities depending on the application or customer. In reality the number of discernible colours achievable from 100 primaries is probably more than 1 million if it is considered that humans are estimated to be able to see up to 10 million discernible colours (Goldstein, 1996; Judd & Wyszecki, 1975). It is also worth noting that this gamut is particularly large with very saturated outer primaries. In reality a company may not be able to physically produce spun-dyed fibres of this saturation. In a practical application the outer primaries of a gamut must be defined using known colours that can be produced using the spun-dyeing process.

It may be that this number of primaries, despite covering a large proportion of colour space is too many for a company to stock. In this case, offering a select number of colours or the most popular colours may be more appealing. The next sub-section will build upon this idea, defining a smaller gamut of colour space and calculating the number of primaries that would be required to cover it.

4.3 Colour space and the distribution of primaries within a small gamut

Depending on the production capabilities of a textile company, or the range of coloured textiles they offer, it may not be necessary to have a system whereby almost any possible colour is produced. It may be more appropriate for a textile company to offer a select range of colours which covers one or more smaller areas of colour space.

Therefore, in this section, the method of plotting tetrahedral blends (developed in section 4.2) is applied to a smaller volume of colour space.

4.3.1 Producing a small gamut

Using a similar MATLAB script as described in section 4.2, the same large gamut (defined by 12 highly chromatic colours and filled with 10,000 colours) was produced. However, in this instance, the gamut was reduced to only include primaries with an L^* value of less than 27. This resulted in 68 colours within the bottom section of colour space, see Figure 4.12.

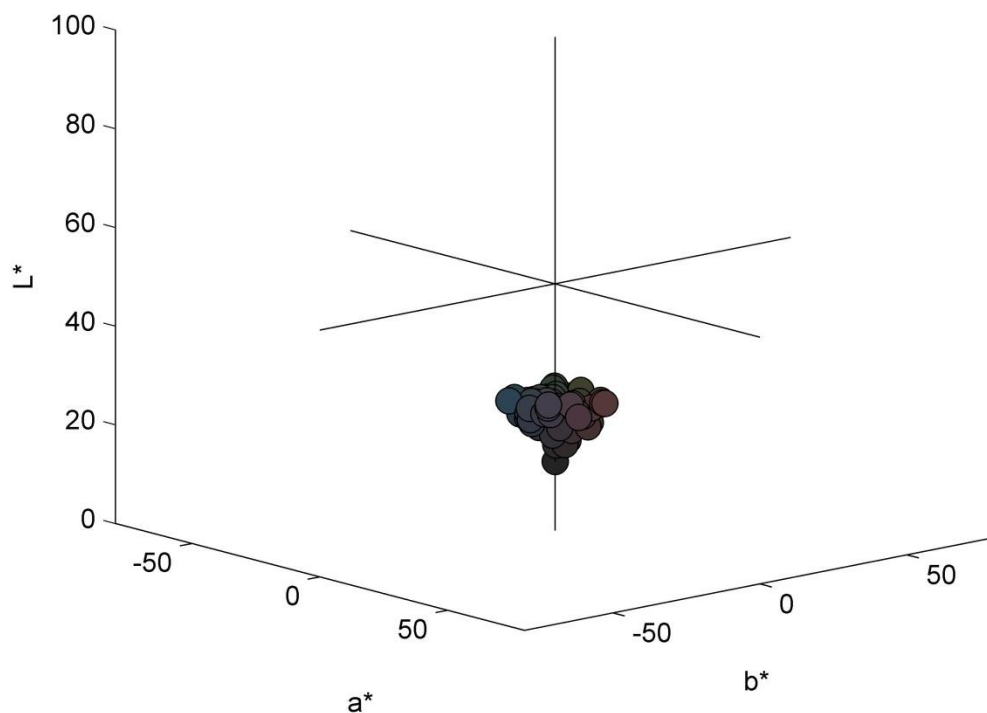


Figure 4.12 Small gamut of dark colours plotted within CIELAB colour space

For plotting this smaller area of colour space, the same code as seen in Appendix IX is followed up to the point where the 10,012 points are generated. At this stage, the points within the gamut are reduced to points with an L^* value of less than 27. For example code see Appendix XII. The code then continues in a similar way to Appendix IX, however, the test numbers (from 10 colours to 200 colours previously) were reduced (from 10 colours to 55 colours in this instance) as the gamut is much smaller. Example code can be found in Appendix XIII. Similarly to section 4.2, the script was run

ten times and an average of the results was recorded. The standard deviation of the results was also recorded.

4.3.2 Results

The results (Table 4.2) showed that for a much smaller volume or gamut of colour space the number of primaries required is dramatically reduced.

Table 4.2 MATLAB results showing the number of primaries within the gamut against the mean colour difference of the tetrahedral blends

No. of Primaries	Average no. of tetrahedra	Standard deviation of no. of tetrahedra	Average mean CIELAB ΔE of tetrahedra	Standard deviation of mean CIELAB ΔE of tetrahedra
5	3	0.48	27	1.89
10	18	0.95	19	1.13
15	40	1.81	17	0.69
20	64	2.87	15	0.83
25	87	4.05	13	0.69
30	111	4.00	12	0.63
35	137	5.13	12	0.49
40	167	6.07	11	0.51
45	196	4.65	10	0.41
50	223	7.15	10	0.41

With only ten primaries, tetrahedral blends could be produced with a predicted average mean colour differences of 19 CIELAB ΔE . From the work done in chapter 3 it was estimated that a colour difference of less than 21 CIELAB ΔE would be sufficient to produce 4-colour blended samples which would appear solid in colour to at least 50 % of people with normal colour vision. It was also observed that samples produced with a mean colour difference of 15 CIELAB ΔE (blends 2.21-2.25) appeared solid to 90-100% of participants. If the small gamut produced in this study were to be produced as

physical primaries for blending as solid colours, a recommended number of primaries would be 10, as this would produce blends with an average mean colour difference of 19 CIELAB ΔE , sufficient to appear as solid blends to the majority of people. As observed with the results produced from the large gamut in section 4.2.4, as the number of primaries increases, so does the number of tetrahedral groups. As also seen in section 4.2.4, as the number of primaries increases, the mean colour difference of the tetrahedral groups reduces. The low standard deviation of the mean colour differences of the tetrahedral groups shows good reliability in predicting what the mean colour difference of the 4-colour tetrahedra will be.

The results of this experiment are plotted in Figure 4.13. It can be seen that as a higher number of primaries is used, the speed at which the mean colour difference reduces begins to slow. The number of primaries required to reduce the mean colour difference of the tetrahedral blends past approximately 10 CIELAB ΔE becomes impractical.

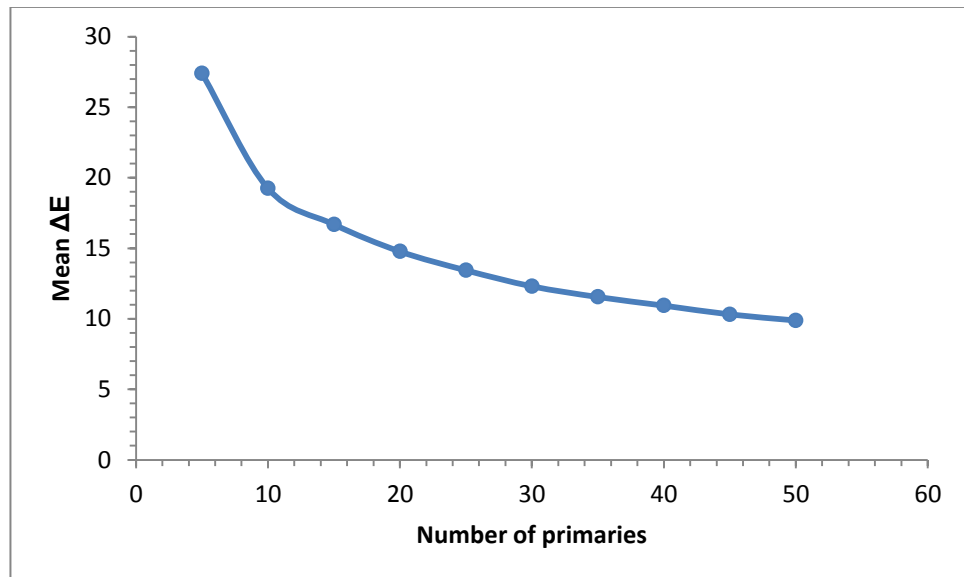


Figure 4.13 Number of primaries versus mean colour difference (CIELAB ΔE) of blends

Reducing the mean colour difference of the blends past 10 CIELAB ΔE would require a substantial increase in the number of primaries which would be disproportionate to the number of blended colours that could be produced. The colour difference between the blends would likely be too insignificant to make the increase in primaries worthwhile.

Again, if we use Table 4.2 as a reference, with 10 primaries there would be approximately 18 tetrahedral groups of four primaries. Again, if only ten blends are made from each tetrahedral group then there would still be a significant increase in the number of solid spun-dyed colours a company could offer at 180 colours (18 x 10).

Ultimately however, the number of primaries that it is appropriate to hold depends on the range of colours a textile company would want to produce. It is also dependent on the level of acceptability of the mean colour difference of a blend in order for it to appear as a solid colour to a given industry's consumer. For example, a textile company producing furnishings for public transport would perhaps accept a higher mean colour difference of 4-colour blends than a textile company producing fabrics for fashion as the interaction and ownership of the fabrics with the public is different. If a mean colour difference of 24 CIELAB ΔE is acceptable for a 4-colour blend then in this example, only 5 primaries are required. However, if a mean colour difference of 13 CIELAB ΔE is desirable then 15 primaries would be required.

The number of primaries required to produce a range of 4-colour blends is therefore dependent on two factors. Firstly, what is the acceptable mean colour difference of a blend for a particular application (this could include the use, fibre type or distance at which the textile piece is seen at)? Secondly, what range of colours is desired (the larger the range of colours, the higher the number of primaries required)? These are questions that must be answered in order to create a tetrachromatic system that is suitable for a particular application. Once these variables are known however, the methods described in this thesis could be used to design colour systems around a defined gamut of colours. The number and specification of the primaries within the

gamut can be defined and the mean colour difference of the tetrahedral blends can be specified according to the end use.

As discussed in the literature review, an appropriate end use for these 4-colour blends would be within fashion. With fast-fashion becoming increasingly popular and with new fashion seasons appearing more regularly throughout the year (often monthly rather than the traditional bi-annual seasons of spring-summer and autumn-winter) this method of colouring textiles could provide a more flexible approach to dyeing textiles. Textile waste from the manufacturing of spun-dyed fibre could definitely be reduced. Whilst individual, bespoke spun-dyed colours must be produced in minimum quantities of between 5 and 10 tonnes depending on the company (in order for their production to be cost effective) 4-colour blended samples could be produced in much smaller amounts.

The next section of this chapter will look at the application of the 4-colour blends in knit form. Tetrahedral groups of coloured fibre will be carded, spun into yarn and knitted. Participants will then view the knitted samples to see if the mean colour difference of the blends translates well into a fashion application or not.

4.4 Applying fibre blending in a fashion context

Sections 4.2 and 4.3 have demonstrated that depending on the requirements of a textile producer, bespoke colour systems using tetrahedral blends of a given number of primaries can be produced. Key decisions which shape the size of such a colouration system include:

1. The acceptable mean colour difference of a tetrahedral blend depending on the particular product application or viewing distance;
2. The size or range of colours (and therefore gamut volume) that want to be offered.






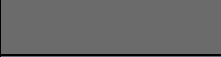



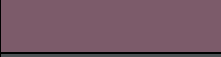






In order to demonstrate the application of this work within the fashion industry, a further small study (experiment 3) was conducted which combined the colouration

system developed in MATLAB with the production of physical, knitted samples. Using a small gamut, a selection of primaries were defined and produced as dyed fibre. These primaries were blended in 4-colour groups with mean colour differences of between 8 CIELAB ΔE and 13 CIELAB ΔE . As knitted fabrics are widely used within fashion garments (rather than woven or non-woven fabrics), some of the blends were spun into yarn and knitted using an outsourced company (Lenzing AG). The knitted samples were visually assessed for their solidity of colour by 10 participants (again most, but not all, of these participants took part in experiment 1 of chapter 3). To provide a means of comparison, participants were also shown samples made from some of the 4-colour blends produced in section 3.3 of chapter 3. These blends had slightly higher mean colour differences of between 15 CIELAB ΔE and 25 CIELAB ΔE . The results showed a good correlation between the knitted samples which had a lower mean colour difference and the appearance of the samples as a solid colour. It is acknowledged that the process of spinning and knitting the fibre can change the colour appearance of the blends; however the main objective of this experiment was to check that fibre blends which appear solid in web form correspondingly appear solid in knit form as this would most likely be how the blended colours would be experienced within fashion. The following sub-sections detail the production of the new primaries, blended samples and participant results.

4.4.1 The primaries

The primaries for this experiment were selected using MATLAB. A small gamut within CIELAB colour space was defined similarly to the methods detailed in sections 4.2 and 4.3. The gamut was filled with 15 primaries. These primaries were produced as dyed fibre by an outsourced pack dyer as described in section 2.1.3 of Chapter 2. All 15 primaries were carded using the method described in section 2.2 and their spectral reflectance factors were measured using the method described in section 2.3. This ensured that accurate colour differences between each of the primaries could be recorded. This was particularly important for these pack-dyed primaries as slight spectral differences may have occurred between the sample dyer and the pack dyer's finished dyed fibre. Table 4.3 shows the $L^*a^*b^*$ and sRGB values of the primaries and also a representation of the appearance of the primaries using sRGB values.

Table 4.3 L*a*b* and sRGB values for the primaries used in experiment 3

Primary number	L*	a*	b*	R	G	B	General appearance (sRGB)
1.2	13.87	-0.03	-0.05	36	36	36	
3.1	47.24	-2.58	0.30	108	114	111	
3.2	42.13	-5.94	1.03	90	103	97	
3.3	46.45	2.98	4.43	119	109	102	
3.4	39.33	3.78	-5.13	96	92	101	
3.5	44.95	0.15	-0.40	107	107	107	
3.6	45.99	0.20	-7.26	104	110	121	
3.7	34.86	11.07	0.63	100	76	81	
3.8	32.50	1.31	-0.38	79	76	77	
3.9	42.41	16.27	-3.48	124	91	106	
3.10	34.02	-1.37	-2.82	76	81	84	
3.11	40.75	-8.64	-10.56	68	102	113	
3.12	33.61	9.58	-0.86	94	74	80	
3.13	44.86	-1.60	10.33	111	107	89	
3.14	50.19	-10.69	0.18	99	125	118	
3.15	38.89	-9.06	-0.20	75	96	91	

The spectral reflectance factors of each primary were plotted in CIELAB colour space (Figure 4.14) and the colour difference (CIELAB ΔE) between each pair of primaries was calculated using the method described in section 2.3. The exact colour of the primaries produced altered slightly from the L*a*b* coordinates of the primaries specified using MATLAB. This was due to technical constraints at the colour matching stage.

4.4.2 Preparing blended samples

Figure 4.14 illustrates the close proximity of the 15 pack-dyed primaries in CIELAB colour space. The largest colour difference between a pair of primaries within the set

of primaries was 20 CIELAB ΔE , the smallest colour difference was 4 CIELAB ΔE . The 15 primaries were used to produce 22 blended samples, each composed of four colours.

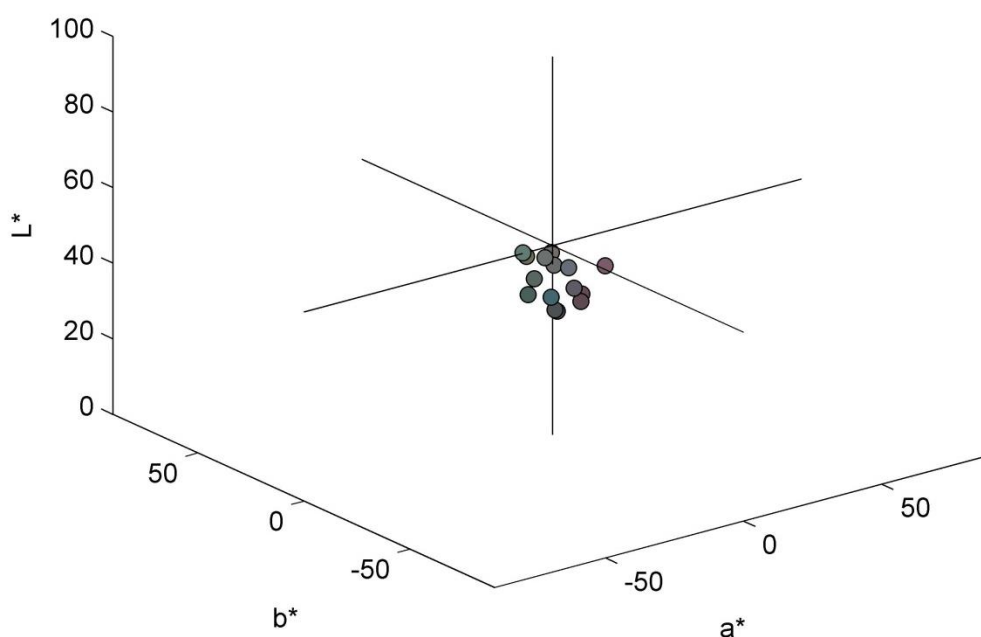


Figure 4.14 The 15 primaries used to produce 22 blended samples, plotted in CIELAB colour space

Table 4.4 shows the two recipes used to create the blended samples. The primaries were blended in tetrahedral groups with varying mean CIELAB colour differences. The sample size for each blend was 30 g and the blends were prepared using the same method as described in section 2.2.

Table 4.4 Experiment 3 generic blend recipes

	Primary a (%)	Primary b (%)	Primary c (%)	Primary d (%)
Recipe 1	25	25	25	25
Recipe 2	80	10	5	5

The spectral reflectance factors of each blend were recorded using the spectrophotometer and the data was converted to $L^*a^*b^*$ and sRGB values in MATLAB using the method described in section 2.3. The position of the blends in CIELAB colour space can be seen in Figure 4.15.

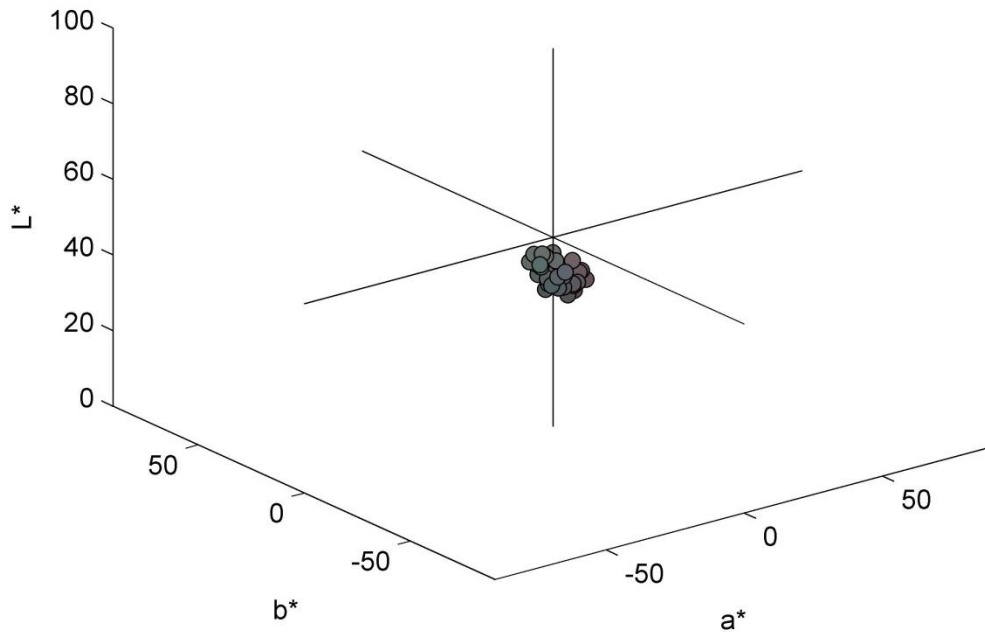


Figure 4.15 Position of the blends in CIELAB colour space

4.4.3 Producing knitted samples














Five of the blended samples and two of the primaries from this experiment were spun and knitted into fabric samples by Lenzing AG. Knitted samples were also produced from five of the blended samples produced in experiment 2 of chapter 3. The method of constructing the knitted samples and their specification can be found in section 2.4 of chapter 2.

4.4.3.1 Visual assessment results

The knitted samples were observed by 10 participants using the same method described in section 2.5 of chapter 2. However instead of asking participants whether a sample appeared as either a) a solid colour, b) almost a solid colour or c) not a solid colour, participants were instead asked whether a given knitted sample was acceptable to them as a solid colour or not. If a knitted sample was acceptable as one

colour to a participant it scored 1, if the knitted sample was not acceptable as a solid colour then it scored 0. The results of the participant observations can be seen in Table 4.5.

Table 4.5 Visual assessment results of knitted fabrics composed of one or more primaries

Knit sample	Mean ΔE	Total participant score	Score as a %	RGB colour
Primary 3.2	n/a	10	100 %	
Primary 3.4	n/a	10	100 %	
Blend 3.1	8	10	100 %	
Blend 3.2	9	10	100 %	
Blend 3.3	10	10	100 %	
Blend 3.4	11	10	100 %	
Blend 3.5	13	8	80 %	
Blend 2.22	15	8	80 %	
Blend 2.23	15	8	80 %	
Blend 2.19	18	4	40 %	
Blend 2.7	23	5	50 %	
Blend 2.4	25	5	50 %	
Blend 2.5	25	7	70 %	

The results showed a high acceptance of the 4-colour blends as solid colours in knitted form. The threshold for determining whether a sample appeared solid in experiment 2 of chapter 3 was determined as when blends were acceptable as one colour to 50 % or more of participants. If the same threshold is applied to these participant results then all but one blend (Blend 2.19) are acceptable as solid colours in knitted form. The results confirm that blends with low colour differences (of less than 25 CIELAB ΔE) appear as solid colours when assessed at the viewing distance used in this thesis. Secondary to this the results show that these same 4-colour blends translate well into knitted fabrics which also appear solid to the majority of observers.

4.4.4 Conclusions

This chapter used two different methods (firstly using MATLAB and secondly using visual assessments) to further the understanding and methodology of a blend colouration system applicable to industry. MATLAB was used in section 4.2 to distribute primaries within a large gamut, and in section 4.3 to distribute primaries within a much smaller gamut. The primaries within each gamut were spaced as tetrahedral groups of four. For the large gamut, if the mean colour difference of the tetrahedral blends was required to be approximately 20 CIELAB ΔE (similar to the mean colour difference of 21 CIELAB ΔE found to produce solid blends in experiment 2 of chapter 3), then it was calculated that 150 primaries would be required to fill the whole gamut. When using a much smaller gamut, as in section 4.3, it was calculated that only 10 primaries would be required to cover the whole of the small gamut so that solid blends with a mean colour difference of 19 CIELAB ΔE could be produced.

MATLAB was also used to define a range of primaries which were blended, spun and knitted into samples for visual assessment by participants. The results of this section showed that 4-colour blends with a mean colour difference of less than 25 CIELAB ΔE could produce solid colour effects in the form of knitted fabrics (when viewed at a distance of 45 cm).

Most importantly however, this section highlights that if the acceptable mean colour difference of a 4-colour blend, depending on the distance at which it is to be viewed at, is known, as well as the size of gamut (or range of colours) that are desirable, then it is possible to define both the number of primaries required and which primaries to mix together to produce solid colour effects. Table 4.1 and Table 4.2 show that it is possible to predict the number of primaries required to fill a gamut depending on the mean colour difference (CIELAB ΔE) of the tetrahedral blends. It was observed that as the mean colour difference (CIELAB ΔE) of the blends increased, the number of primaries required to fill a given gamut decreased. The question of whether a certain number of primaries (for example 150 as in the large gamut produced in section 4.2) is feasible for a company to stock is dependent on individual circumstances. However, it is not an unreasonable amount when the number of subsequent colours that can be

achieved is taken into consideration. It is also likely that it would not be quite as many as 150 as this number was based on a particularly large gamut (actual gamuts for fibre companies will probably be smaller). With companies such as Birla Cellulose already producing 69 spun-dyed colours (Birla Cellulose, 2012b), it can be concluded that a blend colouration system is a viable option for colouring textiles for fashion.

Chapter 5 Colour prediction of fibre blends

In this chapter, existing and novel methods for predicting the colour of a blended sample (a blended sample being a carded web composed of more than one coloured fibre) were explored. Two standard prediction models were tested; the Stearns-Noechel equation and Friele's equation. A standard feedforward multi-layer perceptron (MLP) neural network and a novel MLP neural network were also tested.

The spectral reflectance factors of the 8 primaries and 333 blended viscose samples produced in experiment 1 of chapter three of this thesis provided the data set. The 333 blended samples composed of 8 one-colour blends, 52 two-colour blends, 117 three-colour blends and 37 four-colour blends. The data set was pseudo randomly split using MATLAB into a training set (273 samples) and a testing set (60 samples).

The training set was used to optimise the variables of each of the models. For example, it was used to optimise b in the Stearns-Noechel model (see Equation 2), s in the Friele model (see Equation 3) and the number of hidden units (and the values of the weights) in the ANN models. Performance of the models was then evaluated using the independent testing set.

To evaluate the performance of the prediction models, CIELAB ΔE and CIEDE2000 colour differences were calculated between the predicted CIELAB values of a blend and the real measured reflectance values of the blend (obtained from a spectrophotometer). A target colour difference of < 1 CIELAB ΔE would be desirable for application within industry. In order to process the data, MATLAB was used.

5.1 Standard prediction models

As identified in the literature review, two main methods of predicting colour from reflectance have been used; Stearns-Noechel's equation and Friele's equation. The success and practicality of these models when applied to fibre blends has varied. However, when comparing the two models, the Stearns-Noechel model appears to give the best colour prediction performance measured in terms of colour difference between predicted and measured colour of blended samples. MLP neural networks

have also been used as a model for colour prediction; however, the existing literature is mostly concerned with dyes and pigments and with conventional colouration. Here, Stearns-Noechel's equation, Friele's equation and MLP neural networks are used to predict the colour of 2-, 3- and 4-colour viscose blends using the 333 sample data set prepared in chapter three.

5.1.1 Stearns-Noechel equation

Stearns and Noechel (1944) believed that the reflectance of a blend could not be predicted by simply averaging the weighted reflectance of each fibre component as seen in Equation 22; where the reflectance of the blend is $R_M(\lambda)$ and the reflectance factors of the components are $R_1(\lambda)$ and $R_2(\lambda)$.

$$R_M(\lambda) = c_1 R_1(\lambda) + c_2 R_2(\lambda)$$

Equation 22

Instead, Stearns and Noechel developed an additive formula for predicting the colour of blends where the reflectance factors were transformed using the function $f_{SN}(\lambda)$, as seen in Equation 23, where the dimensionless constant b was empirically derived to be 0.15 for wool blends (Stearns & Noechel, 1944).

$$f_{SN}[R(\lambda)] = \frac{1 - R(\lambda)}{b[R(\lambda) - 0.01] + 0.01}$$

Equation 23

Depending on the fibre type, b is expected to vary. Subsequently, authors have found b to be between 0.09 for viscose (Rong & Feng 2005) and 0.25 for acrylic (Davidson & Taylor 1965). In this thesis the Stearns-Noechel equation was used and b was varied from 0.01 to 0.4 (in steps of 0.01) to find the best experimental fit (measured as the lowest mean colour difference (CIELAB ΔE) between measured colour of blend and predicted colour of blend) using the training data. The best fit was achieved when $b = 0.1$ as can be seen in Figure 5.1. When $b = 0.1$, the mean CIELAB ΔE was 2.92 with a

maximum CIELAB ΔE of 7.08 (for the training data). The MATLAB code used to run Stearns-Noechel's model can be seen in Appendix XIV.

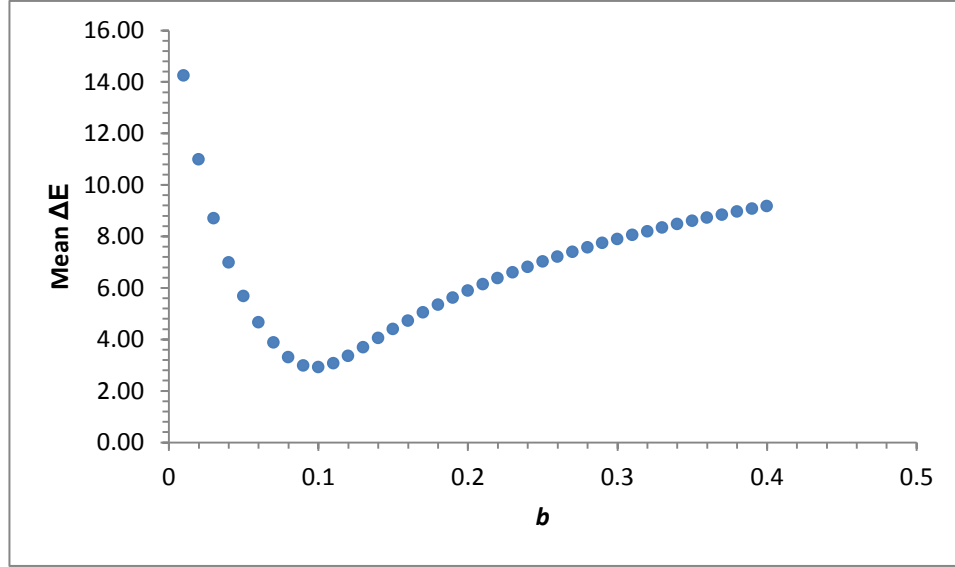


Figure 5.1 Variation of mean CIELAB ΔE (for the training data) with b varied for the Stearns-Noechel model

5.1.2 Friele's equation

Friele's approach to blend prediction was less empirical than Stearns-Noechel's equation and built upon the principles of Kubelka-Munk theory. Friele related K/S to the function $f_F(R(\lambda))$ to produce his own equation as seen in Equation 24 (Friele, 1952), where s is the Friele parameter, or scattering coefficient. In Friele's original work on wool blends the scattering coefficient was theoretically derived as $s = 0.30$ (Friele, 1952).

$$f_F(R(\lambda)) = \frac{-s(1 - R(\lambda))^2}{2R(\lambda)}$$

Equation 24

Successive authors within the literature have altered the s coefficient depending on the fibre type (Miller *et al.*, 1952; Davidson & Taylor, 1965; Burlone, 1984). In order to find the optimum scattering coefficient for this data set s was increased from 0.01 to 0.4 (in steps of 0.01). Figure 5.2 shows that the optimum coefficient is reached when s

= 0.23, giving a mean CIELAB ΔE of 2.18 ΔE . The maximum CIELAB ΔE recorded for $s = 0.23$ was 6.08 ΔE using a 3-colour blend. The MATLAB code used to run Friele's model can be seen in Appendix XV.

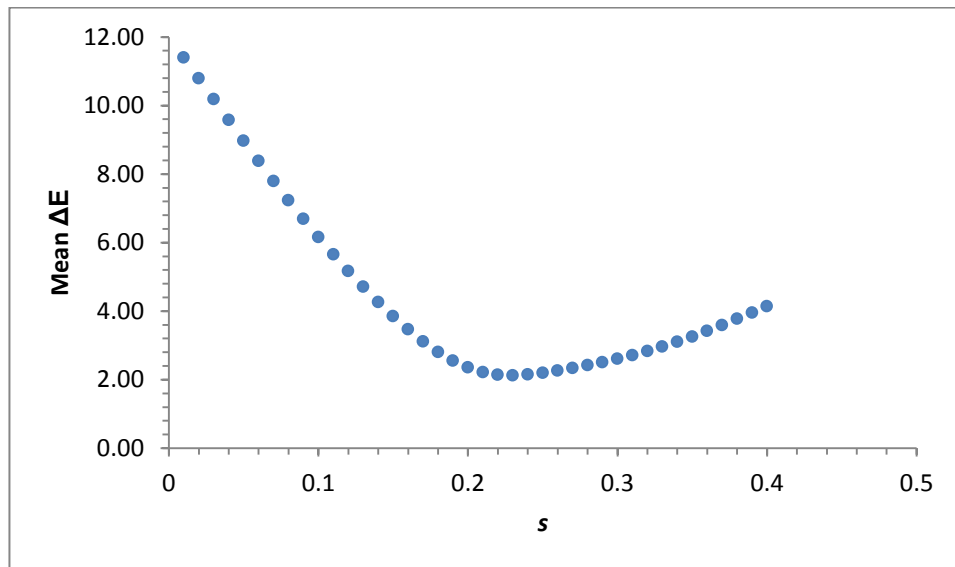


Figure 5.2 Variation of average colour difference (training data) with s for the Friele model

5.2 Standard neural network model

Whilst some work has been done using artificial neural networks (ANNs) to predict the colour of dyes or printing inks (Bishop *et al.*, 1991; Westland, 2001), their success has so far been limited and has not been applied to fibre blend prediction. Here, a standard multilayer perceptron neural network from MATLAB's 'Neural Network Toolbox™' (MathWorks, 2014b) was trained and tested using the 273 training samples and 60 testing samples prepared in this thesis.

For the standard neural network, the number of inputs was defined by the number of primaries (8) used to make the 273 training samples and the number of outputs was defined by the number of wavelengths (35) for which the spectral data was available. A single hidden layer was used, and to derive the optimum number of hidden units in that layer for the network, the network was trained and tested in a loop, with the

number of hidden units varying from 1 to 60. Figure 5.3 illustrates the structure of the standard neural network using two hidden units.

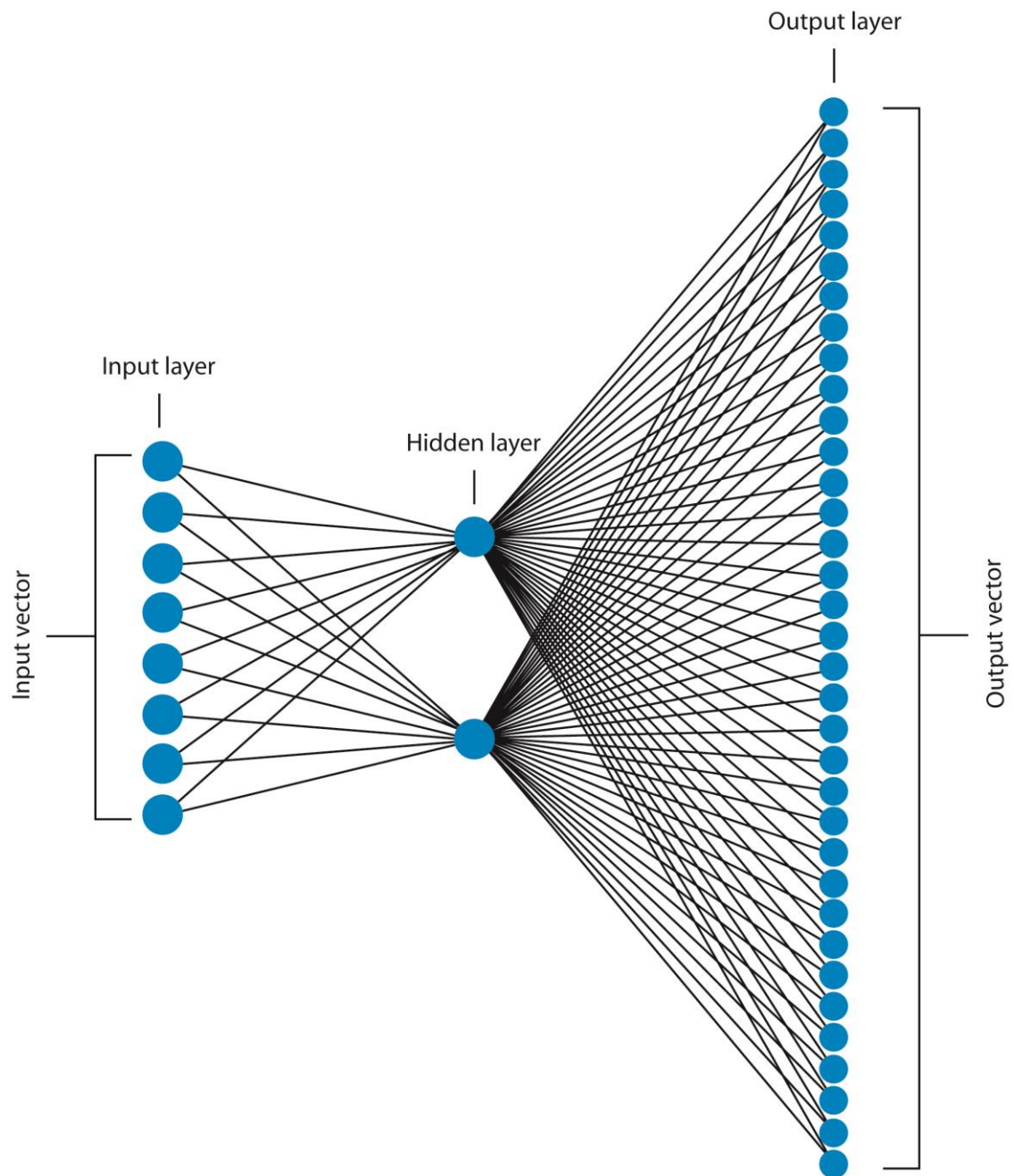


Figure 5.3 Illustration of the standard neural network using 8 input vectors, 35 output vectors and two hidden units (note that each hidden and output unit also receives weighted input from a bias unit, but this is not illustrated)

The standard neural network was run using the built-in settings from MATLAB's 'Neural Network Toolbox™' (MathWorks, 2014b). The network, which uses the

Levenberg-Marquardt training method, is programmed to stop training when one of the progress parameters is fulfilled. Table 5.1 shows the built-in settings for stopping the network. The network will stop when the first of three possible stopping criteria is reached. This could be the maximum number of epochs, the minimum gradient or the maximum MU.

Table 5.1 The progress parameters for the standard neural network using the built-in MATLAB toolbox settings

Progress parameter	Stopping criteria
Epoch	Maximum of 1000
Time	Unlimited
Performance	Unlimited
Gradient	Minimum of $100\text{e-}05$
MU	Maximum of $1.00\text{e+}10$
Validation checks	Maximum of 6

Through testing it was identified that the network would most commonly stop when the minimum gradient ($1\text{e-}05$) was reached. However, as the number of hidden units increased, the maximum number of epochs (1000) also began to stop the neural network. To identify whether the built-in setting of the MATLAB 'Neural Network Toolbox™' (MathWorks, 2014b) were optimised for the data set within this thesis, adjustments were made, firstly to the minimum gradient, and secondly to the maximum number of epochs.

The minimum gradient was varied from $1\text{e-}04$ to $1\text{e-}06$ (in increments of $5\text{e-}06$) but the network trained in a similar way to the standard settings with minimal change in results recorded. Adjustments were then made to the maximum number of epochs, increasing the maximum number of epochs from 1000 to 10,000 epochs. In this instance, the network was consistently stopped by the minimum gradient being reached (rather than a mixture of the minimum gradient and the maximum epochs).

To understand the effect that this stopping parameter was having on the mean error of the training data, two standard neural networks were therefore run.

The first standard neural network used the standard MATLAB settings without any adjustments. This network was called Standard Network 1. The second standard neural network used the standard MATLAB settings with the maximum number of epochs adjusted to 10,000. This network was called Standard Network 2.

Both Standard Network 1 and Standard Network 2 were trained and tested using the 333 sample data set produced in this thesis. The networks were each run ten times and mean training and testing errors were calculated in both CIELAB ΔE and CIEDE2000. The standard error of the results was also calculated. The MATLAB code to run each network can be seen in Appendix XVI.

5.2.1 Standard network results

Standard Network 1 and Standard Network 2 were run ten times each with the mean training and testing errors calculated in CIELAB ΔE and CIEDE2000. The standard neural networks took approximately 70 minutes to complete one run of the code seen in Appendix XVI.

5.2.1.1 Standard Network 1

The results of Standard Network 1 showed that as the number of hidden units increases, the mean colour difference of the training data reduces, showing an improved performance. For the mean testing data, as the number of hidden units increases the performance of the test data also improves up to 25 hidden units. At 25 hidden units the optimum mean training and testing errors are reached. After 25 hidden units the network becomes over trained and the mean testing errors become higher and irregular.

The results of Standard Network 1 can be seen in Table 5.2.

**Table 5.2 Number of hidden units versus mean training and testing errors for
Standard Network 1 using CIELAB ΔE**

Number of hidden units	Mean training CIELAB ΔE	Mean testing CIELAB ΔE	Mean training CIEDE2000	Mean testing CIEDE2000
1	18.15	19.62	12.27	13.10
3	6.12	6.10	5.10	4.70
5	2.93	3.24	2.20	2.35
7	2.06	2.53	1.60	1.78
9	1.57	1.98	1.21	1.43
10	1.26	1.68	0.95	1.20
15	0.98	1.29	0.75	0.93
20	0.80	1.27	0.59	0.86
25	0.73	1.20	0.53	0.80
30	0.69	2.00	0.49	0.98
35	0.64	1.39	0.47	0.94
40	0.64	1.52	0.46	1.00
50	0.54	6.56	0.40	1.19
60	0.46	2.02	0.34	1.35

This result can be seen more clearly in Figure 5.4 where the average training and testing results are plotted against the number of hidden units. It can be seen that above 25 hidden units, the test errors begin to increase indicating that the network is becoming over trained. The results indicate that for Standard Network 1, 25 hidden units produce the optimum results with a mean training error of 0.73 CIELAB ΔE and a mean testing error of 1.20 CIELAB ΔE .

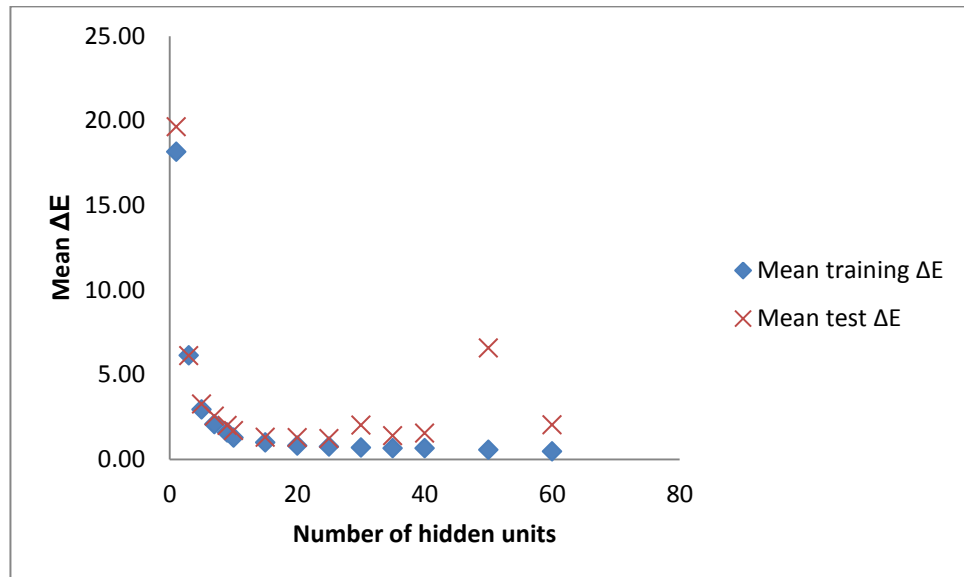


Figure 5.4 The mean training and test errors of Standard Network 1 using CIELAB ΔE (varying the number of hidden units from 1 to 60)

The standard error of the mean training and testing errors for Standard Network 1 can be seen in Table 5.3. When using 25 hidden units the standard error for the training data was 0.012 and 0.027 for the testing data. This indicates good reliability of the results.

Table 5.3 The standard error of the mean training and testing errors of Standard Network 1 using CIELAB ΔE (varying the number of hidden units from 1 to 60)

Number of hidden units	Standard error of mean training CIELAB ΔE	Standard error of mean testing CIELAB ΔE
1	0.000	0.000
3	0.023	0.001
5	0.045	0.039
7	0.041	0.056
9	0.057	0.080
10	0.054	0.066
15	0.031	0.043
20	0.033	0.060
25	0.012	0.027
30	0.014	0.579
35	0.013	0.047
40	0.014	0.103
50	0.018	4.931
60	0.023	0.156

The standard errors for the training and testing data using CIELAB ΔE can be seen in Figure 5.5 and Figure 5.6 where standard error bars have been used. The figures illustrate the small standard errors for both sets of data. The large standard error seen at 50 hidden units in Figure 5.6 is a characteristic associated with overtraining.

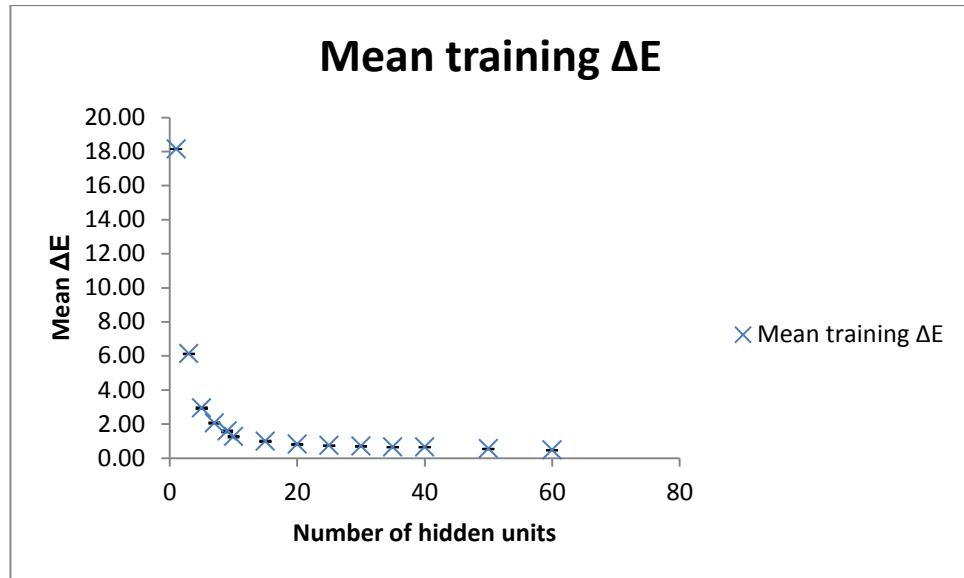


Figure 5.5 Mean training errors of Standard Network 1 using CIELAB ΔE with the standard errors shown

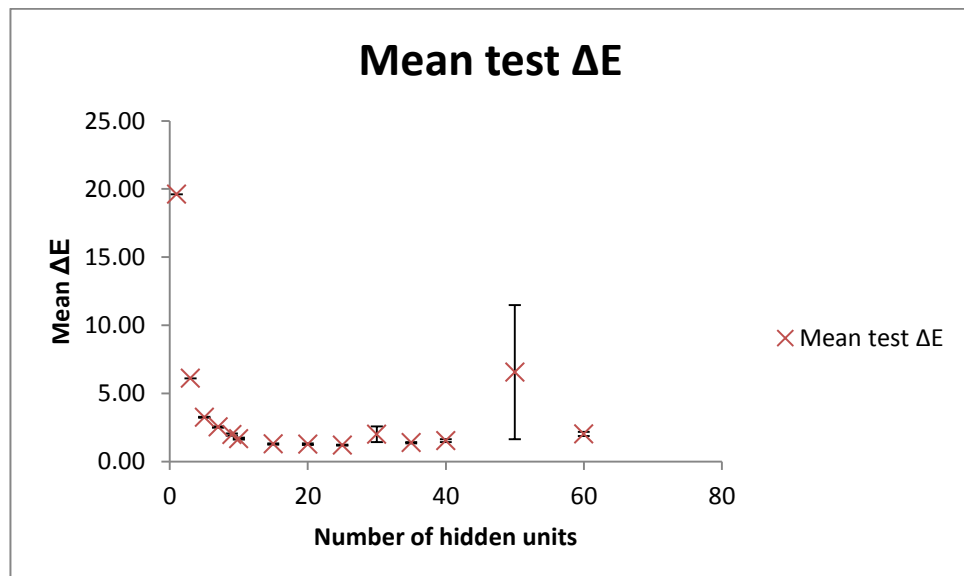


Figure 5.6 Mean testing errors of Standard Network 1 using CIELAB ΔE with the standard errors shown

5.2.1.2 Standard Network 2

Table 5.4 shows the results for Standard Network 2. As Standard Network 1 showed the optimum number of hidden units to be 25, it was decided that running Standard Network 2 to 60 hidden units would be unnecessary. The network was therefore run until 40 hidden units.

Similarly to Standard Network 1, the results show that as the number of hidden units increases, the mean colour difference of the training data reduces to show an improved performance. For the mean test data, as the number of hidden units increases the performance of the test data also improves until 25 hidden units. After this the testing error begins to increase again.

Table 5.4 Number of hidden units versus mean training and testing errors for Standard Network 2 using CIELAB ΔE

Number of hidden units	Mean training CIELAB ΔE	Mean testing CIELAB ΔE	Mean training CIEDE2000	Mean testing CIEDE2000
1	18.15	19.62	12.27	13.10
3	6.14	6.10	5.11	4.71
5	2.86	3.23	2.16	2.34
7	2.06	2.48	1.62	1.75
9	1.59	1.97	1.20	1.38
10	1.35	1.85	1.02	1.25
15	1.00	1.36	0.74	0.96
20	0.81	1.41	0.59	0.92
25	0.73	1.22	0.53	0.83
30	0.70	1.29	0.51	0.88
35	0.66	1.41	0.48	0.93
40	0.63	1.43	0.46	0.95

The performance of Standard Network 2 is illustrated in Figure 5.7 which again shows that the optimum number of hidden units for this data set is 25. The mean training

error for Standard Network 2 was 0.73 CIELAB ΔE and the mean testing error was 1.22 CIELAB ΔE .

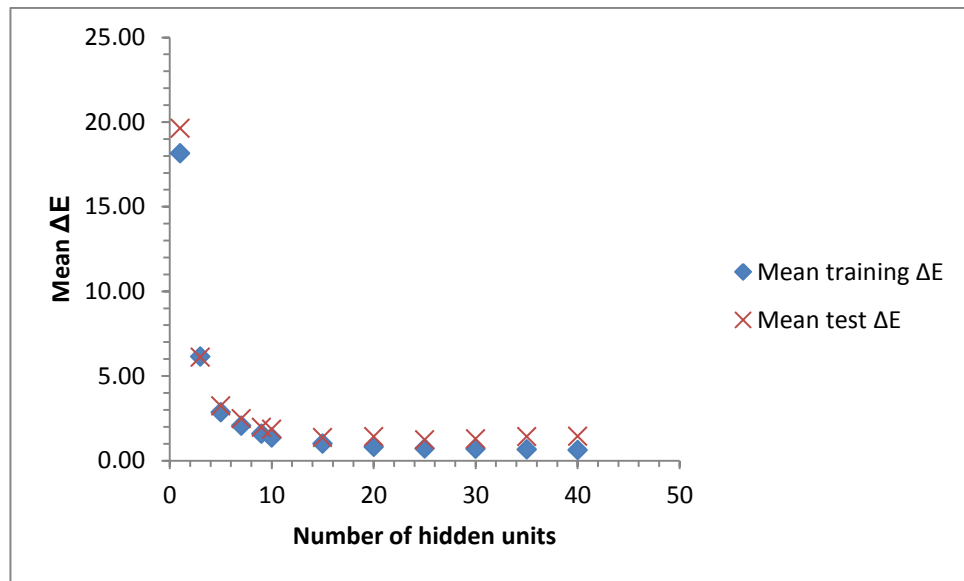


Figure 5.7 The mean training and testing errors of Standard Network 2 using CIELAB ΔE (varying the number of hidden units from 1 to 40)

The standard errors for the mean training and testing errors for Standard Network 2 can be seen in Table 5.5.

Table 5.5 The standard error of the mean training and testing errors of Standard Network 2 using CIELAB ΔE (varying the number of hidden units from 1 to 40)

Number of hidden units	Standard error of mean training CIELAB ΔE	Standard error of mean testing CIELAB ΔE
1	0.000	0.000
3	0.020	0.001
5	0.020	0.015
7	0.064	0.083
9	0.118	0.159
10	0.086	0.195
15	0.039	0.057
20	0.017	0.196
25	0.013	0.020
30	0.013	0.030
35	0.015	0.079
40	0.018	0.043

The standard errors for Standard Network 2 are again very small as seen with Standard Network 1. This is further illustrated in Figure 5.8 and Figure 5.9 which show the mean training and testing errors with standard error bars.

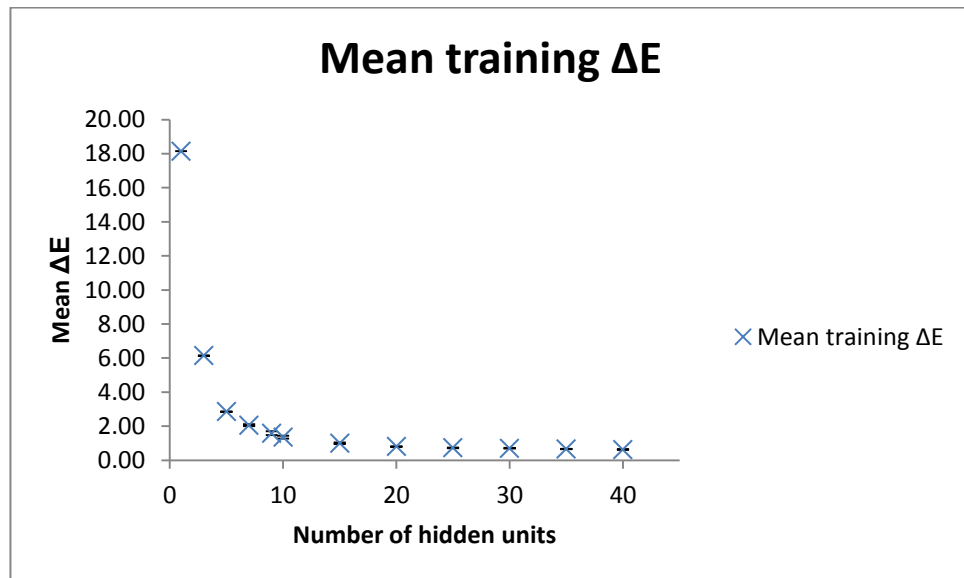


Figure 5.8 Mean training errors of Standard Network 2 using CIELAB ΔE with the standard errors shown

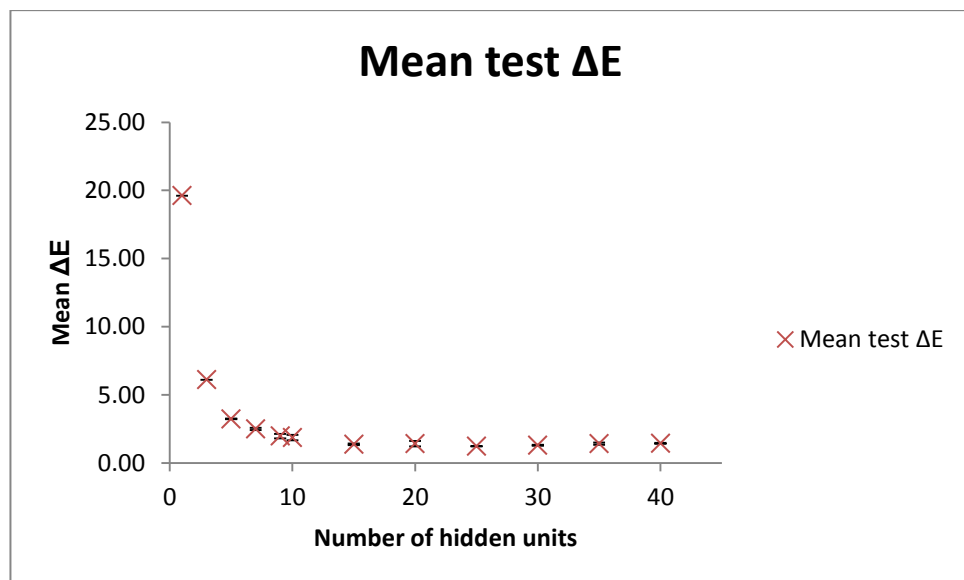


Figure 5.9 Mean testing errors of Standard Network 2 using CIELAB ΔE with the standard errors shown

Standard Network 2 performed very similarly to Standard Network 1 despite altering the stopping criteria of the epochs to a maximum of 10,000 (rather than 1000). The training error (0.73 CIELAB ΔE) was the same for both Standard Network 1 and Standard Network 2. The testing error for Standard Network 2 was slightly higher at 1.22 CIELAB ΔE , compared to the 1.20 CIELAB ΔE that was produced using the standard stopping criteria in Standard Network 1. It can be concluded that in this instance, the standard MATLAB settings provided an optimum training and testing environment for the standard neural network with this particular data set. The optimum number of hidden units was 25 which produced a mean training error of 0.73 CIELAB ΔE (or 0.53 CIEDE2000) and mean test error of 1.20 CIELAB ΔE (or 0.77 CIEDE2000). The small standard error of the results indicated a high reproducibility of results.

5.3 Novel neural network model

To investigate whether the predictive capabilities of a standard neural network could be improved upon, a novel neural network, where the structure of the network was altered (rather than the stopping criteria), was considered.

Instead of using eight input vectors (8 primaries) to predict 35 output vectors (35 reflectance factors between 360 and 700 nm), the novel neural network was constructed to predict the spectral reflectance of a blended sample from the eight primary input vectors at one specific wavelength. Instead of one large neural network, 35 small neural networks were created, each predicting one of the 35 wavelengths from 360 nm to 700 nm (in 10 nm intervals). Figure 5.10 shows an example of one small neural network used to predict the reflectance of a blended sample at 360 nm. In this particular example two hidden units have been used.

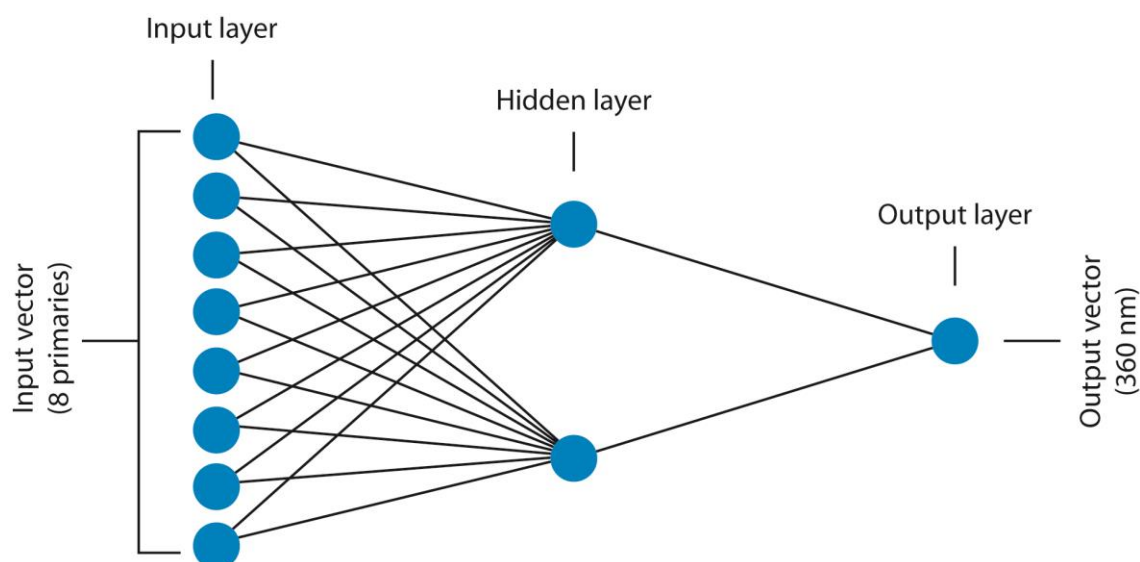


Figure 5.10 Diagram showing a small neural network used to predict the reflectance of a sample at 360 nm

MATLAB's 'Neural Network Toolbox™' (MathWorks, 2014b) was again used to test the novel application neural network (described in this thesis as the novel network). To be consistent with the standard neural network, the novel neural network (composing of 35 small networks) was firstly run using the standard MATLAB parameters (Novel Network 1) and secondly using the altered MATLAB parameters (Novel Network 2) where the maximum number of epochs was increased from 1000 to 10,000.

Novel Network 1 and Novel Network 2 were both given the same training and testing samples as were used to test Standard Network 1 and 2, Stearns-Noechel model and Friele's model. Novel Network 1 and Novel Network 2 were run 20 times (it was possible to run them more times as they ran quicker than the standard networks) and the mean training and testing errors were recorded in both CIELAB ΔE and CIEDE2000. The standard error was also calculated and the MATLAB code for running the novel neural networks can be seen in Appendix XVII.

5.3.1 Novel network results

Novel Network 1 and Novel Network 2 were each run twenty times and the average mean training and test errors calculated in both CIELAB ΔE and CIEDE2000. The novel neural networks took approximately 10 minutes to complete one run of the code seen in Appendix XVII. Novel Network 1 was tested first and the number of hidden units was varied from 1 to 20 in order to find the optimum number of hidden units required. On the basis of the results of Novel Network 1, Novel Network 2 was tested using 1 to 12 hidden units.

5.3.1.1 Novel Network 1

The results of Novel Network 1 (where the standard MATLAB stopping criteria were used) can be seen in Table 5.6.

Table 5.6 Number of hidden units versus mean training and testing errors for Novel Network 1 using CIELAB ΔE

Number of hidden units	Mean training CIELAB ΔE	Mean testing CIELAB ΔE	Mean training CIEDE2000	Mean testing CIEDE2000
1	3.60	4.18	2.66	2.93
2	1.25	1.63	0.92	1.14
3	0.99	1.33	0.73	0.94
4	0.85	2.50	0.62	1.04
5	0.77	5.64	0.56	1.06
6	0.73	5.56	0.54	1.36
7	0.69	2.04	0.50	1.16
8	0.66	3.65	0.48	1.32
9	0.63	4.26	0.46	1.37
10	0.61	7.41	0.45	1.80
11	0.58	12.31	0.43	1.82
12	0.57	17.80	0.42	1.56
13	0.55	13.04	0.41	1.80
14	0.53	17.23	0.40	1.91

15	0.49	6.67	0.37	1.34
16	0.46	8.88	0.35	1.73
17	0.46	6.85	0.35	1.80
18	0.42	7.37	0.32	2.24
19	0.40	5.86	0.30	1.77
20	0.38	4.51	0.29	1.77

Similarly to the standard neural networks, as the number of hidden units increases, the training error decreases. The optimum number of hidden units was 3 which produced a mean training error of 0.99 CIELAB ΔE and a mean training error of 1.33 CIELAB ΔE testing error. When more than 3 hidden units are used, the network becomes over trained and the data becomes unreliable.

The results are illustrated in Figure 5.11 which shows the irregularity of the testing errors when more than 3 hidden units are used, indicating the overtraining. It is not surprising that only three hidden units are required for the novel neural network as the structure of the neural network is much smaller than the standard neural network.

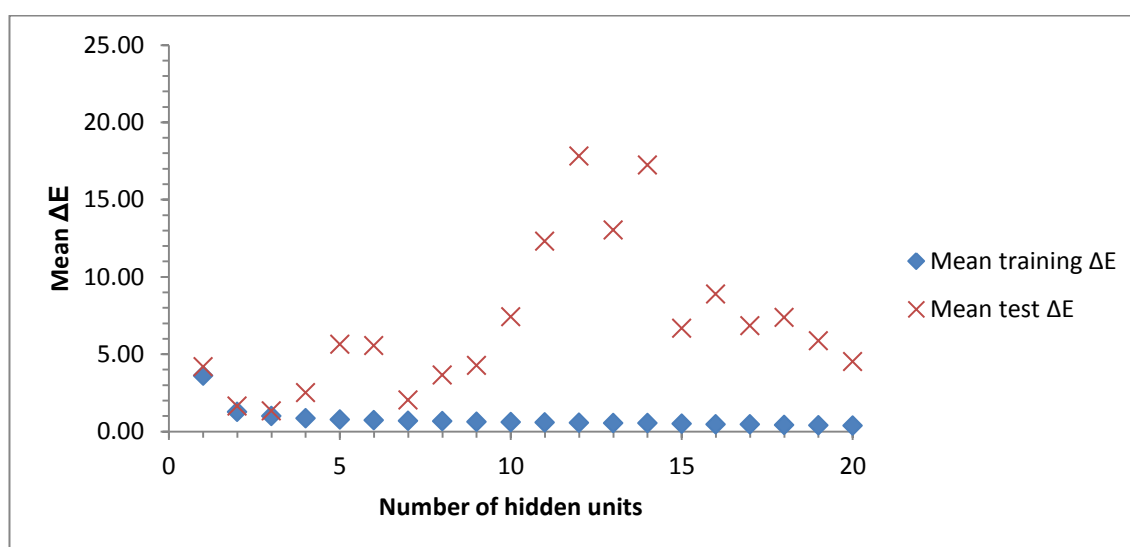


Figure 5.11 The mean training and test errors of Novel Network 1 using CIELAB ΔE (varying the number of hidden units from 1 to 20)

The standard error of the mean training and testing errors for Novel Network 1 can be seen in Table 5.7. When using 3 hidden units the standard error was 0.035 for the

training data and 0.040 for the testing data. The small standard errors for Novel Network 1 indicate good reliability and reproducibility of the results when using the optimum number of hidden units (3).

Table 5.7 The standard errors of the mean training and testing errors for Novel Network 1 using CIELAB ΔE (varying the number of hidden units from 1 to 20)

Number of hidden units	Standard error of mean training CIELAB ΔE	Standard error of mean testing CIELAB ΔE
1	0.023	0.021
2	0.178	0.194
3	0.035	0.040
4	0.032	1.197
5	0.017	4.161
6	0.015	2.839
7	0.009	0.355
8	0.008	0.962
9	0.006	1.840
10	0.010	2.634
11	0.008	7.140
12	0.007	15.869
13	0.009	6.447
14	0.007	9.467
15	0.007	4.750
16	0.007	4.522
17	0.007	3.309
18	0.006	2.912
19	0.007	2.432
20	0.007	2.074

The standard error of the mean training errors was consistently low, from 1 hidden unit to 20 hidden units. This is illustrated in Figure 5.12.

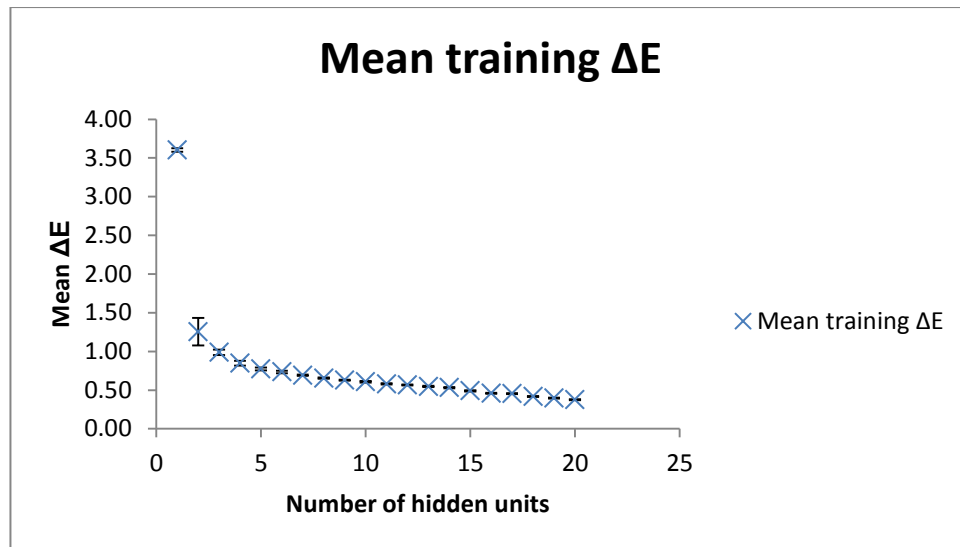


Figure 5.12 Mean training errors of Novel Network 1 using CIELAB ΔE with the standard errors shown

In contrast to the mean training errors, the standard errors of the mean testing errors had much greater variation across the different number of hidden units, varying from a minimum standard error of 0.021 to a maximum standard error of 15.869 (see Figure 5.13).

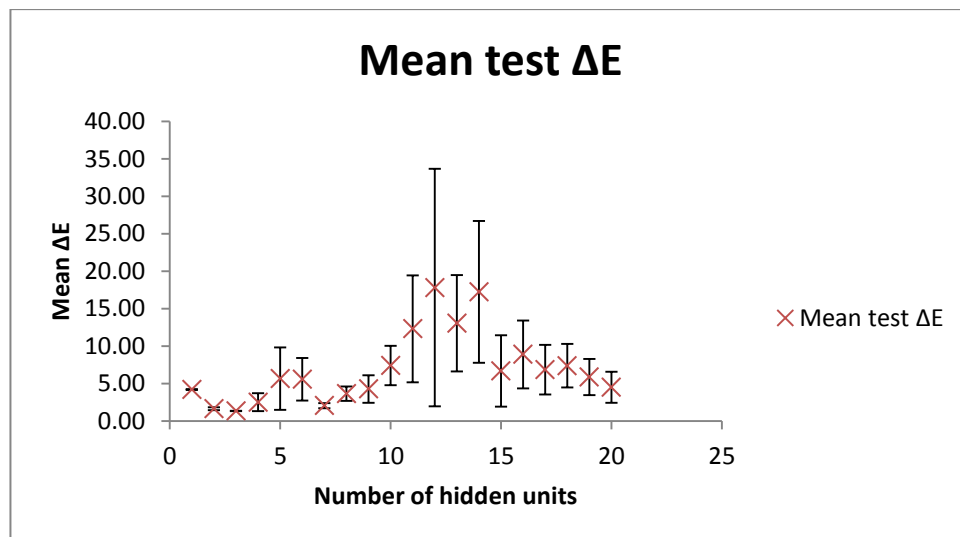


Figure 5.13 Mean testing errors of Novel Network 1 using CIELAB ΔE with the standard errors shown

However, the standard error of the testing data, where the optimum number of hidden units (3) was used, produced a low standard error of 0.040 for Novel Network 1. The increased standard errors seen in the results of the network when more than 3 hidden units are used confirms that the network is becoming over trained.

5.3.1.2 Novel Network 2

Table 5.8 shows the results for Novel Network 2 (where the maximum number of epochs was increased to 10,000 in the network stopping criteria). The network was tested using 1 to 12 hidden units. Similarly to Novel Network 1, the results showed that only a small number of hidden units are required to train and test the small networks. With the maximum number of epochs (stopping parameter) increased to 10,000, Novel Network 2 produced slightly improved results compared to Novel Network 1, with all the training and testing errors slightly reduced from their comparative result.

Novel Network 2 produced an optimum result when four hidden units were used. With four hidden units the mean training error was 0.84 CIELAB ΔE (or 0.62 CIEDE2000) and the mean testing error was 1.17 CIELAB ΔE (or 0.81 CIEDE2000).

The results of Novel Network 2 can be seen in Table 5.8.

Table 5.8 Number of hidden units versus mean training and testing errors for Novel Network 2 using CIELAB ΔE

Number of hidden units	Mean training CIELAB ΔE	Mean testing CIELAB ΔE	Mean training CIEDE2000	Mean testing CIEDE2000
1	3.58	4.16	2.63	2.90
2	1.10	1.45	0.81	1.02
3	0.94	1.26	0.69	0.88
4	0.84	1.17	0.62	0.81
5	0.82	1.47	0.60	0.95
6	0.71	5.29	0.52	1.13
7	0.70	1.97	0.51	1.03
8	0.69	11.52	0.50	1.40
9	0.63	17.31	0.46	1.68
10	0.61	4.38	0.45	1.45
11	0.59	9.67	0.44	1.47
12	0.57	3.15	0.43	1.35

The mean training and testing errors of Novel Network 2 using CIELAB ΔE are illustrated in Figure 5.14. The results show that after 4 hidden units the network produces irregular results which indicate that the network has become over trained.

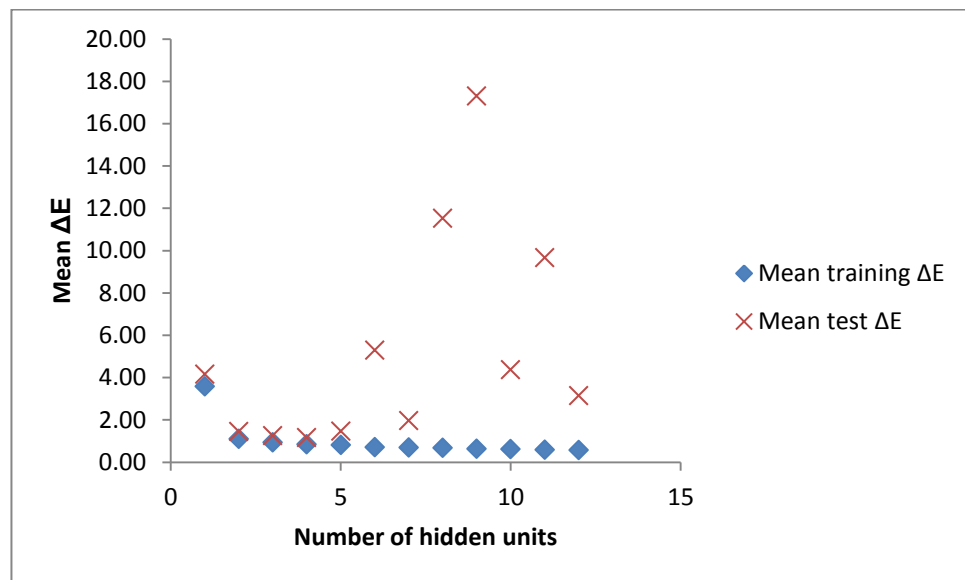


Figure 5.14 The mean training and testing errors of Novel Network 2 using CIELAB ΔE (varying the number of hidden units from 1 to 20)

The overtraining of Novel Network 2 when using more than four hidden units can be further seen when looking at the standard error of the mean training and testing errors in Table 5.9. Whilst the standard errors of the mean training errors remain low, the standard errors of the mean testing errors increase up to 9.085.

Table 5.9 The standard errors of the mean training and testing errors for Novel Network 2 using CIELAB ΔE (varying the number of hidden units from 1 to 12)

Number of hidden units	Standard error of mean training CIELAB ΔE	Standard error of mean testing CIELAB ΔE
1	0.000	0.000
2	0.109	0.112
3	0.036	0.047
4	0.020	0.037
5	0.042	0.243
6	0.015	3.590
7	0.014	0.534
8	0.016	7.885
9	0.009	9.085
10	0.008	1.681
11	0.009	5.785
12	0.011	1.332

Whilst the standard error of the mean training errors (as seen in Figure 5.15) are consistently small as the number of hidden units increased, the standard error of the mean testing error (as seen in Figure 5.16) increases after 4 hidden units. This is an indication that above 4 hidden units the network is becoming over trained.

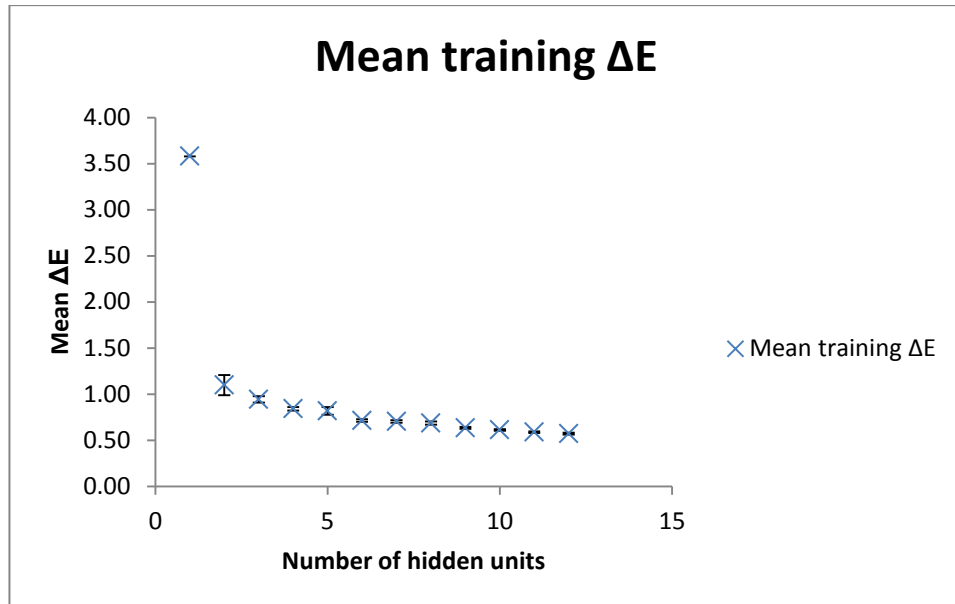


Figure 5.15 Mean training errors of Novel Network 2 using CIELAB ΔE with the standard errors shown

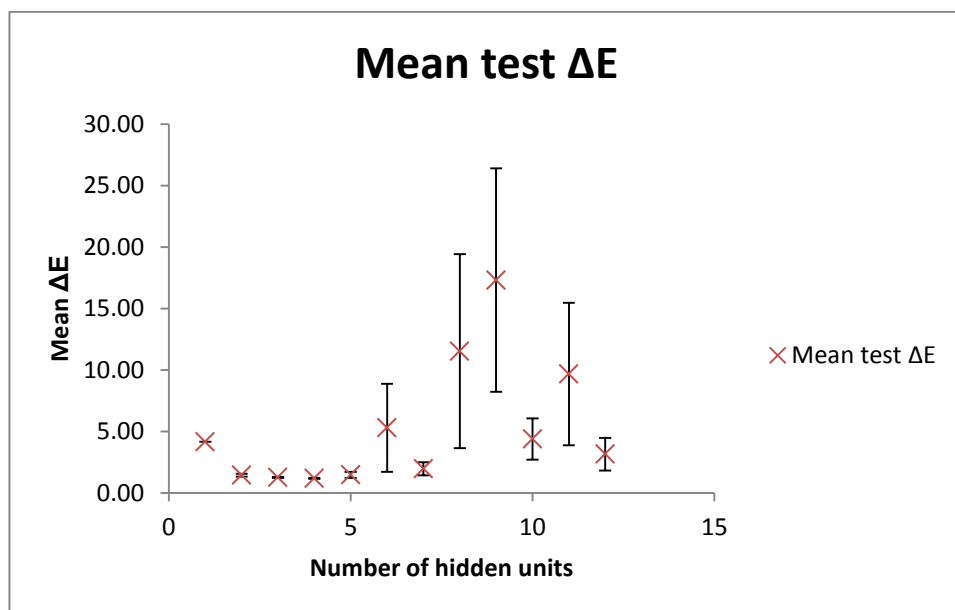


Figure 5.16 Mean testing errors of Novel Network 2 using CIELAB ΔE with the standard errors shown

The standard error for Novel Network 2 when using 4 hidden units was 0.037. This was slightly less than the standard error recorded for Novel Network 1 using 3 hidden units (0.040). Novel Network 2 produced a mean training error of 0.84 CIELAB ΔE which was an improvement to the training error of 0.99 CIELAB ΔE produced using Novel Network 1. The mean testing error of Novel Network 2 (1.17 CIELAB ΔE) was also an improvement on the mean testing error of Novel Network 1 which had a mean error of 1.33 CIELAB ΔE . This result indicates that in this instance, when using much smaller neural networks, altering the standard stopping criteria (which was the maximum number of epochs in this example) of the standard MATLAB parameters was advantageous, giving an optimised result.

5.4 Comparison and conclusions of all models using the test set

The success of each of the prediction models in predicting the colour of a blend was quantified for each model using the mean colour difference between the predicted spectral reflectance of a blend and the measured spectral reflectance of a blend. The mean colour differences for each model were calculated and can be compared using CIELAB ΔE (see Table 5.10) and CIEDE2000 (Table 5.11). Each table shows the mean training and mean testing errors, as well as the maximum training and testing errors for each model. The optimisation coefficient for each model is also included under the prediction method. For Stearns-Noechel's model this was b , for Friele's model this was s , and for the neural networks (both standard and novel) this was primarily the number of hidden units.

Table 5.10 Comparison of results of blend prediction methods using CIELAB ΔE

Prediction method	Training data		Testing data	
	Mean ΔE	Max ΔE	Mean ΔE	Max ΔE
Stearns-Noechel $b = 0.1$	2.92	7.08	3.05	6.55
Friele $s = 0.23$	2.18	6.08	2.42	6.05
Standard Network 1 Hidden units = 25	0.73	3.57	1.20	5.32
Standard Network 2 Hidden units = 25	0.73	4.00	1.22	5.94
Novel Network 1 Hidden units = 3	0.99	17.77	1.33	9.96
Novel Network 2 Hidden units = 4	0.84	9.80	1.17	5.81

Table 5.11 Comparison of results of blend prediction methods using CIEDE2000

Prediction method	Training data		Testing data	
	Mean ΔE	Max ΔE	Mean ΔE	Max ΔE
Stearns-Noechel $b = 0.1$	1.91	3.56	1.87	4.20
Friele $s = 0.23$	1.54	4.17	1.74	4.61
Standard Network 1 Hidden units = 25	0.53	3.55	0.80	3.03
Standard Network 2 Hidden units = 25	0.53	4.39	0.83	4.16
Novel Network 1 Hidden units = 3	0.73	12.39	0.94	7.74
Novel Network 2 Hidden units = 4	0.62	8.50	0.81	4.68

The results clearly show that neural networks (both the standard neural networks and the novel neural networks) outperform the traditional blend prediction models of Stearns-Noechel and Friele.

Out of all four models, Stearns-Noechel's model (where $b = 0.1$) performed the least well (it had the largest mean colour difference between predicted colour of a blend and measured colour of a blend). The model produced a mean training error of 2.92 CIELAB ΔE and a mean testing error of 3.05 CIELAB ΔE . This error was found to be much higher than recorded in similar experiments using viscose within the literature. Rong and Feng (2005) found $b = 0.09$ for viscose blends with a mean error of 0.69 CIELAB ΔE recorded between predicted and measured colour of their blends. However, their data set was much smaller (54 samples) than the sample set (333 samples) used in this thesis. Additionally, only three of their samples were made from 4-colour blends (whereas this thesis included 37 4-colour blends). The majority of their samples were made from 3-colour blends (36 samples) with another 15 samples made from 2-colour blends. The smaller and more limited data set used by Rong and Feng (2005) may account for the discrepancy in the mean colour differences that they found and the mean colour differences which were found in this thesis as 4-colour blends are more complex than 2- and 3-colour blends.

Friele's model (where $s = 0.23$) performed slightly better than Stearns-Noechel's model, producing a mean training error of 2.18 CIELAB ΔE and a mean testing error of 2.42 CIELAB ΔE . This error is slightly lower than other examples of Friele's model being used in the literature. Burlone (1984) used Friele's model to predict the colour of 42 4-colour carded puffs of nylon with s varied between 0.19 and 0.27. Burlone's work produced a minimum average colour difference of 2.7 CIELAB ΔE with the mean colour difference within ± 1 unit of the minimum colour difference (Burlone, 1984).

As identified, in this work both Stearns-Noechel's model and Friele's model were outperformed by the neural network models. When comparing the results of the neural networks, the standard neural networks (Standard Network 1 and Standard Network 2) gave the lowest mean training errors at 0.73 CIELAB ΔE . The second lowest

training error was found using Novel Network 2, where the epoch stopping criteria was increased from 1000 epochs to 10,000 epochs. This gave a mean training error of 0.84 CIELAB ΔE . This was followed closely by Novel Network 1 (where the epoch stopping criteria was 1000 epochs). This gave a mean training error of 0.99 CIELAB ΔE . Whilst the standard networks produced lower training errors than the novel networks, Novel Network 2 produced the lowest testing error of all the networks at 1.17 CIELAB ΔE (compared to 1.20 CIELAB ΔE for Standard Network 1, 1.22 CIELAB ΔE for Standard Network 2 and 1.33 CIELAB ΔE for Novel Network 1). This is perhaps the most important error as this calculates a network's ability to predict unseen data. If the mean errors of the neural networks are examined using CIEDE2000, as in Table 5.11, it can be seen that both the standard networks and the novel neural networks perform excellently, with CIEDE2000 training and testing errors all less than 1 CIEDE2000 unit. This result is highly encouraging as it falls within most acceptable colour differences within commercial industries (Rigg, 1997).

The use of neural networks in the prediction of coloured blends has been shown to outperform existing methods of prediction, namely Stearns-Noechel and Friele's equations, by a significant amount. There was little performance difference between the standard neural networks and the novel neural networks; however, both networks produced low training and testing errors (between 1.17 and 1.33 CIELAB ΔE or 0.80 and 0.94 CIEDE2000), making them a reliable method for the prediction of coloured blends. One advantage to using the novel network, rather than the standard neural network, is the reduced time it takes to run the novel network; the novel network takes approximately 10 minutes per run compared to the standard network which takes approximately 70 minutes per run. This significant reduction in processing time is a great advantage as it allows quick and accurate colour prediction that would be attractive for industry.

Chapter 6 Conclusions and future work

6.1 Conclusions

The aim of this thesis was to identify a method of sustainable colouration for fashion and textiles through the blending of spun-dyed viscose fibre. An overview of the current textiles for fashion industry highlighted both the fast pace of the retail industry and the environmental impact that textile production and dyeing is having globally. Lenzing Viscose Austria and Tencel® were identified as appealing fibre choices to meet increasing global textile demand due to their renewability, biodegradability and low water, energy and chemical consumption compared to other fibres. The colouration of these fibres during their manufacture (spun-dyeing) was also identified as a more sustainable method of textile colouration; due to the reduced consumption of water, energy, chemicals and colorant compared with conventional dyeing. Production limitations of spun-dyed fibre have however limited their application within textiles for fashion. It was therefore proposed that fibre blending of spun-dyed primaries, rather than producing unique colours for a customer, would provide an exciting colouration solution.

In order to develop a methodology for the colouration of textiles using blended fibre from a set of primaries, investigations were made into the following; the visual appearance of blended samples; the selection and number of primaries that would be required within a colouration system; and finally blend prediction models. These areas were explored through experimental work across the course of chapters 3, 4 and 5.

In chapter 3 (Colour difference and sample appearance), the relationship between blend composition and its appearance as a solid colour (or not) was investigated. Both experiment 1 and experiment 2 of chapter 3 showed a strong relationship between the mean colour difference of a blend in CIELAB ΔE (calculated by averaging the colour differences between each pair of primaries within a blend) and the appearance of a blend as a solid colour. In experiment 1, 325 2-, 3- and 4-colour blends of fibre were produced from a set of 8 primaries. The mean colour differences (computed as described above) of the blends were wide ranging, from 11 CIELAB ΔE to 119 CIELAB ΔE , and this is due to the restricted choice of primaries. Participants observed each

sample under controlled viewing conditions to assess the solid colour appearance of each blend. The results collected from this first experiment showed that for 2-colour blends (composed of two spun-dyed primaries) the maximum mean colour difference of a blend for it to appear solid to 50 % or more participants was 36 CIELAB ΔE . For 3-colour blends composed of spun-dyed primaries this was 25 CIELAB ΔE . There were no 4-colour blends composed of four spun-dyed primaries that were found to appear solid to over 50 % of participants, although one sample which contained three spun-dyed primaries and the undyed primary did appear solid at 50 CIELAB ΔE . This first experiment indicated that for blends composed of three spun-dyed primaries or more, a mean colour difference of less than 25 CIELAB ΔE would be required to produce solid colours. Therefore a more concentrated range of primaries, with smaller CIELAB ΔE colour differences between them, was required for further experimental work. The first experiment also indicated that more 4-colour blends should be produced (rather than 2- and 3-colour blends) as this would more accurately reflect the likely blending method that would be used within industry in order to produce practical colour gamuts. In experiment 2 of chapter 3, 25 new 4-colour blends with mean colour differences of between 15 CIELAB ΔE and 25 CIELAB ΔE were produced. This experiment produced more realistic blends of primaries that would be used commercially. The results of the participant observations indicated that in order for the samples to appear solid to 50 % or more of observers, then the mean colour difference of blends should be 21 CIELAB ΔE or less.

Two important conclusions can be drawn from these first two experiments. Firstly, the mean colour difference of a blend is directly related to whether it appears as a solid colour. Secondly, the recommended mean colour difference of the blends in order for them to appear solid in this particular case was 21 CIELAB ΔE or less; however, note that this number is based on the specific viewing conditions and method of sample preparation implemented in this study. This study used a viewing distance of 45 cm, if the viewing distance was to be increased then it would be expected that the acceptable mean colour difference of a blend would also be likely to increase. The experiments highlighted that once the acceptable mean colour difference of a 4-colour blend is known (depending on the specific viewing distance or application), predictions

can then be made as to the number of primaries that would be required to cover a given volume of colour space. This idea was explored further in chapter 4; Developing a relevant colouration system for industry.

In chapter 4 a method for defining the number and colour of primaries within a colouration system, based on the acceptable mean colour difference of a blend so that it appears solid, was developed using MATLAB. This process involved defining the outer boundaries of a gamut with known primaries, filling the whole of the gamut with a very large number (N) of primaries, reducing this number by specifying the value of n primaries that are required for a colouration system, and finally grouping these n primaries into evenly spaced tetrahedral groups of four. The mean colour difference (CIELAB ΔE) of the tetrahedral groups could then be calculated. Depending on the size of gamut, the value of n can be adjusted so that the tetrahedral blends have a mean colour difference appropriate for a particular application or viewing distance.

For example, two gamuts were produced in chapter 4 in order to illustrate this process; one was very large (including highly saturated outer primaries), the other was comparatively small. The number of primaries required to cover the very large gamut so that each tetrahedral blend would have a mean colour difference of 20 CIELAB ΔE or less, was found to be 150. For the small gamut, only 10 primaries were required so that all blends had a mean colour difference of 19 CIELAB ΔE or less. This method of defining a gamut, the number of primaries within it and consequently seeing whether this number of primaries fulfils the mean colour difference requirements of each 4-primary group can be applied to any given set of primaries. Within industry, the size of gamut and therefore number of primaries required to fill the gamut, would likely be determined on individual production and storage capabilities. Importantly, however, this chapter showed that it is possible to predict the number of primaries required within a blend colouration system depending on the size of gamut and target mean colour difference of the 4-colour blends, and that simple adjustments can be made so that the primaries are spaced to achieve solid colour effects. This chapter also illustrated through the use of carded, spun and knitted samples, that blends which appear as solid colours in web form, also appear solid in knitted form. This is an

important finding as the application of this research is aimed at the fashion industry; where this technology would be received as knitted or woven garments, rather than non-woven webs of fibre.

A practical colouration system also requires effective methods for predicting the colour of a given blend from the colour of the primaries (and their proportions) within the blend. Therefore, in chapter 5, four different blend prediction models were tested; Stearns-Noechel's equation (Stearns & Noechel, 1944), Friele's equation (Friele, 1952), a standard neural network and a novel application of neural networks (the novel networks). To date, Stearns-Noechel and Friele's equations (or variations of) have been the most widely used methods of predicting the colour of blends. Whilst neural networks have been used to predict dye concentrations and the colour of printed inks (Bishop *et al.*, 1991; Westland, 1994; Westland, 1998; Westland *et al.*, 1991;), their application within colour prediction of fibre blends has been less prominent. The comparison of these prediction models using the large sample set prepared in chapter 3 of this thesis provided interesting results. The results showed that both Stearns-Noechel and Friele's equations were outperformed by the neural networks. Stearns-Noechel's model gave a testing error of 3.05 CIELAB ΔE (or 1.87 CIEDE2000) and Friele's equation a testing error of 2.42 CIELAB ΔE (or 1.74 CIEDE2000). The lowest testing error using the standard neural network was 1.20 CIELAB ΔE (or 0.80 CIEDE2000) and for the novel neural network 1.17 CIELAB ΔE (or 0.81 CIEDE2000). The results showed clear benefits of using neural networks to predict the colour of blends as opposed to Stearns-Noechel or Friele's equations.

It was anticipated that the novel neural network might show an improvement on the standard neural network results due to the smaller size of each small network in relation to the training data. However, this was not observed; the novel neural network and the standard neural network performed very similarly with both networks showing excellent results. One notable advantage to using the novel neural network is the reduced time that it takes to run compared to the standard neural network. The novel networks took approximately 85 % less time to run than the standard networks, showing a clear advantage if they are to be used within industry. The improved

performance of the neural networks in predicting blend colours compared to Stearns-Noechel and Friele's equations can most likely be attributed to the ability of the neural networks to learn and generalise complex relationships between inputs and outputs. With some further alterations to MATLAB's standard neural network settings, it may be possible to improve the performance of both the standard neural network and the novel neural network. As the networks are however, they would be acceptable methods for predicting the colour of fibre blends with accuracy akin to industry standards.

To return to the aim of this thesis, a sustainable method of colouration has been outlined through the exploration of existing literature and experimental work. The first objective outlined for this work included identifying the maximum mean colour difference of a group of primaries so that once blended they appear solid. This forms the first step to the methodology of sustainable colouration through fibre blending. It was found that by using example 4-colour blends viewed at a specific viewing distance by a group of participants with normal colour vision, the mean acceptable colour difference of a group of blends could be determined.

The second objective of this thesis involved defining the number of primaries required to fill a given gamut of colour space. This objective was addressed in chapter 4. It was found that by plotting a select number of primaries (to form the outer perimeter of a target gamut) it is possible to fill the interior volume of that gamut with a specified number of primaries. The method developed uses MATLAB functions to distribute n number of primaries evenly within a gamut and group them into 4-colour tetrahedra. The mean colour differences of these tetrahedral groups can then be calculated. If the mean colour difference is too high then an increased number of primaries must be used and vice versa. It is ultimately up to a company to decide how many spun-dyed primaries is practical to stock, however from the literature it was seen that companies are already storing more than 60 primaries at a time. From the experiments undertaken in chapter 4 it is clear that a gamut containing 60 primaries would have the potential to produce thousands of discernible new colours when blended in specific 4-

colour groups, presenting the method of fibre blending as a truly flexible and appealing method of textile colouration.

Finally, the last objective of this thesis involved the testing and comparison of existing blend prediction models and neural networks. It was found that both the standard neural network and the novel neural network produced much smaller training and testing errors between predicted colour and measured colour of blends compared to Stearns-Noechel's and Friele's equations. Whilst both neural networks performed similarly well, it can be seen that the novel application of the neural network is advantageous in the reduced time that it takes to run, making it an appealing method to be used within industrial applications.

To summarise, the blending of coloured fibre can be a sustainable, economical and flexible way of colouring textiles for fashion. The sustainability of fibre blending is increased when sustainable fibre and dyeing choices such as Lenzing spun-dyed Viscose Austria and Tencel® are integrated into the methodology.

6.2 Further work

Within this thesis, a methodology for predicting the colour of a fibre blend composed of more than one primary was developed. In order to understand how visually successful a set of primaries blended, so that they appeared as one colour, observer experiments were undertaken using blended samples viewed at a distance of 45 cm. Further observer experiments could be done, where the viewing distance between participant and blended sample is increased or decreased. This could help to further understand the effect of the viewing distance on the appearance of a blend as a solid colour or not. As the distance between observer and blended samples is increased, it is likely that samples with a greater mean colour difference than identified in this thesis (for example, above 25 CIELAB ΔE) will appear solid to a greater percentage of participants. The number of participants observing the samples could also be increased.

Further work could also include producing a range of knitted samples with varying knit structures. This would contribute to greater understanding of the effect of structure on the appearance of the blended primaries. Again, the viewing distance at which the knitted samples are observed could be increased or decreased, and the number of participants observing the samples could also be increased.

The neural networks used in this thesis were run using MATLAB's standard neural network settings. Adjustments were made to the stopping criteria of Standard Network 2 and Novel Network 2 by increasing the number of epochs from 1000 to 10,000. Further alterations to the stopping criteria, for example increasing the gradient, could also be explored to determine whether the performance of the neural networks could be further improved upon. It is possible that with further alteration to the standard MATLAB settings, the novel network could perform better (as well as more quickly) than the standard neural network.

Finally, whilst this thesis has investigated methods of predicting the colour of a blend depending on its composition of primaries, further work could be done to predict the inverse problem; predicting the specific primaries and quantities thereof to match a target colour.

References

- Allwood, J. M., Laursen, S. E., Malvido de Roderiguez, C. and Bocken, N. M. P. 2006. *Well dressed? The present and future sustainability of clothing and textiles in the UK*. Cambridge: University of Cambridge Institute for Manufacturing.
- American Association of Textile Chemists and Colorists (AATCC). 2000. AATCC technical manual (Vol. 75). North Carolina: American Association of Textile Chemists and Colorists.
- Anson, R. 2010. Editorial: End of the line for cheap clothing? *Textile Outlook International*. **147**, pp.4-10.
- Aspland, J. R. and Zhou, M. 2000. Influence of blending on color appearance of black and white fiber blends. *Textile Chemist and Colorist and American Dyestuff Reporter*. **32**(10), pp.47-51.
- Battle, D. R. 1997. The measurement of colour. In: McDonald, R. *Colour physics for industry*. 2nd ed. Bradford: Society of Dyers and Colourists, pp.57-80.
- Berfield, S. and Baigorri, M. 2013. *Zara's fast-fashion edge*. [Online]. [Accessed 17 July 2014]. Available from: <http://www.businessweek.com/articles/2013-11-14/2014-outlook-zaras-fashion-supply-chain-edge>
- Berns, R. 2000. *Billmeyer and Saltzman's principles of color technology*. 3rd ed. Chichester: John Wiley.
- Bezerra, C. de M. and Hawkyard, C. J. 2000. Computer match prediction for fluorescent dyes by neural networks. *Journal of the Society of Dyers and Colourists*. **116**(5-6), pp.163-169.

Bide, M. 2007. Environmentally responsible dye application. In: Christie, R. M. ed. *Environmental aspects of textile dyeing*. Cambridge: Woodhead Publishing Limited, pp.74-92.

Birla Cellulose. 2012a. *Colour that loves water that loves colour*. [Online]. [Accessed: 14 August 2014]. Available from: <http://www.birlacellulose.com/#/fibre/birlaspun>.

Birla Cellulose. 2012b. *Birla spunshades*. [Online]. [Accessed 25 September 2014]. Available from: <http://birlacellulose.com/#/innovation/spun>.

Black, S. 2011. *Eco-Chic: the fashion paradox*. London: Black Dog Publishing Limited.

Burlone, D. A. 1983. Formulation of blends of precoloured nylon fiber. *Color Research and Application*. **8**(2), pp.114-120.

Burlone, D. A. 1984. Theoretical and practical aspects of selected fiber-blend color-formulation functions. *Color Research and Application*. **9**(4), pp.213-219.

Burlone, D. A. 1990. Effect of fiber translucency on the color of blends of precolored fibers. *Textile Research Journal*. **60**, pp.162-167.

Campbell, C. 2006. Consuming goods and the good of consuming. In: Jackson, T. ed. *The earthscan reader in sustainable consumption*. London: Earthscan, pp.278-290.

Cattoor, T. 2007. European legislation relating to textile dyeing. In: Christie, R. M. ed. *Environmental aspects of textile dyeing*. Cambridge: Woodhead Publishing Limited, pp.1-29.

Cegarra, J., Puente, P. and Valdeperas, J. 1992. *The dyeing of materials: the scientific bases and the techniques of application*. Biella: Texilia.

Cheung, V., Westland, S., Connah, D. and Ripamonti, C. 2004. A comparative study of the characterisation of colour cameras by means of neural networks and polynomial transforms. *Coloration Technology*. **120**(1), pp.19-25.

Cheung, V. and Westland, S. 2006. Methods for optimal color selection. *The Journal of Imaging Science Technology*. **50**(5), pp.481-488.

Christie, R. M. 2007. *Environmental aspects of textile dyeing*. Cambridge: Woodhead Publishing Limited.

Chu, K. 2014. *Why Zara is a 'Fast Fashion' pioneer*. [Online]. [Accessed 8 September 2014]. Available from: <http://blogs.wsj.com/corporate-intelligence/2014/06/24/why-zara-is-a-fast-fashion-pioneer/>

Ciechanska, D., and Nousiainen, P. 2005. Cellulosic fibres and fabric processing. In: Blackburn, R. S. ed. *Biodegradable and sustainable fibres*. Cambridge: Woodhead Publishing Limited, pp.111-156.

CIRFS (European man-made fibres association). 2014. *Cellulosics in Europe*. [Online]. [Accessed 8 September 2014]. Available from: <http://www.cirfs.org/KeyStatistics/CellulosicsinEurope.aspx>

Clay, J. 2004. *World agriculture and the environment: a commodity-by-commodity guide to impacts and practices*. London: Island Press.

Commission Internationale de L'Eclairage (CIE) and International Electrotechnical Commission (IEC). 1987. *International lighting vocabulary: CIE 017.4-1987*. 4th ed. Austria: CIE.

Commission Internationale de L'Eclairage (CIE). 2004. *Colorimetry*. 3rd ed. Austria: CIE.

Datacolor. 2007. *Datacolor 650/600/400 user's guide*. China: Datacolor.

Davidson, H.R. and Taylor, M. 1965. Prediction of the color of fiber blends. *Journal of the Optical Society of America*. **55**(1), pp.96-100.

Denton, M. J. and Daniels, P. N. 2002. *Textile terms and definitions*. 11th ed. Manchester: Textile Institute.

D'Errico, J. 2012. *File Exchange: Inhull*. [Online]. [Accessed 31 July 2014]. Available from: <http://www.mathworks.co.uk/matlabcentral/fileexchange/10226-inhull/content/inhull.m>

East, A. J. 2005. Polyester fibres. In: McIntyre, J. E. ed. *Synthetic fibres: nylon, polyester, acrylic, polyolefin*. Cambridge: Woodhead Publishing Limited, pp.95-166.

Environmental Justice Foundation (EJF) and Pesticide Action Network UK. 2007. *The Deadly Chemicals in Cotton*. Environmental Justice Foundation in collaboration with Pesticide Action Network UK, London.

Environmental Justice Foundation (EJF). 2014. *Cotton and water*. [Online]. [Accessed 10 September 2014]. Available from: <http://ejfoundation.org/cotton/cotton-and-water>

ENDS Report. 2007. Calls for energy labelling overhaul as sales of efficient white goods stall. *The ENDS Report*. **387**, p.26.

Fairchild, M. D. 2005. *Color appearance models*. Chichester; John Wiley.

Ferdows, K., Lewis, M. A. and Machuca, J. A. D. 2005. *Zara's secret for fast fashion*. [Online]. [Accessed: 17 July 2014]. Available from: <http://hbswk.hbs.edu/archive/4652.html>

Fiber Economics Bureau. 2013. *Fiber Organon*. **84**. Washington: Fiber Economics Bureau, Inc.

Filature Miroglio. 2009. *Decora; dope dye yarns*. [Online]. [Accessed: 23 August 2011]. Available from: <http://www.filaturemiroglio.com/eng/decora.php>

Flanagan, M. 2013. Can the clothing industry ever be sustainable? In: Black, S. ed. *The sustainable fashion handbook*. London: Thames and Hudson, pp.213-214.

Fletcher, K. 2008. *Sustainable fashion and textiles: design journeys*. London: Earthscan.

Fletcher, K. 2015 Forthcoming. Introduction. In: Fletcher, K. and Tham, M. eds. *Routledge handbook of sustainability and fashion*. Abingdon: Routledge, pp.1-11.

Fletcher, K. and Grose, L. 2012. *Fashion and sustainability: design for change*. London: Laurence King Publishing.

Fletcher, K. and Tham, M. 2004. *Lifetimes: Clothing Rhythms*. [Online]. [Accessed 8 April 2014]. Available from: <http://www.katefletcher.com/lifetimes/cr3a.html>

Franklin Associates. 1993. *Resource and Environmental Profile Analysis of a Manufactured Apparel Product: Woman's knit polyester blouse*. Washington DC: American Fiber Manufacturers Association.

Friele, L. F. C. 1952. The application of colour measurement in relation to fibre-blending. *Journal of the Textile Institute Proceedings*. **43**(8), pp.104-111.

Funahashi, K. 1989. On the approximate realization of continuous mappings. *Neural Networks*. **2**(3), pp.183-192.

Gangakhedkar, N. S. 2010. Colour measurement methods for textiles. In: Gulrajani, M. L. ed. *Colour Measurement* Cambridge: Woodhead Publishing Limited, pp.221-252.

Gibson, P. M. 2013. Sustainable fashion in the age of celebrity culture. In: Black, S. ed. *The sustainable fashion handbook*. London: Thames and Hudson, pp.20-23.

Goldstein E.B. 1996. *Sensation and perception*. 4th ed. California: Brooks/Cole Publishing Co.

Gregory, P. 2007. Toxicology of textile dyes. In: Christie, R. M. ed. *Environmental aspects of textile dyeing*. Cambridge: Woodhead Publishing Limited, pp.44-73.

Grose, L. 2009. Sustainable cotton production. In: Blackburn, R. S. ed. *Sustainable Textiles: Life Cycle and Environmental Impact*. Cambridge: Woodhead Publishing Limited, pp.33-62.

Guild, J. 1931. The colorimetric properties of the spectrum. *Philosophical Transactions of the Royal Society of London*. A230, pp.149-187.

Gupte, V. 2010. Expressing colours numerically. In: Gulrajani, M. L. ed. *Colour measurement: principles, advances and industrial applications*. Cambridge: Woodhead Publishing Limited, pp.70-87.

Guthrie, J. C. and Oliver, P. H. 1957. Applications of colour physics to textiles. *The Journal of the Society of Dyers and Colourists*. **73**(12), pp.533-542.

Guthrie, J. C., Moir, J. and Oliver, P. H. 1962. Two problems associated with the blending of coloured fibres. *Journal of the Society of Dyers and Colourists*. **78**(1), pp.27-34.

Hawley, J. M. 2006. Textile recycling: a system perspective. In: Wang, Y. ed. *Recycling in textiles*. Cambridge: Woodhead Publishing Limited, pp.7-24.

Haykin, S. 1999. *Neural networks: a comprehensive foundation*. 2nd ed. Upper Saddle River, New Jersey: Prentice Hall.

Hecht, J. 2014. *History shows that parched Aral Sea can be restored*. [Online]. [Accessed 6 June 2014]. Available from: <http://www.newscientist.com/article/dn25620-history-shows-that-parched-aral-sea-can-be-restored.html#.VBCgsfldXTo>

Hill, A. R. 1997. How we see colour. In: McDonald, R. ed. *Colour Physics for Industry*. Bradford: The Society of Dyers and Colourists, pp.426-513.

Hunger, K. and Sewekow, U. 2003. Health and safety aspects. In: Hunger, K. ed. *Industrial dyes: chemistry, properties, applications*. Cambridge: Wiley-VCH, pp.625-641.

Hunt, R. 1998. *Measuring colour*. Kingston-upon-Thames: Fountain Press.

Hunter Associates Laboratory, Inc. 2008. *Measuring fibres*. [Online]. [Accessed 18 July 2011]. Available from: <http://www.hunterlab.com/measurementmethods/fibers.html>

Ingamells, W. 1993. *Colour for Textiles: a user's handbook*. Bradford: Society of Dyers and Colourists.

International Organization for Standardization (ISO). 2006a. ISO 14040:2006. *Environmental management. Life cycle assessment. Principals and framework*. Geneva: International Organization for Standardization.

International Organization for Standardization (ISO). 2006b. ISO 14044:2006. *Environmental management. Life cycle assessment. Requirements and guidelines*. Geneva: International Organization for Standardization.

International Organization for Standardization (ISO). 2011a. ISO 11664-2:2011. *Colorimetry - Part 1: CIE standard colorimetric observers*. Geneva: International Organization for Standardization.

International Organization for Standardization (ISO). 2011b. ISO 11664-2:2011. *Colorimetry - Part 2: CIE standard illuminants*. Geneva: International Organization for Standardization.

International Organization for Standardization (ISO). 2011c. ISO 11664-4:2011. *Colorimetry - Part 4: CIE 1976 L*a*b* Colour space*. Geneva: International Organization for Standardization.

Ishihara, S. 1972. *Tests for colour-blindness*. 38 plates ed. Tokyo: Kanehara Shuppan Co.

Judd D. B. and Wyszecki G. 1975. *Color in business, science, and industry*. 3rd ed. New York: John Wiley and Sons.

Klemm, D., Heublein, B., Fink, H. -P. and Bohn, A. 2005. Cellulose: fascinating biopolymer and sustainable raw material. *Angewandte Chemie (International Edition)*. **44**(22), pp.3358–3393

Kubelka, P. and Munk, F. 1931. Ein Beitrag Zur Optik der Farbanstriche. *Zeitschrift fur technische Physik*. **12**, pp.593-601.

Kuehni, R. 2005. *Color: an introduction to practice and principles*. 2nd ed. Chichester: John Wiley.

Laursen, S. E. and Hansen, J. 1997. *Environmental assessment of textiles*. Copenhagen: Danish Environmental Protection Agency, p.84.

Lee, K. M. 2013a. Sustainable products and sustainable production: Introduction. In: Kauffman, J. and Lee, K. M. eds. *Handbook of sustainable engineering*. London: Springer, pp.261-267.

Lee, K. M. 2013b. Product life cycle assessment (PLCA) and product carbon footprint (PCF). In: Kauffman, J. and Lee, K. M. eds. *Handbook of sustainable engineering*. London: Springer, pp.371-388.

Lenzing. 2008. *Focus Sustainability; Sustainability in the Lenzing group 2008*. Austria: Lenzing Aktiengesellschaft.

Lenzing. 2012. *Focus sustainability: sustainability in the Lenzing Group 2012*. Austria: Lenzing Aktiengesellschaft.

Lenzing. 2014a. *Certifications, Eco-labels, Awards*. [Online]. [Accessed 18th June 2014]. Available from: <http://www.lenzing.com/en/concern/sustainability/certifications-eco-labels-awards.html>

Lenzing. 2014b. *Lenzing Group: Difficult Market Situation Continued in Q1/2014 – Countermeasures Have a Positive Impact*. [Press release]. [Accessed 18th June 2014]. Available from: <http://www.lenzing.com/en/concern/press/info/2014.html>

Lenzing. 2014c. *Lenzing Viscose: specifications*. [Online]. [Accessed 5 May 2014]. Available from: <http://www.lenzing.com/en/fibers/lenzing-viscose/specifications.html>

Lenzing. 2014d. *Tencel: revolutionary and eco-friendly*. [Online]. [Accessed 10 September 2014]. Available from: <http://www.lenzing.com/sites/botanicprinciples/website/sustainability04.htm>

Lenzing. 2014e. *Lenzing Viscose*. [Online]. [Accessed 5 May 2014]. Available from: <http://www.lenzing.com/en/fibers/lenzing-viscose.html>

Lewis, H., Gertsakis, J., Grant, T., Morelli, N. and Sweatman, A. 2001. *Design and environment: a guide to designing greener goods*. Sheffield: Greenleaf Publishing Limited.

Li, R., Song, Y., Gu, F. and Pan, W. 2009. A spectrophotometric color matching algorithm for precolored fiber blends. *Color Research and Application*. **34**(2), pp.108-114.

Luo, R. 2002. Development of colour-difference formulae. *Review of Progress in Coloration and Related Topics*. **32**(1), pp.28-39.

Luo, R., Cui, R. and Rigg, B. 2000. The development of the CIE 2000 colour-difference formula: CIEDE2000. *Color Research and Application*. **26**(5), pp.340-350.

MacAdam, D. L. 1947. Note on the number of distinct chromaticities. *Journal of the Optical Society of America*. **37**(4), pp.308-309.

Manian, A., Ruef, H. and Bechtold, T. 2007. Spun-dyed lyocell. *Dyes and pigments*. **74**(3), pp.519-524.

MathWorks. 2014b. *Neural Network Toolbox*. [Online]. [Accessed 31 July 2014]. Available from: <http://www.mathworks.co.uk/products/neural-network/>

MathWorks. 2014a. *Documentation Centre: delaunay*. [Online]. [Accessed 31 July 2014]. Available from: <http://www.mathworks.co.uk/help/matlab/math/delaunay-triangulation.html>

McIntyre, J. E. 2005. Historical background. In: McIntyre, J. E. ed. *Synthetic fibres: nylon, polyester, acrylic, polyolefin*. Cambridge: Woodhead Publishing Limited, pp.1-19.

Mehrotra, K., Mohan, C. K. and Ranka, S. 1997. *Elements of Artificial Neural Networks*. London: MIT Press.

Miller, A., Moir, J., Guthrie, J. C. and Oliver, P. H. 1963. A computed colour catalogue of fibre blends and its use in match prediction. *Journal of the Society of Dyers and Colourists*. **79**, pp.604-612.

Munsell, A. H. 1905. *A color notation*. Boston: Geo. H. Ellis Co.

Munsell, A. H. 1907. *Atlas of the Munsell Color System*. Malden, MA: Wadsworth-Howland.

Munsell, A. H. 1915. *Atlas of the Munsell Color System*. 2nd ed. Malden, MA: Wadsworth-Howland.

Munsell Color Company. 1929. *Munsell Book of Color*. Baltimore: Munsell Color Company.

Nevell, T. 1995. Cellulose: structure, properties and behaviour in the dyeing process. In: Shore, J. ed. *Cellulosics dyeing*. Bradford: Society of Dyers and Colourists, pp.1-80.

Newhall, S. M., Nickerson, D. and Judd, D. B. 1943. Final report of the O.S.A. subcommittee on the spacing of the Munsell Colors. *Journal of the Optical Society of America*, **33**(7), pp.385-418.

Nousiainen, P. 1997. Modern textile dyeing takes note of the environment. *Kemia-Kemi*. **24**(5), pp.376-380.

Nobbs, J. H. 1985. Kubelka-Munk theory and the prediction of reflectance. *Review of Progress in Coloration and Related Topics*. **15**(1), pp.66-75.

Ohta, N., and Robertson, A. R. 2005. *Colorimetry: fundamentals and applications*. Chichester: John Wiley and Sons Ltd.

Osherson, D. N., Weinstein, S. and Stob, M. 1990. Modular learning. In: Schwartz, E. L. ed. *Computational Neuroscience*. Cambridge, Massachusetts: MIT Press, pp.369-377.

Oxford English Dictionary (OED). 2013. *Mélange*, *n.* 3rd ed. Oxford: Oxford University Press. [Online]. [Accessed 28 November 2014]. Available from: <http://www.oed.com/view/Entry/116016?rskey=WlwQpW&result=1#eid>

Oxford English Dictionary (OED). 2014. *Primary*, *adj. and n.; primary colour*. 3rd ed. Oxford: Oxford University Press. [Online]. [Accessed 28 November 2014]. Available from: <http://www.oed.com/view/Entry/151280?rskey=uPaqKN&result=1#eid>

Pantone. 2011. *Pantone fashion and home cotton planner*. X-rite: [no place]. ISBN 978-1-590651-92-6.

Pantone. 2014. *Pantone: What we do*. [Online]. [Accessed 10 May 2014]. Available from: <http://www.pantone.co.uk/pages/pantone/pantone.aspx?pg=19295&ca=10>

Park, R. H. and Stearns, E. I. 1944. Spectrophotometric Formulation. *Journal of the Optical Society of America*. **34**(2), pp.112-113.

Perkins, W. S. 1996. *Textile coloration and finishing*. Durham, North Carolina: Carolina Academic Press.

Philips-Invernizzi, B. and Caze, C. 2000. Sustainability and recycling of textile materials: Modelling colorimetric behaviour of cotton fiber blends. *Proceedings of the spring 2000 meeting of the Fiber Society*. Guimaraes, Portugal: University of Minho, pp.53-56.

Philips-Invernizzi, B., Dupont, D. and Caze, C. 2002a. Formulation of colored fiber blends from Friele's theoretical model. *Color Research and Application*. **27**(3), pp.191-198.

Philips-Invernizzi, B., Dupont, D., Jolly-Desodt, A. –M. and Caze, C. 2002b. Color formulation by fiber blending using the Stearns-Noechel model. *Color Research and Application*. **27**(2), pp.100-107.

Rigg, B. 1997. Colorimetry and the CIE system. In: McDonald, R. ed. *Colour physics for industry*. 2nd ed. Bradford: Society of Dyers and Colourists, pp.81-120.

Rong, L.I. and Feng, G.U. 2005. Tristimulus algorithm of colour matching for precoloured fibre blends based on the Stearns-Noechel model. *Coloration Technology*. **122**(2), pp.74-81.

Rumelhart, D. and McClelland, J. 1987. *Parallel distributed processing: explorations in the microstructure of cognition: Foundations*. Cambridge, Massachusetts: MIT Press.

Russell, I. M. 2009. Sustainable wool production and processing. In: Blackburn, R. S. ed. *Sustainable Textiles: Life Cycle and Environmental Impact*. Cambridge: Woodhead Publishing Limited, pp.64-87.

Sarle, W. S. 2002. *Subject: What is overfitting and how can I avoid it?* [Online]. [Accessed 20 August 2014]. Available from: <ftp://ftp.sas.com/pub/neural/FAQ3.html>

Shamey, R. and Hussain, T. 2003. Artificial intelligence in the colour and textile industry. *Review of Progress in Coloration and Related Topics*. **33**, pp.33-45.

Schalkoff, R. J. 1997. *Artificial Neural Networks*. New York: The McGraw-Hill Companies, Inc.

Shen, L., Worrell, E. and Patel, M. K. 2010. Environmental impact assessment of man-made cellulose fibres. *Resources, Conservation and Recycling*. **55**(2), pp.260-274.

Shen, L. and Patel, M. 2008. *Life Cycle Assessment of Lenzing Fibers*. Netherlands: University Utrecht.

Sherburne, A. 2009. Achieving sustainable textiles: a designer's perspective. In: Blackburn, R. S. ed. *Sustainable textiles: life cycle and environmental impact*. Cambridge: Woodhead Publishing Limited, pp.3-32.

Simpson, P. 2013. Global trends in fibre prices, production and consumption. *Textile Outlook International*. **165**, pp.50-69.

Sinclair, R. S. 1997. Light, light sources and light interactions. In: McDonald, R. ed. *Colour Physics for Industry*. 2nd ed. Bradford: Society of Dyers and Colourists, pp.1-56.

Soth, J., Grasser, C. and Salerno, R. 1999. *The impact of cotton on fresh water resources and ecosystems: a preliminary synthesis*. Switzerland: WWF.

Speranskaya, N. I. 1959. Determination of spectrum color coordinates for twenty-seven normal observers. *Optics and Spectroscopy*. **7**, pp.424-428.

Stearn, C. 1898. Patent No. 1020. Britain.

Stearns, E.L. and Noechel, F. 1944. Spectrophotometric prediction of color of wool blends. *American Dyestuff Reporter*. **33**, pp.177-180.

Stiles, W. S. and Burch, J. M. 1959. NPL colour-matching investigation: Final report. *Optica Acta*. **6**, pp.1-26.

Taylor, J. 2012. *Meeting with Jim Taylor at Lenzing, Austria, 29 October*.

Terinte, N., Manda, B. M. K., Taylor, J., Schuster, K. C. and Patel, M. K. 2014. Environmental assessment of coloured fabrics and opportunities for value creation: spin-dyeing versus conventional dyeing of modal fabrics. *Journal of cleaner production*. **72**, pp.127-138.

Textiles Intelligence. 2013. Man-made Fibre Production and Consumption in Europe. *Textile Outlook International*. **166**, pp.145-157.

Tham, M. 2013. Slow and fast fashion. In: Black, S. ed. *The sustainable fashion handbook*. London: Thames and Hudson, pp.216-218.

The Economist. 2005. *Inditex: the future of fast fashion*. [Online]. [Accessed 19 June 2014]. Available from: <http://www.economist.com/node/4086117>

Tilley, R. J. D. 2011. *Colour and the optical properties of materials*. Chichester: John Wiley & Sons Limited.

United Nations (Department of Economic and Social Affairs). 2013. *World Population Prospects: The 2012 Revision, Highlights and Advance Tables*. [Online]. New York: United Nations. [Accessed 18 June 2014]. Available from: http://esa.un.org/unpd/wpp/Documentation/pdf/WPP2012_HIGHLIGHTS.pdf

Virtual Colour Systems Ltd (VCS). 2013. *Virtual Atlas*. [Online]. [Accessed 21 July 2014]. Available from: <http://www.vcsconsulting.co.uk/Colour/colourpage2.html>

Viqueira Pérez, V., De Fez Saiz, D. and Martinez Verdú, F. 2010. Colour vision: theories and principles. In: Gulrajani, M. *Colour measurement: principles, advances and industrial applications*. Cambridge: Woodhead Publishing Limited, pp.3-18.

Wakelyn, P. J. and Chaudhry, M. R. 2007. Organic cotton. In: Gordon, S. and Hsieh, Y.L. eds. *Cotton: science and technology*. Cambridge: Woodhead Publishing Limited, pp.130-170.

Warburton, P. and Lund, G. V. 1956. Colour and textiles: II-The modification of colour due to juxtaposition. *Journal of the Textile Institute Proceedings*. **47**(5), pp.319-346.

Warburton, P. and Oliver, P. H. 1956. Colour and textiles: IV-The blending of coloured fibres. *Journal of the Textile Institute Proceedings*. **47**(5), pp.361-373.

Westland, S., Bishop, J. M., Bushnell, M. J. and Usher, A. L. 1991. An intelligent approach to colour recipe prediction. *Journal of the Society of Dyers and Colourists*. **107**, pp.235-237.

Westland, S. 1994. Advances in artificial intelligence for the colour industry. *Journal of the Society of Dyers and Colourists*. **110**(11), pp.370-375.

Westland, S. 1998. Artificial neural networks explained - part 2. *Journal of the Society of Dyers and Colourists*. **114**(10), pp.312-315.

Westland, S. 2001. Artificial neural networks and colour recipe prediction. *Proceedings of Colour Science 98*. University of Leeds, UK. **3**, pp.225-233.

Westland, S. and Ripamonti, C. 2004. *Computational colour science using MATLAB®*. 1st ed. Chichester: John Wiley & Sons Limited.

Westland, S., Ripamonti, C. and Cheung, V. 2012. *Computational colour science using MATLAB®*. 2nd ed. Chichester: John Wiley & Sons Limited.

Wilkes, A. 2000. The viscose process. In: Woodings, C. ed. *Regenerated cellulose fibres*. Cambridge: Woodhead Publishing Limited, pp.37-61.

Woodings, C. 2000. A brief history of regenerated cellulosic fibres. In Woodings, C. ed. *Regenerated Cellulose*. Cambridge: Woodhead Publishing Limited, pp.1-21.

World Wide Fund for Nature (WWF). 2003. *Thirsty crops: Our food and clothes: eating up nature and wearing out the environment?* Switzerland: WWF.

Wright, W. D. 1929. A re-determination of the trichromatic coefficients of the spectral colours. *Transactions of the Optical Society*. **30**(4), pp.141-164.

X-rite. 2007. *Munsell Color: Defining color: Systems for precise color validation*. [Online]. [Accessed 24 July 2012]. Available from: http://www.xrite.com/documents/literature/en/L10-315_Defining_Color_Munsell_en.pdf

Appendices

Appendix I MATLAB code for plotting tristimulus values in CIELAB colour space

```
% p is a 35 x 1 example vector of reflectance percent
p = [7.47
8.19
8.89
9.63
10.13
10.41
10.62
10.82
10.95
11.05
11.07
11.01
10.88
10.73
10.52
10.21
9.81
9.57
9.45
9.14
8.48
8.09
8.67
9.51
9.59
9.56
9.51
9.53
9.66
9.95
10.32
10.49
10.52
10.36
10.04];
```



```

% divide by 100 and transform the 35 x 1 vector into a 1 x 35 vector
data = (p/100)';

% calculate XYZ using standard r2xyz function
xyz = r2xyz(data,360,700,'d65_64');

% calculate CIELAB coordinates using standard xyz2lab function
lab = xyz2lab(xyz,'d65_64');

% calculate sRGB using standard xzy2srgb function
rgbface=xyz2srgb(xyz(:, :)/100)/255;
[rows clmns]=size(rgbface);

% plot CIELAB coordinates, coloured with sRGB values
for i=1:rows
plot3(lab(i,2),lab(i,3),lab(i,1),'ko','MarkerFaceColor',rgbface(i,:), '
MarkerEdgeColor','k');
hold on
end

% plot axes
hold on
plot3([0 0],[0 0],[0 100],'k-')
hold on
plot3([-90 90],[0 0],[50 50],'k-')
hold on
plot3([0 0],[-90 90],[50 50],'k-')
axis([-90 90 -90 90 0 100])

```

Appendix II MATLAB code for calculating the CIELAB ΔE between two colours

```

% p1 and p2 are example 35 x 1 vectors of reflectance percent
% as in Appendix I but not shown here

% group p1 and p2 together to create a 35 x 2 vector
p = [p1 p2];

save p.mat
close all
load p.mat

% divide by 100 and transform the 35 x 2 vector into a 2 x 35 vector
data = (p/100)';

% calculate XYZ using standard r2xyz function
xyz = r2xyz(data,360,700,'d65_64');

% calculate CIELAB coordinates using standard xyz2lab function
lab = xyz2lab(xyz,'d65_64');

% calculate colour difference between p1 and p2
lab(1,:);
lab(2,:);
cielabde(lab(1,:),lab(2,:))

```

Appendix III MATLAB code for calculating the average CIELAB ΔE of a blend of three colours

```
% p1, p2 and p3 are 35 x 1 example vectors of reflectance percent

% group p1, p2 and p3 together to create a 35 x 3 vector
pp = [p1 p2 p3];

% divide by 100 and transform the 35 x 3 vector into a 3 x 35 vector
data = (pp/100)';

% calculate XYZ using standard r2xyz function
xyz = r2xyz(data,360,700,'d65_64');

% calculate CIELAB coordinates using standard xyz2lab function
lab = xyz2lab(xyz,'d65_64');

% calculate colour difference between p1 and p2, p1 and p3, p2 and p3
% these three numbers can then be averaged
cielabde(lab(1,:),lab(2,:))

cielabde(lab(1,:),lab(3,:))

cielabde(lab(2,:),lab(3,:))
```

Appendix IV Example directions for observer experiment

The purpose of this experiment is to determine, from a group of observers, which of the carded samples provided appear solid in colour.

X webs of coloured fibre have been created by a process of carding loose stock fibre. Each individual sample is different and is composed of either one, two, three or four different colours per sample. You will not be told how many colours are in each sample.

For each sample, you must indicate whether you think the given sample appears to be either;

a) A solid colour

(the sample appears like one colour)

b) Almost a solid colour

(the sample is very close to appearing like it is one colour, but you can see that there may be another colour present)

c) Not a solid colour

(the sample definitely appears to be made up from more than one colour)

Notes:

- Your results are confidential and anonymous.
- No personal data will be asked for or used in any way.
- Your help in my research will allow me to identify which blends of coloured fibre, made from either singular or multiple colours, appear solid in colour.

Appendix V Example data capture form for recording observer responses

Record observers responses using the following numbering system:

- | | |
|--------------------------|------------|
| a) A solid colour | 1 point |
| b) Almost a solid colour | 0.5 points |
| c) Not a solid colour | 0 points |

[illegible]

Appendix VI First experiment recipes and CIELAB ΔE

P1 = Primary 1;

P2 = Primary 2;

P3 = Primary 3;

P4 = Primary 4;

P5 = Primary 5;

P6 = Primary 6;

P7 = Primary 7;

P8 = Primary 8.

Blend no.	P1 (%)	P2 (%)	P3 (%)	P4 (%)	P5 (%)	P6 (%)	P7 (%)	P8 (%)	ΔE
Blend 1.1	50.00	50.00	0.00	0.00	0.00	0.00	0.00	0.00	82
Blend 1.2	0.00	0.00	50.00	0.00	0.00	25.00	25.00	0.00	78
Blend 1.3	0.00	50.00	16.67	16.67	0.00	16.67	0.00	0.00	74
Blend 1.4	0.00	0.00	0.00	0.00	0.00	0.00	75.00	25.00	38
Blend 1.5	75.00	0.00	25.00	0.00	0.00	0.00	0.00	0.00	43
Blend 1.6	0.00	0.00	25.00	25.00	25.00	0.00	0.00	25.00	69

Blend 1.7	16.67	16.67	0.00	0.00	50.00	16.67	0.00	0.00	78
Blend 1.8	0.00	25.00	0.00	0.00	25.00	50.00	0.00	0.00	76
Blend 1.9	0.00	0.00	16.67	0.00	0.00	16.67	50.00	16.67	72
Blend 1.10	0.00	25.00	25.00	25.00	25.00	0.00	0.00	0.00	71
Blend 1.11	0.00	0.00	0.00	25.00	50.00	0.00	25.00	0.00	73
Blend 1.12	25.00	25.00	0.00	0.00	0.00	25.00	25.00	0.00	79
Blend 1.13	0.00	50.00	0.00	0.00	0.00	50.00	0.00	0.00	109
Blend 1.14	16.67	16.67	0.00	16.67	0.00	0.00	0.00	50.00	74
Blend 1.15	0.00	25.00	0.00	25.00	0.00	0.00	25.00	25.00	69
Blend 1.16	50.00	0.00	0.00	0.00	50.00	0.00	0.00	0.00	80
Blend 1.17	0.00	16.67	50.00	0.00	16.67	0.00	0.00	16.67	77
Blend 1.18	25.00	0.00	0.00	0.00	0.00	25.00	0.00	50.00	88
Blend 1.19	0.00	50.00	0.00	0.00	25.00	0.00	25.00	0.00	91
Blend 1.20	0.00	0.00	0.00	25.00	25.00	0.00	25.00	25.00	77
Blend 1.21	16.67	16.67	50.00	16.67	0.00	0.00	0.00	0.00	68

Blend 1.22	0.00	50.00	16.67	0.00	16.67	0.00	16.67	0.00	77
Blend 1.23	0.00	0.00	50.00	0.00	16.67	16.67	16.67	0.00	72
Blend 1.24	25.00	0.00	0.00	25.00	0.00	25.00	0.00	25.00	76
Blend 1.25	0.00	16.67	16.67	50.00	16.67	0.00	0.00	0.00	71
Blend 1.26	0.00	0.00	75.00	25.00	0.00	0.00	0.00	0.00	57
Blend 1.27	16.67	0.00	0.00	16.67	50.00	0.00	16.67	0.00	67
Blend 1.28	0.00	16.67	0.00	50.00	0.00	0.00	16.67	16.67	69
Blend 1.29	33.33	33.33	33.33	0.00	0.00	0.00	0.00	0.00	64
Blend 1.30	0.00	33.33	33.33	0.00	0.00	33.33	0.00	0.00	88
Blend 1.31	0.00	0.00	0.00	0.00	0.00	0.00	25.00	75.00	38
Blend 1.32	0.00	0.00	50.00	0.00	0.00	0.00	50.00	0.00	42
Blend 1.33	16.67	50.00	16.67	0.00	0.00	0.00	16.67	0.00	55
Blend 1.34	16.67	0.00	0.00	0.00	16.67	0.00	50.00	16.67	73
Blend 1.35	25.00	0.00	0.00	0.00	0.00	0.00	0.00	75.00	67
Blend 1.36	0.00	0.00	50.00	25.00	25.00	0.00	0.00	0.00	55

Blend 1.37	25.00	25.00	25.00	0.00	0.00	25.00	0.00	0.00	78
Blend 1.38	33.33	0.00	0.00	33.33	33.33	0.00	0.00	0.00	58
Blend 1.39	0.00	75.00	0.00	0.00	0.00	0.00	25.00	0.00	61
Blend 1.40	0.00	0.00	25.00	0.00	25.00	0.00	0.00	50.00	79
Blend 1.41	0.00	0.00	25.00	25.00	25.00	25.00	0.00	0.00	50
Blend 1.42	0.00	16.67	16.67	0.00	50.00	0.00	0.00	16.67	77
Blend 1.43	0.00	0.00	0.00	0.00	0.00	25.00	75.00	0.00	106
Blend 1.44	16.67	0.00	16.67	0.00	0.00	16.67	0.00	50.00	73
Blend 1.45	0.00	33.33	33.33	0.00	0.00	0.00	33.33	0.00	57
Blend 1.46	25.00	0.00	0.00	0.00	0.00	0.00	50.00	25.00	47
Blend 1.47	25.00	0.00	50.00	0.00	0.00	0.00	25.00	0.00	40
Blend 1.48	0.00	0.00	0.00	75.00	25.00	0.00	0.00	0.00	27
Blend 1.49	50.00	0.00	16.67	0.00	16.67	0.00	0.00	16.67	71
Blend 1.50	16.67	16.67	0.00	0.00	50.00	0.00	16.67	0.00	78
Blend 1.51	0.00	0.00	33.33	0.00	0.00	33.33	33.33	0.00	78

Blend 1.67	16.67	50.00	16.67	0.00	16.67	0.00	0.00	0.00	77
Blend 1.68	0.00	75.00	25.00	0.00	0.00	0.00	0.00	0.00	68
Blend 1.69	0.00	0.00	25.00	0.00	0.00	75.00	0.00	0.00	87
Blend 1.70	33.33	0.00	0.00	0.00	33.33	0.00	33.33	0.00	74
Blend 1.71	50.00	0.00	0.00	25.00	25.00	0.00	0.00	0.00	58
Blend 1.72	25.00	25.00	0.00	0.00	0.00	50.00	0.00	0.00	90
Blend 1.73	0.00	0.00	0.00	25.00	0.00	25.00	25.00	25.00	79
Blend 1.74	0.00	50.00	0.00	0.00	0.00	16.67	16.67	16.67	80
Blend 1.75	0.00	0.00	0.00	50.00	25.00	0.00	0.00	25.00	77
Blend 1.76	0.00	0.00	0.00	0.00	75.00	25.00	0.00	0.00	11
Blend 1.77	0.00	50.00	25.00	0.00	25.00	0.00	0.00	0.00	85
Blend 1.78	0.00	33.33	0.00	0.00	33.33	0.00	33.33	0.00	91
Blend 1.79	50.00	0.00	0.00	25.00	0.00	25.00	0.00	0.00	61
Blend 1.80	0.00	33.33	0.00	0.00	33.33	0.00	0.00	33.33	90
Blend 1.81	0.00	0.00	0.00	50.00	0.00	0.00	0.00	50.00	91

Blend 1.82	0.00	25.00	25.00	0.00	50.00	0.00	0.00	0.00	85
Blend 1.83	16.67	0.00	16.67	0.00	50.00	0.00	0.00	16.67	68
Blend 1.84	16.67	0.00	16.67	50.00	16.67	0.00	0.00	0.00	59
Blend 1.85	0.00	16.67	0.00	0.00	16.67	16.67	0.00	50.00	85
Blend 1.86	16.67	0.00	50.00	16.67	0.00	0.00	0.00	16.67	61
Blend 1.87	0.00	0.00	0.00	25.00	50.00	25.00	0.00	0.00	25
Blend 1.88	0.00	0.00	50.00	0.00	25.00	25.00	0.00	0.00	60
Blend 1.89	50.00	0.00	0.00	0.00	16.67	16.67	16.67	0.00	70
Blend 1.90	0.00	0.00	0.00	50.00	0.00	25.00	0.00	25.00	82
Blend 1.91	33.33	0.00	0.00	0.00	33.33	0.00	0.00	33.33	87
Blend 1.92	0.00	0.00	50.00	0.00	25.00	0.00	25.00	0.00	76
Blend 1.93	0.00	33.33	0.00	33.33	0.00	0.00	0.00	33.33	76
Blend 1.94	0.00	0.00	16.67	0.00	16.67	0.00	50.00	16.67	70
Blend 1.95	50.00	0.00	0.00	50.00	0.00	0.00	0.00	0.00	67
Blend 1.96	0.00	0.00	0.00	0.00	25.00	75.00	0.00	0.00	11

Blend 1.97	0.00	0.00	0.00	50.00	0.00	0.00	25.00	25.00	72
Blend 1.98	16.67	50.00	0.00	0.00	16.67	0.00	16.67	0.00	78
Blend 1.99	0.00	0.00	16.67	50.00	0.00	16.67	16.67	0.00	69
Blend 1.100	0.00	0.00	25.00	0.00	0.00	25.00	25.00	25.00	72
Blend 1.101	0.00	0.00	16.67	50.00	0.00	0.00	16.67	16.67	59
Blend 1.102	0.00	0.00	16.67	16.67	50.00	0.00	0.00	16.67	69
Blend 1.103	0.00	0.00	0.00	0.00	50.00	25.00	0.00	25.00	82
Blend 1.104	25.00	25.00	0.00	0.00	25.00	0.00	0.00	25.00	83
Blend 1.105	0.00	16.67	16.67	0.00	0.00	16.67	50.00	0.00	79
Blend 1.106	50.00	25.00	0.00	0.00	0.00	25.00	0.00	0.00	90
Blend 1.107	16.67	0.00	16.67	0.00	50.00	16.67	0.00	0.00	64
Blend 1.108	25.00	0.00	0.00	0.00	25.00	50.00	0.00	0.00	57
Blend 1.109	0.00	25.00	0.00	50.00	25.00	0.00	0.00	0.00	74
Blend 1.110	0.00	25.00	0.00	50.00	0.00	0.00	25.00	0.00	79
Blend 1.111	0.00	25.00	0.00	0.00	0.00	25.00	0.00	50.00	92

Blend 1.112	25.00	0.00	25.00	0.00	0.00	0.00	0.00	50.00	50
Blend 1.113	25.00	0.00	0.00	50.00	0.00	0.00	0.00	25.00	75
Blend 1.114	0.00	0.00	0.00	0.00	50.00	0.00	25.00	25.00	86
Blend 1.115	25.00	0.00	0.00	0.00	50.00	0.00	0.00	25.00	87
Blend 1.116	25.00	0.00	25.00	0.00	0.00	0.00	50.00	0.00	40
Blend 1.117	0.00	25.00	0.00	0.00	75.00	0.00	0.00	0.00	106
Blend 1.118	25.00	0.00	25.00	0.00	25.00	0.00	25.00	0.00	65
Blend 1.119	0.00	0.00	50.00	0.00	0.00	0.00	0.00	50.00	41
Blend 1.120	0.00	50.00	0.00	16.67	0.00	0.00	16.67	16.67	69
Blend 1.121	25.00	0.00	0.00	0.00	0.00	75.00	0.00	0.00	79
Blend 1.122	0.00	0.00	0.00	50.00	16.67	16.67	16.67	0.00	62
Blend 1.123	25.00	0.00	0.00	25.00	0.00	25.00	25.00	0.00	68
Blend 1.124	0.00	25.00	0.00	25.00	0.00	0.00	50.00	0.00	79
Blend 1.125	0.00	0.00	0.00	25.00	25.00	25.00	0.00	25.00	66
Blend 1.126	0.00	0.00	50.00	16.67	16.67	16.67	0.00	0.00	50

Blend 1.127	25.00	25.00	0.00	0.00	0.00	0.00	25.00	25.00	55
Blend 1.128	0.00	0.00	0.00	25.00	0.00	75.00	0.00	0.00	36
Blend 1.129	25.00	0.00	50.00	0.00	25.00	0.00	0.00	0.00	69
Blend 1.130	0.00	50.00	25.00	0.00	0.00	0.00	25.00	0.00	57
Blend 1.131	16.67	16.67	50.00	0.00	0.00	16.67	0.00	0.00	78
Blend 1.132	0.00	0.00	50.00	16.67	0.00	16.67	16.67	0.00	69
Blend 1.133	0.00	16.67	16.67	50.00	0.00	16.67	0.00	0.00	74
Blend 1.134	0.00	0.00	0.00	0.00	0.00	50.00	25.00	25.00	88
Blend 1.135	75.00	0.00	0.00	0.00	25.00	0.00	0.00	0.00	80
Blend 1.136	0.00	16.67	0.00	16.67	16.67	50.00	0.00	0.00	63
Blend 1.137	0.00	0.00	0.00	0.00	33.33	33.33	0.00	33.33	82
Blend 1.138	0.00	0.00	0.00	33.33	0.00	33.33	0.00	33.33	82
Blend 1.139	16.67	0.00	16.67	0.00	16.67	0.00	0.00	50.00	71
Blend 1.140	0.00	25.00	0.00	0.00	0.00	75.00	0.00	0.00	109
Blend 1.141	0.00	0.00	0.00	50.00	16.67	0.00	16.67	16.67	77

Blend 1.142	25.00	0.00	50.00	0.00	0.00	25.00	0.00	0.00	70
Blend 1.143	25.00	0.00	25.00	50.00	0.00	0.00	0.00	0.00	56
Blend 1.144	0.00	0.00	0.00	0.00	25.00	0.00	75.00	0.00	105
Blend 1.145	25.00	50.00	0.00	0.00	25.00	0.00	0.00	0.00	89
Blend 1.146	50.00	0.00	0.00	16.67	0.00	0.00	16.67	16.67	64
Blend 1.147	0.00	0.00	0.00	25.00	25.00	25.00	25.00	0.00	62
Blend 1.148	25.00	0.00	25.00	0.00	0.00	0.00	25.00	25.00	45
Blend 1.149	25.00	25.00	0.00	25.00	0.00	0.00	25.00	0.00	70
Blend 1.150	0.00	50.00	16.67	0.00	0.00	0.00	16.67	16.67	50
Blend 1.151	0.00	25.00	0.00	25.00	25.00	0.00	0.00	25.00	79
Blend 1.152	0.00	0.00	25.00	0.00	25.00	0.00	50.00	0.00	76
Blend 1.153	50.00	25.00	25.00	0.00	0.00	0.00	0.00	0.00	64
Blend 1.154	0.00	16.67	0.00	50.00	16.67	16.67	0.00	0.00	63
Blend 1.155	16.67	16.67	0.00	0.00	0.00	50.00	0.00	16.67	84
Blend 1.156	0.00	0.00	33.33	33.33	0.00	0.00	0.00	33.33	63

Blend 1.157	0.00	50.00	0.00	16.67	0.00	16.67	0.00	16.67	82
Blend 1.158	50.00	0.00	25.00	0.00	25.00	0.00	0.00	0.00	69
Blend 1.159	0.00	0.00	0.00	0.00	25.00	0.00	50.00	25.00	86
Blend 1.160	0.00	16.67	0.00	0.00	50.00	0.00	16.67	16.67	79
Blend 1.161	0.00	0.00	0.00	0.00	0.00	25.00	0.00	75.00	119
Blend 1.162	50.00	16.67	0.00	0.00	16.67	0.00	16.67	0.00	78
Blend 1.163	0.00	16.67	16.67	16.67	0.00	50.00	0.00	0.00	74
Blend 1.164	0.00	25.00	0.00	25.00	25.00	25.00	0.00	0.00	63
Blend 1.165	25.00	50.00	0.00	0.00	0.00	25.00	0.00	0.00	90
Blend 1.166	0.00	25.00	0.00	25.00	0.00	0.00	0.00	50.00	76
Blend 1.167	0.00	0.00	25.00	25.00	0.00	0.00	0.00	50.00	63
Blend 1.168	25.00	0.00	0.00	0.00	0.00	50.00	25.00	0.00	74
Blend 1.169	16.67	0.00	16.67	50.00	0.00	0.00	16.67	0.00	55
Blend 1.170	25.00	0.00	25.00	0.00	0.00	25.00	25.00	0.00	66
Blend 1.171	0.00	50.00	25.00	0.00	0.00	0.00	0.00	25.00	52

Blend 1.172	16.67	0.00	16.67	50.00	0.00	16.67	0.00	0.00	52
Blend 1.173	0.00	50.00	0.00	16.67	16.67	16.67	0.00	0.00	63
Blend 1.174	0.00	16.67	0.00	0.00	16.67	50.00	0.00	16.67	85
Blend 1.175	0.00	50.00	0.00	0.00	25.00	25.00	0.00	0.00	76
Blend 1.176	0.00	25.00	25.00	0.00	0.00	0.00	25.00	25.00	50
Blend 1.177	0.00	16.67	0.00	0.00	0.00	16.67	16.67	50.00	80
Blend 1.178	0.00	16.67	50.00	0.00	0.00	0.00	16.67	16.67	50
Blend 1.179	0.00	0.00	16.67	50.00	16.67	0.00	16.67	0.00	67
Blend 1.180	0.00	0.00	16.67	16.67	16.67	0.00	50.00	0.00	67
Blend 1.181	0.00	16.67	0.00	16.67	0.00	16.67	0.00	50.00	82
Blend 1.182	0.00	16.67	16.67	0.00	0.00	0.00	50.00	16.67	50
Blend 1.183	0.00	0.00	0.00	0.00	16.67	16.67	50.00	16.67	82
Blend 1.184	0.00	0.00	0.00	0.00	0.00	50.00	0.00	50.00	119
Blend 1.185	33.33	0.00	33.33	0.00	33.33	0.00	0.00	0.00	69
Blend 1.186	0.00	0.00	0.00	25.00	50.00	0.00	0.00	25.00	77

Blend 1.187	50.00	0.00	0.00	25.00	0.00	0.00	0.00	25.00	75
Blend 1.188	0.00	0.00	0.00	0.00	0.00	75.00	25.00	0.00	106
Blend 1.189	50.00	0.00	25.00	25.00	0.00	0.00	0.00	0.00	56
Blend 1.190	0.00	25.00	0.00	0.00	0.00	50.00	25.00	0.00	92
Blend 1.191	50.00	16.67	0.00	0.00	16.67	0.00	0.00	16.67	83
Blend 1.192	50.00	0.00	0.00	0.00	0.00	0.00	0.00	50.00	67
Blend 1.193	0.00	75.00	0.00	0.00	0.00	25.00	0.00	0.00	109
Blend 1.194	0.00	75.00	0.00	0.00	0.00	0.00	0.00	25.00	48
Blend 1.195	0.00	0.00	25.00	50.00	0.00	0.00	25.00	0.00	62
Blend 1.196	0.00	0.00	0.00	25.00	0.00	0.00	0.00	75.00	91
Blend 1.197	0.00	0.00	0.00	16.67	16.67	50.00	0.00	16.67	66
Blend 1.198	50.00	0.00	0.00	0.00	0.00	0.00	50.00	0.00	36
Blend 1.199	16.67	0.00	0.00	0.00	0.00	16.67	50.00	16.67	74
Blend 1.200	75.00	0.00	0.00	0.00	0.00	0.00	25.00	0.00	36
Blend 1.201	0.00	0.00	16.67	16.67	50.00	0.00	16.67	0.00	67

Blend 1.202	50.00	0.00	0.00	0.00	16.67	16.67	0.00	16.67	78
Blend 1.203	0.00	0.00	50.00	0.00	0.00	16.67	16.67	16.67	72
Blend 1.204	25.00	0.00	0.00	50.00	0.00	0.00	25.00	0.00	63
Blend 1.205	0.00	0.00	50.00	25.00	0.00	25.00	0.00	0.00	60
Blend 1.206	25.00	50.00	0.00	25.00	0.00	0.00	0.00	0.00	79
Blend 1.207	0.00	0.00	0.00	25.00	0.00	25.00	0.00	50.00	82
Blend 1.208	25.00	50.00	25.00	0.00	0.00	0.00	0.00	0.00	64
Blend 1.209	0.00	0.00	0.00	25.00	0.00	50.00	25.00	0.00	76
Blend 1.210	16.67	0.00	0.00	50.00	16.67	16.67	0.00	0.00	50
Blend 1.211	0.00	25.00	25.00	0.00	0.00	0.00	50.00	0.00	57
Blend 1.212	0.00	0.00	0.00	16.67	16.67	16.67	50.00	0.00	62
Blend 1.213	0.00	16.67	50.00	16.67	0.00	0.00	16.67	0.00	67
Blend 1.214	0.00	33.33	0.00	0.00	0.00	33.33	0.00	33.33	92
Blend 1.215	16.67	0.00	0.00	50.00	0.00	16.67	0.00	16.67	76
Blend 1.216	0.00	0.00	0.00	50.00	0.00	50.00	0.00	0.00	36

Blend 1.217	16.67	0.00	16.67	50.00	0.00	0.00	0.00	16.67	61
Blend 1.218	0.00	75.00	0.00	0.00	25.00	0.00	0.00	0.00	106
Blend 1.219	0.00	50.00	50.00	0.00	0.00	0.00	0.00	0.00	68
Blend 1.220	0.00	0.00	25.00	50.00	0.00	25.00	0.00	0.00	60
Blend 1.221	0.00	25.00	0.00	75.00	0.00	0.00	0.00	0.00	88
Blend 1.222	50.00	16.67	0.00	16.67	0.00	0.00	0.00	16.67	74
Blend 1.223	33.33	0.00	0.00	33.33	0.00	0.00	33.33	0.00	63
Blend 1.224	0.00	0.00	0.00	0.00	75.00	0.00	0.00	25.00	114
Blend 1.225	0.00	0.00	0.00	50.00	16.67	16.67	0.00	16.67	66
Blend 1.226	16.67	0.00	0.00	16.67	50.00	0.00	0.00	16.67	74
Blend 1.227	16.67	0.00	50.00	16.67	0.00	16.67	0.00	0.00	62
Blend 1.228	50.00	0.00	0.00	16.67	16.67	0.00	16.67	0.00	67
Blend 1.229	25.00	0.00	0.00	0.00	25.00	25.00	25.00	0.00	70
Blend 1.230	0.00	0.00	50.00	0.00	50.00	0.00	0.00	0.00	82
Blend 1.231	16.67	0.00	16.67	0.00	50.00	0.00	16.67	0.00	65

Blend 1.232	0.00	16.67	0.00	0.00	50.00	16.67	16.67	0.00	83
Blend 1.233	0.00	25.00	0.00	0.00	50.00	0.00	25.00	0.00	91
Blend 1.234	0.00	0.00	0.00	16.67	50.00	0.00	16.67	16.67	77
Blend 1.235	50.00	16.67	16.67	0.00	16.67	0.00	0.00	0.00	77
Blend 1.236	50.00	0.00	16.67	0.00	0.00	0.00	16.67	16.67	45
Blend 1.237	25.00	25.00	0.00	25.00	25.00	0.00	0.00	0.00	75
Blend 1.238	0.00	16.67	50.00	0.00	0.00	16.67	16.67	0.00	79
Blend 1.239	0.00	0.00	25.00	0.00	50.00	0.00	25.00	0.00	76
Blend 1.240	25.00	0.00	0.00	0.00	0.00	0.00	75.00	0.00	36
Blend 1.241	16.67	0.00	0.00	0.00	50.00	16.67	16.67	0.00	70
Blend 1.242	16.67	16.67	0.00	50.00	0.00	16.67	0.00	0.00	77
Blend 1.243	0.00	0.00	16.67	16.67	0.00	50.00	0.00	16.67	72
Blend 1.244	0.00	0.00	16.67	0.00	50.00	16.67	0.00	16.67	76
Blend 1.245	0.00	0.00	33.33	0.00	0.00	33.33	0.00	33.33	82
Blend 1.246	0.00	0.00	0.00	33.33	0.00	33.33	33.33	0.00	76

Blend 1.247	0.00	0.00	33.33	0.00	0.00	0.00	33.33	33.33	40
Blend 1.248	25.00	0.00	25.00	25.00	0.00	25.00	0.00	0.00	62
Blend 1.249	16.67	16.67	0.00	0.00	0.00	16.67	50.00	0.00	79
Blend 1.250	16.67	0.00	16.67	16.67	0.00	50.00	0.00	0.00	62
Blend 1.251	25.00	0.00	0.00	25.00	25.00	25.00	0.00	0.00	50
Blend 1.252	0.00	50.00	16.67	0.00	16.67	0.00	0.00	16.67	77
Blend 1.253	0.00	25.00	0.00	50.00	0.00	25.00	0.00	0.00	78
Blend 1.254	0.00	25.00	25.00	0.00	25.00	0.00	25.00	0.00	77
Blend 1.255	25.00	0.00	0.00	0.00	25.00	0.00	25.00	25.00	73
Blend 1.256	25.00	25.00	0.00	0.00	25.00	0.00	25.00	0.00	78
Blend 1.257	0.00	0.00	0.00	0.00	33.33	0.00	33.33	33.33	86
Blend 1.258	16.67	0.00	0.00	0.00	0.00	16.67	16.67	50.00	74
Blend 1.259	16.67	50.00	0.00	0.00	16.67	0.00	0.00	16.67	83
Blend 1.260	0.00	0.00	16.67	16.67	0.00	16.67	0.00	50.00	72
Blend 1.261	0.00	0.00	0.00	25.00	25.00	0.00	0.00	50.00	77

Blend 1.262	16.67	50.00	16.67	0.00	0.00	16.67	0.00	0.00	78
Blend 1.263	0.00	50.00	0.00	25.00	0.00	0.00	0.00	25.00	76
Blend 1.264	33.33	0.00	33.33	0.00	0.00	0.00	0.00	33.33	50
Blend 1.265	25.00	0.00	0.00	0.00	0.00	50.00	0.00	25.00	88
Blend 1.266	16.67	0.00	50.00	0.00	0.00	16.67	16.67	0.00	66
Blend 1.267	50.00	0.00	50.00	0.00	0.00	0.00	0.00	0.00	43
Blend 1.268	0.00	25.00	0.00	25.00	50.00	0.00	0.00	0.00	74
Blend 1.269	16.67	0.00	0.00	16.67	50.00	16.67	0.00	0.00	50
Blend 1.270	0.00	25.00	50.00	0.00	0.00	0.00	25.00	0.00	57
Blend 1.271	0.00	25.00	50.00	0.00	25.00	0.00	0.00	0.00	85
Blend 1.272	16.67	16.67	0.00	0.00	0.00	0.00	50.00	16.67	55
Blend 1.273	50.00	0.00	25.00	0.00	0.00	0.00	0.00	25.00	50
Blend 1.274	16.67	0.00	16.67	0.00	0.00	0.00	16.67	50.00	45
Blend 1.275	0.00	16.67	0.00	0.00	16.67	0.00	16.67	50.00	79
Blend 1.276	50.00	16.67	16.67	0.00	0.00	16.67	0.00	0.00	78

Blend 1.277	50.00	16.67	0.00	0.00	0.00	0.00	16.67	16.67	55
Blend 1.278	50.00	0.00	0.00	16.67	0.00	16.67	0.00	16.67	76
Blend 1.279	16.67	0.00	0.00	0.00	50.00	0.00	16.67	16.67	73
Blend 1.280	0.00	0.00	0.00	0.00	0.00	0.00	50.00	50.00	38
Blend 1.281	0.00	25.00	0.00	25.00	0.00	50.00	0.00	0.00	78
Blend 1.282	16.67	0.00	0.00	16.67	0.00	0.00	16.67	50.00	64
Blend 1.283	0.00	0.00	0.00	25.00	25.00	0.00	50.00	0.00	73
Blend 1.284	25.00	25.00	0.00	0.00	0.00	25.00	0.00	25.00	84
Blend 1.285	0.00	0.00	25.00	0.00	50.00	25.00	0.00	0.00	60
Blend 1.286	0.00	0.00	50.00	0.00	0.00	25.00	0.00	25.00	82
Blend 1.287	0.00	0.00	25.00	0.00	0.00	50.00	0.00	25.00	82
Blend 1.288	0.00	0.00	25.00	0.00	0.00	0.00	50.00	25.00	40
Blend 1.289	0.00	50.00	0.00	0.00	0.00	25.00	25.00	0.00	92
Blend 1.290	16.67	50.00	0.00	16.67	16.67	0.00	0.00	0.00	75
Blend 1.291	50.00	0.00	0.00	0.00	25.00	0.00	0.00	25.00	87

Blend 1.292	50.00	0.00	0.00	0.00	0.00	0.00	25.00	25.00	47
Blend 1.293	0.00	16.67	0.00	16.67	0.00	50.00	0.00	16.67	82
Blend 1.294	0.00	0.00	25.00	25.00	0.00	0.00	50.00	0.00	62
Blend 1.295	75.00	25.00	0.00	0.00	0.00	0.00	0.00	0.00	82
Blend 1.296	25.00	25.00	25.00	0.00	25.00	0.00	0.00	0.00	77
Blend 1.297	0.00	0.00	50.00	0.00	0.00	50.00	0.00	0.00	87
Blend 1.298	16.67	16.67	0.00	0.00	16.67	50.00	0.00	0.00	78
Blend 1.299	0.00	0.00	0.00	16.67	0.00	50.00	16.67	16.67	79
Blend 1.300	0.00	16.67	16.67	0.00	0.00	0.00	16.67	50.00	50
Blend 1.301	0.00	16.67	0.00	0.00	50.00	16.67	0.00	16.67	85
Blend 1.302	0.00	25.00	0.00	25.00	25.00	0.00	25.00	0.00	79
Blend 1.303	0.00	50.00	0.00	0.00	0.00	25.00	0.00	25.00	92
Blend 1.304	0.00	0.00	25.00	50.00	0.00	0.00	0.00	25.00	63
Blend 1.305	50.00	0.00	0.00	16.67	0.00	16.67	16.67	0.00	68
Blend 1.306	0.00	16.67	16.67	16.67	50.00	0.00	0.00	0.00	71

Blend 1.307	75.00	0.00	0.00	0.00	0.00	0.00	0.00	25.00	67
Blend 1.308	0.00	0.00	0.00	16.67	16.67	16.67	0.00	50.00	66
Blend 1.309	0.00	0.00	0.00	0.00	25.00	50.00	0.00	25.00	82
Blend 1.310	25.00	25.00	0.00	0.00	0.00	0.00	0.00	50.00	66
Blend 1.311	25.00	75.00	0.00	0.00	0.00	0.00	0.00	0.00	82
Blend 1.312	0.00	50.00	0.00	50.00	0.00	0.00	0.00	0.00	88
Blend 1.313	0.00	0.00	25.00	75.00	0.00	0.00	0.00	0.00	88
Blend 1.314	0.00	16.67	0.00	16.67	0.00	0.00	50.00	16.67	69
Blend 1.315	0.00	0.00	16.67	16.67	0.00	50.00	16.67	0.00	69
Blend 1.316	0.00	50.00	0.00	16.67	16.67	0.00	0.00	16.67	79
Blend 1.317	50.00	25.00	0.00	0.00	25.00	0.00	0.00	0.00	89
Blend 1.318	16.67	0.00	0.00	16.67	0.00	16.67	50.00	0.00	68
Blend 1.319	33.33	0.00	0.00	0.00	0.00	33.33	0.00	33.33	88
Blend 1.320	16.67	50.00	0.00	16.67	0.00	0.00	0.00	16.67	74
Blend 1.321	0.00	50.00	0.00	25.00	0.00	25.00	0.00	0.00	78

Blend 1.322	0.00	0.00	0.00	16.67	50.00	16.67	16.67	0.00	62
Blend 1.323	0.00	0.00	50.00	16.67	16.67	0.00	0.00	16.67	69
Blend 1.324	16.67	0.00	0.00	0.00	0.00	50.00	16.67	16.67	74
Blend 1.325	0.00	0.00	16.67	16.67	0.00	0.00	16.67	50.00	63

Appendix VII Visual assessment results of experiment 1

Sample no.	Total score	Mean CIELAB ΔE	Visual score as %
Primary 1	10	n/a	100 %
Primary 2	10	n/a	100 %
Primary 3	10	n/a	100 %
Primary 4	10	n/a	100 %
Primary 5	10	n/a	100 %
Primary 6	10	n/a	100 %
Primary 7	10	n/a	100 %
Primary 8	10	n/a	100 %
Blend 1.48	10	27	100 %
Blend 1.65	10	80	100 %
Blend 1.76	10	11	100 %
Blend 1.87	10	25	100 %
Blend 1.96	10	11	100 %
Blend 1.121	10	79	100 %
Blend 1.128	10	36	100 %
Blend 1.210	10	50	100 %
Blend 1.240	10	36	100 %
Blend 1.38	9.5	58	95 %
Blend 1.108	9.5	57	95 %
Blend 1.216	9.5	36	95 %
Blend 1.269	9.5	50	95 %
Blend 1.198	9	36	90 %
Blend 1.267	9	43	90 %
Blend 1.35	8.5	67	85 %
Blend 1.251	8.5	50	85 %
Blend 1.16	8	80	80 %
Blend 1.27	8	67	80 %

Blend 1.31	8	38	80 %
Blend 1.112	8	50	80 %
Blend 1.5	7.5	43	75 %
Blend 1.192	7.5	67	75 %
Blend 1.247	7.5	40	75 %
Blend 1.264	7.5	50	75 %
Blend 1.274	7.5	45	75 %
Blend 1.26	7	57	70 %
Blend 1.41	7	50	70 %
Blend 1.59	7	79	70 %
Blend 1.69	7	87	70 %
Blend 1.95	7	67	70 %
Blend 1.119	7	41	70 %
Blend 1.148	7	45	70 %
Blend 1.172	7	52	70 %
Blend 1.200	7	36	70 %
Blend 1.209	7	76	70 %
Blend 1.220	7	60	70 %
Blend 1.241	7	70	70 %
Blend 1.273	7	50	70 %
Blend 1.288	7	40	70 %
Blend 1.292	7	47	70 %
Blend 1.313	7	88	70 %
Blend 1.322	7	62	70 %
Blend 1.4	6.5	38	65 %
Blend 1.32	6.5	42	65 %
Blend 1.46	6.5	47	65 %
Blend 1.47	6.5	40	65 %
Blend 1.62	6.5	74	65 %
Blend 1.71	6.5	58	65 %

Blend 1.107	6.5	64	65 %
Blend 1.122	6.5	62	65 %
Blend 1.143	6.5	56	65 %
Blend 1.147	6.5	62	65 %
Blend 1.168	6.5	74	65 %
Blend 1.179	6.5	67	65 %
Blend 1.188	6.5	106	65 %
Blend 1.236	6.5	45	65 %
Blend 1.248	6.5	62	65 %
Blend 1.250	6.5	62	65 %
Blend 1.280	6.5	38	65 %
Blend 1.285	6.5	60	65 %
Blend 1.11	6	73	60 %
Blend 1.54	6	67	60 %
Blend 1.61	6	69	60 %
Blend 1.79	6	61	60 %
Blend 1.84	6	59	60 %
Blend 1.116	6	40	60 %
Blend 1.126	6	50	60 %
Blend 1.169	6	55	60 %
Blend 1.189	6	56	60 %
Blend 1.201	6	67	60 %
Blend 1.205	6	60	60 %
Blend 1.229	6	70	60 %
Blend 1.246	6	76	60 %
Blend 1.36	5.5	55	55 %
Blend 1.39	5.5	61	55 %
Blend 1.56	5.5	41	55 %
Blend 1.57	5.5	40	55 %
Blend 1.88	5.5	60	55 %

Blend 1.135	5.5	80	55 %
Blend 1.195	5.5	62	55 %
Blend 1.204	5.5	63	55 %
Blend 1.228	5.5	67	55 %
Blend 1.230	5.5	82	55 %
Blend 1.231	5.5	65	55 %
Blend 1.307	5.5	67	55 %
Blend 1.315	5.5	69	55 %
Blend 1.1	5	82	50 %
Blend 1.23	5	72	50 %
Blend 1.99	5	69	50 %
Blend 1.123	5	68	50 %
Blend 1.227	5	62	50 %
Blend 1.305	5	68	50 %
Blend 1.64	4.5	67	45 %
Blend 1.68	4.5	68	45 %
Blend 1.132	4.5	69	45 %
Blend 1.142	4.5	70	45 %
Blend 1.158	4.5	69	45 %
Blend 1.170	4.5	66	45 %
Blend 1.185	4.5	69	45 %
Blend 1.239	4.5	76	45 %
Blend 1.266	4.5	66	45 %
Blend 1.283	4.5	73	45 %
Blend 1.297	4.5	87	45 %
Blend 1.311	4.5	82	45 %
Blend 1.89	4	70	40 %
Blend 1.194	4	48	40 %
Blend 1.212	4	62	40 %
Blend 1.223	4	63	40 %

Blend 1.70	3.5	74	35 %
Blend 1.92	3.5	76	35 %
Blend 1.129	3.5	69	35 %
Blend 1.33	3	55	30 %
Blend 1.43	3	106	30 %
Blend 1.295	3	82	30 %
Blend 1.86	2.5	61	25 %
Blend 1.118	2.5	65	25 %
Blend 1.130	2.5	57	25 %
Blend 1.139	2.5	71	25 %
Blend 1.144	2.5	105	25 %
Blend 1.152	2.5	76	25 %
Blend 1.180	2.5	67	25 %
Blend 1.196	2.5	91	25 %
Blend 1.318	2.5	68	25 %
Blend 1.325	2.5	63	25 %
Blend 1.14	2	74	20 %
Blend 1.22	2	77	20 %
Blend 1.44	2	73	20 %
Blend 1.45	2	57	20 %
Blend 1.51	2	78	20 %
Blend 1.55	2	52	20 %
Blend 1.63	2	59	20 %
Blend 1.83	2	68	20 %
Blend 1.127	2	55	20 %
Blend 1.171	2	52	20 %
Blend 1.176	2	50	20 %
Blend 1.211	2	57	20 %
Blend 1.294	2	62	20 %
Blend 1.300	2	50	20 %

Blend 1.2	1.5	78	15 %
Blend 1.40	1.5	79	15 %
Blend 1.49	1.5	71	15 %
Blend 1.52	1.5	72	15 %
Blend 1.60	1.5	73	15 %
Blend 1.66	1.5	66	15 %
Blend 1.75	1.5	77	15 %
Blend 1.94	1.5	70	15 %
Blend 1.102	1.5	69	15 %
Blend 1.103	1.5	82	15 %
Blend 1.113	1.5	75	15 %
Blend 1.125	1.5	66	15 %
Blend 1.150	1.5	50	15 %
Blend 1.153	1.5	64	15 %
Blend 1.156	1.5	63	15 %
Blend 1.161	1.5	119	15 %
Blend 1.165	1.5	90	15 %
Blend 1.167	1.5	63	15 %
Blend 1.178	1.5	50	15 %
Blend 1.182	1.5	50	15 %
Blend 1.186	1.5	77	15 %
Blend 1.187	1.5	75	15 %
Blend 1.207	1.5	82	15 %
Blend 1.208	1.5	64	15 %
Blend 1.215	1.5	76	15 %
Blend 1.224	1.5	114	15 %
Blend 1.225	1.5	66	15 %
Blend 1.226	1.5	74	15 %
Blend 1.234	1.5	77	15 %
Blend 1.244	1.5	76	15 %

Blend 1.245	1.5	82	15 %
Blend 1.258	1.5	74	15 %
Blend 1.262	1.5	78	15 %
Blend 1.265	1.5	88	15 %
Blend 1.272	1.5	55	15 %
Blend 1.282	1.5	64	15 %
Blend 1.286	1.5	82	15 %
Blend 1.287	1.5	82	15 %
Blend 1.304	1.5	63	15 %
Blend 1.310	1.5	66	15 %
Blend 1.312	1.5	88	15 %
Blend 1.321	1.5	78	15 %
Blend 1.323	1.5	69	15 %
Blend 1.9	1	72	10 %
Blend 1.13	1	109	10 %
Blend 1.18	1	88	10 %
Blend 1.19	1	91	10 %
Blend 1.20	1	77	10 %
Blend 1.30	1	88	10 %
Blend 1.58	1	79	10 %
Blend 1.67	1	77	10 %
Blend 1.77	1	85	10 %
Blend 1.81	1	91	10 %
Blend 1.90	1	82	10 %
Blend 1.97	1	72	10 %
Blend 1.100	1	72	10 %
Blend 1.101	1	59	10 %
Blend 1.106	1	90	10 %
Blend 1.114	1	86	10 %
Blend 1.115	1	87	10 %

Blend 1.136	1	63	10 %
Blend 1.138	1	82	10 %
Blend 1.140	1	109	10 %
Blend 1.141	1	77	10 %
Blend 1.146	1	64	10 %
Blend 1.162	1	78	10 %
Blend 1.173	1	63	10 %
Blend 1.177	1	80	10 %
Blend 1.181	1	82	10 %
Blend 1.184	1	119	10 %
Blend 1.197	1	66	10 %
Blend 1.202	1	78	10 %
Blend 1.203	1	72	10 %
Blend 1.217	1	61	10 %
Blend 1.218	1	106	10 %
Blend 1.232	1	83	10 %
Blend 1.243	1	72	10 %
Blend 1.257	1	86	10 %
Blend 1.260	1	72	10 %
Blend 1.261	1	77	10 %
Blend 1.263	1	76	10 %
Blend 1.277	1	55	10 %
Blend 1.278	1	76	10 %
Blend 1.279	1	73	10 %
Blend 1.291	1	87	10 %
Blend 1.298	1	78	10 %
Blend 1.308	1	66	10 %
Blend 1.309	1	82	10 %
Blend 1.320	1	74	10 %
Blend 1.6	0.5	69	5 %

Blend 1.15	0.5	69	5 %
Blend 1.17	0.5	77	5 %
Blend 1.21	0.5	68	5 %
Blend 1.24	0.5	76	5 %
Blend 1.28	0.5	69	5 %
Blend 1.29	0.5	64	5 %
Blend 1.34	0.5	73	5 %
Blend 1.37	0.5	78	5 %
Blend 1.72	0.5	90	5 %
Blend 1.73	0.5	79	5 %
Blend 1.74	0.5	80	5 %
Blend 1.78	0.5	91	5 %
Blend 1.91	0.5	87	5 %
Blend 1.98	0.5	78	5 %
Blend 1.109	0.5	74	5 %
Blend 1.110	0.5	79	5 %
Blend 1.111	0.5	92	5 %
Blend 1.117	0.5	106	5 %
Blend 1.120	0.5	69	5 %
Blend 1.131	0.5	78	5 %
Blend 1.133	0.5	74	5 %
Blend 1.137	0.5	82	5 %
Blend 1.145	0.5	89	5 %
Blend 1.154	0.5	63	5 %
Blend 1.159	0.5	86	5 %
Blend 1.163	0.5	74	5 %
Blend 1.164	0.5	63	5 %
Blend 1.166	0.5	76	5 %
Blend 1.175	0.5	76	5 %
Blend 1.183	0.5	82	5 %

Blend 1.190	0.5	92	5 %
Blend 1.193	0.5	109	5 %
Blend 1.199	0.5	74	5 %
Blend 1.206	0.5	79	5 %
Blend 1.219	0.5	68	5 %
Blend 1.221	0.5	88	5 %
Blend 1.233	0.5	91	5 %
Blend 1.242	0.5	77	5 %
Blend 1.249	0.5	79	5 %
Blend 1.252	0.5	77	5 %
Blend 1.253	0.5	78	5 %
Blend 1.255	0.5	73	5 %
Blend 1.256	0.5	78	5 %
Blend 1.259	0.5	83	5 %
Blend 1.268	0.5	74	5 %
Blend 1.275	0.5	79	5 %
Blend 1.281	0.5	78	5 %
Blend 1.289	0.5	92	5 %
Blend 1.290	0.5	75	5 %
Blend 1.299	0.5	79	5 %
Blend 1.302	0.5	79	5 %
Blend 1.303	0.5	92	5 %
Blend 1.306	0.5	71	5 %
Blend 1.314	0.5	69	5 %
Blend 1.316	0.5	79	5 %
Blend 1.317	0.5	89	5 %
Blend 1.319	0.5	88	5 %
Blend 1.324	0.5	74	5 %
Blend 1.3	0	74	0 %
Blend 1.7	0	78	0 %

Blend 1.8	0	76	0 %
Blend 1.10	0	71	0 %
Blend 1.12	0	79	0 %
Blend 1.25	0	71	0 %
Blend 1.42	0	77	0 %
Blend 1.50	0	78	0 %
Blend 1.53	0	85	0 %
Blend 1.80	0	90	0 %
Blend 1.82	0	85	0 %
Blend 1.85	0	85	0 %
Blend 1.93	0	76	0 %
Blend 1.104	0	83	0 %
Blend 1.105	0	79	0 %
Blend 1.124	0	79	0 %
Blend 1.134	0	88	0 %
Blend 1.149	0	70	0 %
Blend 1.151	0	79	0 %
Blend 1.155	0	84	0 %
Blend 1.157	0	82	0 %
Blend 1.160	0	79	0 %
Blend 1.174	0	85	0 %
Blend 1.191	0	83	0 %
Blend 1.213	0	67	0 %
Blend 1.214	0	92	0 %
Blend 1.222	0	74	0 %
Blend 1.235	0	77	0 %
Blend 1.237	0	75	0 %
Blend 1.238	0	79	0 %
Blend 1.254	0	77	0 %
Blend 1.270	0	57	0 %

Blend 1.271	0	85	0 %
Blend 1.276	0	78	0 %
Blend 1.284	0	84	0 %
Blend 1.293	0	82	0 %
Blend 1.296	0	77	0 %
Blend 1.301	0	85	0 %

Appendix VIII MATLAB code to define the boundaries of a gamut

```
% define the CIELAB values of the boundaries of the gamut
lab = [95      0      0; ...
      14      0      0; ...
      50     57     28; ...
      69     39     74; ...
      79      7     99; ...
      70    -23     79; ...
      52    -50     18; ...
      53    -42     -3; ...
      54    -30    -22; ...
      54     -8    -44; ...
      52     24    -29; ...
      51     46     -7];

% plot CIELAB coordinates, coloured with sRGB values
rgb = (xyz2srgb((lab2xyz(lab,'d65_31'))/100))/255;

for i=1:length(rgb)
    hold on
    c = rgb(i,:);

    plot3(lab(i,2),lab(i,3),lab(i,1),'o','MarkerEdgeColor','k','MarkerFace
    Color',c,'MarkerSize',10)

end

hold on
plot3([80 -80],[0 0],[50 50],'k-');
hold on
plot3([0 0],[-80 80],[50 50],'k-');
hold on
plot3([0 0],[0 0],[0 100],'k-');
hold on

xlabel('a*')
ylabel('b*')
zlabel('L*')
```

Appendix IX MATLAB code for creating 4-colour tetrahedra within a given gamut

```

% set N, the number of samples generated to fill the gamut
N = 10000;

% define the CIELAB values of the primaries forming the boundaries of
the gamut
lab = [95      0      0; ...
      14      0      0; ...
      50     57     28; ...
      69     39     74; ...
      79      7     99; ...
      70    -23     79; ...
      52    -50     18; ...
      53    -42     -3; ...
      54    -30    -22; ...
      54     -8    -44; ...
      52     24    -29; ...
      51     46     -7];

% plot CIELAB coordinates, coloured with sRGB values
rgb = (xyz2srgb((lab2xyz(lab,'d65_31'))/100))/255;
for i=1:length(rgb)
    hold on
    c = rgb(i,:);
    plot3(lab(i,2),lab(i,3),lab(i,1),'o','MarkerEdgeColor','k','MarkerFace
Color',c,'MarkerSize',10)
end

hold on
plot3([80 -80],[0 0],[50 50],'k-');
hold on
plot3([0 0],[-80 80],[50 50],'k-');
hold on
plot3([0 0],[0 0],[0 100],'k-');
hold on
xlabel('a*')
ylabel('b*')
zlabel('L*')

```

```

% specify the rectangular box from which to grab random colours
maxvals = max(lab);
minvals = min(lab);
maxL = maxvals(1)+2;
maxa = maxvals(2)+2;
maxb = maxvals(3)+2;
minL = minvals(1)-2;
mina = minvals(2)-2;
minb = minvals(3)-2;

% generate N new primaries that are inside the gamut of the outer 12
% index is 0 and N is 10,000
while index<N
    index = 0;

    % a loop creates random colours and tests whether they are in the hull
    % if they are in the hull the loop accepts them; if not they are
    % rejected

    while index<N
        % generate a random colour - [L a b]
        p = [rand*(maxL-minL)+minL rand*(maxa-mina)+mina rand*(maxb-
            minb)+minb];
        if inhull(p, lab)
            index = index+1;
            morelab(index,:) = p;
        end
    end

    disp(index)

    % combine the 12 x 3 array (outer primaries) with the 10,000 x 3 array
    % (inner primaries)
    lab = [lab; morelab];

    % at this point there are 10,012 samples (12 + N samples)
    % plot CIELAB coordinates, coloured with sRGB values
    rgb = (xyz2srgb((lab2xyz(lab,'d65_31'))/100))/255;

```

```

figure
for i=1:length(rgb)
    hold on
    c = rgb(i,:);
    plot3(lab(i,2),lab(i,3),lab(i,1),'o','MarkerEdgeColor','k','MarkerFace
    Color',c,'MarkerSize',10)
end

hold on
plot3([80 -80],[0 0],[50 50],'k-');
hold on
plot3([0 0],[-80 80],[50 50],'k-');
hold on
plot3([0 0],[0 0],[0 100],'k-');

```

Appendix X Example MATLAB code for plotting Delaunay triangles in CIELAB colour space

```
% tester is a 50 x 3 matrix of L*a*b* values
X = tester;

% plot tetrahedra using Delaunay function
tet = delaunay(X);

% colour faces of tetrahedra
faceColor = [0.6875 0.8750 0.8984];

tetramesh(tet,X,'FaceColor', faceColor,'FaceAlpha',0.3);
```

Appendix XI MATLAB code for generating tetrahedra using points within the gamut

```

% the 10,012 random primaries provide the points to select from
% test_num is the number of primaries to select in each loop
test_num = [10 20 30 40 50 60 70 80 90 100 150 200]

for i=1:12
    disp(i)
    this_num = test_num(i);

    % this is the arbitrary first sample to select
    p = 1;

    sublab = maxminc(lab,this_num,p);

    tri = delaunay(sublab(:,2)',sublab(:,3)',sublab(:,1)');

    % this tells us the number of tetrahedral subsystems
    N = length(tri)
    for j=1:N
        a = tri(j,1);
        b = tri(j,2);
        c = tri(j,3);
        d = tri(j,4);
        prim = [sublab(a,:); sublab(b,:); sublab(c,:); sublab(d,:)];
        % this calculates the mean colour difference of the tetrahedral
        subsystems depending on the test_num
        index=0;
        for k=1:3
            for m=k+1:4
                index=index+1;
                e(index) = cielabde(prim(k,:),prim(m,:));
            end
        end
        storee(j) = mean(e);
    end
    disp(storee)
    store(i,:) = [this_num N mean(storee)];
end

```

```
disp(store)
```

```
figure
```

```
plot(store(:,1),store(:,3),'r-')
```

```
hold on
```

```
plot([0 150],[20 20],'b-')
```

```
hold on
```

```
plot([0 150],[23 23],'b-')
```

Appendix XII MATLAB code for reducing the points to those with an L* value of less than 27

```
% at this point there are 10,012 samples
% reduced the gamut so that it has an L* value of less than 27
lab = lab((lab(:,1)<27),:);
rgb = (xyz2srgb((lab2xyz(lab,'d65_31'))/100))/255;

figure
for i=1:length(rgb)
    hold on
    c = rgb(i,:);

    plot3(lab(i,2),lab(i,3),lab(i,1),'o','MarkerEdgeColor','k','MarkerFace
    Color',c,'MarkerSize',10)
end

hold on
plot3([80 -80],[0 0],[50 50],'k-');
hold on
plot3([0 0],[-80 80],[50 50],'k-');
hold on
plot3([0 0],[0 0],[0 100],'k-');
```


Appendix XIII MATLAB code for creating the tetrahedra within the smaller gamut

```

% test_num is the number of colours to select in each loop
% note the test numbers are reduced as the gamut is smaller
test_num = [5 10 15 20 25 30 35 40 45 50]
for i=1:10
    disp(i)
    this_num = test_num(i);
    p = 1;
    blacklab = maxminc(lab,this_num,p);

    tri = delaunay(blacklab(:,2)',blacklab(:,3)',blacklab(:,1)');
    s = size(tri);
    N = s(1);

    for j=1:N
        a = tri(j,1);
        b = tri(j,2);
        c = tri(j,3);
        d = tri(j,4);

        prim = [blacklab(a,:); blacklab(b,:); blacklab(c,:);
        blacklab(d,:)];
        index=0;
        for k=1:3
            for m=k+1:4
                index=index+1;
                e(index) = cielabde(prim(k,:),prim(m,:));
            end
        end
        storee(j) = max(e);
    end
    store(i,:) = [this_num N mean(storee)];
end

disp(store)
this_num=15
p = 1;
blacklab = maxminc(lab,this_num,p);

```

```
disp(blacklab)

hold on
plot3([80 -80],[0 0],[50 50],'k-');
hold on
plot3([0 0],[-80 80],[50 50],'k-');
hold on
plot3([0 0],[0 0],[0 100],'k-');

hold on
xlabel('a*')
ylabel('b*')
zlabel('L*')
```

Appendix XIV MATLAB code for applying Stearns-Noechel's model

```

clear
close all
load firstexperimentall.mat
% firstexperimentdata 333x35 93240 double
% firstexperimentrecipes 333x8 21312 double

% convert the firstexperimentdata into fractional data
data = firstexperimentdata/100;

% converts the firstexperimentrecipes from 0-6 to 0-1
recipes = firstexperimentrecipes/6;

% assumes the first eight are the primaries
% and that they are in the right order
primary = data(1:8,:);

% create a variable for plotting
w = linspace(360,700,35);

% define the empirically derived b value of the Stearns-Noechel model
b = 0.1;

% calculate the transformed values of the primaries
sn = (1-primary)./(b*(primary-0.01)+0.01);

% predict the reflectance of every sample
pred_sn = sn'*recipes';

% now convert back to reflectance
pred_R = (1 + 0.01*pred_sn*(b-1))./(1+b*pred_sn);
pred_R = pred_R';
LAB1 = xyz2lab(r2xyz(data,360,700,'d65_64'),'d65_64');
LAB2 = xyz2lab(r2xyz(pred_R,360,700,'d65_64'),'d65_64');

% calculate CIELAB DE and CIEDE2000 mean, minimum and maximum colour
% differences between actual blended samples and the predicted

```

```
% reflectance of the samples  
DE = cielabde(LAB1,LAB2);  
DE00 = cie00de(LAB1,LAB2);  
disp([mean(DE) min(DE) max(DE); mean(DE00) min(DE00) max(DE00)])
```

Appendix XV MATLAB code for running Friele's model

```

clear
close all
load firstexperimentall.mat
% firstexperimentdata 333x35 93240 double
% firstexperimentrecipes 333x8 21312 double

% converting % data into fractional data
data = firstexperimentdata/100;

% convert the recipes from 0-6 to 0-1
recipes = firstexperimentrecipes/6;

% assumes the first eight are the primaries
% and also that they are in the right order
primary = data(1:8,:);

% create a variable for plotting
w = linspace(360,700,35);

% define the empirically derived s value of the Friele model
s = 0.35;

% calculate the K/S values of the primaries
ks = ((1-primary).^2)./(2*primary);

% apply the Friele model
friele = exp(-s*ks);

% predict the reflectance of every sample
pred_fks = friele'*recipes';

% first convert back to standard K/S
pred_ks = log(pred_fks)/(-s);

% then convert back to reflectance
pred_R = 1 + pred_ks - ((1 + pred_ks).^2 - 1).^(0.5);

```

```

pred_R = pred_R';

% calculate CIELAB DE and CIEDE2000 mean, minimum and maximum colour
% differences actual blended samples and the predicted reflectance of
% the samples

LAB1 = xyz2lab(r2xyz(data,360,700,'d65_64'),'d65_64');
LAB2 = xyz2lab(r2xyz(pred_R,360,700,'d65_64'),'d65_64');

DE = cielabde(LAB1,LAB2);
DE00 = cie00de(LAB1,LAB2);

disp([mean(DE) min(DE) max(DE); mean(DE00) min(DE00) max(DE00)])

```

Appendix XVI MATLAB code for running standard neural network

```

clear
close all

% the number of hidden units to test
hunits = [1 3 5 7 9 10 15 20 25 30 35 40 50 60];
for counter = 1:length(hunits)

% load reflectance data of 325 blended samples and 8 primaries
load data.mat

% train_recipes = 273 x 8
% train_reflect = 273 x 35
% test_recipes = 60 x 8
% test_reflect = 60 x 35

hiddenLayerSize = hunits(counter);

% create a network object (structure) using the fitnet command
net = fitnet(hiddenLayerSize);

net.divideParam.trainRatio = 100/100;
net.divideParam.valRatio = 0/100;
net.divideParam.testRatio = 0/100;

% for the network each column is a sample (rather than each row)
[net,tr] = train(net,train_recipes',train_reflect');

% now that the network is trained its performance can be tested
outputs = net(train_recipes');
train_outputs = outputs';
outputs = net(test_recipes');
test_outputs = outputs';

train_xyz = r2xyz(train_reflect,360,700,'d65_64');
train_xyzp = r2xyz(train_outputs,360,700,'d65_64');
test_xyz = r2xyz(test_reflect,360,700,'d65_64');

```

```

test_xyzp = r2xyz(test_outputs,360,700,'d65_64');

train_lab = xyz2lab(train_xyz,'d65_64');
train_labp = xyz2lab(train_xyzp,'d65_64');
test_lab = xyz2lab(test_xyz,'d65_64');
test_labp = xyz2lab(test_xyzp,'d65_64');

% calculate CIELAB DE and CIEDE2000 mean and maximum colour
% differences between actual blended samples and the predicted
% reflectance of samples
train_de = cielabde(train_lab,train_labp);
test_de = cielabde(test_lab,test_labp);
train_de1 = cie00de(train_lab,train_labp);
test_de1 = cie00de(test_lab,test_labp);

disp([mean(train_de) max(train_de) mean(test_de) max(test_de)
mean(train_de1) max(train_de1) mean(test_de1) max(test_de1)])

% calculate results for each number of hidden layers and save
savedata(counter,:) = [hiddenLayerSize mean(train_de) mean(test_de)
mean(train_de1) mean(test_de1)];
end

```


Appendix XVII MATLAB code for running the novel neural network

```

clear
close all

load firstexperimentsplitdata.mat
% train_recipes = 273 x 8
% train_reflect = 273 x 35
% test_recipes = 60 x 8
% test_reflect = 60 x 35

hiddenunits = [1 2 3 4 5 6 7 8 9 10 11 12 13 14 15 16 17 18 19 20];

for i=1:length(hiddenunits)
N = hiddenunits(i);

% create a network object (structure) using the fitnet command
net = fitnet(N);

% these lines are necessary because the train and test sets are
% already formed and all the data should be treated as training data
net.divideParam.trainRatio = 100/100;
net.divideParam.valRatio = 0/100;
net.divideParam.testRatio = 0/100;

for w = 1:35
disp([N w])
% for the network each column is a sample (rather than each
% row) and therefore the transpose (') command must be used to flip
% the data
[net,tr] = train(net,train_recipes',train_reflect(:,w)');

% now that the network is trained its performance can be
% tested
outputs = net(train_recipes');
train_outputs(:,w) = outputs';
outputs = net(test_recipes');
test_outputs(:,w) = outputs';

```

end

```

train_xyz = r2xyz(train_reflect,360,700,'d65_64');
train_xyzp = r2xyz(train_outputs,360,700,'d65_64');
test_xyz = r2xyz(test_reflect,360,700,'d65_64');
test_xyzp = r2xyz(test_outputs,360,700,'d65_64');

train_lab = xyz2lab(train_xyz,'d65_64');
train_labp = xyz2lab(train_xyzp,'d65_64');
test_lab = xyz2lab(test_xyz,'d65_64');
test_labp = xyz2lab(test_xyzp,'d65_64');

% calculate CIELAB DE and CIEDE2000 mean and maximum colour
% differences between actual blended samples and the predicted
% reflectance of samples
train_de = cielabde(train_lab,train_labp);
test_de = cielabde(test_lab,test_labp);

disp([mean(train_de) max(train_de) mean(test_de) max(test_de)])

train_de00 = cie00de(train_lab,train_labp);
test_de00 = cie00de(test_lab,test_labp);

disp([mean(train_de00) max(train_de00) mean(test_de00)
max(test_de00)])

store(i,:) = [N mean(train_de) max(train_de) mean(test_de)
max(test_de) mean(train_de00) max(train_de00) mean(test_de00)
max(test_de00)];
end

```